Mosby
An Affiliate of Elsevier

11830 Westline Industrial Drive
St. Louis, Missouri 63146

ATLAS OF EQUINE ENDOSCOPY ISBN 0-323-1848-3

Library of Congress Cataloging-in-Publication Data
Slovis, Nathan M.
Atlas of equine endoscopy / Nathan M. Slovis.
p. cm.
Includes bibliographical references (p.).
ISBN (invalid) 032318483
1. Horses—Diseases—Atlases. 2. Veterinary endoscopy—Atlases. I. Title.

SF951.S624 2004
636.1'089607545—dc22

2003065117

Acquisitions Editor: Liz Fathman
Developmental Editor: Teri Merchant
Publishing Services Manager: Melissa Lastarria
Book Design Manager: Gail Morey Hudson

Printed in the United States of America

Last digit is the print number: 9 8 7 6 5 4 3 2 1

Contributors

FAIRFIELD T. BAIN, DVM
Diplomate ACVIM, ACVP, ACVECC
Hagyard-Davidson-McGee, PLLC
Lexington, Kentucky

JAMES BURNS
General Manager
Endoscopy Support Services, Inc.
Brewster, New York

DOUG BYARS, DVM
Diplomate ACVIM, ACVECC
Director, Internal Medicine
Hagyard-Davidson-McGee, PLLC
Lexington, Kentucky

AURELIO MUTTINI, MED VET
Department of Veterinary Clinical Sciences
University of Teramo—Italy

LUCIO PETRIZZI, MED VET
Associate Professor of Veterinary Clinical Sciences
University of Teramo—Italy

DWAYNE RODGERSON, DVM, MS
Diplomate ACVS
Hagyard-Davidson-McGee, PLLC
Lexington, Kentucky

THOMAS SEAHORN, DVM, MS
Diplomate ACVIM, ACVECC
Hagyard-Davidson-McGee, PLLC
Lexington, Kentucky

NATHAN M. SLOVIS, DVM
Diplomate ACVIM
Hagyard-Davidson-McGee, PLLC
Lexington, Kentucky

KIM SPRAYBERRY, DVM
Diplomate ACVIM
Hagyard-Davidson-McGee, PLLC
Lexington, Kentucky

JOHN STEINER, DVM
Diplomate ACT
Hagyard-Davidson-McGee, PLLC
Lexington, Kentucky

LUCA VALBONETTI, MED VET
Department of Veterinary Sciences and Agriculture—
Surgical Unit
University of Teramo—Italy

EDWARD VOSS, DVM
Diplomate ACVIM
Arizona Equine Centre
Gilbert, Arizona

To my wife
Stacey and **my family**

Norman Slovis, Carol Slovis,
Daniel Slovis, and **Margo Glickman**

Preface

Today's veterinary curriculum places more demands on both students and teachers, and consequently there is generally insufficient time and material available to teach an ever-increasing number of students the art of endoscopy. Endoscopes, videosystems, and therapeutic techniques are constantly being upgraded or redesigned, thus outdating many reports regarding their use. The purpose of this atlas is to provide both the general practitioner and student with a reference guide. The atlas's emphasis is on normal and abnormal findings of different body systems examined by the general equine practitioner. The atlas contains state-of-the-art digital images that provide a base of knowledge on which the reader may build and to describe techniques involved in endoscopy, so as to make learning an easier proposition.

Endoscopy is one of the most diagnostically useful tools available in equine practice. It allows the practitioner a minimally invasive technique in examining different organ systems. We hope that this text will help illustrate the usefulness of diagnostic endoscopy. The atlas provides photographs of endoscopic procedures that will help guide the reader through the different organ systems with an emphasis on normal and abnormal findings.

This book is divided into two major sections. The first section includes newer instrumentation and documentation for endoscopy. The second section illustrates through photographs the art of endoscopy and provides a quick reference guide in the visual form. This atlas should be regarded as a companion to other equine endoscopy texts that have educated the reader on the basics of equine endoscopy. The contributors discuss treatments and management where appropriate.

We have attempted to emphasize the diagnostic features of those conditions the general equine practitioner will be exposed to. The atlas's contributors realize that the most valuable learning resources were the photographs that we took of our patients. Through this book we have oriented many years of clinical experience in endoscopic observation and documentation by leading specialists. The atlas's photographs will provide the reader a large range of appearances from which to learn and compare, while helping the amateur endoscopist gain confidence. In order to orient the anatomy of different organ systems, distant and close-up views are provided where applicable. This is educational, particularly in identifying anatomical variations. The chapters are organized according to the area being discussed. The photographic illustrations reflect the order in which the endoscopic examination is being performed. The atlas begins with a series of photographic and, where applicable, schematic drawing of the normal anatomic conformation and variations to the specific area of the body being discussed. The abnormal findings have been grouped by type of disorder (i.e., inflammatory, neurologic, neoplastic, congenital).

We have seen significant progress being made in equine endoscopy over the last two decades. Today the public demands and insists on more specialized care for their animals. More equine practitioners have realized the importance of endoscopy for the diagnosis of various disorders.

Nathan M. Slovis

CHAPTER 1

Endoscopic Instrumentation

JAMES BURNS

FIBEROPTIC ENDOSCOPE PRINCIPLES

A fiberoptic endoscope system is based on transmission of light and images through long thin fibers of optical glass. The fiberoptic image is made up of thousands of tiny fibers that are made of coated glass. The coating acts as a mirror that reflects light through the fiber into the eyepiece. The eyepiece magnifies the group of fibers into an image that you can visualize with your eye (Figure 1-1). If you look closely, you can observe what appears to be a screen or spider web. This screen is actually all the fibers lined up next to one another. Each fiber displays part of the overall image.

When one of the fibers in the group is broken, it appears as a black dot in your overall image. If the coating on a fiber is scratched or chipped, light can escape from it, causing the fiber to appear as a light gray dot in your overall image.

Light used to visualize your image is sent into the body cavity through light guides and then travels back up through the image guide to the eyepiece for viewing.

To identify the amount of broken fibers in an instrument, you need to hold the distal tip of the insertion tube to a light (Figure 1-2) Note that fluorescent lights work

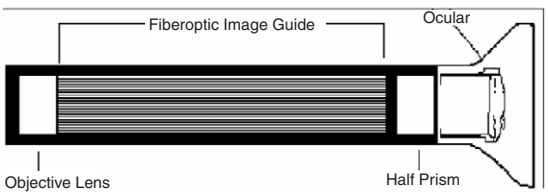

FIGURE 1-1. Optical system of fiberoptic endoscope.

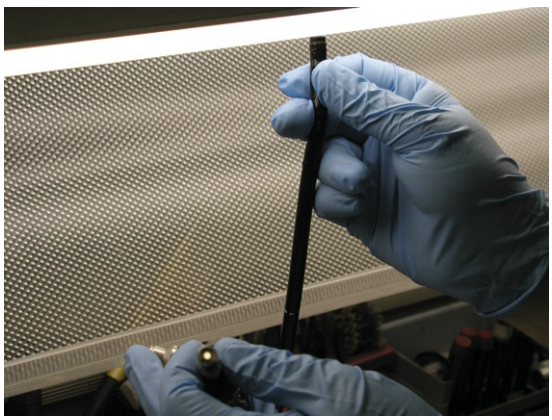

FIGURE 1-2. Identifying the amount of broken fibers in instrument.

best. While holding the tip to the light, look through the eyepiece and focus the scope so you can clearly see the outline of the fibers.

VIDEO ENDOSCOPE PRINCIPLES

Video endoscopy has been used in human medicine for several years and has just recently become widely used in equine medicine for both diagnostic and therapeutic procedures.

Endoscopic external video cameras (Figure 1-3) can be attached to the eyepiece of a fiberoptic endoscope with a coupler (Figure 1-4) and allow you to visualize what you would see through the eyepiece on screen.

There has been an increase in the demand for new and used endoscopic external video cameras. Using cameras can help enhance the visualization of a diagnostic procedure.

When you look into the eyepiece directly, a clear image is noted. However, with a camera the image may appear darker. This visualization occurs because the camera does not have the ability to sense light as well as your eye.

FIGURE 1-3. Endoscopic video camera.

FIGURE 1-4. Couplers.

The use of a fiberoptic instrument with external video cameras may produce the moiré phenomenon (Figure 1-5). This phenomenon is caused when the camera tries to generate an image from the fibers in the endoscope. The charged couple device (CCD) is made up of tiny pixels that convert the light into an electronic signal so it can be sent to the processing unit. The image from the endoscope is made up of tiny fibers that are assembled in the eyepiece as a single image. When the camera looks at the image, the pixels in the CCD will notice the individual fibers, therefore causing interference. This interference shows up as a wave of colors that flow through the image. This interference is known as moiré patterning. There are three approaches to the resolution of this problem.

The first is to fool the camera by taking it out of focus. This allows the camera to see a single image instead of all the fibers. However your image on the screen also appears to be out of focus. Some practitioners do not mind the image being slightly blurred despite the risk of missing a diagnosis when working in these conditions.

The second is to rotate the camera head until the moiré pattern clears up. A disadvantage to this is that the top of your image should appear at the 12 o'clock position on your monitor. If you rotate the camera head, the top of your image could end up in the 4 o'clock position on the monitor. Then when you angulate your scope using the "up control," it appears to move down and right. The change in orientation seems to change the angulation controls, making it difficult to determine your location when you perform a procedure. Nonetheless, some people have learned to deal with this inconvenience.

The third and best way is to use a camera system that incorporates an anti-moiré filter. This filter helps to alleviate the interference and allows you to sharpen the focus as well as position the image correctly on the screen. Only a small number of used cameras on the market incorporate anti-moiré filters in their systems. The cameras that do incorporate this filtering system have been designed for use with flexible and rigid endoscopes.

Most of the newer cameras on the market use a smaller CCD. This has allowed camera manufacturers to develop smaller, lighter camera heads. These lighter camera

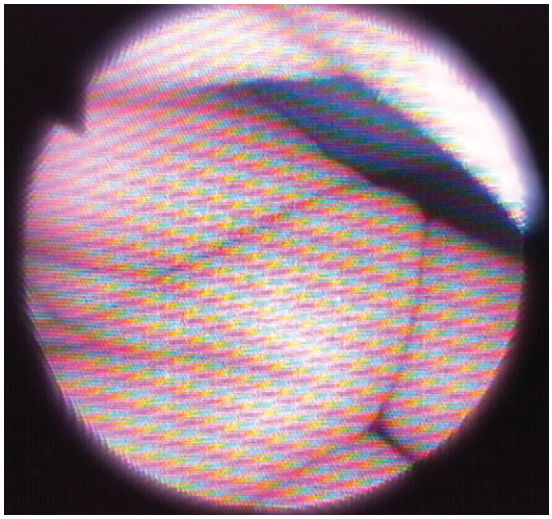

FIGURE 1-5. Moiré phenomenon.

heads prevent addition of excessive weight to the eyepiece, making it harder for the user to hold and control them.

Auto exposure cameras control the light sensitivity electronically and can be used with any light source you prefer. Some of the newer auto exposure cameras have better light sensitivity and offer more advanced manual control of the sensitivity settings. The manual control options have proven to be very useful in low-light situations. These features allow the use of a halogen light source with this type of camera system.

Non-auto exposure cameras do not control the light intensity and must be used with an auto exposure light source. Exposure control is managed by the light source in this type of system. The light source uses a robotic shutter inside the unit to control the light intensity. This prevents the camera from "whiting out" if the light on the object being visualized becomes too intense (Figure 1-6).

Another item to consider when you purchase a camera for use on a fiberoptic endoscope is the endocoupler (see Figure 1-4). The endocoupler is used to obtain mechanical and optical coupling of the fiberscope to the camera head. This device plays a very important part in the overall image. When purchasing a used camera, you do not have a choice of what size or magnification endocoupler will be provided with it. Most rigid cameras have a 32- to 35-mm coupler for use with rod lens endoscopes. Some cameras may come with a zoom coupler that allows you to change the magnification range much like that of a camcorder.

A 22- to 28-mm endocoupler normally works the best with flexible gastroscopes and colonoscopes (typical human instruments used in veterinary endoscopy). A 22- to 28-mm coupler does not overmagnify the fibers and helps reduce moiré interference. Another major advantage is that these couplers normally allow the user to see the entire image on the screen. When higher magnifications are used, the image can appear larger than the screen, causing the user to only view part of the image.

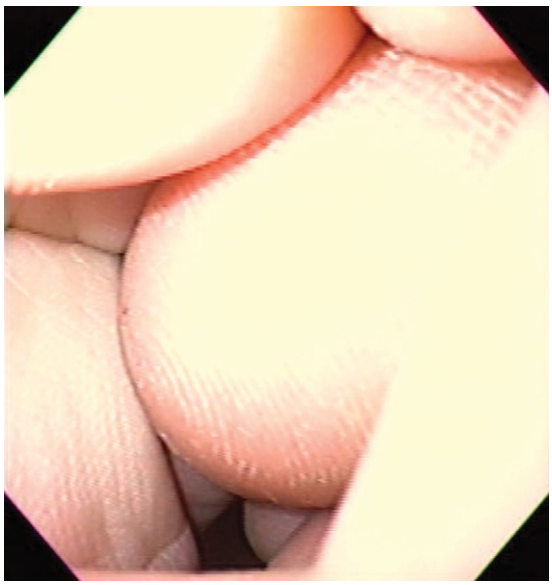

FIGURE 1-6. "White out."

VIDEO ENDOSCOPES

Video endoscopes and endoscopic video cameras gather light via a lens and a CCD. The CCD is made up of many tiny pixels that convert light into an electronic signal that is sent to the processing unit where it is converted for output as a video signal for the monitor to display.

ENDOSCOPE CONSTRUCTION

Figure 1-7 shows the construction of an endoscope.

LIGHT SOURCES

Halogen light sources are most commonly used in equine medicine. Their lightweight portable design and low cost make them the right choice for ambulatory practice. The halogen light source (Figure 1-8, *A*) typically uses a 150-watt halogen projector lamp at an average cost of about $35. When a fiberoptic scope is used optically, the light output of a halogen light source will always be suitable.

Xenon light sources (Figure 1-8, *B*) use a gas-filled lamp that burns the gas over the life of the bulb. When the gas inside the bulb has burned off, the lamp stops functioning.

Xenon light sources produce a high-intensity light as well as cleaner or "whiter" light compared with other types of light sources. When a video camera is used, this higher-intensity light is needed to visualize the subject. (See Figure 1-3.)

The cost of a xenon bulb is usually about $500. Xenon bulbs have an expected life of 600 hours. Most lamps come with a 500-hour warranty, and a lamp timer is used to gauge the lamp's life.

Most of the auto exposure light sources are 300-watt xenon light sources rather than the 150-watt halogen light sources commonly associated with flexible endoscopes. The xenon light source outputs more than twice the amount of light as a halogen unit. Xenon units produce light at a lower color temperature, making it a cleaner or whiter light.

Air and water functions of scopes are controlled by the air pump found in the light source. If you plan to use these functions, you will need a light source that has an air pump.

HUMAN ENDOSCOPES USED BY EQUINE PRACTITIONERS

Equine veterinarians generally use human gastroscopes or colonoscopes.

Human Gastroscopes

The insertion tube of a human gastroscope normally ranges in size from 7.9 to 12 mm in outer diameter with a working length of about 1 m. These scopes can be used for the following equine procedures:

- Rhinoscopy
- Pharyngoscopy and laryngoscopy
- Guttural pouch examination
- Tracheoscopy (proximal)
- Cystoscopy (young colts or geldings, ponies, and adult mares)

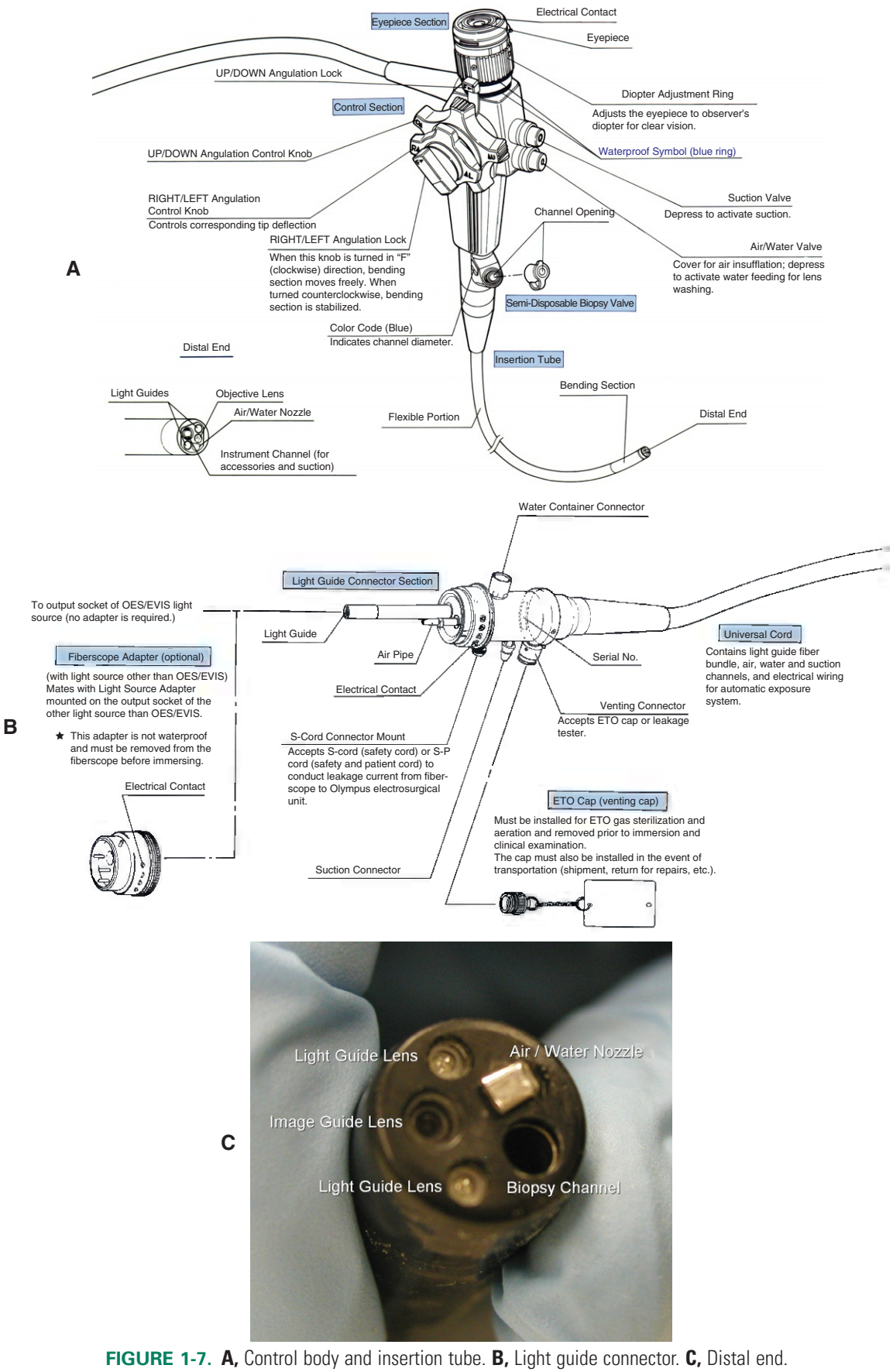

FIGURE 1-7. **A,** Control body and insertion tube. **B,** Light guide connector. **C,** Distal end.

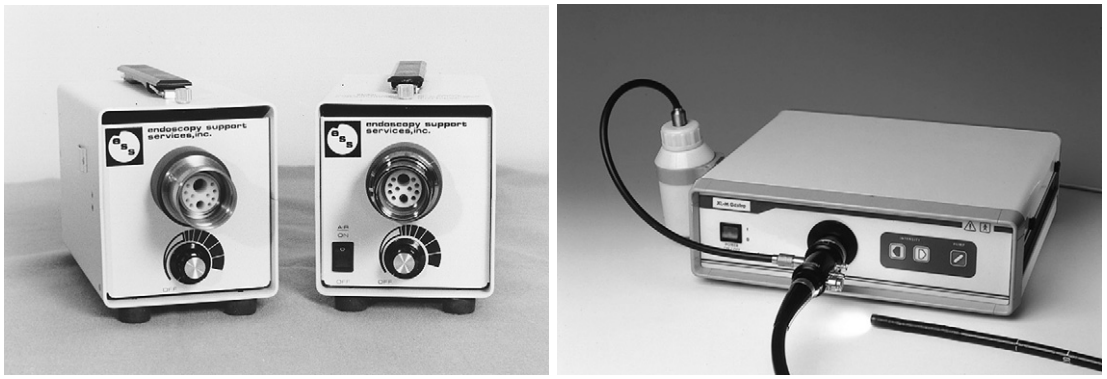

FIGURE 1-8. **A,** Halogen light source. **B,** Xenon light source.

- Proctoscopy
- Otoscopy
- Female reproductive tract examination

Human Colonoscopes

The insertion tube on a human colonoscope ranges in size from 11 to 14 mm in outer diameter with a working length of 133 to 170 cm. These scopes can be used for the same diagnostic procedures as the human gastroscope but can also be used for the following:

- Examination of the adult male reproductive tract and cystoscopy
- Uterotubal junction insemination
- Tracheobronchoscopy

Human Enteroscopes

The insertion tube of a human enteroscope normally ranges in size from 11 to 12 mm in outer diameter with a working length of 218 to 250 cm. These scopes are generally used for equine gastroscopy.

VETERINARY SPECIFIC ENDOSCOPES

General Purpose Veterinary Scopes

The Olympus VR7142 veterinary endoscope (Figure 1-9), also known as the VET-XP20, is a 7.9-mm-diameter instrument with a 140-cm working length. This scope offers a host of applications because of its small diameter and length suitable for upper airway examinations.

Equine Gastroscopes

The Olympus GIF-130-300 equine video gastroscope (Figure 1-10) is 9.8 mm in diameter and 3 m in length. It offers exceptional picture quality. However, this instrument is a special order item and costs $34,000 (pricing from January 2003).

The VFS-300 fiberoptic gastroscope from Vet-Vue (Figure 1-11) offers low-cost entry into the equine gastrointestinal tract. However, because of its length this scope tends

FIGURE 1-9. Olympus VR7142 veterinary endoscope.

FIGURE 1-10. Olympus GIF-130-300 equine video gastroscope.

FIGURE 1-11. Vet-Vue VFS-300 fiberoptic gastroscope.

to be a little more delicate than the typical fiberoptic scope. This scope has a 9.8-mm diameter and a 3-m working length.

The scopes discussed here represent only a sampling of what is available on the market. We have chosen to highlight these models because they are the most popular.

Be very careful if you choose to deal with a company that only makes veterinary endoscopes. Some of these scopes are being imported from China and Russia. The quality of the equipment tends to be far lower than that of the German and Japanese equipment used in human endoscopy. The initial purchase price will look very attractive but you could be trading service for the lower price.

HOW TO INSPECT USED ENDOSCOPES

As discussed earlier, the amount of broken fibers in an instrument can be identified by holding the distal tip of the insertion tube to a fluorescent light (see Figure 1-2) and looking through the eyepiece to clearly see the outline of the fibers. Now

count the number of black dots (broken fibers) you see in the field of view (Figure 1-12). Also look for gray dots (partially broken fibers). Gray fibers can eventually turn black. It is up to the individual using the scope to determine whether the amount of broken fibers in the image is going to make the scope unacceptable for use. Keep in mind that even a new endoscope may have up to five or six broken fibers.

Lay the scope straight out on a table (Figure 1-13). Turn the up/down and left/right angulation control knobs. As soon as you start to move the knob, the tip of the scope should also move. If the angulation cables in the scope are stretched, the knob will turn some before the tip moves. A good scope will have tight cables and the tip will respond immediately to any movement of the controls. If the cables seem to be *VERY LOOSE* you should have the scope checked by a knowledgeable service facility before purchasing the instrument. Minor play in the cables of a scope is acceptable and can be easily repaired for $150 to $250.

To check the light transmission fibers of the endoscope hold the tip of the scope to a light bulb as illustrated in Figure 1-2. Next, look at the end of the light guide probe that plugs into your light source (see Figure 1-7B). The field of fibers should appear to be illuminated evenly almost like a full moon. Try to estimate the percentage of light fibers that are not transmitting light to get a feel for how well the scope will be able to transmit light when you are performing a procedure. If you determine that 30% or more of the light guide fibers are broken, the light guides of the scope may need to be replaced. The typical charge for this repair would be $1000 to $2000, depending on the model of the scope.

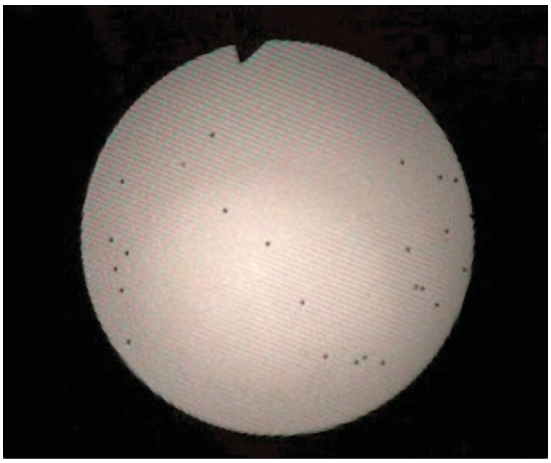

FIGURE 1-12. View of scope with broken fibers.

FIGURE 1-13. Inspecting a used endoscope.

Carefully inspect the flexible bending rubber for holes or wrinkles (Figure 1-14). A good bending rubber will be smooth and tight to the scope. The bending rubber can always be replaced later for about $200.

Pass a biopsy forceps through the instrument channel. Make sure the forceps passes through the channel no matter which way the tip of the instrument is angulated (Figure 1-15). If you have difficulty passing the forceps, *DO NOT* force it. If the channel is good, the forceps will pass smoothly through it. Resistance in the channel could be a sign of a bigger problem. You should have the scope checked by a knowledgeable service facility before purchasing the instrument if you encounter this problem.

Perform a leak test on the instrument with a leak tester (Figure 1-16) to determine whether the scope is vulnerable to fluid invasion. Leak testers are available in hand-held models for about $200 and are very easy to use.

Fluid can cause major damage to your endoscope (Figure 1-17) if it enters the inner cavities of the instrument. If you have no way to perform a leak test before purchasing a scope, you are taking a gamble on its condition. If the scope is an older non-immersible model, send it to a facility that has the proper devices to test the insertion tube and inner channels for air leaks. Make sure you confirm that the service facility

FIGURE 1-14. Inspecting flexible bending rubber.

FIGURE 1-15. Passing biopsy forceps through instrument channel.

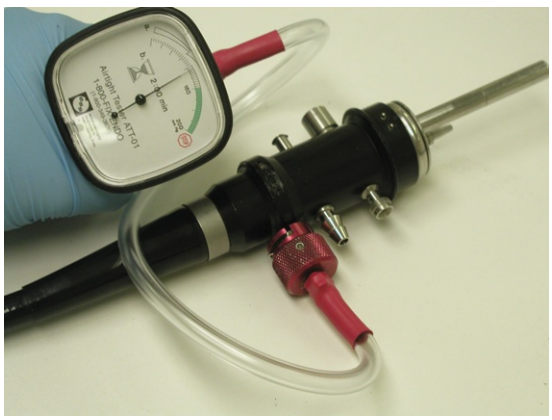

FIGURE 1-16. Leak testing instrument.

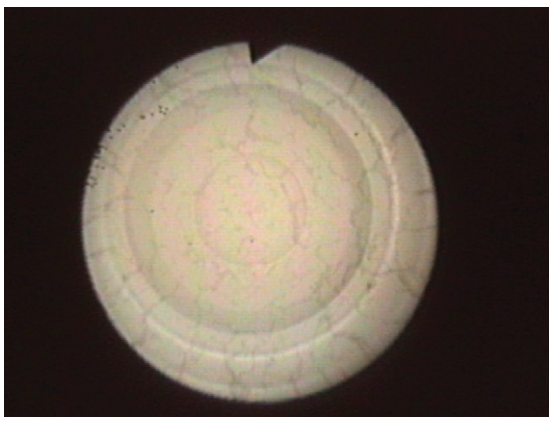

FIGURE 1-17. Fluid-damaged endoscope: note the blurred image caused by water leakage.

has these capabilities before sending in your scope. Only a small number of companies offer this type of equipment testing on older instruments. Note that a small pinhole can destroy an endoscope.

ACCESSORIES

Biopsy and Grasping Forceps

The various styles of forceps and graspers that are available for passage through the instrument channel are shown in Figures 1-18 to 1-25.

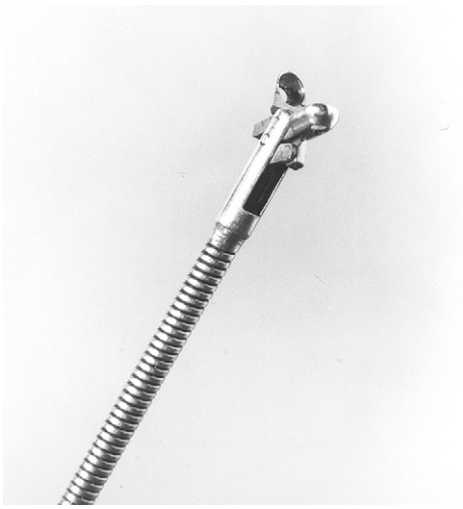

FIGURE 1-18. Standard fenestrated cup biopsy forceps.

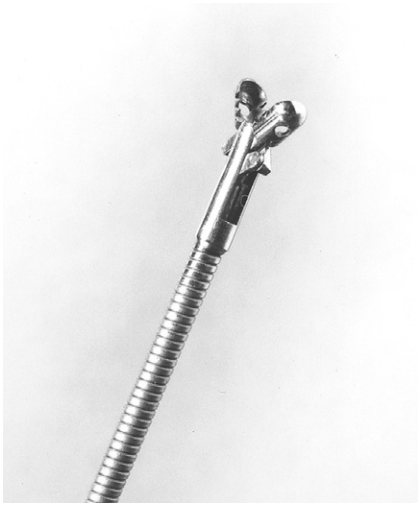

FIGURE 1-19. Serrated fenestrated cup biopsy forceps.

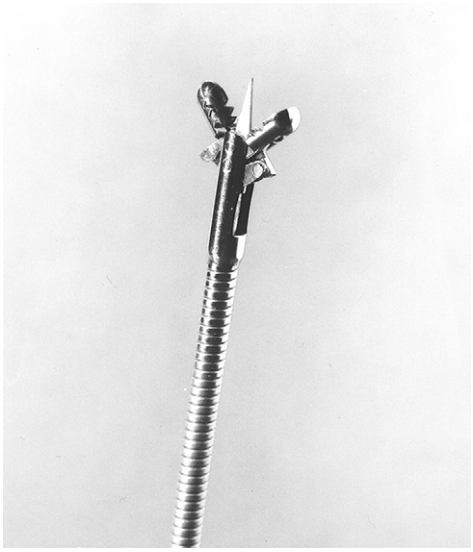

FIGURE 1-20. Serrated fenestrated cup biopsy forceps with needle.

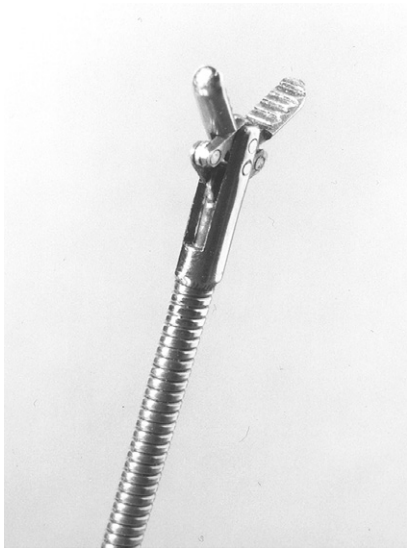

FIGURE 1-21. Alligator grasping forceps.

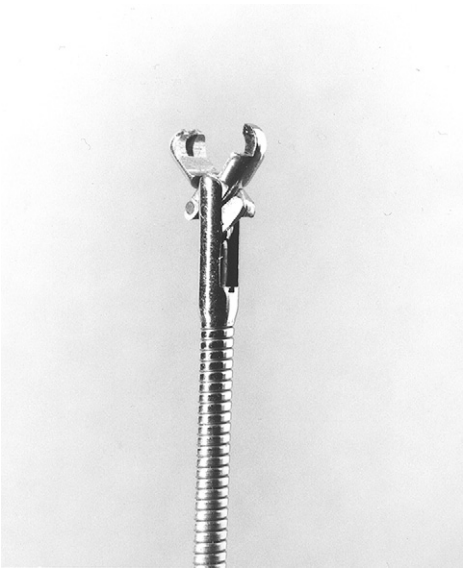

FIGURE 1-22. Rat tooth grasping forceps.

FIGURE 1-23. Forked jaw grasping forceps.

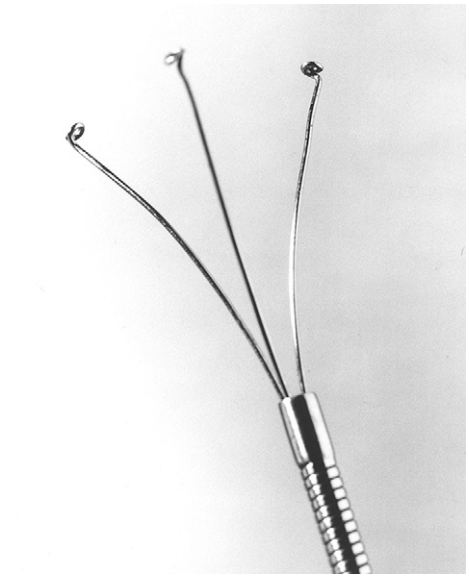

FIGURE 1-24. Tripod grasping forceps.

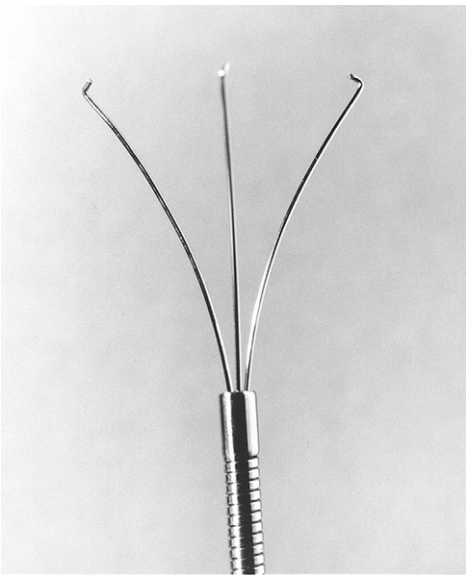

FIGURE 1-25. Three-prong grasping forceps.

Guttural Pouch Probes

The guttural pouch probe (Figure 1-26) is a nontraumatic tipped guide wire that facilitates easy navigation of the guttural pouch. When inserted through the scope and into the pouch, the probe enables the clinician to slide the scope forward over the wire into the guttural pouch.

CATHETERS AND NEEDLES

Various catheters for flushing and aspirating fluids are available. Simple aspiration catheters made of Teflon normally come in two sizes: 1.8-mm or 2.4-mm diameter. The length of these catheters is 240 cm, and they will fit any scope with a 220-cm or shorter working length. The catheters have standard luer fittings for use with a syringe. More advanced catheter systems are also available.

Double-Guarded Tracheal Aspiration Catheter

The double-guarded tracheal aspiration catheter (Figure 1-27) (EMAC800; Mila International, Florence, KY) enables sterile specimen retrieval via an endoscope. This set contains a glycol plug in the outer catheter to maintain sterility as the catheter is being advanced and an inner catheter for retrieval of the sterile specimen. It is ideal for sterile collection of fluid during a tracheal wash procedure.

FIGURE 1-26. Guttural pouch probe.

FIGURE 1-27. Double-guarded tracheal aspiration catheter.

Simple Aspiration Catheter

The single catheter (2.5 mm × 190 or 220 cm) with a female luer lock (EDC 190; Mila International) is used for medication delivery and sampling through an endoscope (Figure 1-28). It is ideal for guttural pouch lavage, respiratory area treatments, and any endoscope-accessible area. It contains a glycol plug in the tip for sterile sampling.

Lance Catheter

The endoscopic aspiration and injection needle (17-gauge; 2.5 mm × 190 cm) with a female luer lock (LAN190, Mila International) (Figure 1-29) is ideal for injecting ethmoid hematomas.

Guttural Pouch Catheter

This catheter (Mila International) is used for guttural pouch empyema (Figure 1-30).

Needles

Human sclerotherapy and transbronchial needles are very popular for injecting ethmoid hematomas and tumors. The needles could also be used to take aspiration samples of abscesses. These needles range in diameter and length; the most popular size is the 17-gauge needle with a 1-cm length.

CLEANING SUPPLIES

When using cleaning supplies, *ALWAYS* follow the manufacturer's cleaning instructions outlined in your equipment's specific instruction manual.

FIGURE 1-28. Simple aspiration catheter.

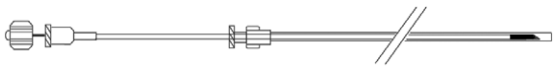

FIGURE 1-29. Lance catheter.

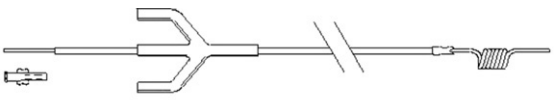

FIGURE 1-30. Guttural pouch catheter.

Leak Tester

The leak tester is the most important accessory item for use with the endoscope (Figure 1-31). The leak tester pressurizes the inside of submersible endoscopes to determine whether the scope is airtight before submersion in liquids. Fluid can cause severe damage if it leaks into the inner body of the endoscope. The best way to protect your investment is to perform a leak test on your scope after every use or before use in a procedure if the scope has been in storage for a long time.

If you detect a leak, contact the service department of an endoscopic repair company. The longer fluid remains in a scope, the worse the damage can become.

Channel-Cleaning Brushes

Channel-cleaning brushes come in various sizes and are available in reusable and disposable versions (Figure 1-32). The disposable version is the most economical because these brushes can be reused until the bristles look worn. Most disposable brushes come in packages of 10 or 20. To properly clean your scope it is important to use the correct size brush. Bristle diameter is important to effectively clean the channel without causing damage to the scope. If you are not sure what size brush your instrument requires, you should contact your scope vendor.

FIGURE 1-31. Leak tester.

FIGURE 1-32. Channel-cleaning brush exiting distal end.

Channel-Flushing Kits

New endoscopes always come with a standard set of cleaning accessories that include the cleaning brush and a channel-flushing kit. Most kits provide a syringe method for flushing fluids through the channel during cleaning and disinfection. However, most practitioners do not properly disinfect the biopsy channels.

Recently a suction-based cleaning product called the PSK cleaning kit has become available with prices ranging from $250 to $325, depending on the model of your endoscope (Figure 1-33). With these kits larger quantities of fluid are moved effectively through the instrument channels in much less time, making it easier to clean, rinse, and disinfect scopes.

Place the scope with the kit attached in enzyme detergent and turn on the suction unit until all of the instrument's channels are filled with detergent (Figure 1-34). For rinsing, lift the scope from the detergent and place it into a basin of clean rinse water. Turn on the suction again to facilitate a rinse cycle. The steps can be repeated with the disinfectant solution.

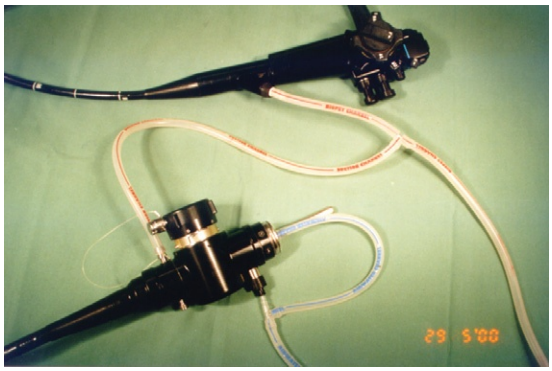

FIGURE 1-33. PSK cleaning kit.

FIGURE 1-34. Filling instrument channels with enzyme detergent.

FIGURE 1-35. Rinsing the endoscope.

FIGURE 1-36. Drying the endoscope with suction.

After the scope has soaked in the disinfectant for the prescribed time, rinse the scope again as explained in the previous paragraph (Figure 1-35). When you have finished cleaning the scope you can also use the PSK kit to dry the channels by keeping the kit attached and suctioning air through the channel (Figure 1-36).

TROUBLESHOOTING GUIDE

Table 1-1 is a troubleshooting guide for flexible endoscopes.

TABLE 1-1 Troubleshooting Guide for Flexible Endoscopes

Symptom	Possible Problem	Remedy
Image is not clear.	Dirty objective lens	Feed water to remove stool, mucus, and other debris from objective lens.
	Dirty eyepiece, camera, or adapter	Clean using cotton swab moistened with alcohol.
	Lens not adjusted to operator's eyesight	Rotate diopter adjustment ring until fiber pattern is clear.
	Internal fluid damage	Moisture within instrument will permanently cloud lenses in distal end or eyepiece (repair by manufacturer).
Image is too dark or too bright.	Dirty light guide	Clean light guide connector and distal tip using gauze moistened with alcohol.
	Improper light source settings	Adjust brightness control knob; check filter.
	Old or improperly installed lamp	Properly install lamp; replace old lamp.
Air or water feeding is absent or insufficient.	Air/water nozzle clogged	Soak distal end in warm, soapy water; feed water or enzymatic soap solution through air/water channels.
	Air/water nozzle missing or deformed	Send instrument for repair.
	Air/water valve dirty	Remove valve; clean and lubricate with silicone oil.
	Air pump not operating	Turn on switch on light source.
	Water bottle cap loose	Tighten cap.
No water is feeding.	Water bottle either empty or too full	Fill two thirds full.
Air/water valve is sticky.	Dirty valve	Remove valve; clean and lubricate with silicone oil.
Constant air is feeding.	Dirty air/water valve	Remove valve; clean and replace.
Suction is absent or insufficient.	Suction channel obstructed	Remove valve and pass cleaning brush through suction channels in both insertion tube and universal cord.
	Dirty suction valve	Remove valve; clean and lubricate with silicone oil.
	Leaky or improperly attached biopsy valve	Check and replace with new valve if necessary.

TABLE 1-1 Troubleshooting Guide for Flexible Endoscopes—cont'd

Symptom	Possible Problem	Remedy
Suction valve is sticky.	Dirty valve	Remove valve; clean and lubricate with silicone oil.
Resistance is present when rotating angulation control knobs.	Angulation valves engaged	Place locks in "free" position.
Tip deflection is not normal.	Amount of tip deflection less than specifications	Send instrument for repair.
Accessory does not pass through channel smoothly.	Bent or kinked forceps shaft	Discard and replace with new forceps; when inserting accessory, use repeated short strokes, grasping accessory close to biopsy valve.
Forceps does not operate smoothly.	Bent or kinked forceps shaft	Discard and replace with new forceps.
Camera cannot attach to fiberscope.	Improperly positioned auto focus pin on fiberscope eyepiece	Refer to instruction manual.
Camera fails to activate light source.	Dirty or bent electrical connection in adapter, eyepiece, or light guide connector.	Clean all contacts using cotton swab moistened with alcohol.
Exposure is incorrect.	Dirty contacts	Clean all contacts using cotton swab moistened with alcohol.
Image is blurred.	Dirty lenses	Clean objective lens, eyepiece lens, and adapter lenses using cotton swab moistened with alcohol.
	Water drops on objective lens	Feed air to remove water drops.
Color is incorrect.	Improper film	Use daylight-balanced film with xenon light sources; use tungsten-balanced film with halogen light sources.

From Tams TR, editor: *Small animal endoscopy*, ed 2, St Louis, 1999, Mosby.

ENDOSCOPE CLEANING

Always refer to the manufacturer's manual for specific cleaning/sterilizing instructions. Box 1-1 provides a checklist for cleaning waterproof endoscopes.

BOX 1-1 Endoscope Cleaning Checklist for Waterproof Endoscopes

1. If your scope is not waterproof, do not use this checklist. If you are not sure that your model is waterproof, consult manufacturer of your scope.
2. Use 4 × 4 gauze pad or equivalent dampened with Endozyme cleaning solution to wipe down insertion tube from insertion cone to distal end. (Endozyme is available from The Ruhof Corporation, Mineola, NY.)
3. Test endoscope to confirm that it is airtight (see Figure 1-16).
   a. If test fails, call endoscope service department about sending unit in for repair. Refer to list of service facilities at end of Chapter 1.
   b. If scope is airtight, continue with cleaning procedure.
4. Hook up to light source, water bottle with Endozyme cleaning solution, and suction unit; prepare 1× soaking tray with cleaning solution and 1× sink with clean water.
   a. Turn all equipment on.
   b. Pump cleaning solution through air/water line for 10 seconds.
   c. Pump air through air/water line for 10 seconds. Repeat steps B and C several times.
   d. Suction cleaning solution for 10 seconds, stop, and repeat second time.
5. Remove all valves (Figure 1-37) and soak entire unit in disinfectant solution for recommended soak time. (See your instrument's instruction manual for approved cleaning solutions.)
6. Use channel-cleaning brush (see Figure 1-32).
   a. Clean biopsy channel from biopsy port to distal end.
   b. Clean suction channel from suction valve housing to suction pump connector.
   c. Clean suction valve housing to distal end. (See instrument's manual for details.)
7. Using soft toothbrush or cotton swab, clean off distal end.
8. Rinse unit with clean water.
   a. Wash and rinse water bottle with clean water.
   b. Wash and rinse all valves.
   c. Wash and rinse instrument.
9. Reattach full hookup, light source, and suction unit, and water bottle filled with clean water.
   a. Reattach all valves.
10. Suction clean water for 15 to 20 seconds.
11. Spray clean air and water for 15 to 20 seconds.

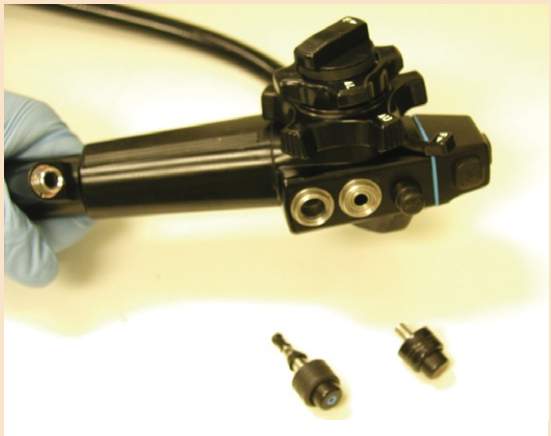

FIGURE 1-37. Removing valves.

BOX 1-1 Endoscope Cleaning Checklist for Waterproof Endoscopes—cont'd

12. Disconnect water bottle from light guide connector (Figure 1-38). While covering water bottle connector port on your instrument with your finger, depress water valve to purge air/water channel. (Scope must be plugged into light source with air pump "on" to purge.)
13. Wipe unit dry.
14. Remove air/water and suction valves. Rinse, dry, and lubricate the O-rings with silicone oil (Figure 1-39).
15. Clean lens with lens cleaner as needed.
16. Hang unit in designated storage area.
17. Soak, clean, rinse, and dry all accessories: channel-cleaning brush, forceps, retrievers, toothbrush, etc. (Lubricate forceps and retrievers with silicone.) Return these items to storage. Note that forceps, retrievers, and cleaning brush should be hung.

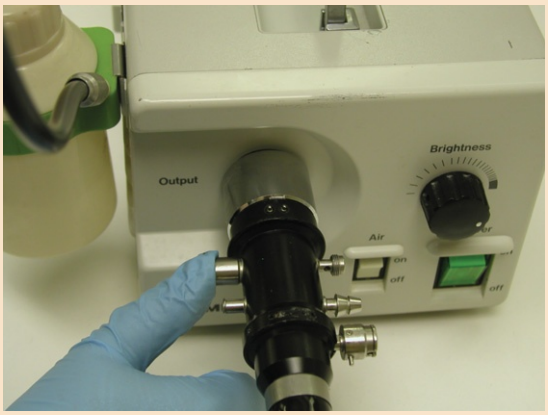

FIGURE 1-38. Depressing water valve.

FIGURE 1-39. Silicone oil.

ENDOSCOPE STORAGE

The preferred storage method for endoscopes is a hanging position with the insertion tube straight. This prevents liquid from settling in the channel and prevents the insertion tube from becoming wavy from prolonged storage inside the case. Forceps and retrievers should also be stored in a hanging position (Figure 1-40).

Damage

Torn Bending Rubber. The articulating portion of the scope is covered with a thin rubber skin commonly referred to as the "bending rubber." This skin can be punctured or torn, causing the scope to lose its watertight seal (Figure 1-41). Always carefully inspect bending rubber of your scopes for damage. It should be tight to the scope and should not look loose or worn.

Fluid Invasion. Fluid invasion happens when the watertight seal of the scope has become compromised, and the scope is soaked in fluid without being properly tested for leaks first. Fluid invasion can cause many types of damage to your endoscope:

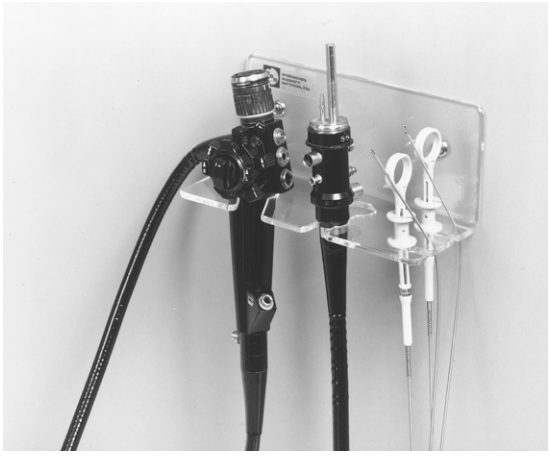

FIGURE 1-40. Storage method for endoscopes.

FIGURE 1-41. Torn bending rubber.

- In fiberoptic scopes fluid can cause irreparable damage to the optic fibers (Figure 1-42). This damage stains the image and the only recourse is to replace the optic fiber bundle in the scope. Note that the fiberoptic bundle is the most expensive part of the scope and that this type of repair can cost thousands of dollars.
- In video endoscopes fluid can damage the internal electronic components, causing the image to break up or display interference or change colors (Figure 1-43). In some cases fluid can cause the video chip to blow out entirely, requiring replacement of the chip.

Stretched Cables. Over time the angulation control cables that run down the inside of the insertion tube may become stretched. As this happens, you will experience a reduction in the angulation range of the scope. Regular maintenance of the scope should include tightening of these cables. If you fail to maintain the cables, they will eventually break.

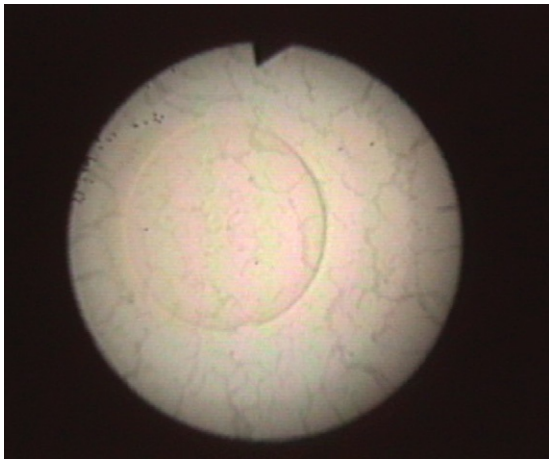

FIGURE 1-42. Damage to optic fibers.

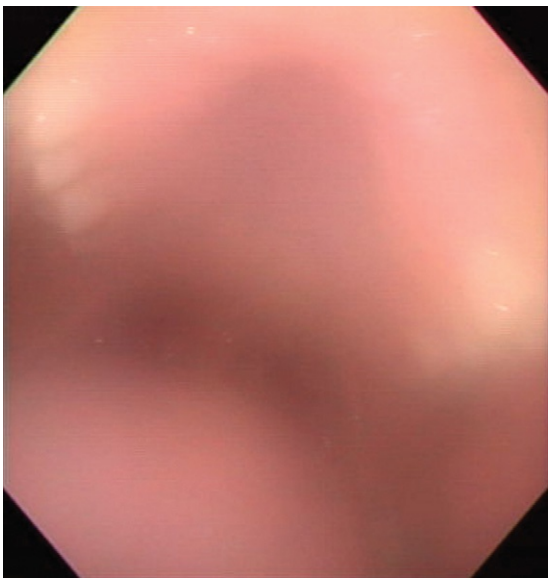

FIGURE 1-43. Fluid causing the image to blur.

Broken Cables. Putting too much torque or pressure on the endoscope with the control knobs can cause the cables that control the angulation of the endoscope to snap. When the cable is broken, the scope will not be able to be turned in the direction the cable controlled.

Bite Damage. It is not uncommon for the bending section of the scope to turn on itself when gastroscopy is performed if the patient does not want to swallow. The scope will accidentally end up in the oral cavity and can be damaged (Figure 1-44). To prevent this, one should lock the control knobs of the scope when passing it into the esophagus and visualize the passage of the scope. If you cannot see where the scope is going, then *STOP* and back up the scope until you can identify where the scope tip is located.

Ruptured Channel. When passing instruments through the scope's biopsy channel, you may encounter some resistance. Never force the instrument because this could cause the internal channel to rupture. Instead, when resistance is encountered, reposition the tip with the control knobs until the instrument can pass. If you encounter an unusually high amount of resistance, it may be the result of a kinked channel or poor cleaning of the instrument.

Kinked Channel. Kinks can develop in the channel wall, causing resistance when instruments are passed. If you suspect the presence of a kink in the channel of your instrument you should send it into a repair center before the site of the kink becomes worn away, causing a rupture in the channel.

Broken Light Guides. Light guide bundles transmit the light needed for visualization into the patient. If the light guide fiber is broken, it can no longer transmit light. If you look through the scope and find the image to be dark, this could indicate that the instrument has a high concentration of broken light guide fibers. As the percentage of broken light guide fibers increases, the ability of the scope to transmit light is lowered.

FIGURE 1-44. **A** and **B,** Crush damage to the distal end. Caused by accidentally entering the scope into the oral cavity during gastroscopy.

Smashed Lenses. When you handle the scope, always be aware of the location of the distal tip. If possible, hold it in your free hand when it is not in the patient. Letting the tip swing freely could result in its banging against objects. This type of trauma to the instrument can smash the distal end lenses, causing loss of the image or the ability to transmit light.

VIDEO ENDOSCOPE MANUFACTURERS

The following companies manufacture video endoscopes:

Olympus America Inc., 2 Corporate Center Drive, Melville, NY 11747; 1-800-848-9024

Pentax Precision Instrument Corporation, 30 Ramland Road, Orangeburg, NY 10962-2699; 800-431-5880, 845-365-0700, fax: 845-365-0822, 1-800-848-9024

Fujinon Inc., 10 Highpoint Drive, Wayne, NJ 07470; 1-800-872-0196

Welch Allyn Inc., 4341 State St., Skaneateles Falls, NY; 1-800-535-6663

CHAPTER 2

Endoscopic Documentation

JAMES BURNS

Advances in computer technology and video printers have made documentation of images easy.

VIDEO PRINTERS

The video printer grabs a single frame of video and prints it as an image. The most popular manufacturer of video printers is Sony. Sony offers a host of video printers that create printed images in all different sizes. The average cost per print (sheet of print paper) ranges from $.50 to $2, depending on the model of the printer and the size of the print.

The newer Sony printers, such as the one pictured in Figure 2-1, print images in about 30 seconds. The newer units also use lower-cost media, making the cost per print about one half the cost of prints created with some of the older printers, which also take much longer to print pictures.

Some video printers, such as the DPP-SV88 in Figure 2-2, also save the image in a format for use in a computer. This unit will save the captured images to a compact disc (CD) or a Sony Memory Stick as JPEG images.

Used video printers are available on the market. For some of the older units print media and paper are becoming difficult to find. Items to be aware of when buying a used printer include the following:

- Where was the printer used before your purchasing it? If the unit was in a hospital in which hundreds of procedures were performed per week, then the life expectancy of the unit's thermal print head will be short. Printers do not keep

FIGURE 2-1. Sony UP-21MD video printer.

track of the number of prints produced. As a buyer you will have no idea how often the printer was used.
- Does the original manufacturer still support the product if it requires service?
- Will print media and supplies be available for the unit long term and at what cost? *NOTE:* A new printer may use lower-priced print media and supplies than an older unit; thus over time a used unit could cost more than purchasing a new unit.

DIGITAL IMAGE CAPTURE

New, faster, and higher-quality storage solutions are emerging daily. The consumer sector offers a host of digital image acquisition and storage solutions such as digital photography cameras and video frame grabbers designed to capture pictures and video from your camcorder or TV.

Many systems output video as an analog video signal. To capture images digitally, the signal is converted by the capture device and saved in a binary format that can be stored electronically.

Once images are in electronic format the possibilities for use are endless. Images can be manipulated or enhanced to point out lesions not easily recognizable. Annotations such as arrows or labels can be placed on the image to bring specific details to the attention of referring practitioners or clients.

There are devices on the market that have been designed for medical and veterinary practice. We present a few of these products here to give you an idea of the features that are available with this type of equipment.

The UPA-P100MD (Figure 2-3) is a medical-grade unit designed to capture and digitize analog images from an external video device. Up to 15,000 images or 15 hours of video can be stored on the internal hard disc drive and are accessible

FIGURE 2-2. Sony DPP-SV88 video capture unit/printer.

FIGURE 2-3. Sony UPA-P100MD digital capture unit.

via a hospital's digital computer network. These images can then be sent to a printer or recorded on CD-R media, from which they can be incorporated into PowerPoint presentations, attached to e-mails, and inserted into medical reports.

Equipped with a built-in CD-R drive, the UPA-P100MD records the images and video stored on the hard disc drive onto CD-R media. CD-R is widely used as recording media for PCs, so you can view the images recorded on a CD-R on your PC easily without special software. When images and their associated information are recorded onto a CD-R, they are unalterable, thus avoiding problems such as overwriting.

Images are automatically saved in three digital image formats: TIFF, JPEG, and MPEG-4. The noncompressed TIFF format is an ideal image recording format when picture quality is a priority. The TIFF format provides easy transfer of the images to DICOM systems that usually require a noncompressed image format. The JPEG compression format is used for viewing images from an Internet browser. Motion images are recorded in the MPEG-4 format.

Equipped with a SCSI port, the UPA-P100MD can be connected to the UP-D50 digital color printer or the UP-D70XR digital color/monochrome printer. The images stored in the UPA-P100MD can be directly printed with great speed at high quality.

By connecting to a PC, the images stored on the UPA-P100MD hard disc drive can be viewed from the PC's Internet browser. One monitor can display both index images and an enlarged image selected from the index images for easy and quick viewing. By connecting to a network, the images stored on a hard disc drive can be viewed by multiple users and from multiple places throughout a network.

i-Cap from Endoscopy Support Services, Inc. (Brewster, NY), was designed specifically as a simple-to-use system for veterinary practice. i-Cap allows you to capture images and video clips directly onto a computer hard drive from any endoscopic video camera or external video source such as an ultrasound or microscope camera.

The i-Cap package includes a CD with the i-Cap software, a universal serial bus (USB) device that acts as a bridge between the computer and your video camera and a foot pedal for hands-free capture of images (Figure 2-4). Simply load the software into your computer; hook up your camera and foot pedal and the result is a simple image-capture and report-writing system.

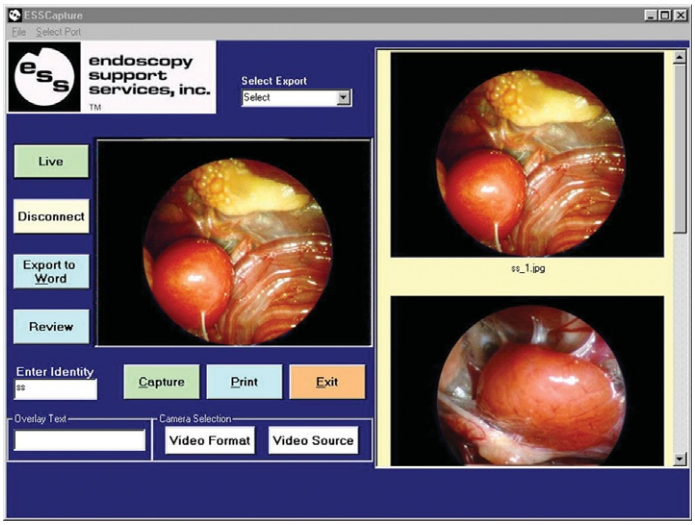

FIGURE 2-4. Screen shot from i-Cap image capture software.

ENDOSCOPY

Hagyard-Davidson-McGee Associates, P.S.C.
Veterinarians
Equine Internal Medicine Hospital
4250 Iron Works Road
Lexington, KY 40511-8412

Phone: (859) 258-0002 Fax: (859) 259-9202

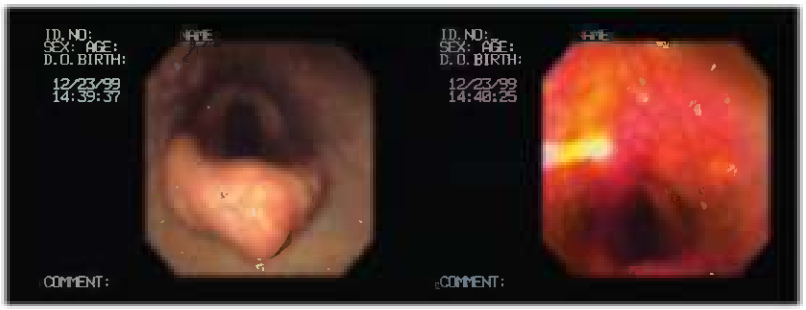

Doctor:

Owner/Farm:
Patient's Name:
History:

Procedures:

Diagnosis:

Medication (s):

Diet:

Exercise:

Special Instructions:

Follow-up Appointment: Date & Time:

Please call the hospital if you have any questions or concerns regarding these instructions.

FIGURE 2-5. i-Cap report.

i-Cap catalogs images and video clips by patient identity for later review, reporting, e-mailing, or printing. The system also offers an image export feature that allows you to place images directly into report templates (Figure 2-5) that you create in Microsoft Word. A sample template is included with the system.

System requirements for i-Cap are the following:

- Pentium II 350MHz PC with 64MB memory
- USB port for capture device
- CD-ROM drive for software installation
- Serial port for foot pedal.
- Microsoft Word 5.0 or higher for reporting

DIGITAL VIDEO AND CAPTURE SOLUTIONS

If you wish to capture video as well as still images, then consider the Sony GV D-1000 digital video (DV) recorder with still image capture (Figure 2-6). The GV D-1000 is a compact and portable DV Walkman for playing, recording, and editing DV footage. Use mini-DV cassettes and or a Sony Memory Stick to capture images or MPEG videos. You can edit or play back your captured movies anywhere and at any time, even through your PC. Edit your still or moving videos with USB Image Capture and

FIGURE 2-6 Sony GV D-1000 Digital Video Recorder.

ImageMixer software, one of Sony's latest digital editing functions. The GV D-1000 makes it easier than ever to edit as a side-by-side companion to your mini-DV camcorder. Alternatively, you can use the GV D-1000 as a video cassette recorder (VCR) and connect it to any television to play back your videos. In addition, the GV D-1000 incorporates a 4-inch LCD monitor for clear, crisp color images for client playback without the need to hook it up with cables to a monitor.

Key features of the GV D-1000 are the following:

- Video: DV format offers up to 500 lines of horizontal resolution and significantly higher signal-to-noise ratio to provide stunning video performance.
- i.LINK: DV in/out (IEEE 1394) lets you edit or dub between another digital camcorder, VCR, or computer equipped with a DV capture card, with virtually no generation loss.
- Digital program editing: The built-in assemble editor lets you mark cut-in and cut-out points for up to 20 separate scenes. Use the Walkman as your source while controlling via infrared almost any remote-capable camcorder or VCR as your recorder.
- Audio: Record PCM digital audio in two modes: 16-bit mode for CD-quality stereo sound on one track, or 12-bit mode for stereo on two tracks so you can add background music or voice-overs.
- LCD: A 4-inch color LCD screen with active matrix technology is incorporated to provide clear, accurate colors for on-the-spot playback of recordings.
- Analog in/out: Increasing your creative possibilities, analog in/out makes it possible to connect your video Walkman to a range of analog devices.
- Control L: A LANC interface for synchronized editing with other Control L–equipped devices is provided.
- USB terminal: USB is a computer industry standard that is designed to simplify interconnection between digital equipment such as audiovisual devices and computers. It makes quality, higher-volume data transfer possible between your video Walkman and PC, printer, or other equipped device via a simple, one-cable connection.

TABLE 2-1 Recording Time on Memory Stick Storage Media

	128MB	64MB	32MB	16MB	8MB	4MB
160 × 112	85 min 20 sec	42 min 40 sec	21 min 20 sec	10 min 40 sec	5 min 20 sec	2 min 40 sec
320 × 240	21 min 20 sec	10 min 40 sec	5 min 20 sec	2 min 40 sec	1 min 20 min	40 sec

TABLE 2-2 Number of Images Stored on Memory Stick Storage Media

VGA (640 × 480)	28MB	64MB	32MB	16MB	8MB	4MB
Standard	1970*	980*	485*	240*	120*	58*
Fine	1310*	650*	325*	160*	80*	39*

*Approximate images.

- USB image capture: This function lets you stream live and recorded moving images to your PC via the USB port.
- *NOTE:* The GV D-1000 includes Image Mixer for Sony software by Pixela, which captures both still and moving images from your camera to your PC. It lets you drag and drop movie materials (i.e., MPEG files, transition patterns, and audio files), set in and out editing points, and combine edited materials into one movie.
- Memory Stick slot: The Memory Stick, Sony's digital storage medium, allows flexible storage of still or moving images, as well as digital audio and other text or command information. The Memory Stick provides a quick and easy transfer from your DV Walkman to a PC, editing device, printer, or display system and back again.
- MPEG movie: MPEG movies can be captured onto Sony's Memory Stick media with the GV D-1000 (Tables 2-1 and 2-2).

VIDEO TAPING

In addition to recording video in DV format, connecting an analog VCR to your system is also an option. VCRs can be acquired at most local video electronics stores.

Combined TV/VCR units are also available for use with your endoscopic video system or video camera. Be careful, however, when purchasing a TV/VCR combination unit because the resolution on most of these units is very low. Panasonic offers a line of combination monitor/TV/VCR units with a monitor function that offers higher resolution than that of a traditional TV/VCR. Models with these features from Panasonic include the AG-513 and AG-520.

CHAPTER 3

Rhinoscopy

NATHAN M. SLOVIS

NORMAL ENDOSCOPIC ANATOMY

The nasal cavity extends from the nostril to the caudal aspect, the choana, which "exits" into the nasopharynx (Figures 3-1 and 3-2).

Most of the nasal septum separating the two halves is a plate of cartilage that fits into the trough of the vomer ventrally to the perpendicular plate of the ethmoid bone *(arrows)* caudally. A highly vascular and glandular mucous membrane covers the nasal septum (Figure 3-3).

The dorsal and ventral conchae form delicate scrolls. The space enclosed within each is divided into two compartments by an internal septum. The caudal part of the dorsal concha comprises the rostral continuation of the frontal sinus, forming the

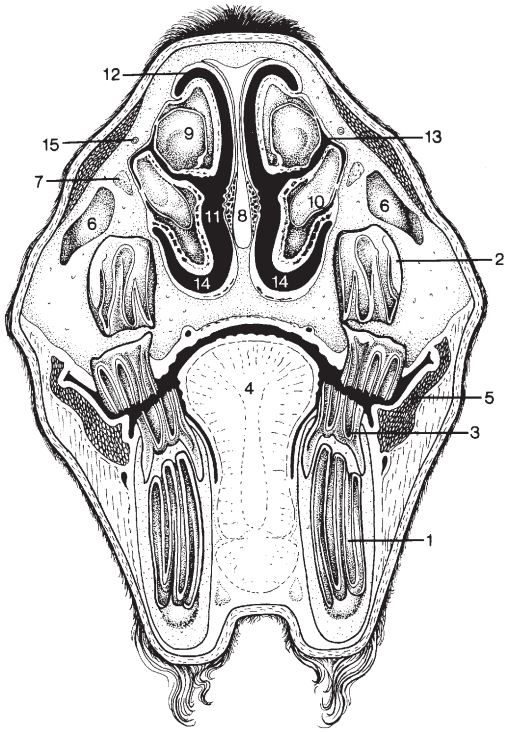

FIGURE 3-1. Transverse section of the head at the level of the rostral maxillary sinus. *1,* P_4; *2,* P^4; *3,* p_4; *4,* tongue; *5,* buccinator; *6,* rostral maxillary sinus; *7,* infraorbital nerve; *8,* nasal septum; *9,* dorsal nasal concha; *10,* ventral nasal concha; *11,* common nasal meatus; *12,* dorsal nasal meatus; *13,* middle nasal meatus; *14,* ventral nasal meatus; *15,* nasolacrimal duct. (From Dyce KM et al: *Textbook of veterinary anatomy,* ed 3, Philadelphia, 2002, WB Saunders.)

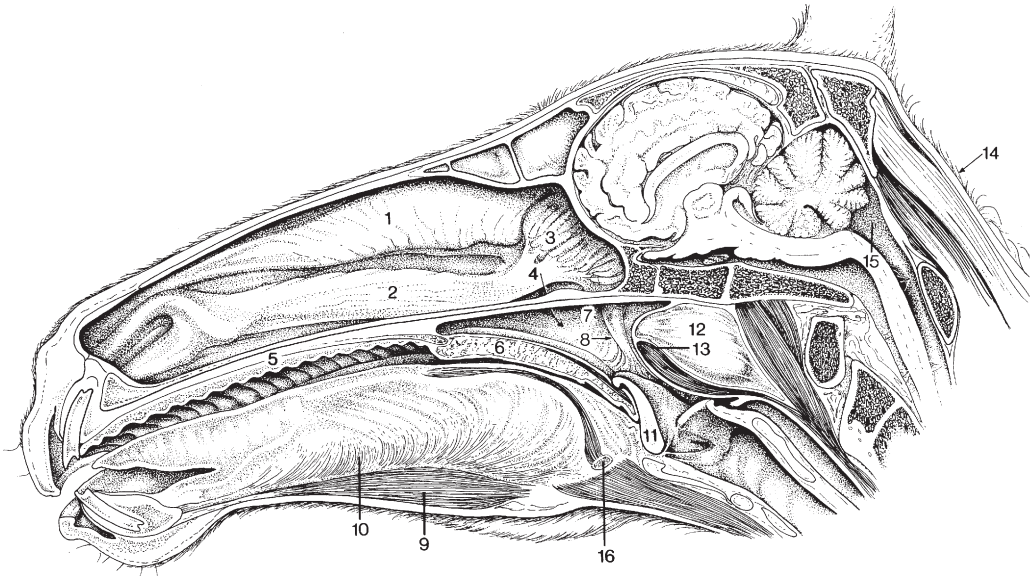

FIGURE 3-2. Median section of the head; most of the nasal septum has been removed. *1,* Dorsal nasal concha; *2,* ventral nasal concha; *3,* ethmoidal conchae; *4,* right choana *(arrow)*; *5,* hard palate with prominent ridges (rugae); *6,* soft palate; *7,* nasopharynx; *8,* pharyngeal opening of auditory tube; *9,* geniohyoideus; *10,* genioglossus; *11,* epiglottis; *12,* medial wall of guttural pouch; *13,* pharyngeal muscles; *14,* site for tapping the cerebellomedullary cistern; *15,* cerebellomedullary cistern; *16,* basihyoid. (From Dyce KM et al: *Textbook of veterinary anatomy,* ed 3, Philadelphia, 2002, WB Saunders.)

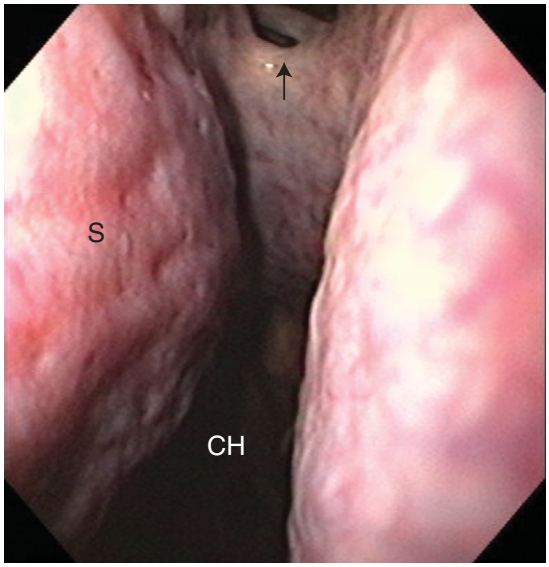

FIGURE 3-3. *CH,* Choana; *S,* septum; ethmoid bone *(arrow).*

combined conchofrontal sinus. The caudal space within the ventral concha communicates with the rostral maxillary sinus.

The dorsal concha extends from the cribriform plate of the ethmoid bone and extends to the nostril (Figure 3-4).

The ventral concha is shorter than the dorsal concha and extends rostral from the level of the last molar to the level of the first cheek tooth (Figure 3-5).

The conchae divide the cavity into four meatuses: dorsal, middle, common, and ventral. The dorsal meatus is the narrowest, bound dorsally by the roof of the nasal cavity and ventrally by the dorsal concha (Figure 3-6).

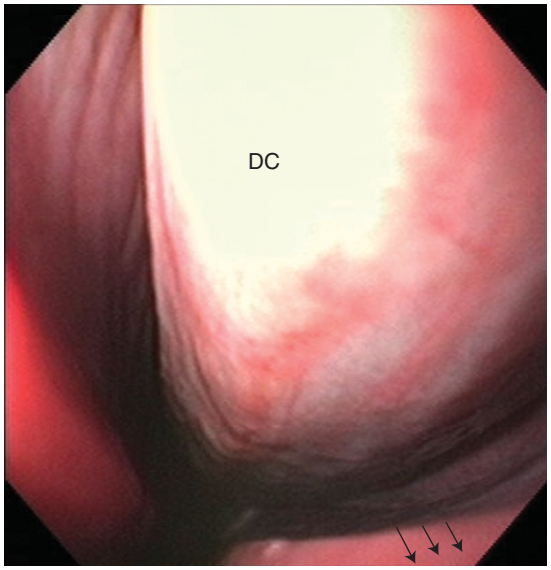

FIGURE 3-4. *DC,* Dorsal concha; ventral concha *(arrows).*

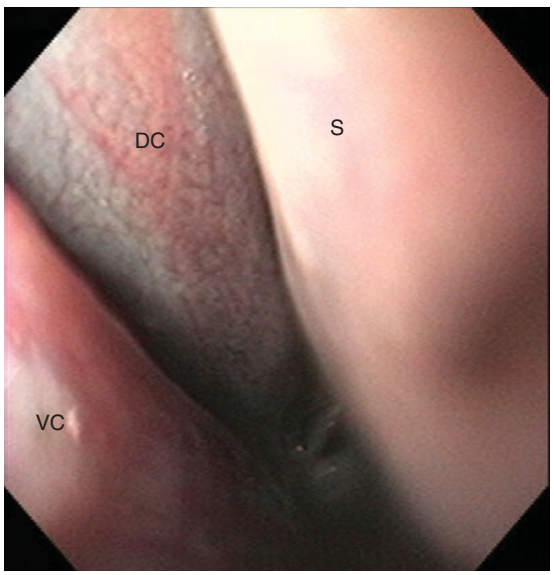

FIGURE 3-5. *DC,* Dorsal concha; *S,* septum; *VC,* ventral concha.

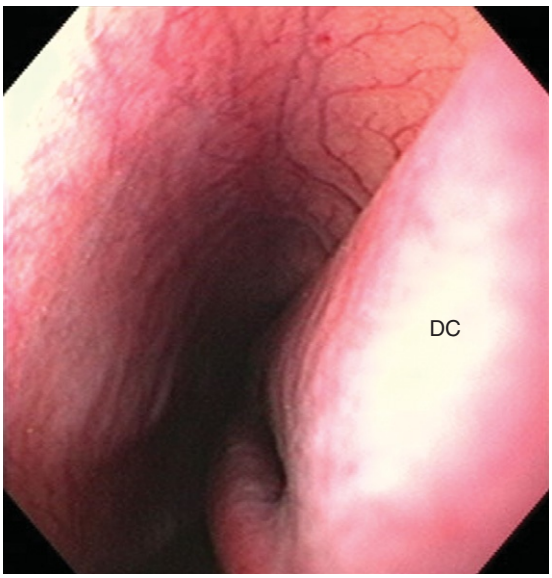

FIGURE 3-6. Dorsal meatus. *DC,* Dorsal concha.

The middle meatus lies between the dorsal and ventral concha. The communication between the nasal cavity and maxillary sinus (nasomaxillary opening) is in the caudal part of the middle meatus. The common meatus is the space between the nasal septum and the conchae and between the roof and floor of the nasal cavity (Figure 3-7). The ventral meatus is the widest meatus that is situated between the ventral concha and the floor of the nasal cavity from the nasal vestibule to the choana leading to the nasopharynx (Figure 3-8).

Among the numerous ethmoid turbinates of the labyrinth, the great ethmoid turbinate (endoturbinate I) *(large arrow)* contains a sinus. This sinus communicates with the maxillary sinus (Figures 3-9A and B). Endoturbinates II, III, and IV are the visible structures of the ethmoid bone (Figure 3-10).

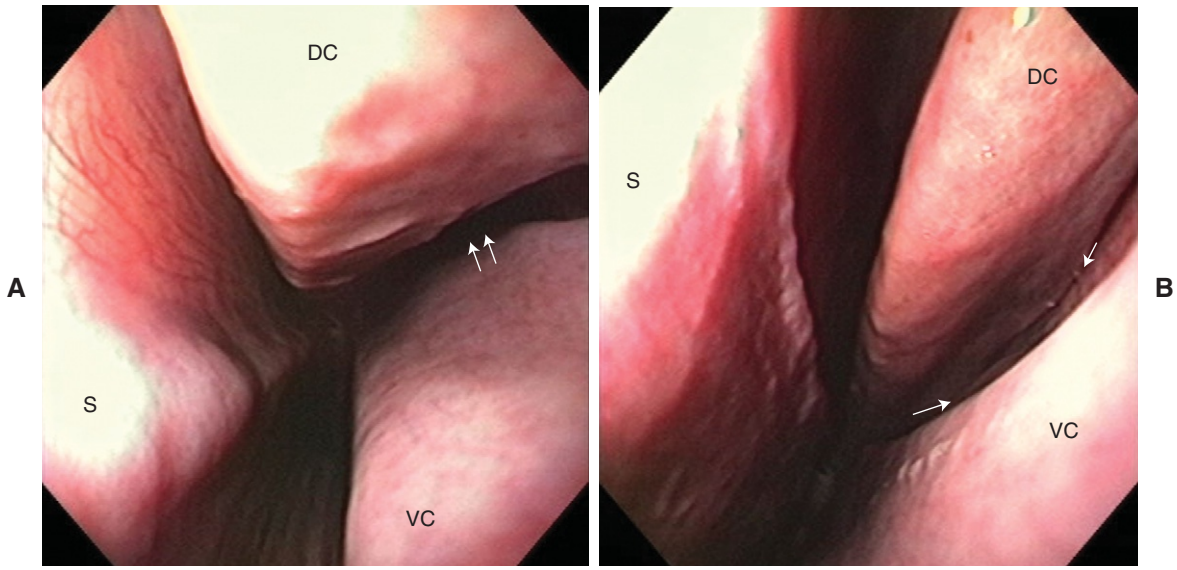

FIGURES 3-7. **A** and **B,** Left rhinoscopy in common meatus. *DC,* Dorsal concha; *S,* septum; *VC,* ventral concha; middle meatus *(arrows).*

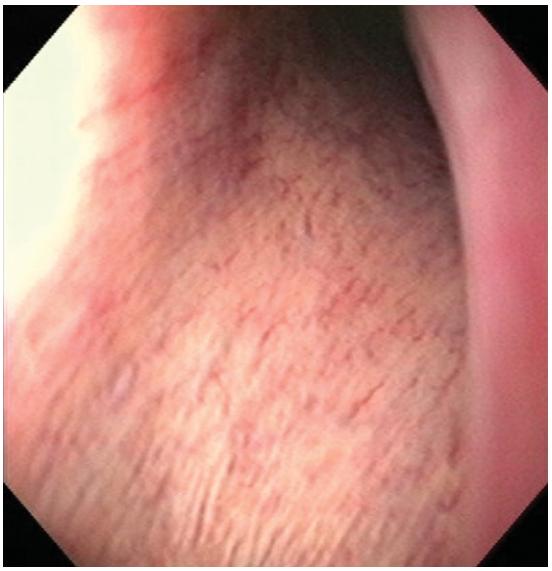

FIGURE 3-8. Ventral meatus.

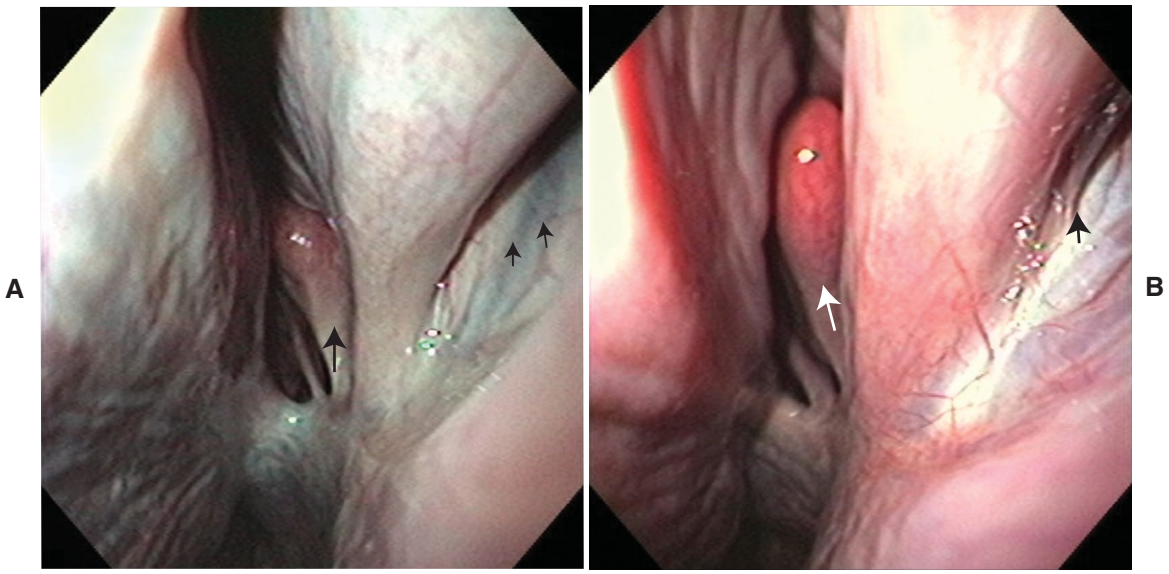

FIGURE 3-9. **A,** Endoturbinate I *(large arrow),* and the left nasal maxillary opening located in the middle meatus *(small arrows).* **B,** Ethmoid turbinates. Middle meatus *(black arrow).* Endoturbinates I *(white arrow).*

FIGURE 3-10. Ethmoid turbinates.

ETHMOID HEMATOMAS

A progressive ethmoid hematoma (PEH) is an expansive mass of unknown etiology that originates in the submucosa of the ethmoid labyrinth of horses. PEHs can be unilateral or bilateral on occasion and can even be located in the paranasal sinuses or nasal cavity. These masses tend to be locally destructive and highly vascular in structure. Older horses are most often affected, but horses of any age may develop an ethmoid hematoma. Noise on respiration and mild intermittent unilateral nasal discharge or epistaxis are the most commonly observed clinical signs. Figures 3-11 through 3-15 illustrate the typical greenish coloration. Figure 3-14 shows an early-stage ethmoid hematoma noted in a 19-year-old gelding with a history of chronic mucoid nasal discharge. The PEH enlarges along the path of least resistance, either rostrally within the nasal cavity or caudally into the nasopharynx (Figure 3-11B).

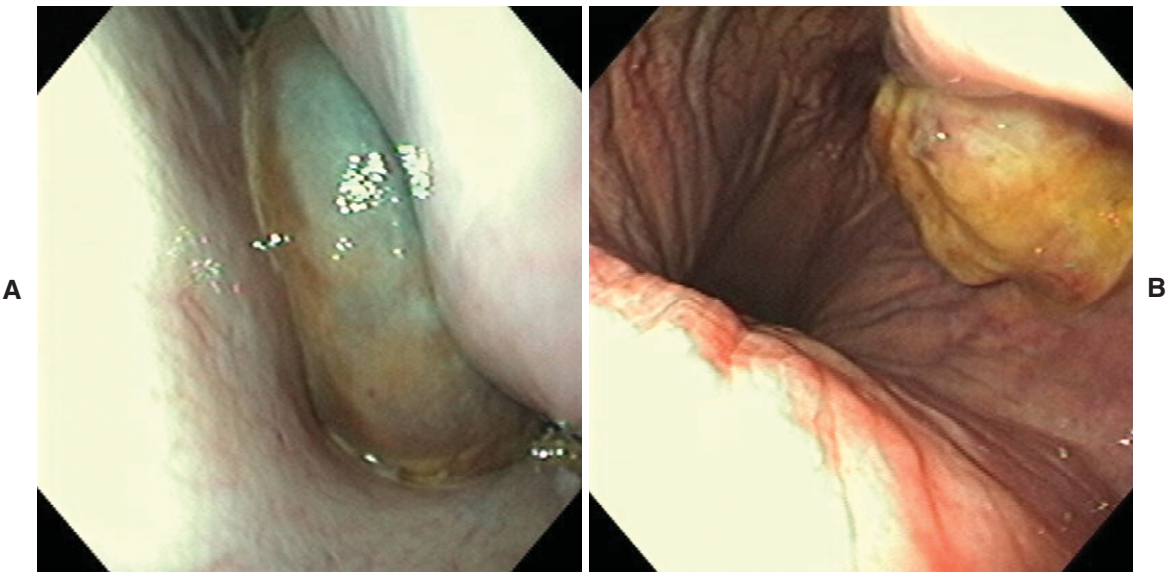

FIGURE 3-11. **A,** Ethmoid hematoma. **B,** Note hematoma extending into Nasopharynx.

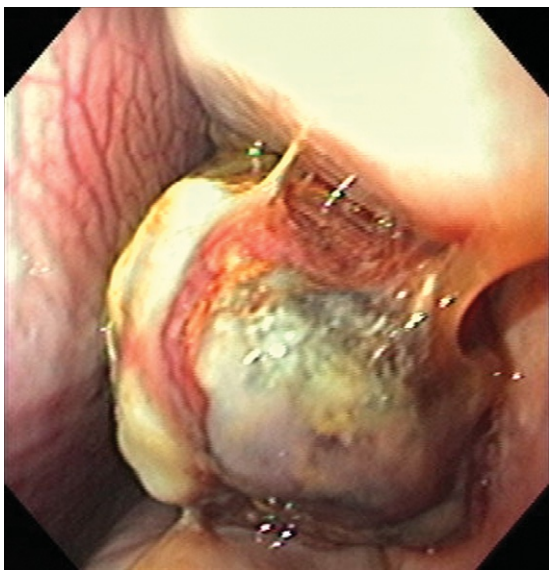

FIGURE 3-12. Ethmoid hematoma.

Intralesional injection of neutral buffered 10% formalin with repetition of injections at 14-day intervals has been used in the treatment of PEH (Figures 13-15 to 13-18). An early recurrence can be treated with a diode laser (Figure 3-19).

Aggressive hematomas can occlude both nasal passages (Figures 3-20 and 3-21).

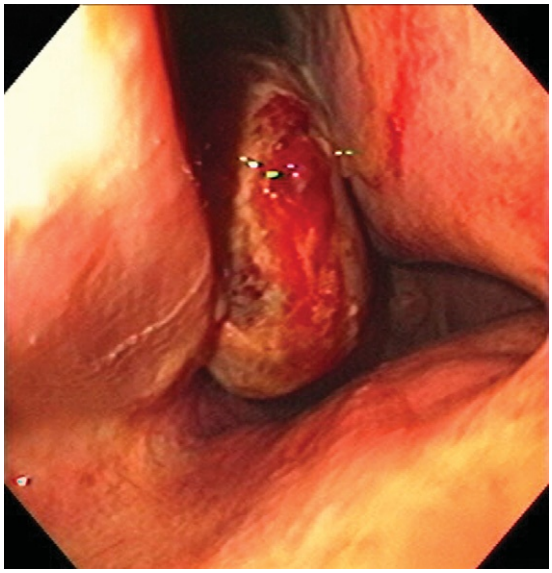

FIGURE 3-13. Ethmoid hematoma.

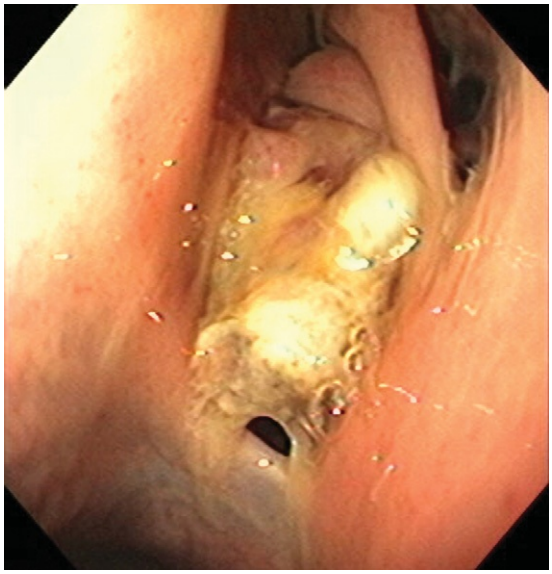

FIGURE 3-14. Ethmoid hematoma.

FIGURE 3-15. Injection of 20 ml of formalin in a 20-year-old mare with chronic serosanguinous discharge. Formalin was injected into the hematoma with use of a transendoscopic 14-gauge retractable needle (after topical administration of lidocaine). Injection is stopped whenever formalin is seen to leak out of hematoma or hematoma becomes rigid.

FIGURE 3-16. Hematoma becoming necrotic 2 weeks after injection. Lesion was injected again with 10 ml of formalin.

FIGURE 3-17. Shows 90% resolution of hematoma 2 weeks after second injection. Note that hematoma originated from ethmoid labyrinth. Hematoma also caused significant local destruction to create frontonasal fistula. Horse received one more injection of formalin and full resolution of mass was achieved.

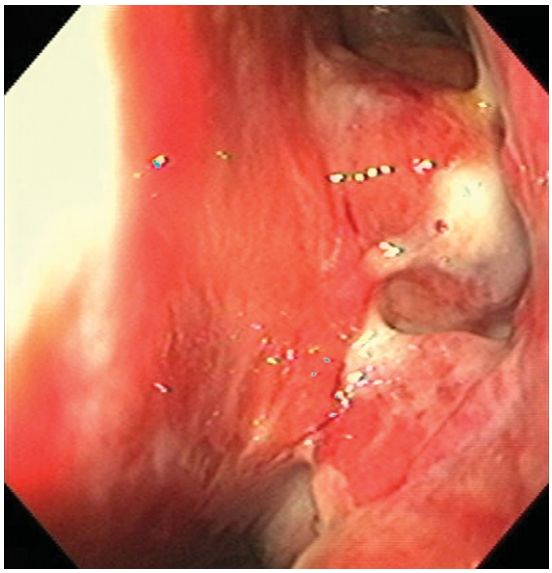

FIGURE 3-18. Complete resolution of ethmoid hematoma after eight formalin injections. Note destruction and remodeling of ethmoid turbinates.

FIGURE 3-19. Early recurrence of ethmoid hematoma 6 weeks after formalin injection. Note destruction of endoturbinate I (not present) because of pressure necrosis from previous ethmoid hematoma. This early-stage hematoma was successfully treated with diode laser.

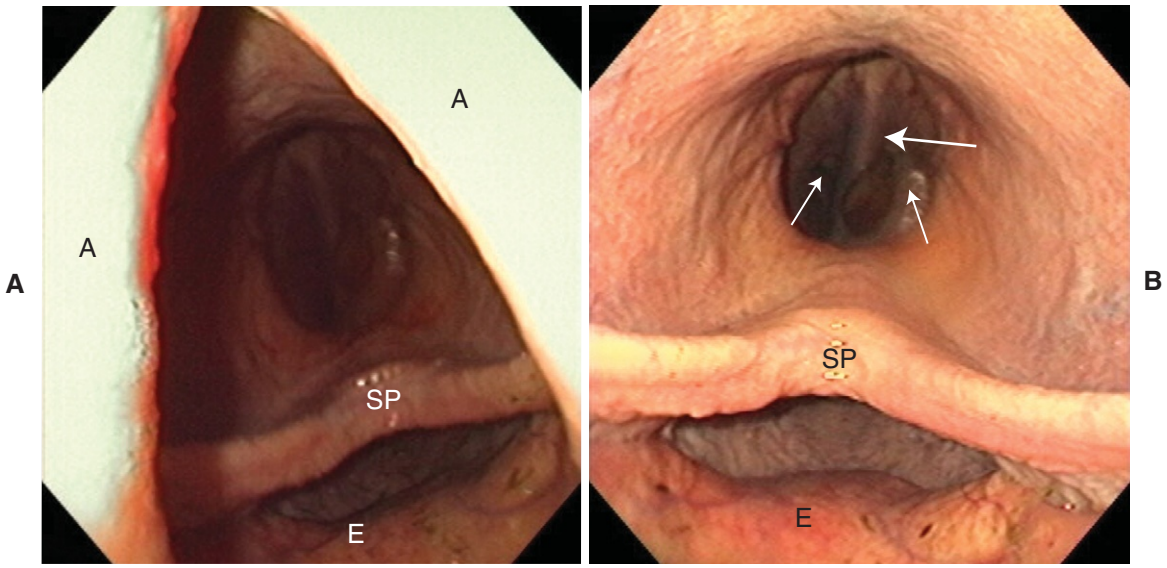

A B

FIGURE 3-20. **A,** and **B,** Pharyngoscopy through tracheostomy site of a 20-year-old Thoroughbred that had complete bilateral nasal occlusion from ethmoid hematomas *(small arrows).* Note dorsal displacement of soft palate. *A,* Arytenoids; *E,* epiglottis; *SP,* soft palate; nasal septum *(large arrow).* **B,** Nasopharyngeal view.

FIGURE 3-21. Close-up examination of nasal septum *(S)* of horse in Figure 3-20. Note aggressive nature of ethmoid hematoma involving and occluding both nasal passages.

NEOPLASIA

An early nasal adenocarcinoma is shown (Figure 3-22).

PHYCOMYCOSIS

Nasal fungal infections are uncommon in horses. Infection can occur in normal or traumatized tissue (Figures 3-23 through 3-29). Differential diagnoses for nasal granulomatous lesions include nasal neoplasms and nasal amyloidosis.

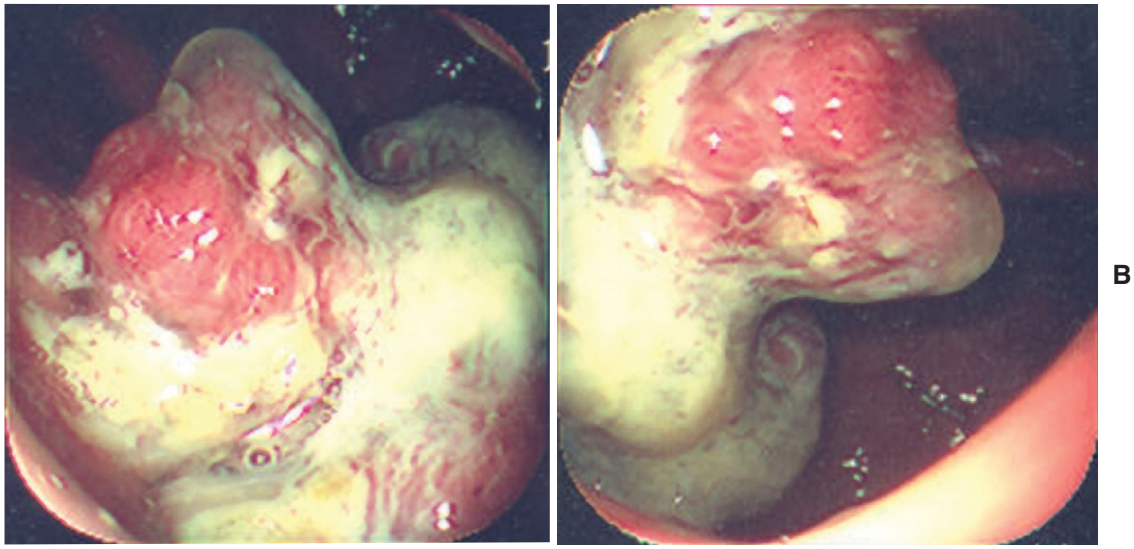

FIGURE 3-22. **A** and **B,** Fifteen-year-old quarter horse gelding with chronic right rhinorrhea. Rhinoscopy revealed a large mass in right common meatus. A biopsy was obtained and revealed adenocarcinoma.

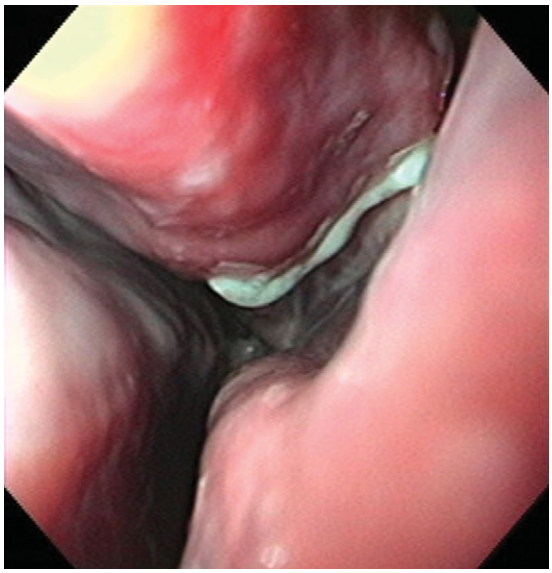

FIGURE 3-23. This 22-year-old gelding had a chronic left-sided nasal discharge for 3 weeks. A nasogastric tube had been placed 1 month previously to reflux distended stomach caused by strangulating lipoma. Biopsy of white plaque was obtained for cytologic examination. Fungal hyphae suggestive of *Aspergillosis* spp. were noted on slide. Plaques were débrided with a cytology brush. The horse was sent home on a regimen of oral ethylenediamine dihydroiodide and recovered uneventfully. Fungal rhinitis was caused by trauma from stomach tube placement.

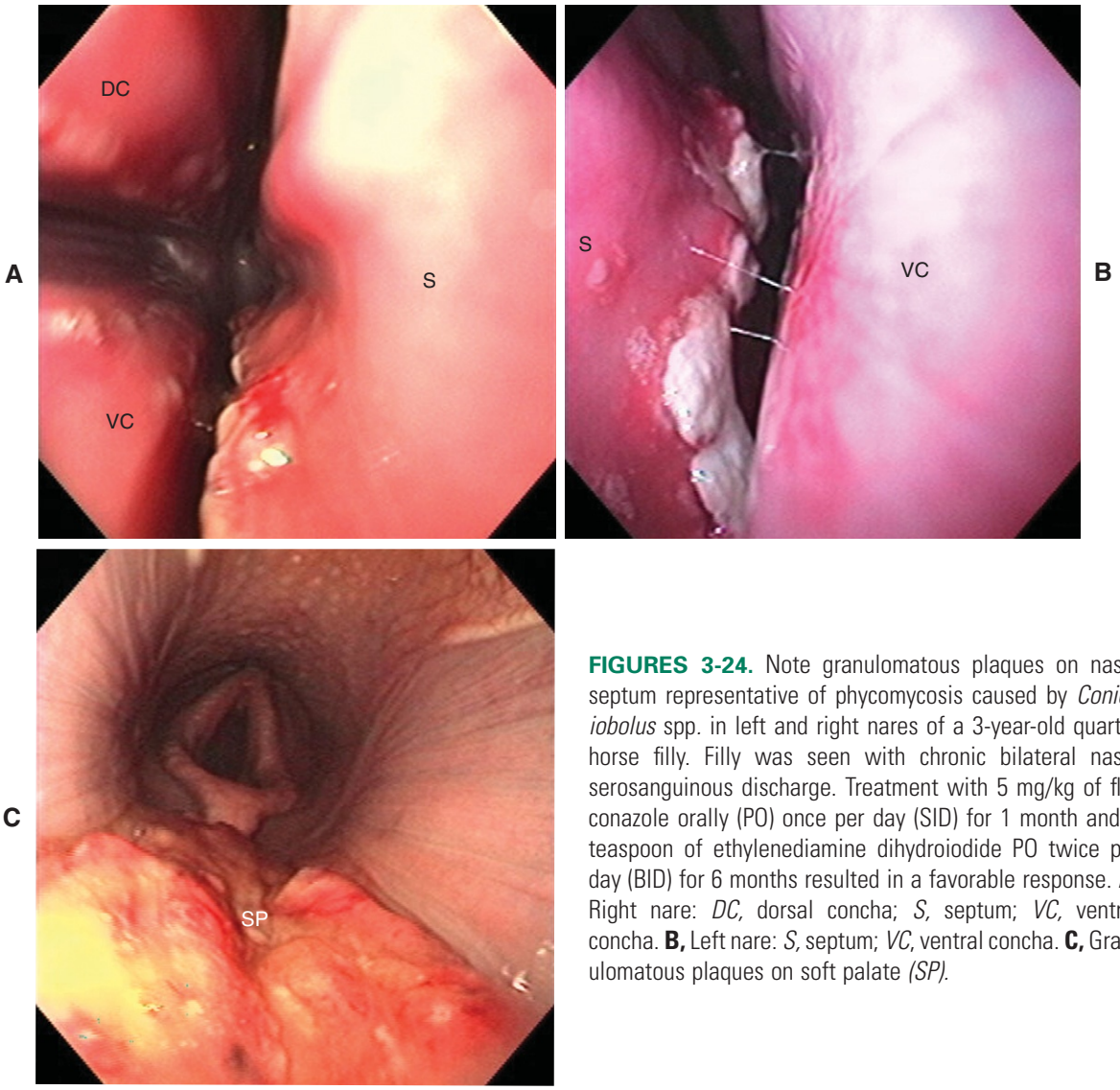

FIGURES 3-24. Note granulomatous plaques on nasal septum representative of phycomycosis caused by *Conidiobolus* spp. in left and right nares of a 3-year-old quarter horse filly. Filly was seen with chronic bilateral nasal serosanguinous discharge. Treatment with 5 mg/kg of fluconazole orally (PO) once per day (SID) for 1 month and 1 teaspoon of ethylenediamine dihydroiodide PO twice per day (BID) for 6 months resulted in a favorable response. **A,** Right nare: *DC,* dorsal concha; *S,* septum; *VC,* ventral concha. **B,** Left nare: *S,* septum; *VC*, ventral concha. **C,** Granulomatous plaques on soft palate *(SP).*

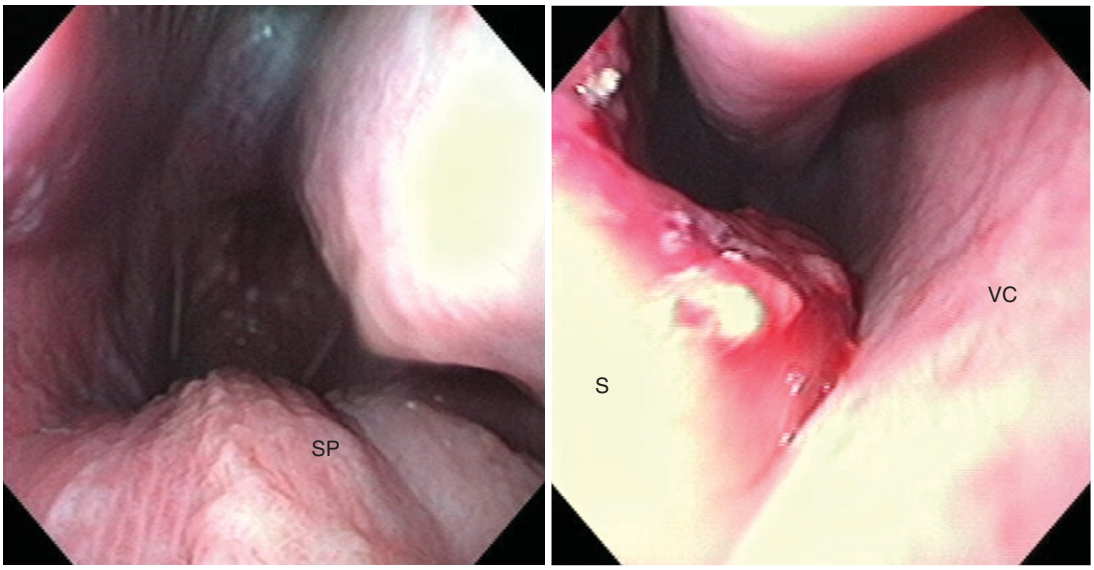

FIGURES 3-25. **A** and **B,** Three-week reevaluation.

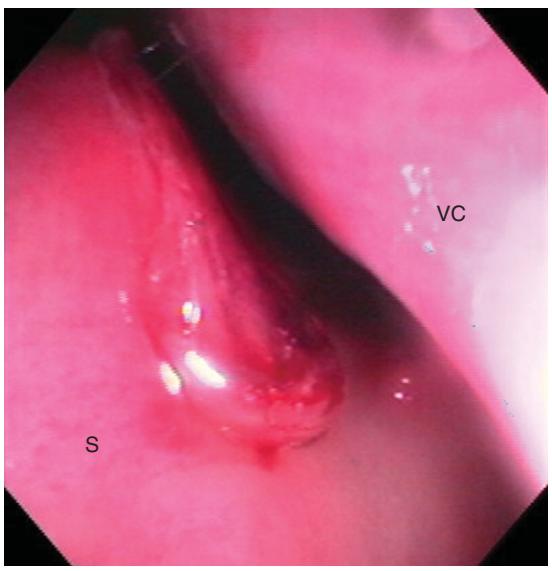

FIGURE 3-26. Seven-week reevaluation.

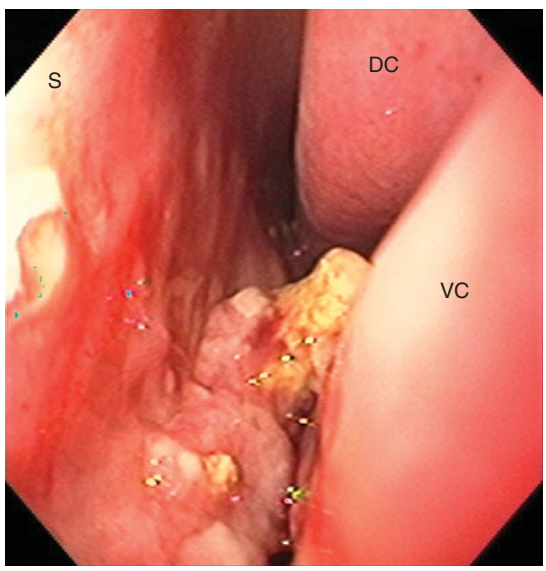

FIGURE 3-27. Filly had exacerbation of phycomycosis caused by *Conidiobolus* spp. in left nare 7 months after initial diagnosis. Treatment was initiated with 5 mg/kg of fluconazole orally (PO) once per day (SID) for 6 weeks and 1 teaspoon of ethylenediamine dihydroiodide PO twice per day (BID) for 6 weeks with local infiltration of amphotericin B (20 mg per granuloma site) at 3-week intervals for four treatments. Left nare: *DC,* dorsal concha; *S,* septum; *VC,* ventral concha.

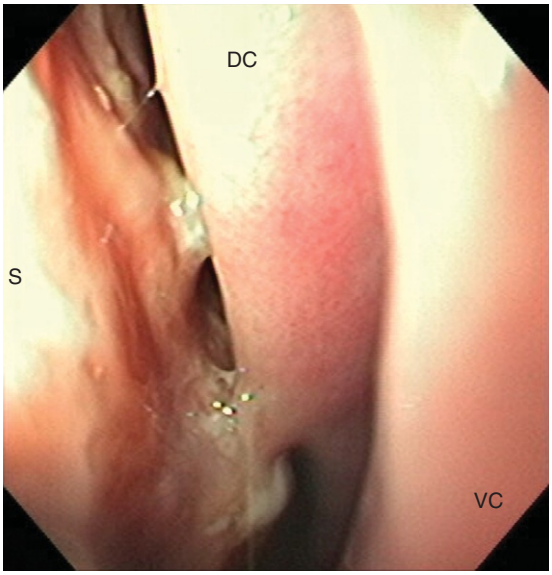

FIGURE 3-28. Three-week left nare reevaluation. *DC,* Dorsal concha; *S,* septum; *VC,* ventral concha.

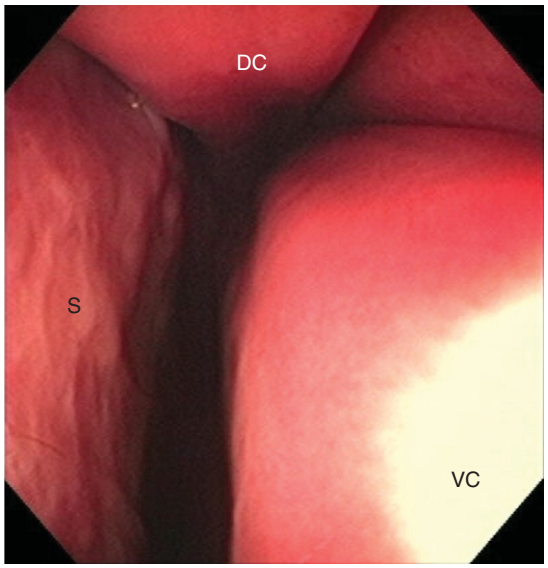

FIGURE 3-29. Twelve-week reevaluation. Complete resolution. *DC,* Dorsal concha; *S,* septum; *VC,* ventral concha.

FOREIGN BODIES

A 14-year-old Thoroughbred was seen with a chronic history of right fetid nasal discharge (Figures 3-30 and 3-31). The gelding's 107 tooth was removed 6 months previously due to dental caries. Feed material was noted in the lateral aspect of the ventral nasal meatus (Figure 3-32). Alligator jaw grasping forceps was used to remove the feed material. Feeding with a complete pelleted diet and pasture turn out was started. No hay was to be offered to the gelding. The gelding recovered uneventfully (Figure 3-33).

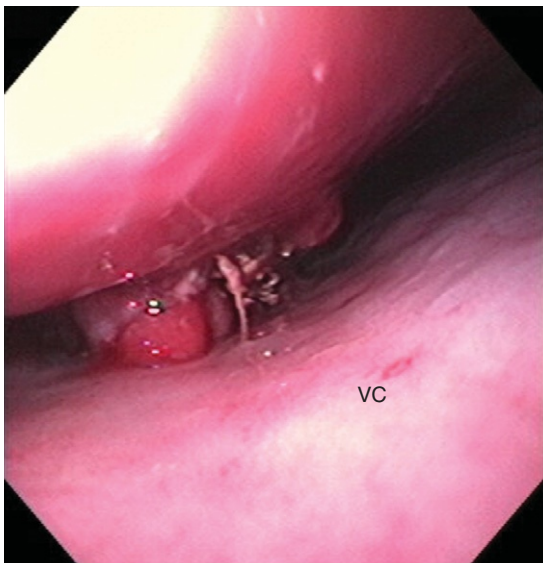

FIGURE 3-30. Feed material in lateral aspect of the ventral nasal meatus. *VC,* Ventral concha.

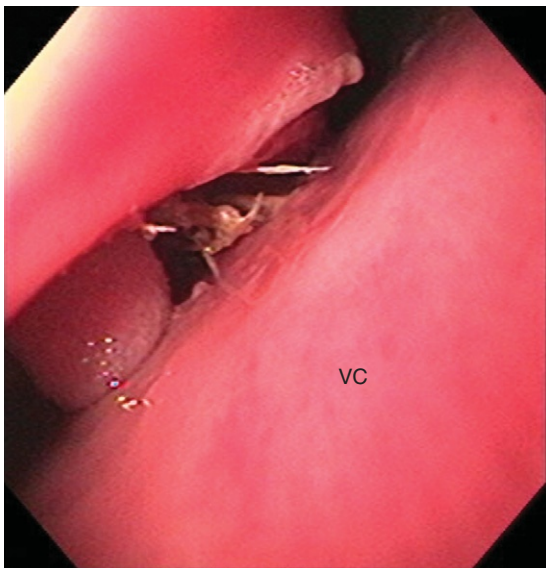

FIGURE 3-31. Two-week checkup. Continued migration of feed material into ventral meatus. *VC,* Ventral concha.

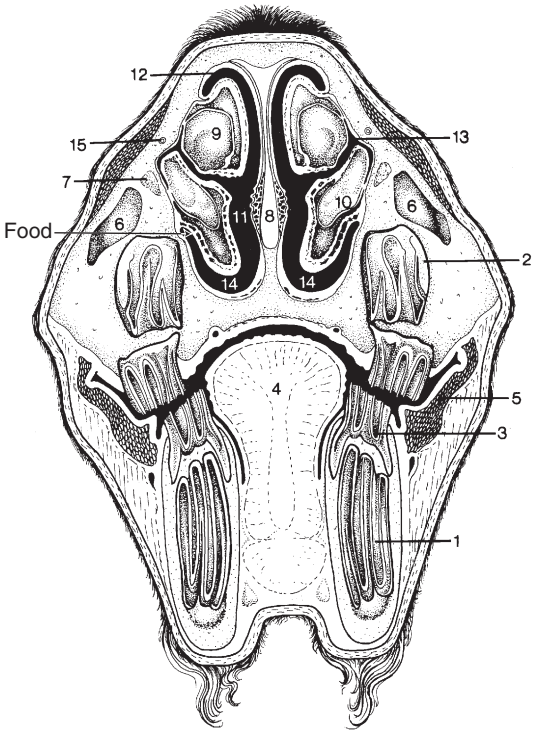

FIGURE 3-32. Location of food material *(arrow).* (From Dyce KM et al: *Textbook of veterinary anatomy,* ed 3, Philadelphia, 2002, WB Saunders.) *1,* P_4; *2,* P^4; *3,* p_4; *4,* tongue; *5,* buccinator; *6,* rostral maxillary sinus; *7,* infraorbital nerve; *8,* nasal septum; *9,* dorsal nasal concha; *10,* ventral nasal concha; *11,* common nasal meatus; *12,* dorsal nasal meatus; *13,* middle nasal meatus; *14,* ventral nasal meatus; *15,* nasolacrimal duct. (From Dyce KM et al: *Textbook of veterinary anatomy,* ed 3, Philadelphia, 2002, WB Saunders.)

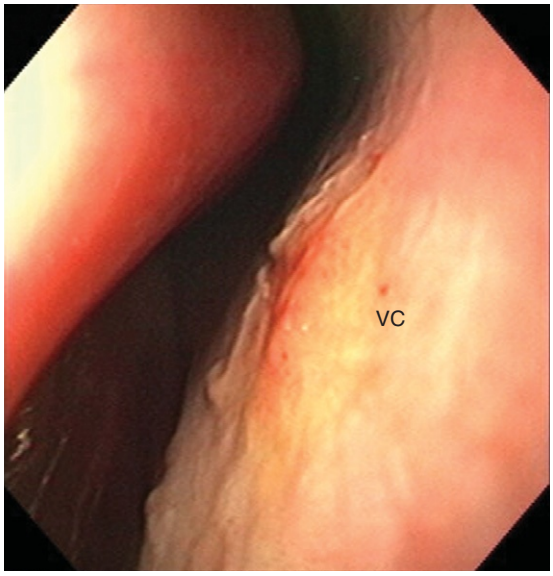

FIGURE 3-33. *VC,* Ventral concha. Recovery of food foreign body.

SINUSITIS

Mucopurulent exudate was noted from the middle meatus, which suggests a maxillary sinusitis or maxillary cyst (Figure 3-34). The communication between the nasal cavity and maxillary sinus (nasomaxillary aperture) is in the caudal part of the middle meatus. Radiographs revealed soft tissue opacity in the left caudal maxillary sinus and frontal sinus. Trephination of the frontal sinus and a sinuscopy were performed. A cyst was noted in the frontomaxillary aperture (Figures 3-35 and 3-36). A biopsy specimen

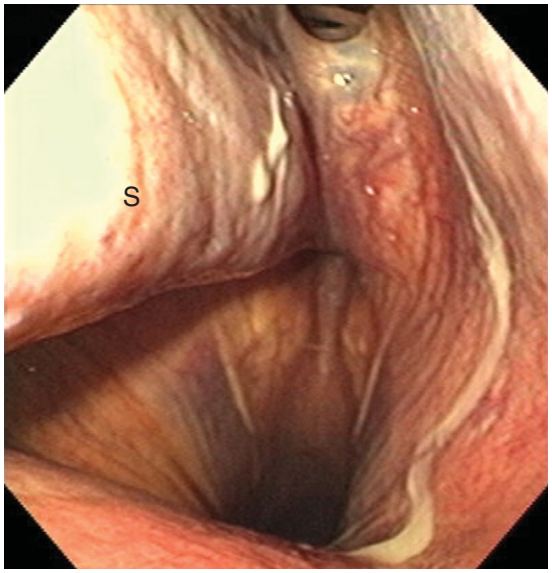

FIGURE 3-34. Mucopurulent exudate noted from middle meatus. *S,* septum.

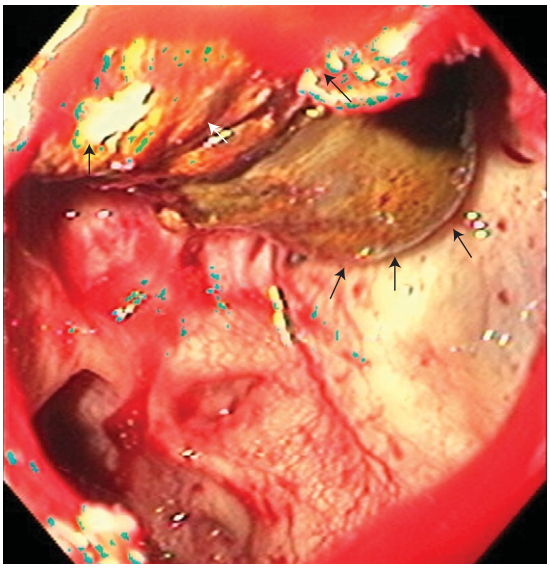

FIGURE 3-35. Cyst *(large arrows)* was noted in frontomaxillary aperture. Trephination site *(small arrows).*

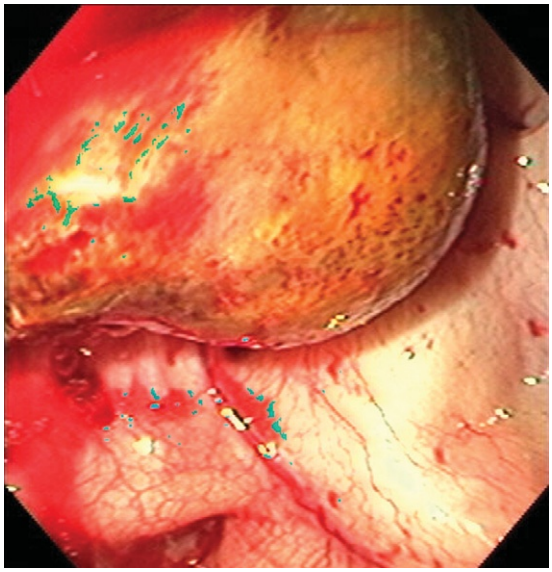

FIGURE 3-36. View of frontomaxillary cyst.

was obtained using an oval jaw with a pin biopsy instrument (Figure 3-37). Results of histopathologic examination were characteristic of a paranasal sinus cyst. Extirpation of the cyst was performed (Figure 3-38).

Hemorrhage from the nasomaxillary aperture into the middle meatus *(arrowhead)* was caused by trauma to the frontal sinus. The foal was noted to have hit a fence post with his head and was obtunded at presentation with unilateral hemorrhagic left nasal discharge.

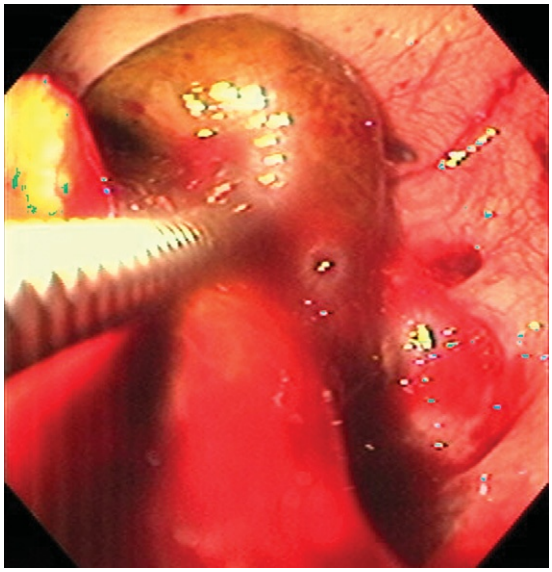

FIGURE 3-37. Capsular biopsy of cyst.

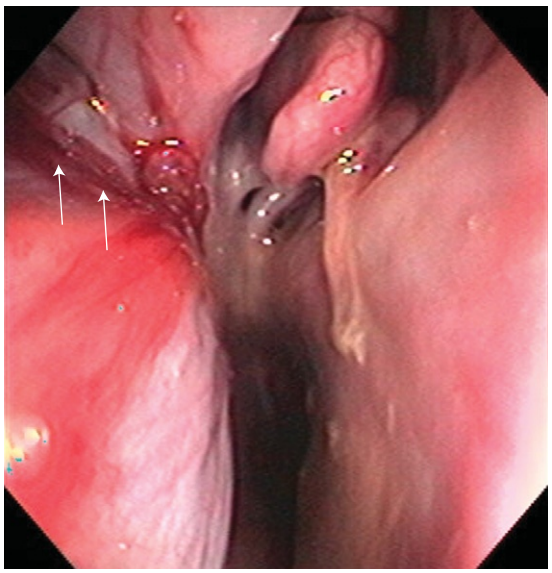

FIGURE 3-38. Left rhinoscopy. Hemorrhage from nasomaxillary aperture into middle meatus *(arrow)* due to trauma of frontal sinus.

CHAPTER 4

Pharyngoscopy and Laryngoscopy

DOUG BYARS

Equine endoscopy is routinely performed in the standing patient using physical or chemical restraint. Endoscopes are ideally 1 m in length and 9 mm or less in diameter for foals and 11 to 12 mm for adults. The actual length needed for an upper airway evaluation is 40 to 60 cm; however, any added length will allow for clinical evaluations of the trachea and esophagus.

EQUINE UPPER AIRWAY EXAMINATION

The equine upper airway examination can be performed by routine endoscopy with physical restraint, a nasal occlusion examination is usually performed with sedation, and a performance treadmill evaluation that most often requires the use of a video endoscope.

Endoscope Evaluation with Restraint

The standard endoscopic evaluation is usually performed with restraint provided by a "twitch." The endoscope is passed forward up either nasal passage via the ventral meatus. If the sinuses or ethmoid turbinates are to be evaluated, the curvature of the endoscope is directed dorsal to view the maxillary sinus opening and then further advanced to view the ethmoid turbinate. The endoscope is further directed downward and forward to view the entry into the pharynx. This view provides observation of the pharynx, the soft palate (usually forced upward by the tongue beneath the palate), the openings to the guttural pouches, and the upper portion of the larynx. In most adult horses the length of the endoscope penetration will be approximately 40 cm. A slight advancement of the scope while turning it downward will produce a view of the larynx and its vestibule opening. The epiglottis is usually visualized unless the soft palate is displaced. If the soft palate occludes the view of the epiglottis, the horse should be encouraged to swallow by advancing and then withdrawing the endoscope. If a water flush is available through the endoscope, spraying of the soft palate and laryngeal orifice will usually elicit a swallowing reflex. If the soft palate is not visualized by the epiglottis being in the proper position, the endoscope is advanced into the uppermost portion of the trachea to elicit either a cough or swallowing reflex. The endoscope is then swiftly withdrawn with a downward view of the pharynx. Further evaluation involves the symmetrical abduction of the arytenoid cartilages during inspiration and expiration. Examination of symmetry involves the oblique or rounded entries into the vocal sacs and the thickness of the respective aryepiglottic folds. The ability to fully abduct during inspiration is a sales criterion for upper airway "soundness of wind."

Under most sales conditions, if disputes regarding throat evaluations arise, an arbitration panel of veterinarians is provided to determine failure or passing of an individual horse for sales purposes.

Occlusion

Nasal occlusion may be produced with or without sedation. The nares are occluded during endoscopy to mimic conditions of the throat most likely to be present during performance. Sedation with approximately 2 ml (200 mg) of intravenous xylazine in the adult horse causes an accentuation of paresis, which can either be interpreted as falsely causing hemiparesis or mimicking the condition of the throat during performance-related fatigue. The horse should be encouraged to "work" the throat with full abduction during the occlusion period and then be allowed to have air by release of the hand clasp of the nares to observe arytenoid function, soft palate displacement, swallowing, pharyngeal collapse, or flutter of the aryepiglottic folds. The confidence limit for the nasal occlusion will match that of a treadmill evaluation by approximately 90% (Dr. Frederick J. Derksen, personal communication, 2002). Nasal occlusion is used to evaluate the upper airways, when indicated, in a stable environment instead of during actual performance.

Nasal Sound Recording Device

An additional upper airway test is to use a nasal sound recording device (WindTest™) in conjunction with endoscopy to assess upper airway lesions not able to be observed directly. For this test a nasal recording microphone is placed into the nares, and the horse is then maximally exercised. Endoscopy is performed immediately upon arrival into the stable, and the airway noise turbulence is compared with that from lesions of the upper airways. Although still experimental, the procedure is promising because it has potential for evaluation of noise tracings similar to those of electrocardiogram tracings referred for interpretation by a computerized diagnostic center.

Endoscopic Treatment

Disorders revealed by endoscopic examinations can occasionally be treated through the endoscope. Foreign bodies may be removed by grasping objects with biopsy forceps or snares, laser procedures can be used to remove polyps and granulomas, and local anesthetics or therapeutic lavage may be given through the biopsy port.

ENDOSCOPY OF THE UPPER AIRWAY

Endoscopy of the upper airways was the first introduction of using endoscopy in equine medicine, originating from the need to examine the airways of the horse. The original endoscopes were rigid and battery powered. These endoscopes were difficult to pass through the ventral nasal meatus, and the light bulb generated heat, which limited the time for examination. The introduction of fiberoptics allowed for flexible endoscopes and a "cool" light source that did not limit the examination time. Knowledge of upper airway disorders increased exponentially with recognition of impairment and obstructive lesions of the pharynx and larynx, which set standards for performance evaluations eventually used in routine prepurchase examinations now adopted by sales

companies as "conditions of sales." Today, equine endoscopy is considered a routine service component of equine practice.

The equine throat comprises multiple functional structures that maintain normal upper airway airflow at rest and during performance for the horse as an obligate nasal breather. The competence of both inspiration and expiration depends on the absence of stricture, occlusive masses, and accumulation of secretions and the presence of normal functional anatomy. Upper airway disorders can affect aerodynamics and can predispose a horse to abnormal function of the lower airways.

NORMAL ANATOMY

The anatomic structures of the throat function to maintain inspiratory and expiratory airflow. Laryngeal function is influenced by the rostral airways from the dynamic nares, including the area from the alar cartilages to the static nasal passages (meatus) that warm and humidify the air leading to the pharyngeal vault. The larynx provides for a proportionally sized opening to the trachea at rest and during performance and for the functional aspects of swallowing.

Figures 4-1 to 4-5 show the normal anatomic structures of the functional pharynx and larynx.

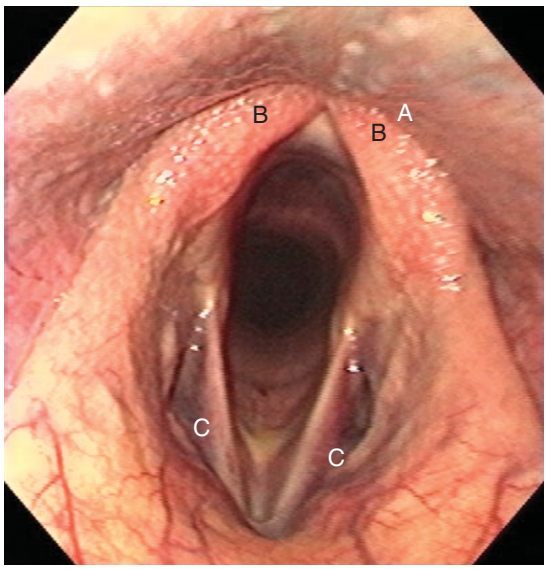

FIGURE 4-1. Normal larynx. *A,* Opening to esophagus behind and dorsal to *B,* corniculate process of arytenoids cartilage, vocal sacs; *C,* ventricles.

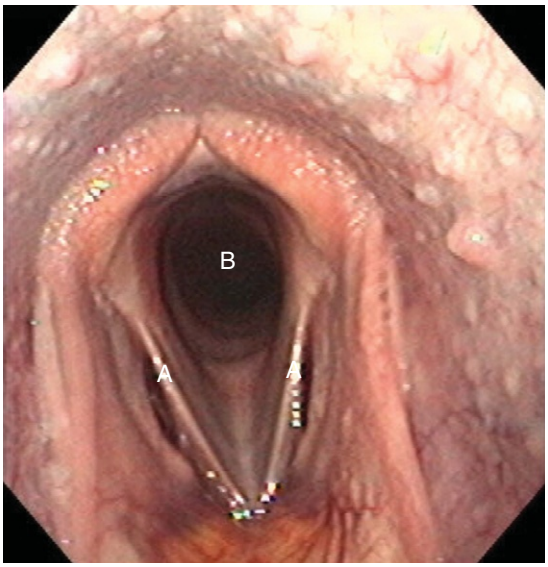

FIGURE 4-2. Normal larynx. *A,* Vocal cord; *B,* rima glottidis. Pharyngeal lymphoid tissues are obvious as nodules in dorsum of pharynx.

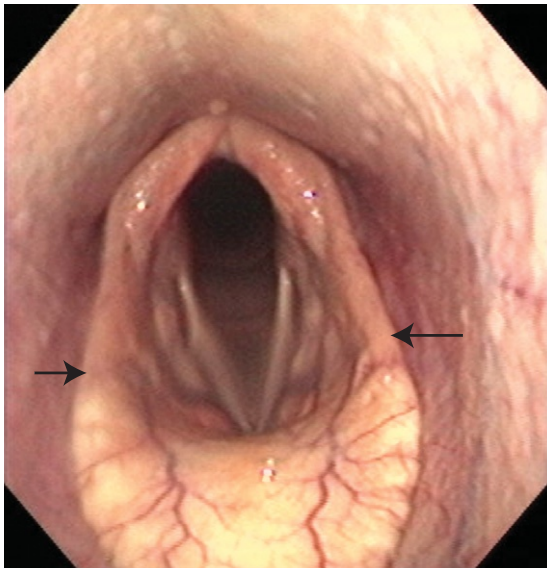

FIGURE 4-3. Normal trachea and aryepiglottic folds *(arrows).*

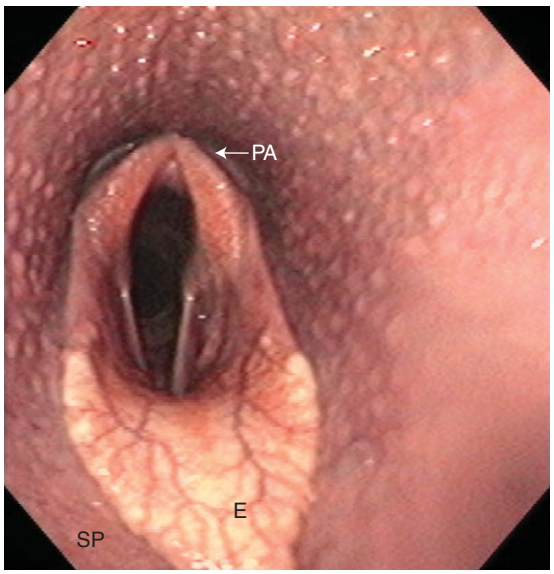

FIGURE 4-4. Correct position for palatopharyngeal arch *(PA),* epiglottis *(E)* with surrounding ventral soft palate *(SP)* and further view of pharynx with lymphoid tissue nodules.

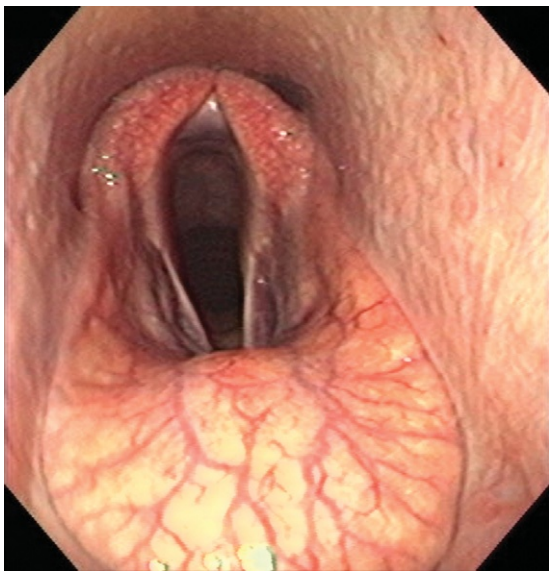

FIGURE 4-5. Moderate deviation from normal showing grade II laryngeal hemiplegia during abduction.

DEVIATIONS FROM NORMAL FUNCTIONAL ANATOMY

Functional lesions of the upper airways may not be obvious without specialized endoscopic examination; however, results of each examination should be evaluated meticulously with the recognition that there are few symmetrically normal equine throats. Although asymmetry and other apparent lesions in the patient can be obvious, they are often overcome or compensated for if the clinical result indicates subtle problems that do not compromise performance. Decompensation often is consistent with a performance complaint or the presence of noise. Some presumptive endoscopic assessments of the upper airways are discussed in the following sections.

Recurrent Laryngeal Neuropathy

Grading systems vary slightly among clinicians. I use the grading system shown in Figures 4-6 to 4-10. Practitioners should be aware that sedation may accentuate paretic lesions.

Laser Abduction Surgery

A laser can be used through the biopsy channel of an endoscope to perform surgical procedures or ablation of lesions. CO_2, neodymium:yttrium-aluminum-garnet (Nd:YAG), or diode lasers can be used. The diode laser, which is the most recent generation of laser for upper-airway surgical procedures, has some advantages: it is compatible with 110-volt electrical power, it is lightweight and portable, it does not require calibration time, and fiber use can be extended over multiple procedures. The power capability achieved is usually 25 watts, which is comparable to 75 watts with a Nd-YAG laser.

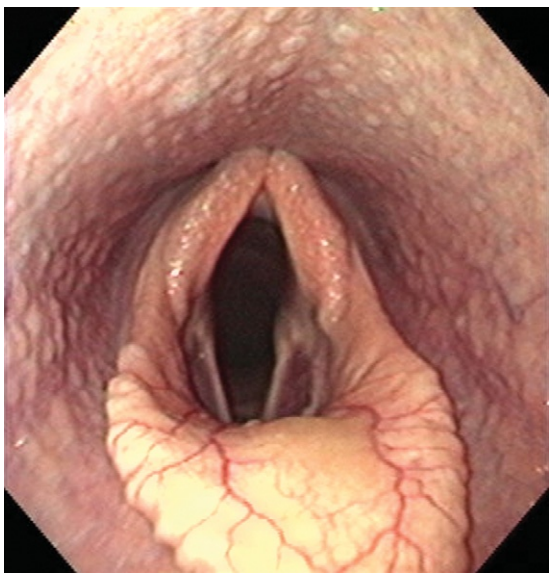

FIGURE 4-6. Grade I: all movements, both adductory and abductory, are synchronized at rest and after exercise. Normal larynx.

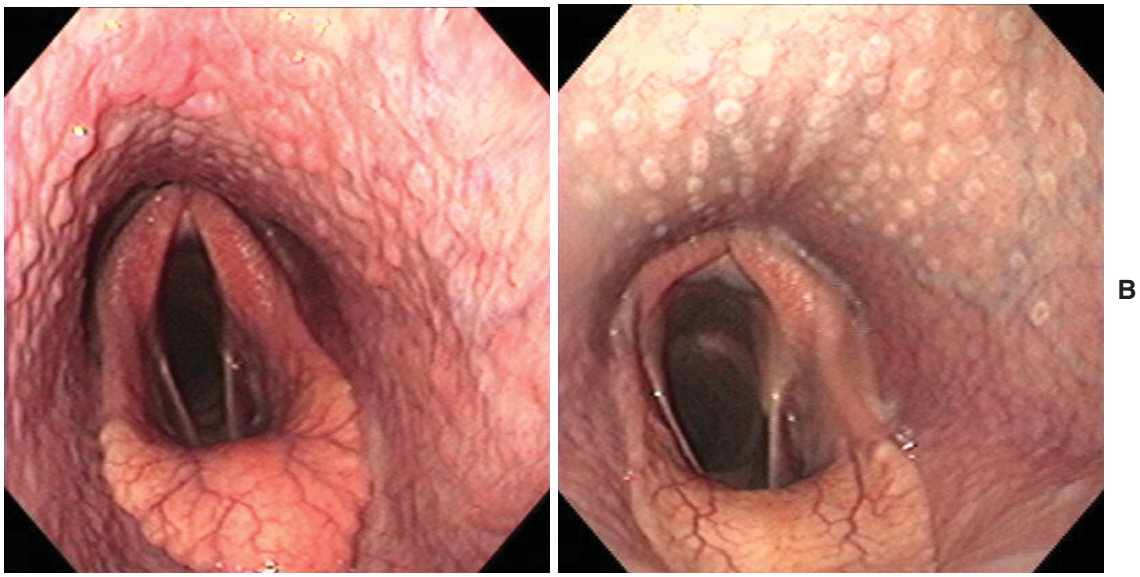

FIGURE 4-7. **A** and **B,** Grade II: all major movements are symmetrical with full range of abduction or adduction. Transient asynchrony or delayed abduction may be seen. Asymmetry of vocal sac and thickening of aryepiglottic fold may be noted.

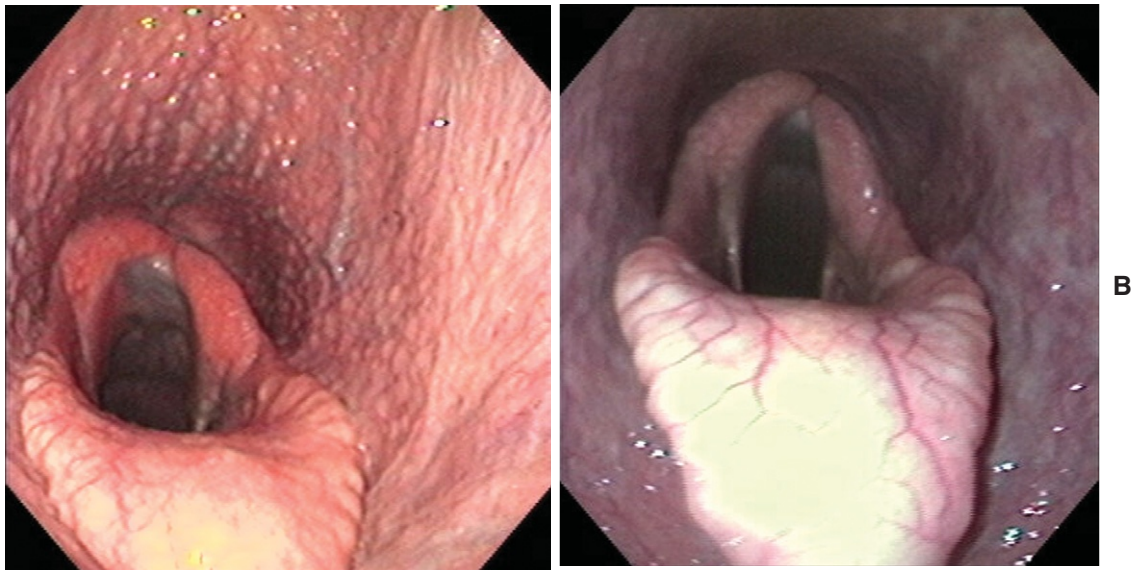

FIGURE 4-8. **A** and **B,** Grade III: asynchronous, incomplete abduction.

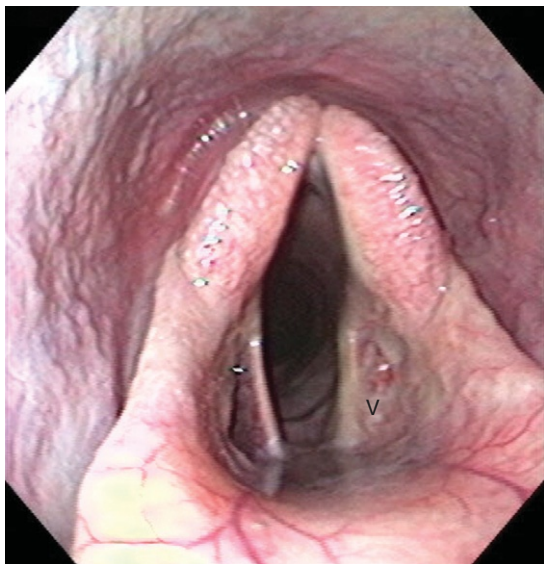

FIGURE 4-9. Note left ventriculectomy *(V)* in this grade III left laryngeal hemiplegia (LLH).

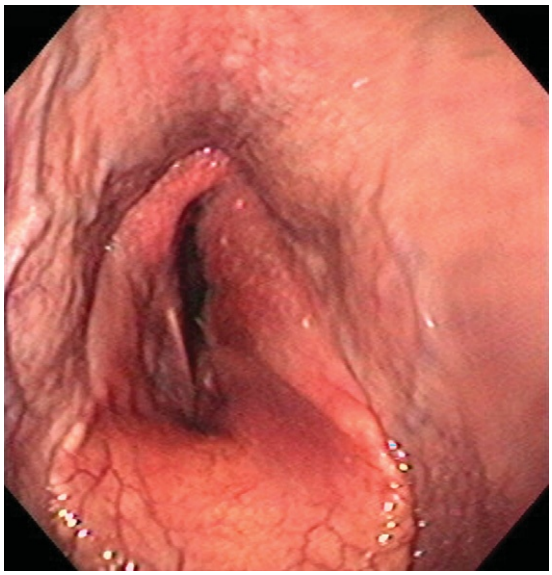

FIGURE 4-10. Grade IV: complete paralysis of affected arytenoid.

Laser procedures include the ablation of masses by intense "paintbrush" techniques, amputation of granulomas or other pedunculated lesions by line-cutting at the stalk, arytenoidectomy, sacculectomy, and the use of strategic burns to scar soft tissues. Additional uses include cutting through membranes (e.g., in guttural pouch tympany a laser can be used to equalize pressures by creating a common air passage between the guttural pouches).

The most common laser abduction procedure currently being performed is provided for horses having impaired upper airway performance caused by lesser grades of laryngeal hemiplegia with functional motion of the paretic arytenoid that precludes the success of a traditional "tie-back" surgical procedure. With the abduction procedure strategic spot burns are made at 12 to 14 A voltage with the diode laser along a line behind the paretic arytenoid (usually on the left side) and then extended to an aryepiglottic fold and triangulated toward the saccule. The affected saccule is aggressively cauterized using the laser in a "blanket" pattern for a relative complete sacculectomy. (Bleeding may occur in the ventral aspect of the saccule that cauterization with the laser does not effectively stop.) The rightmost and leftmost lateral portions of the soft palate are tucked with spot burns and the pharyngeal dorsal wall is similarly "spotted" to create scarring and decrease pharyngeal collapse during performance. Although the results for this procedure are not consistent, it is performed with limited success on performance horses for which relatively few other procedures are available.

Other laser procedures include the drainage of congenital or acquired cysts, abscesses, or hematomas. In the later, the laser should not be considered adequate for hemostasis, and provision of drainage is more appropriate for seromas already being sufficiently coagulated. Use of a laser for choanal atresia has been attempted but has not yet been successful (Figures 4-11 to 4-15).

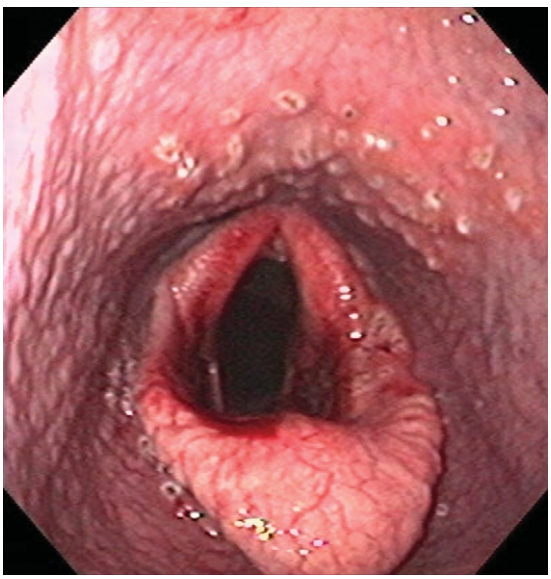

FIGURE 4-11. Laser treatment of grade II LLH. Note laser points to dorsal pharyngeal wall and left aryepiglottic fold.

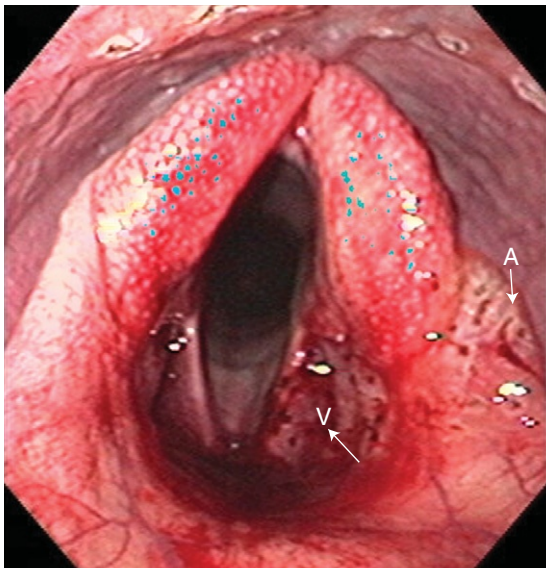

FIGURE 4-12. Close-up view of Figure 4-11. Note laser treatment points on left aryepiglottic fold *(A)* and left ventricle *(V)*.

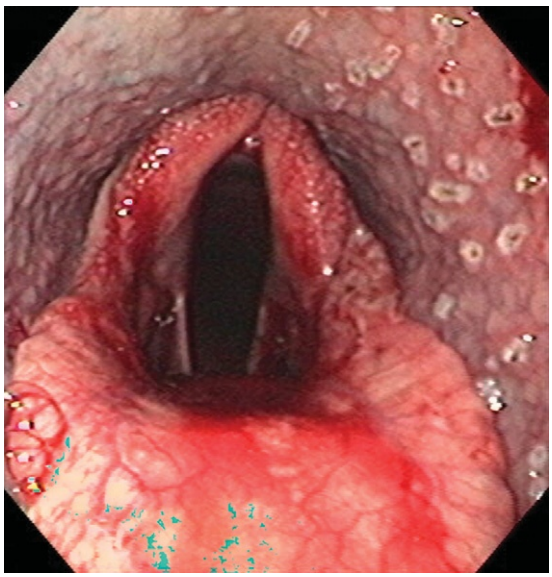

FIGURE 4-13. Laser abduction surgery. Note laser treatment points of left dorsal pharyngeal wall and aryepiglottic fold.

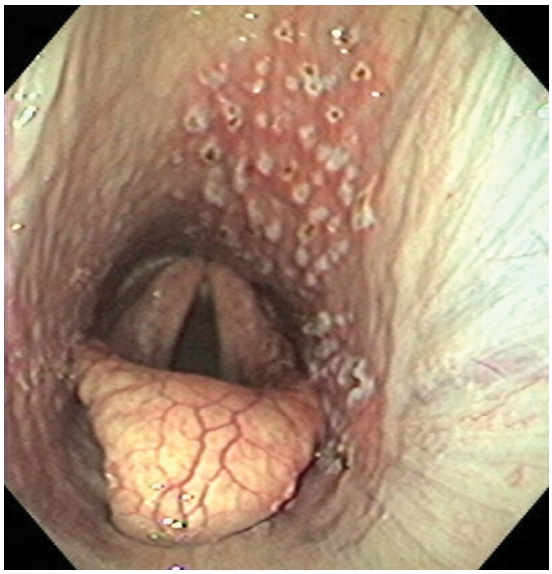

FIGURE 4-14. Grade II: LLH after laser abduction surgery. Note curled epiglottis that occurred from dorsal displacement of soft palate.

A

B

FIGURE 4-15. **A** and **B,** Laser ablation of an aryepiglottic hyperplasia.

LARYNGEAL GRANULOMATOSIS

Figures 4-16 through 4-21 show formation of slight to severe laryngeal granulomas. Most granulomas are associated with motion-induced irritation due to hemiplegia and chondritis formation.

FIGURE 4-16. Note thickening and inflammation of left corniculate cartilage *(arrow)*.

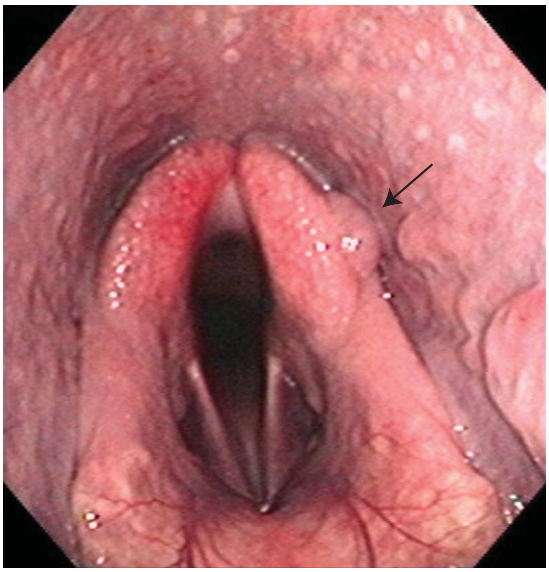

FIGURE 4-17. Small granuloma noted on abaxial aspect of corniculate cartilage *(arrow)*.

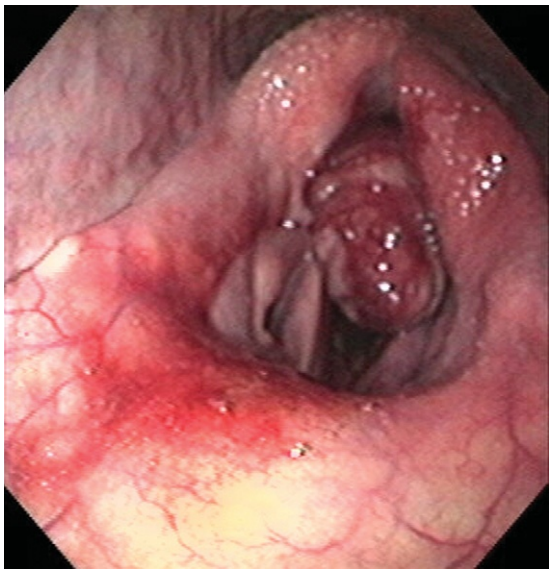

FIGURE 4-18. Horse was seen with chronic history of stertorous respiration. Note large granuloma obstructing rima glottidis.

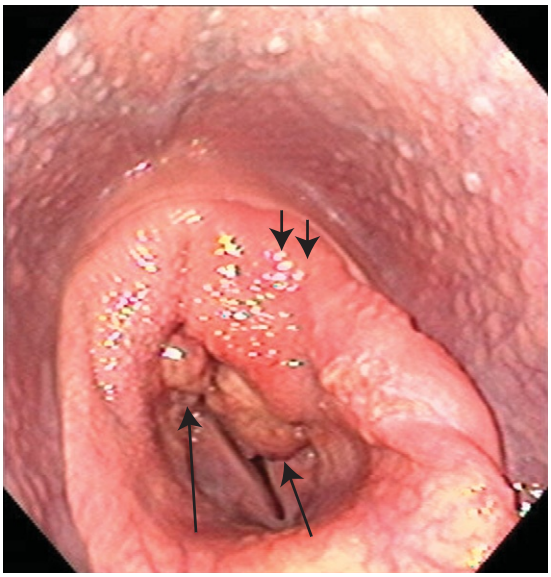

FIGURE 4-19. Severe chondritis with granulomas *(large arrows).* The left arytenoid chondritis *(small arrows)* is also seen.

FIGURE 4-20. Grade IV: LLH with severe granuloma formation.

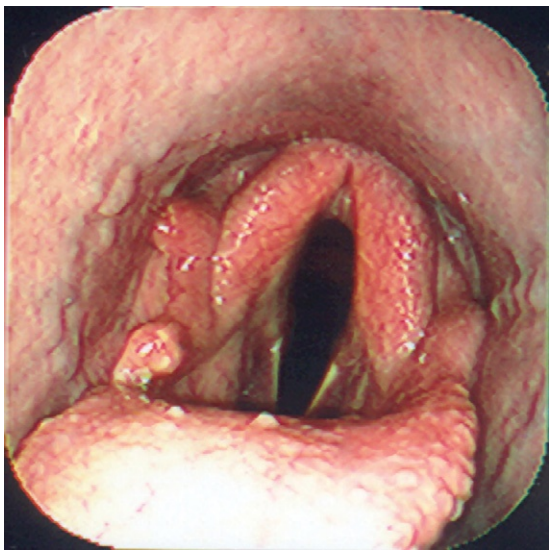

FIGURE 4-21. Granuloma noted on right aryepiglottic fold.

CHONDRITIS

Chondritis is the result of chronic inflammation and may be complicated by secondary infection and eventual granuloma formation or calcification. It is often unclear if unilateral chondritis can be a consequence of or a precipitating event for recurrent laryngeal neuropathy (Figures 4-22 to 4-24).

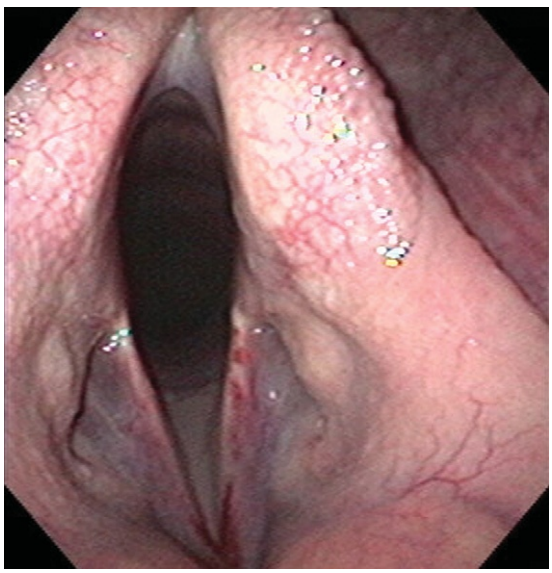

FIGURE 4-22. Mild chondritis of left arytenoid. Compare thickening of ventral aspect of corniculate process in this picture to that in Figure 14-3.

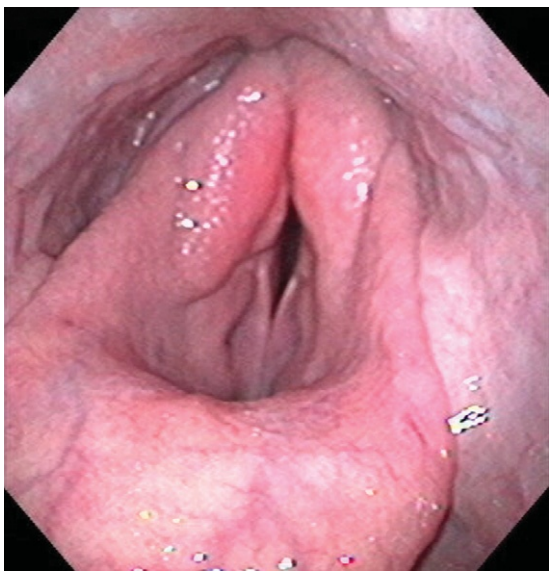

FIGURE 4-23. Severe chondritis of left and right arytenoids.

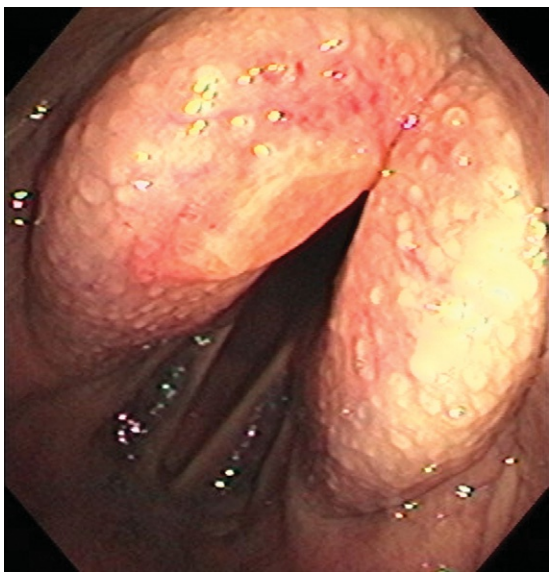

FIGURE 4-24. Mild chondritis of right corniculate process. Note that medial surface of corniculate process is swollen and inflamed.

DORSAL DISPLACEMENT OF THE SOFT PALATE

Dorsal displacement of the soft palate (DDSP) may be persistent or intermittent. Persistent DDSP due to guttural pouch mycosis, severe epiglottic hypoplasia, subepiglottic cysts, or persistent frenulum of the epiglottis has been reported. Identifying the causes of intermittent DDSP is frustrating. Several contributing factors must be considered: pharyngeal inflammation, excitement, fatigue, excessive flexion at the poll, and placing the tongue over the bit have all been implicated (Figures 4-25 to 4-32).

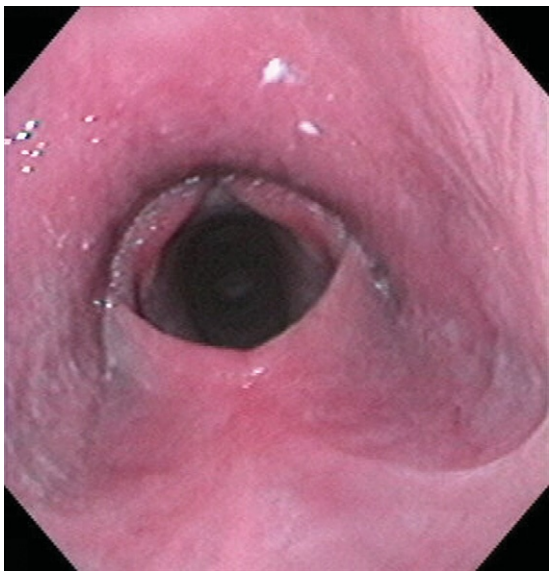

FIGURE 4-25. DDSP of an 8-hour-old foal that had oronasal reflux. Persistent epiglottic frenulum was identified and transected (not shown).

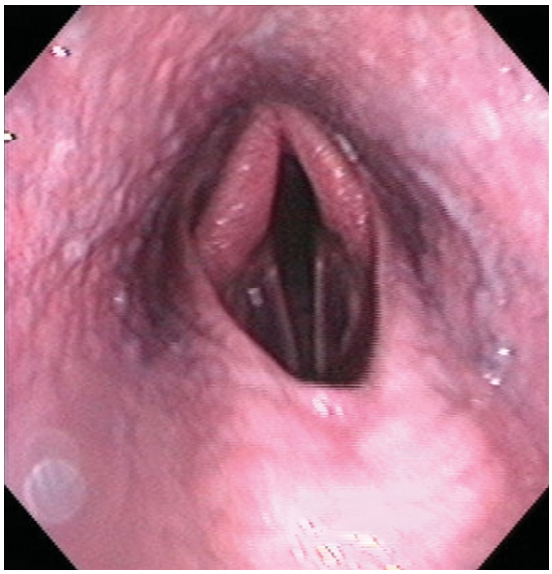

FIGURE 4-26. DDSP in 2-year-old race filly. This is typical DDSP.

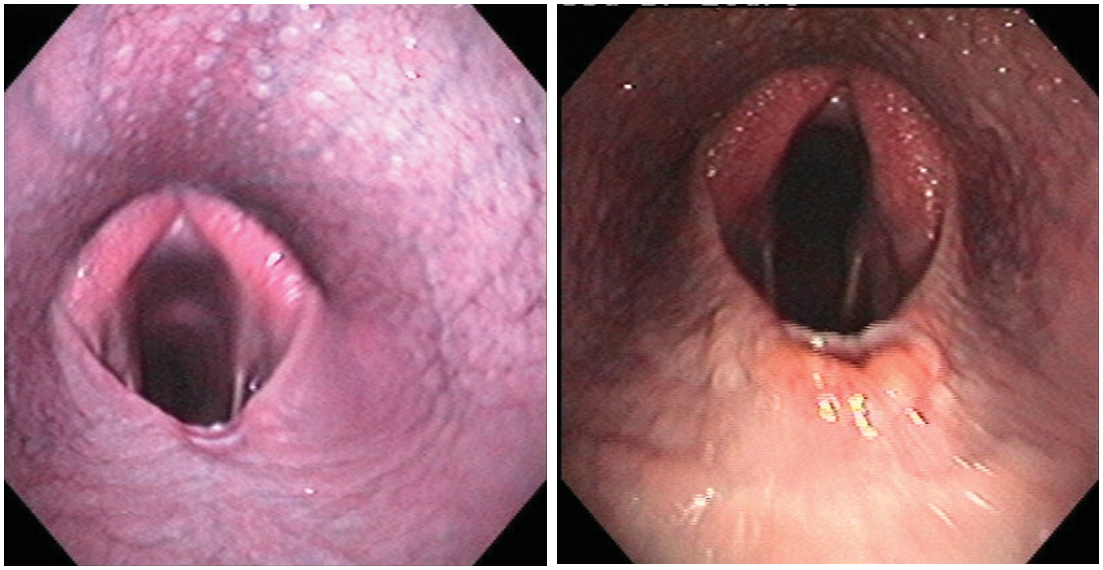

FIGURES 4-27. **A** and **B,** Pharyngoscopy of these two horses revealed secondary soft palate central ulceration caused by intermittent erosion caused by inability of the epiglottis to maintain normal position above soft palate. These figures were obtained when displacement was induced and ulceration observed to soft palate were consistent with epiglottic curvature. Displacement can often be induced by passing endoscope into upper portion of trachea, awaiting swallow or "gag reflex," and then withdrawing endoscope while directing scope ventral to observe soft palate.

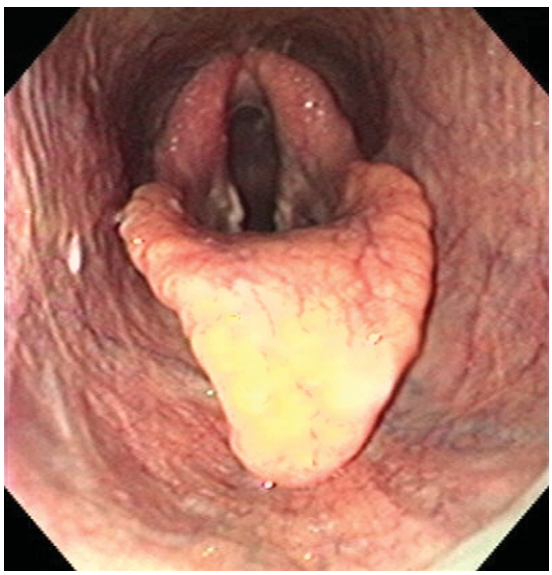

FIGURE 4-28. Epiglottic curvature associated with DDSP and ulceration of soft palate. DDSP can be seen in Figure 4-29.

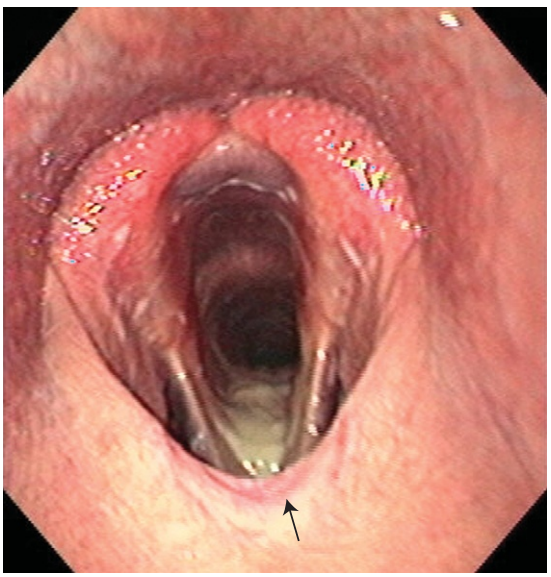

FIGURE 4-29. This horse had aspiration associated with DDSP. Note ulceration on soft palate *(arrow).*

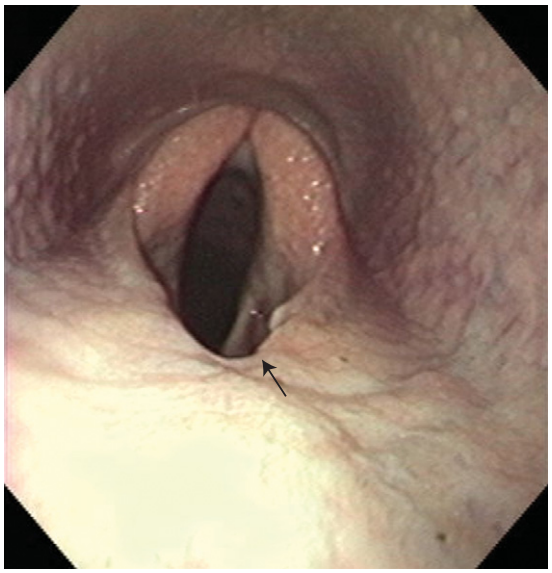

FIGURE 4-30. Soft palate notching due to chronic displacement of soft palate *(arrow)*.

FIGURE 4-31. Soft palate notching associated with chronic displacement of soft palate. Horse also had an aryepiglottic fold entrapment *(arrows)*.

FIGURE 4-32. Ulceration of epiglottic tip *(arrow)* due to chronic displacement.

ARYEPIGLOTTIC ENTRAPMENT (Figures 4-33 to 4-37)

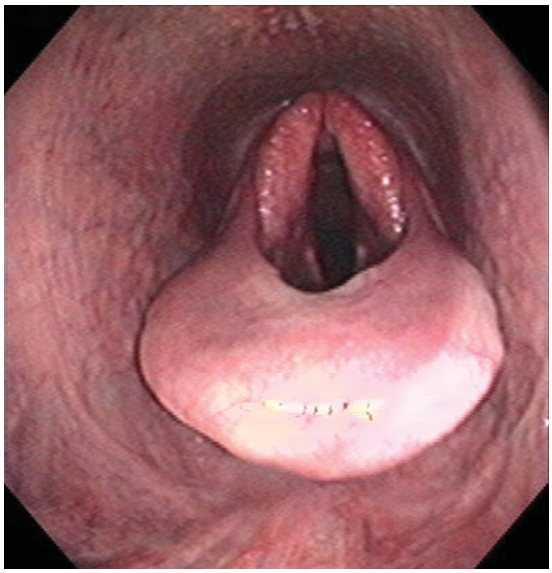

FIGURE 4-33. Typical full aryepiglottic entrapment by displaced aryepiglottic fold.

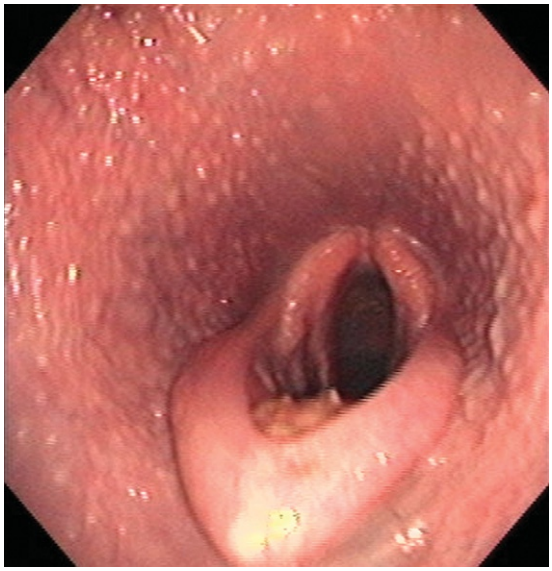

FIGURE 4-34 Weanling that was seen with history of choke. On pharyngoscopy an aryepiglottic fold entrapment that was considered incidental was noted. Surgical correction with bistoury was successful.

FIGURE 4-35. Surgical correction of aryepiglottic fold entrapment in Figure 4-33. Surgical correction was approached through laryngotomy.

FIGURE 4-36. Asymmetric chronic aryepiglottic entrapment. Outline of compromised epiglottis can be observed *(dashed line)*.

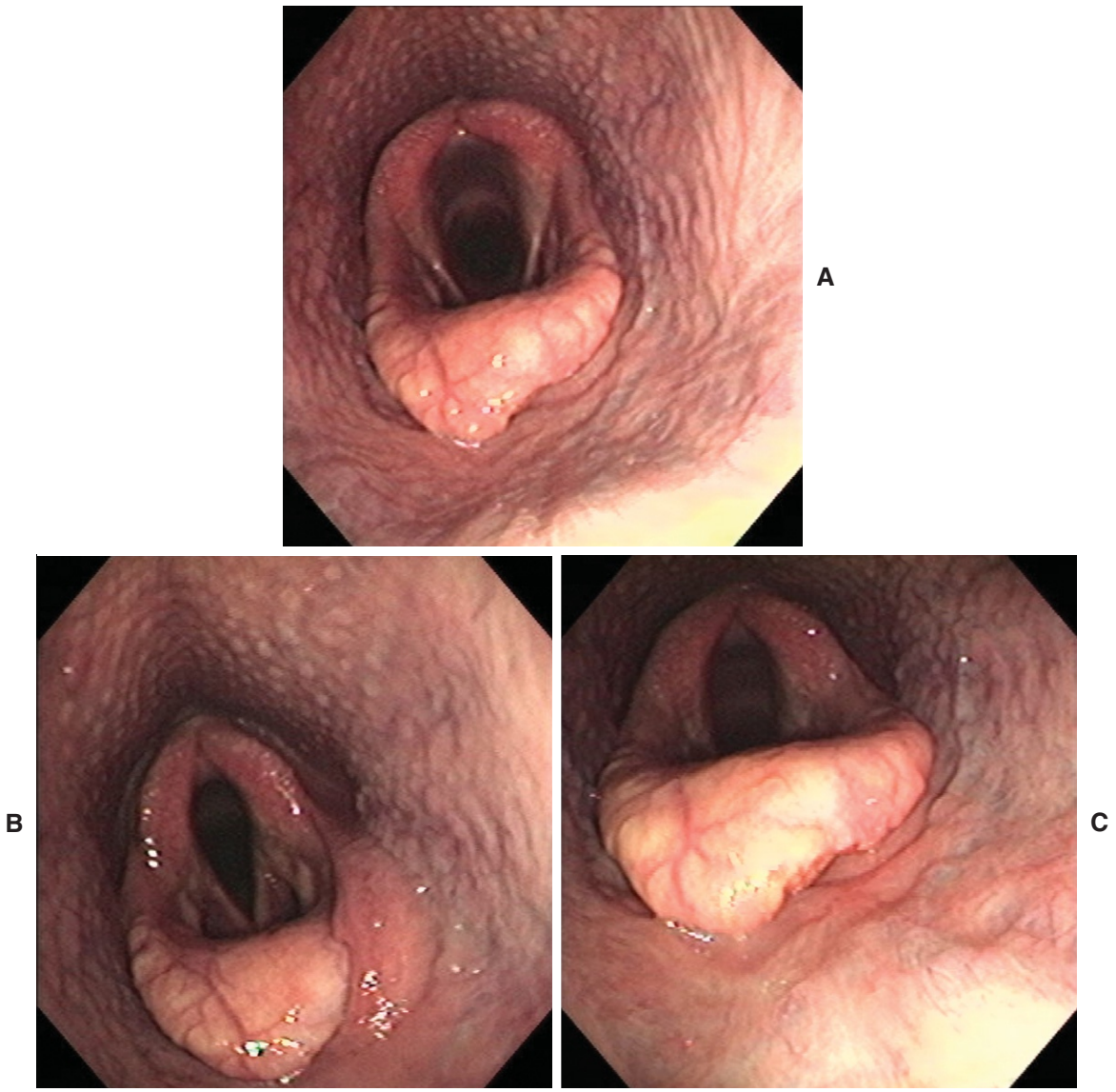

FIGURE 4-37. **A, B,** and **C,** Partial and intermittent left-sided aryepiglottic displacement. Note resulting epiglottic ulceration caused by intermittent partial "entrapment."

EPIGLOTTAL HYPOPLASIA (Figure 4-38)

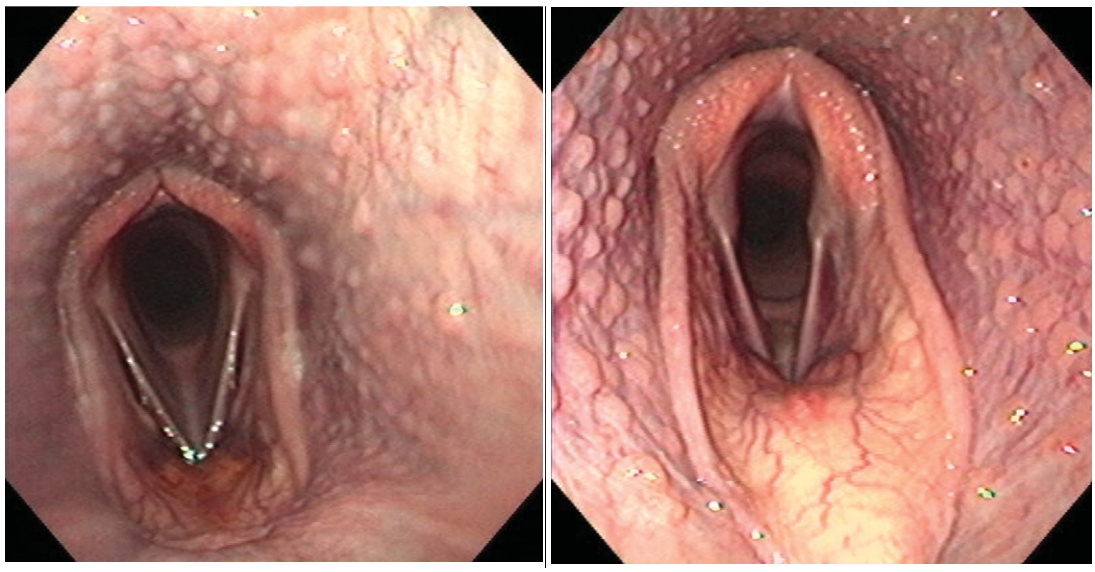

FIGURE 4-38. **A** and **B,** Hypoplasia of epiglottal cartilage observed in yearlings or younger horses. Horses older than 2 years may be seen with coughing due to aspiration or dysphagia or impairment of performance. Epiglottic augmentation by surgical intervention may be performed in older horses, but prognosis is guarded.

PHARYNGEAL LYMPHOID HYPERPLASIA

A grading system has been created to document the severity of pharyngeal lymphoid hyperplasia and its response to therapy.[1] This system is based on the degree of hyperplasia of the tonsillar tissue in the dorsal pharyngeal recess and of the roof of the pharynx[2] (Figures 4-39 to 4-42).

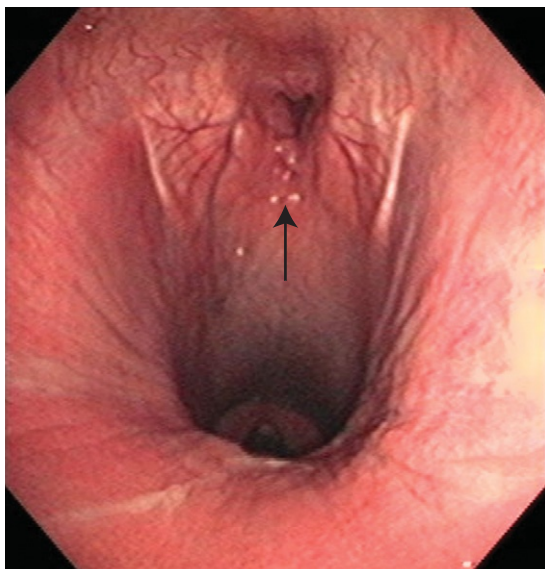

FIGURE 4-39. Grade 1: lymphoid hypertrophy is limited to less than 180 degrees of dorsal pharyngeal recess *(arrow)*.

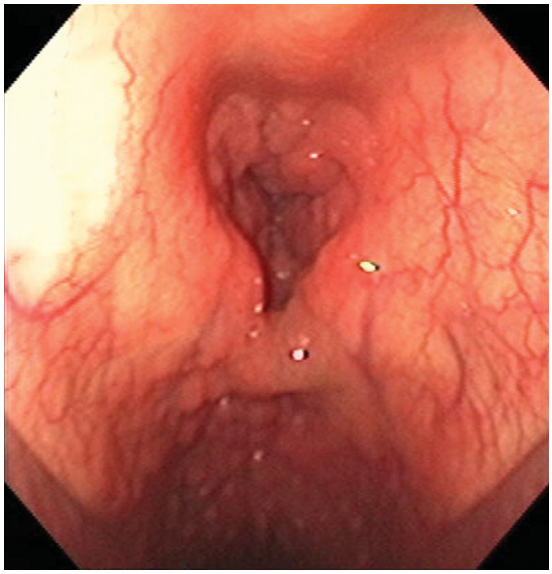

FIGURE 4-40. Grade 2: lymphoid hypertrophy extends to circumference of dorsal pharyngeal recess.

FIGURE 4-41. Grade 3: lymphoid hypertrophy makes midline contact of dorsal pharyngeal recess. Note difference between this figure and Figure 4-40.

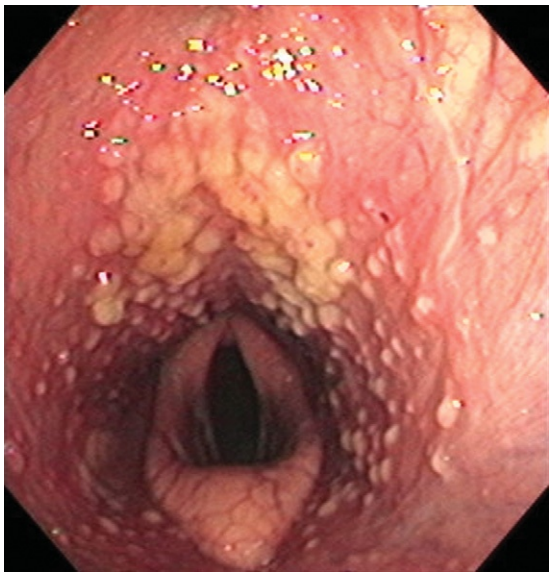

FIGURE 4-42. Grade 4: lymphoid hypertrophy with small masses (some are small abscesses) that arise from either dorsal pharyngeal recess or pharyngeal walls.

EPIGLOTTIC CYSTS (Figure 4-43)

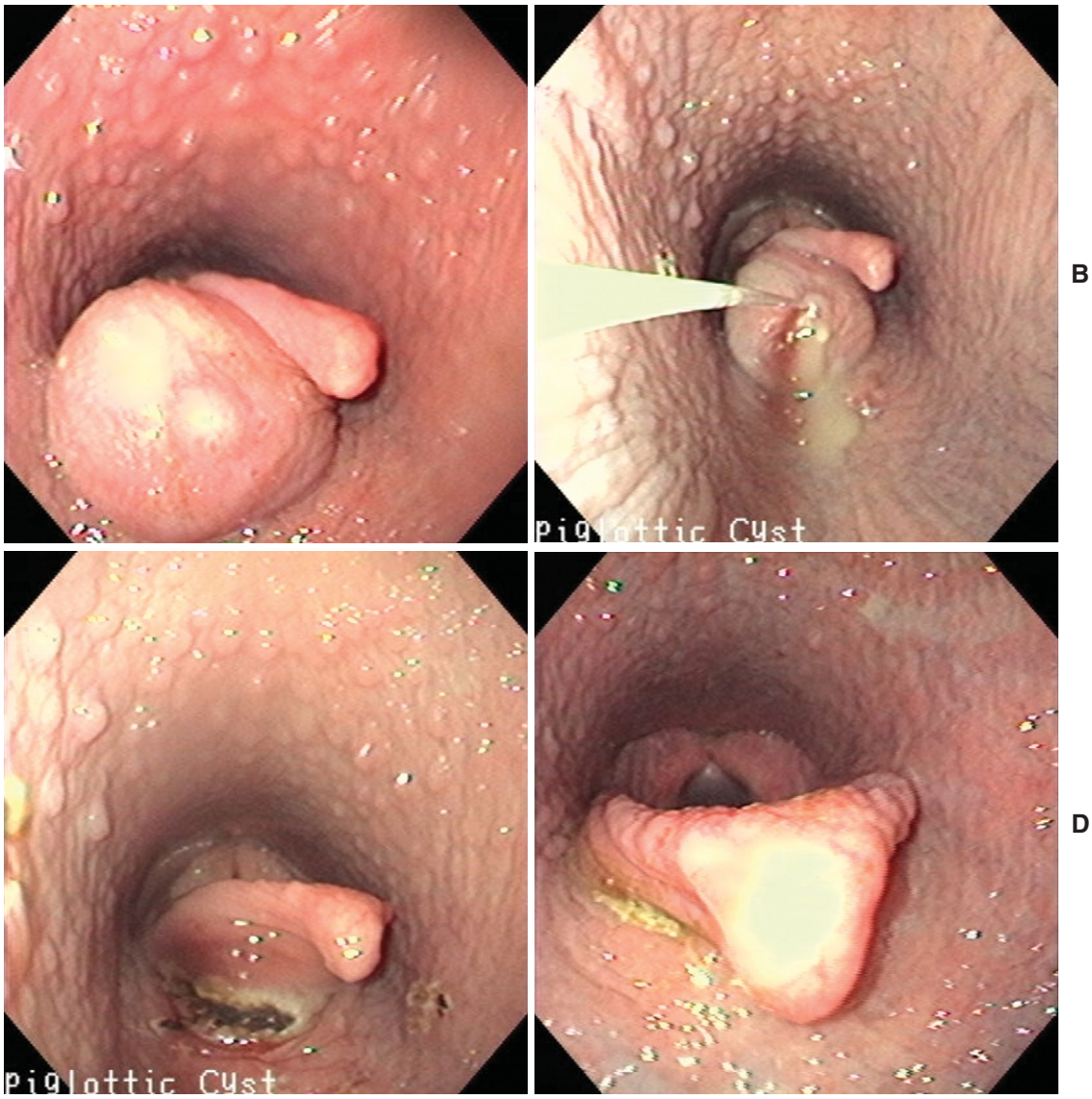

FIGURE 4-43. A 15-month-old Percheron/Saddlebred colt with 3+-month history of intermittent coughing and stertorous breathing. As colt's trainers started to train horse in hand they noted that when colt became excited he would make more stertorous breath sounds. **A,** Note large subepiglottic cyst. Laser surgery was performed using diode laser (14 watts). **B,** Flexible fiber of laser is contacting cyst, causing thermal necrosis of cyst's capsule. After cyst's capsule was excised, mucoid discharge was released. Discharge was cultured, and no significant bacterial species were isolated. **C,** Flexible fiber of laser was then introduced into cyst to completely ablate cyst's lining. **D,** Reevaluation of horse 9 weeks after laser therapy revealed that some granulation tissue was present in remnants of the cyst's wall. Granulation tissue was not excessive and was approximately 10% original cyst. No coughing or stertorous breathing was noted.

OROPHARYNX AND LARYNGOPHARYNX

The oropharynx is the most caudal aspect of the oral cavity. The oropharynx can be observed in a well-sedated horse with a full mouth speculum. The dorsal margin of the oropharynx is the ventral surface of the soft palate, and the ventral surface shows the large glossoepiglottic fold in the median plane and the palatoglossal arches laterally[2] (Figure 4-44).

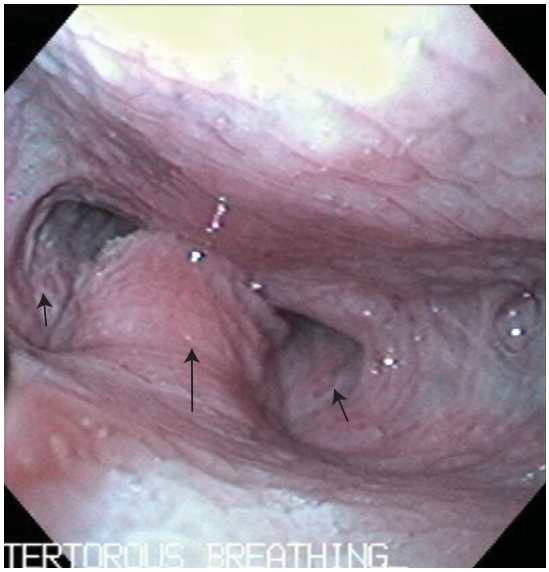

FIGURE 4-44. Oropharynx of normal horse: glossoepiglottic fold *(large arrow);* palatoglossal arch *(small arrows).*

MISCELLANEOUS LARYNGEAL DISORDERS

Right-Sided Hemiplegia (Figure 4-45)

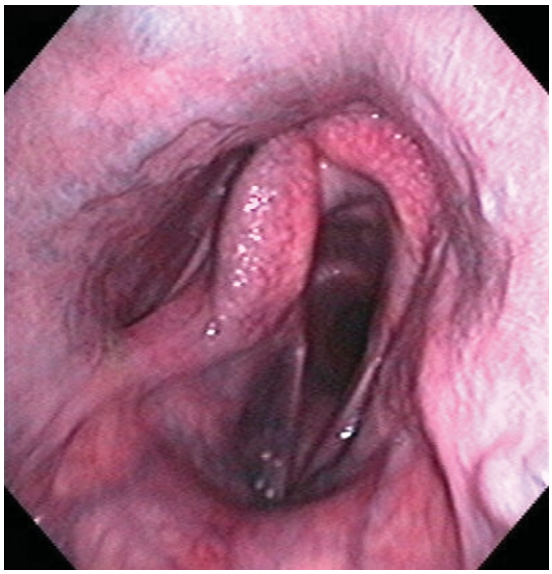

FIGURE 4-45. Right-sided grade III hemiplegia in horse that had received left-sided "tie-back" operation.

Arytenoidectomy (Figure 4-46)

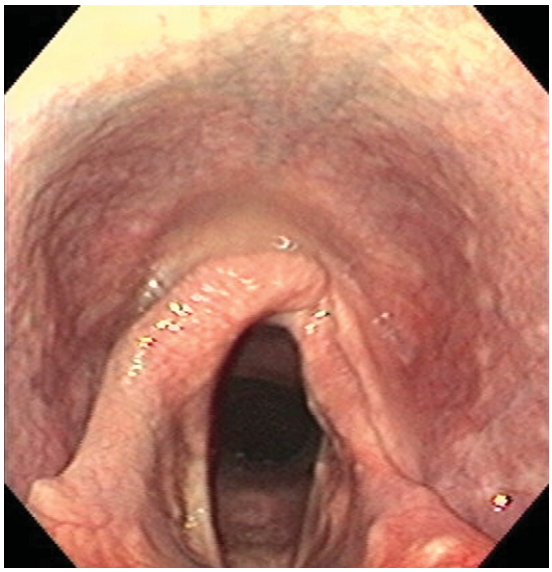

FIGURE 4-46. Left arytenoidectomy that had been performed because of severe chondritis.

Stertorous Respiration (Figure 4-47)

FIGURE 4-47. Miniature horse with stertorous respiration due to retraction of tongue caudally and pushing of soft palate dorsally. This horse had severe dental anomalies that did not allow tongue to be properly placed in oral cavity.

Laryngeal Purpura Granuloma (Figure 4-48)

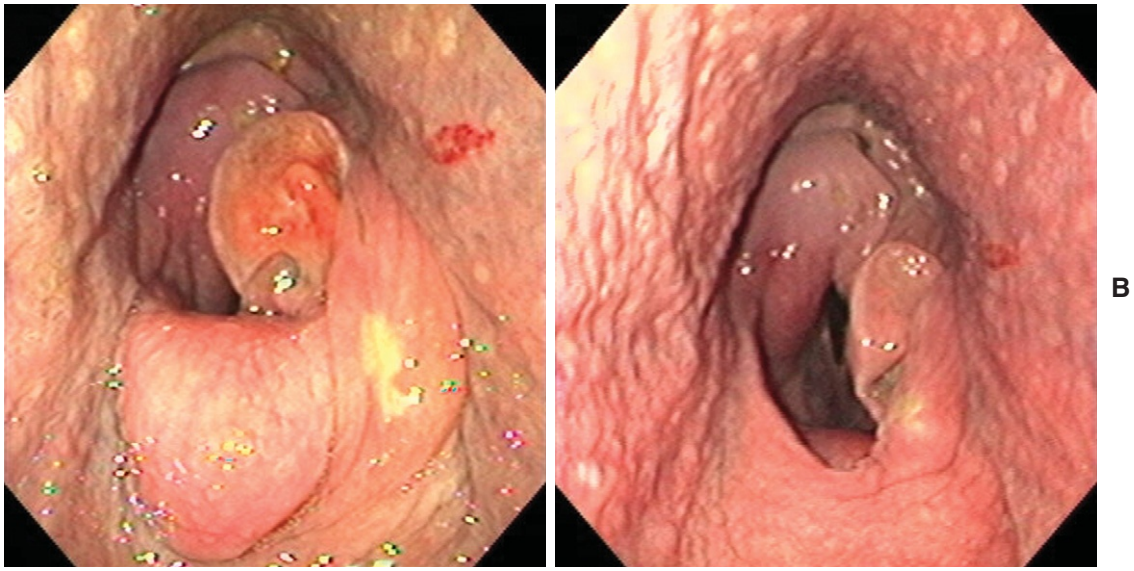

FIGURE 4-48. **A** and **B,** Before and after laser surgery for treatment of laryngeal purpura granuloma.

Obstruction in Rima Glottidis (Figure 4-49)

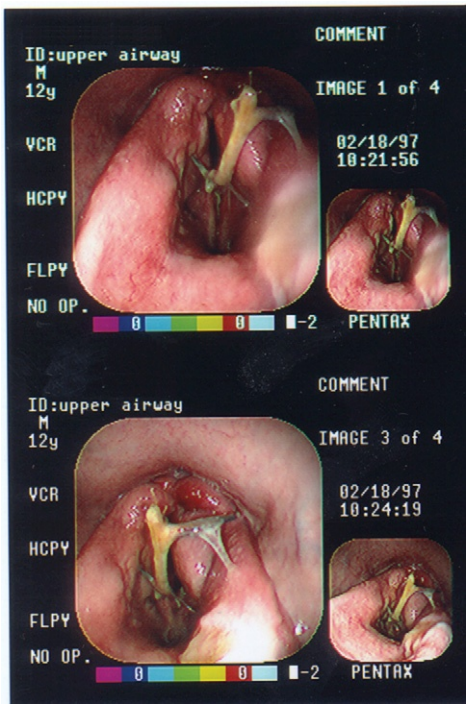

FIGURE 4-49. Ten-year-old quarter horse was seen with 1-month history of coughing and weight loss. Pharyngoscopy revealed mesquite branch in rima glottidis.

Cleft Palate (Figure 4-50)

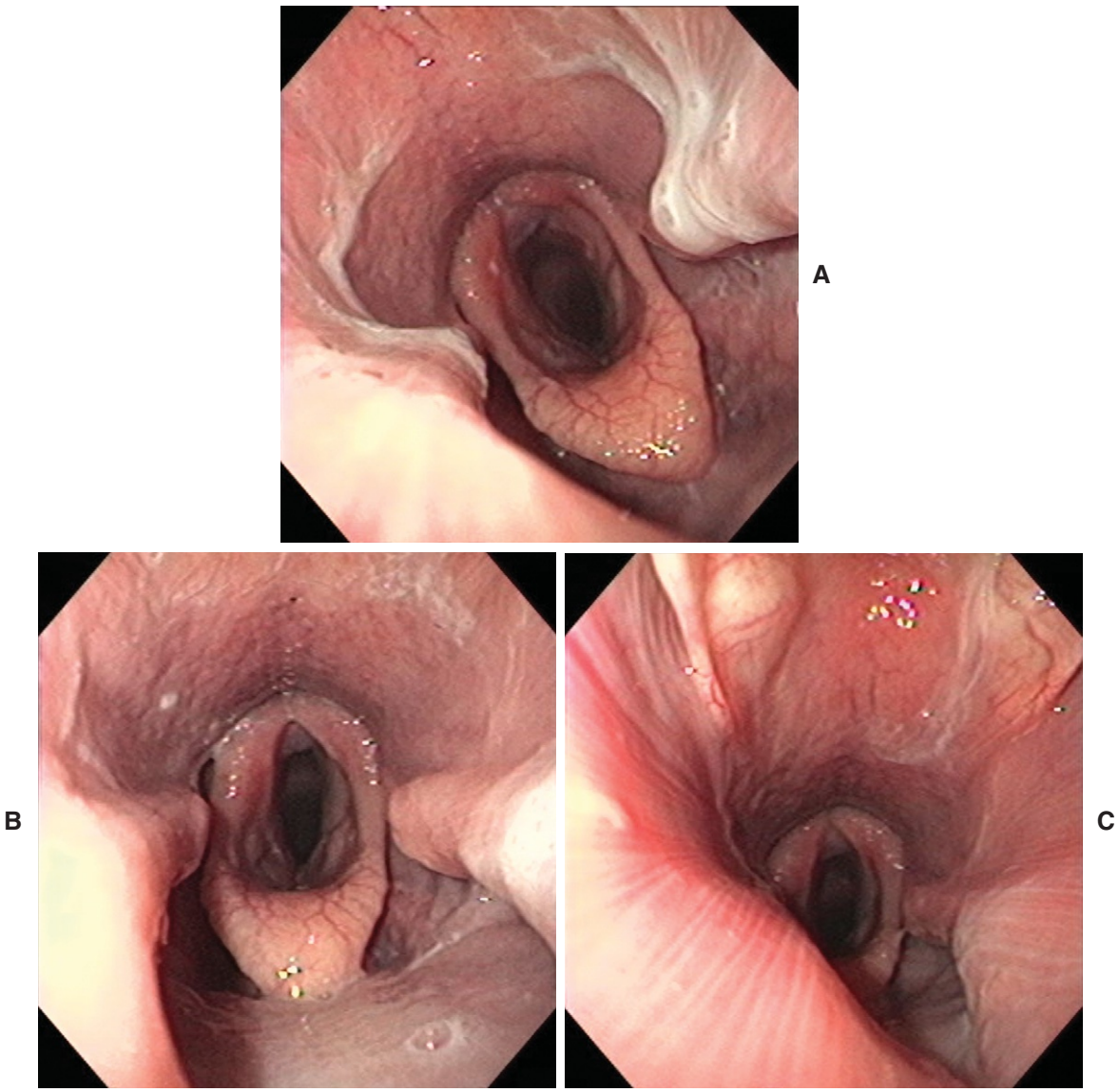

FIGURE 4-50. **A, B,** and **C,** Severe cleft of hard palate.

Aryepiglottic Congenital Cyst (Figure 4-51)

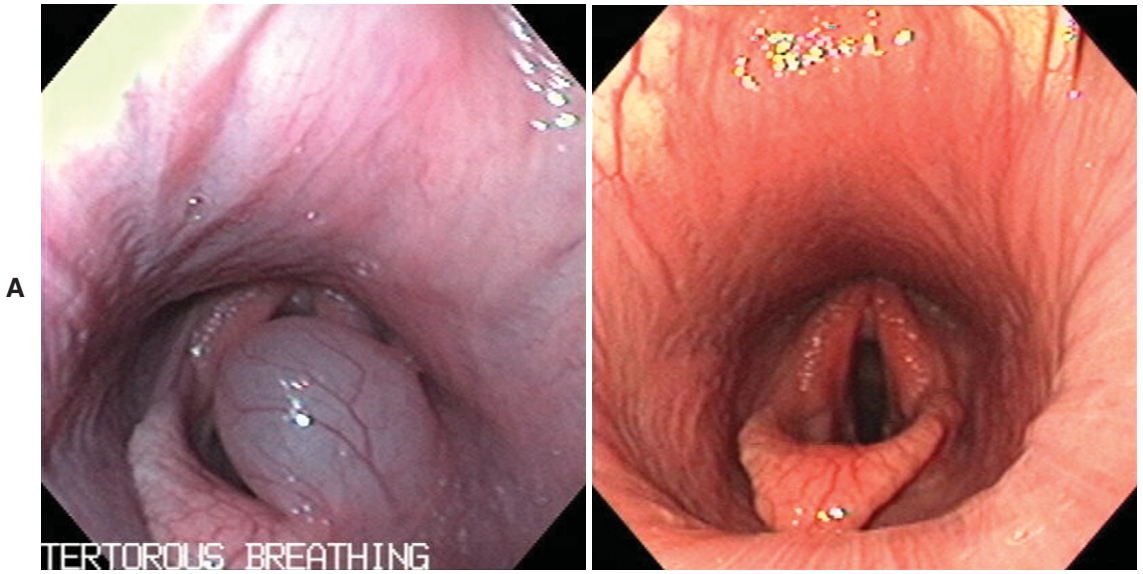

FIGURE 4-51. **A,** Three-hour-old foal was seen with history of stertorous respiratory pattern. Aryepiglottic congenital cyst was noted. **B,** Diode laser was used for ablation of cyst.

Laryngeal Purpura (Figure 4-52)

FIGURE 4-52. Laryngeal purpura due to intranasal *Streptococcus equi* vaccination.

Rostral Displacement of the Palatal Arch (Figure 4-53)

FIGURE 4-53. Rostral displacement of palatopharyngeal arch. Absence of cricopharyngeus musculature has allowed caudal pillars of palatal arch to move rostral to corniculate processes, and proximal esophagus is open. (From Traub-Dargatz JL, Brown CM: *Equine endoscopy,* ed 2, St Louis, 1997, Mosby.)

REFERENCES

1. Baker GJ: Disease of the pharynx. In Robinson NE, editor: *Current therapy in equine medicine,* ed 2, Philadelphia, 1987, WB Saunders.
2. Baker GJ: Pharynx. In Traub-Dargatz JL, editor: *Equine endoscopy,* ed 2, St Louis, 1997, Mosby.

CHAPTER 5

Endoscopic Examination of the Guttural Pouches

THOMAS SEAHORN

ANATOMY OF THE GUTTURAL POUCH

The guttural pouches are diverticula of the eustachian tubes. These pouches are formed by protrusion of the mucosal lining of the tube through a ventral slit between the supporting cartilages. They do not communicate but contact one another medially, ventral to the rectus capitis ventralis muscles. Each guttural pouch has a capacity of approximately 300 to 500 ml. The pouches lie between the base of the skull and atlas dorsally and the pharynx and commencement of the esophagus ventrally. The pouches are covered laterally by the pterygoid muscles and parotid and mandibular glands. The floor of the pouches lies on the pharynx and is molded to the stylohyoid bone, which divides them into medial and lateral compartments. The medial compartment is larger and extends more caudally and ventrally. Each pouch communicates with the pharynx through a slitlike opening rostral and ventral to the pharyngeal recess along the lateral pharyngeal wall (Figure 5-1). A thin plate of fibrocartilage is located in the mucosa of the medial aspect of the opening. The pharyngeal opening is located near the dorsal aspect of the guttural pouch, and drainage from the pouch is thus poor unless the head is lowered (Figure 5-2).

EXAMINATION OF THE GUTTURAL POUCHES

To enter the guttural pouch with the endoscope, a wire guide is first passed through the endoscopic biopsy port into the guttural pouch opening (Figure 5-3). The endoscope is pushed forward and rotated to roll the fibrocartilage axially, thus allowing entry. As the endoscope passes through the opening, the salpingopharyngeal fold will be apparent (Figure 5-4).

The walls of the guttural pouch are thin and intimately associated with many vital structures, including the pharynx, larynx, esophagus, parotid and mandibular salivary glands, and retropharyngeal lymph nodes. A fold of mucous membrane extending from the roof of the guttural pouch along the caudal aspect of the medial compartment contains the vagus, accessory, and cranial sympathetic nerves, cranial cervical ganglion, and internal carotid artery. The hypoglossal and glossopharyngeal nerves are associated with the caudolateral aspect of the medial compartment, and the pharyngeal branch of the vagus with the ventral aspect (Figure 5-5). The external carotid artery and its branches and the facial nerve traverse over the lateral compartment (Figure 5-6).

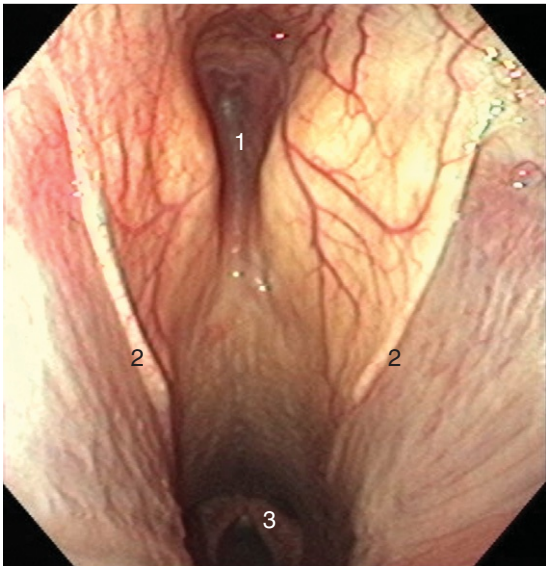

FIGURE 5-1. *1,* Dorsal pharyngeal recess; *2,* pharyngeal openings of auditory tubes; *3,* corniculate process of arytenoid cartilage.

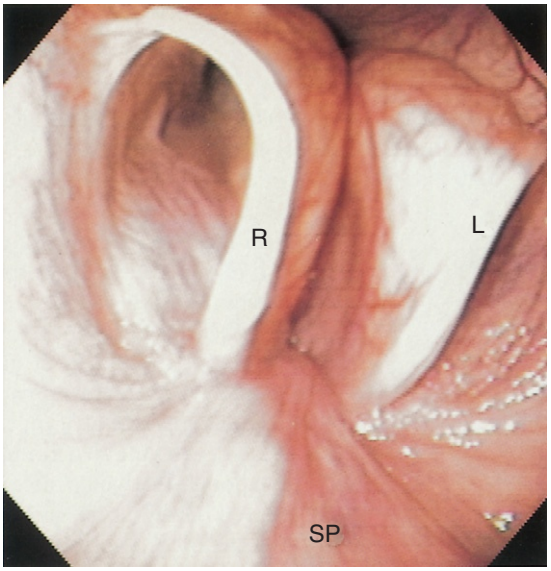

FIGURE 5-2. Right *(R)* and left *(L)* cartilaginous flaps of guttural pouches open during swallowing; *SP,* soft palate. (From Traub-Dargatz JL, Brown CM: *Equine endoscopy,* ed 2, St Louis, 1997, Mosby.)

FIGURE 5-3. Wire guide is passed through endoscopic biopsy port into left guttural pouch. Endoscope is pushed forward and rotated to gain entry into guttural pouch.

FIGURE 5-4. Salpingopharyngeal fold *(arrows).* It is theorized that excessive length of this fold causes air trapping in guttural pouch, resulting in guttural pouch tympany.

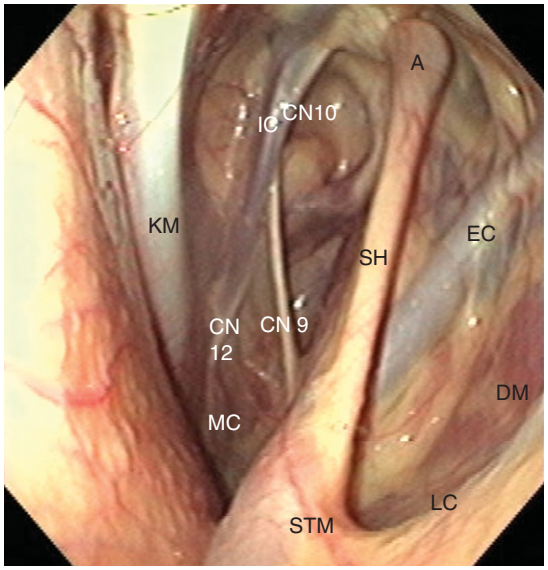

FIGURE 5-5. Normal left guttural pouch. *A,* Articulation of stylohyoid and petrous part of temporal bone; *CN9,* cranial nerve 9; *CN10,* cranial nerve 10; *CN12,* cranial nerve 12; *DM,* digastricus muscle; *EC,* external carotid artery; *IC,* internal carotid artery; *LC,* lateral compartment; *LCM,* long capitis muscle; *MC,* medial compartment; *SH,* stylohyoid bone; *STM,* stylopharyngeus muscle.

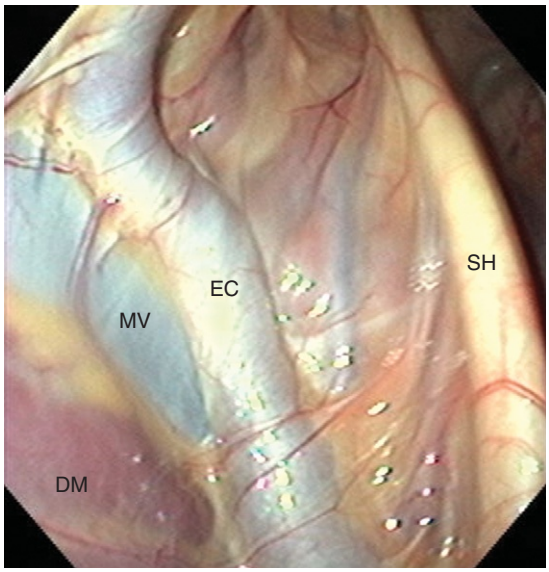

FIGURE 5-6. Normal lateral compartment. *DM,* Digastricus muscle; *EC,* external carotid artery; *MV,* maxillary vein; *SH,* stylohyoid bone.

There have been many functions proposed for the guttural pouch, but none have been proven. The pharyngeal orifice is known to dilate during swallowing, and there is an exchange of air during respiration. It has been shown experimentally that ventilation of the guttural pouch cools the blood within the internal carotid artery. The normal exchange of air during respiration may be a brain-cooling device to dissipate heat produced by muscular exertion.

DISORDERS OF THE GUTTURAL POUCH (Figures 5-7 to 5-42)

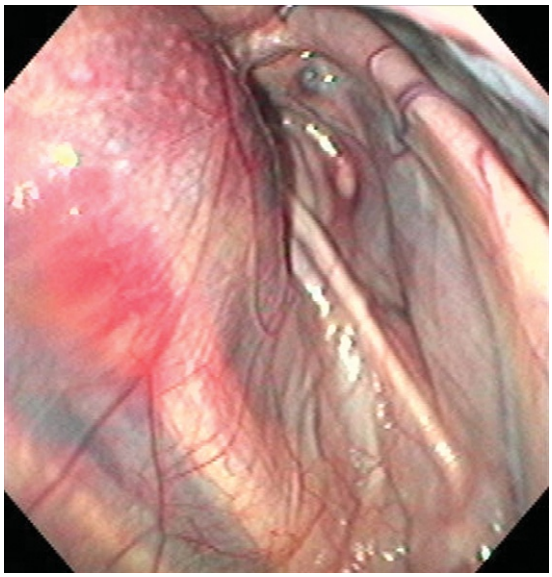

FIGURE 5-7. Left guttural pouch. Swelling associated with dorsal and medial aspect of medial compartment is caused by hemorrhage due to trauma and fracture of basisphenoid bone at attachment of longus capitis muscle. Similar hemorrhage and swelling were apparent in right guttural pouch. Clinically foal exhibited head tilt and nystagmus.

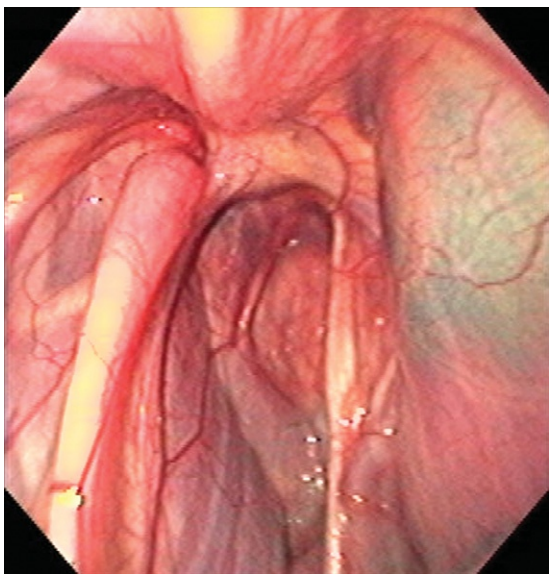

FIGURE 5-8. Right guttural pouch. Less swelling caused by hemorrhage from fracture of basisphenoid bone.

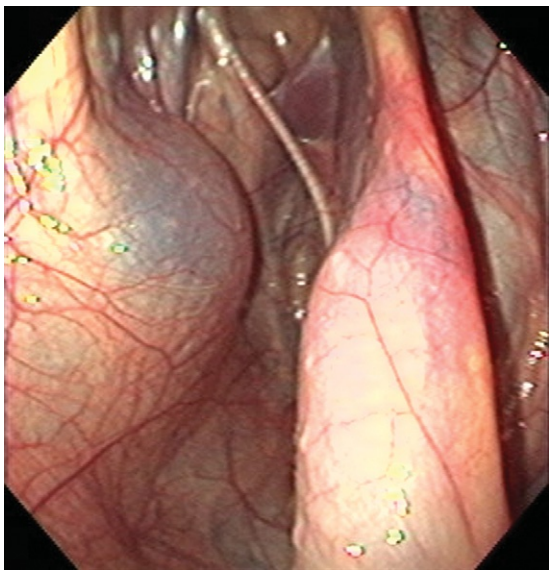

FIGURE 5-9. Left guttural pouch. Swelling associated with ventral and medial aspect of medial compartment is caused by tympany of adjacent guttural pouch.

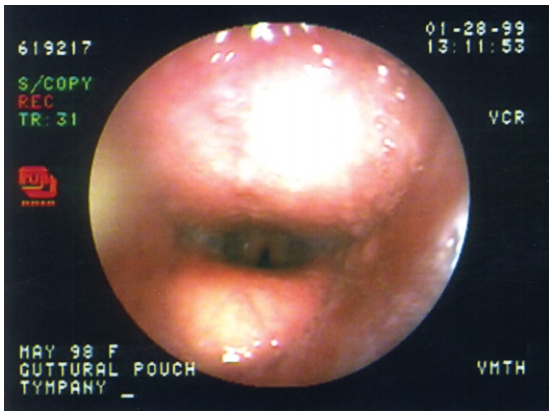

FIGURE 5-10. One-year-old miniature horse was seen with stertorous respiratory distress. Pharyngeal compression due to bilateral guttural pouch tympany was found.

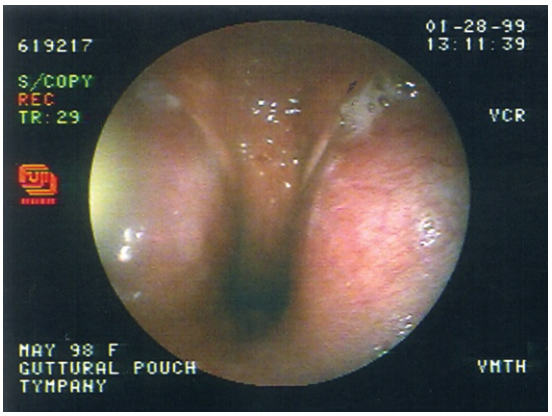

FIGURE 5-11. Another view of nasopharynx illustrating marked air distention of both guttural pouches.

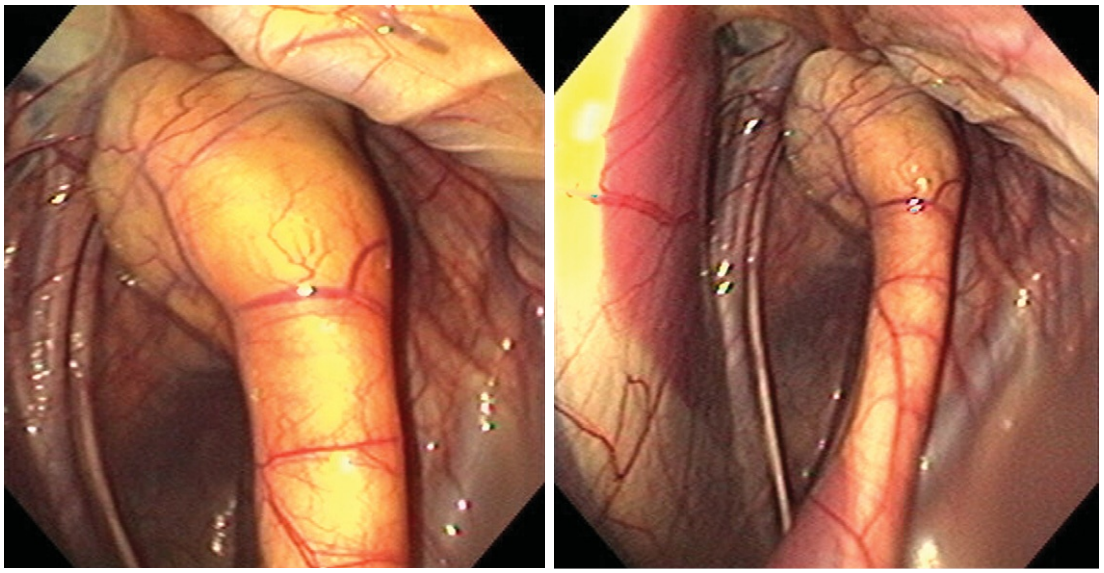

FIGURE 5-12. **A** and **B,** Both photos depict osseous proliferation of proximal portion of stylohyoid bone in left guttural pouch resulting from otitis media/interna. Clinically this colt exhibited facial paralysis and head tilt.

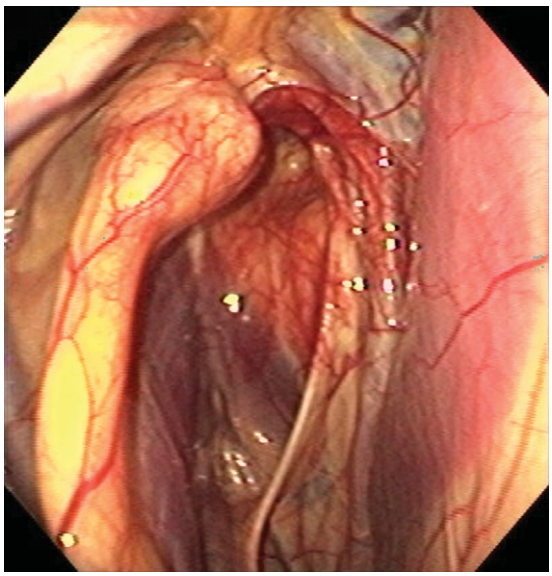

FIGURE 5-13. Right guttural pouch. Additional example of moderate proliferation of proximal portion of stylohyoid bone. Note hyperemic mucosa in dorsal aspect of medial compartment.

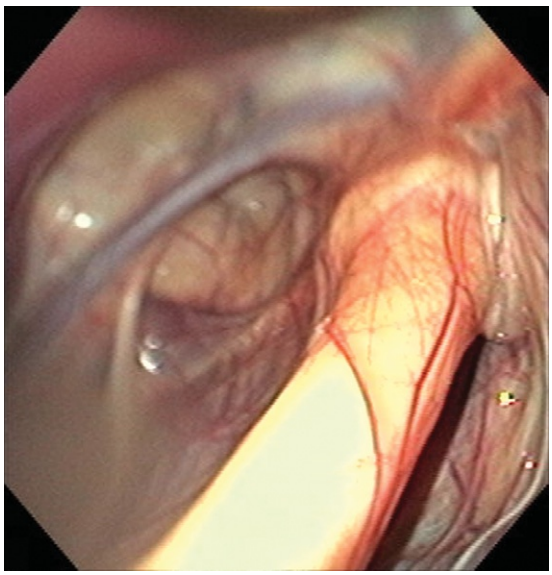

FIGURE 5-14. Mild proliferation of proximal portion of stylohyoid bone.

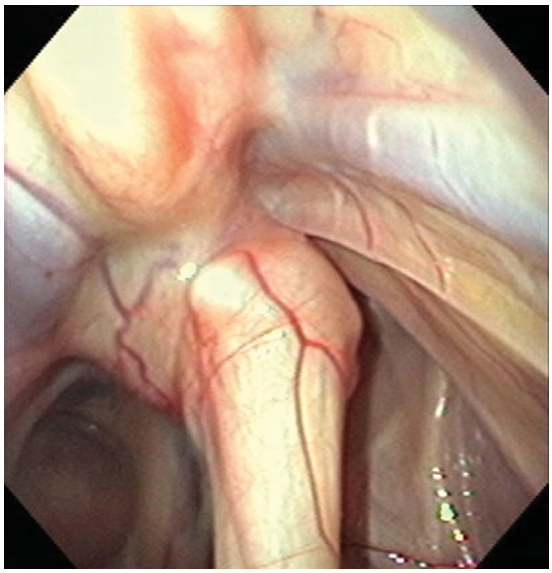

FIGURE 5-15. Mild proliferation of proximal portion of stylohyoid bone.

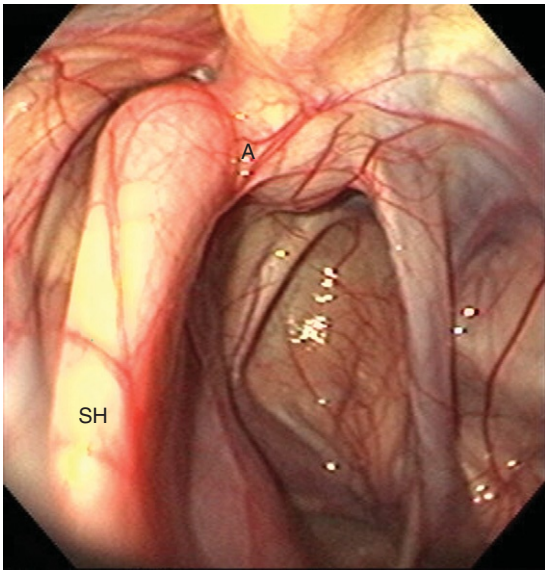

FIGURE 5-16. Normal stylohyoid bone *(SH)* articulation *(A)* with petrous temporal bone (temporohyoid joint) in right guttural pouch of 3-month-old foal.

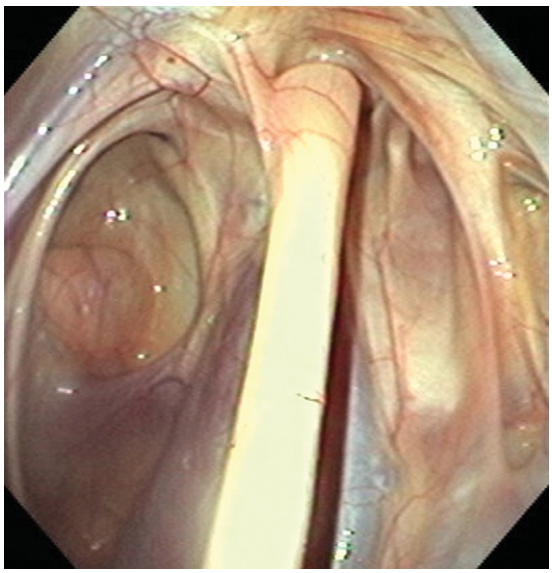

FIGURE 5-17. Normal stylohyoid bone in left guttural pouch of adult horse.

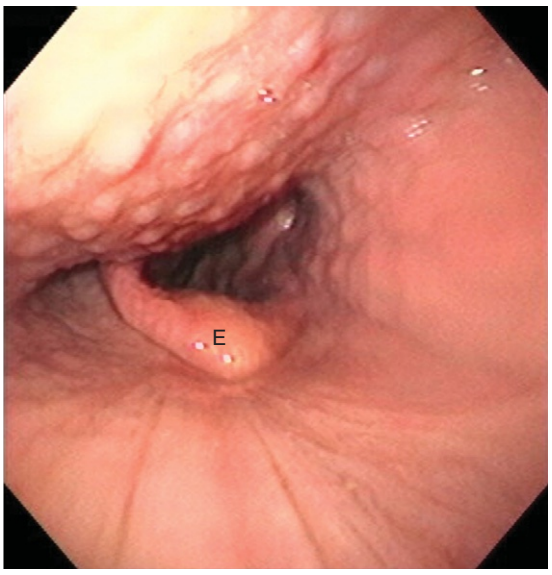

FIGURE 5-18. Dorsal and lateral pharyngeal compression resulting from retropharyngeal lymph node enlargement into right guttural pouch. *E,* Epiglottis.

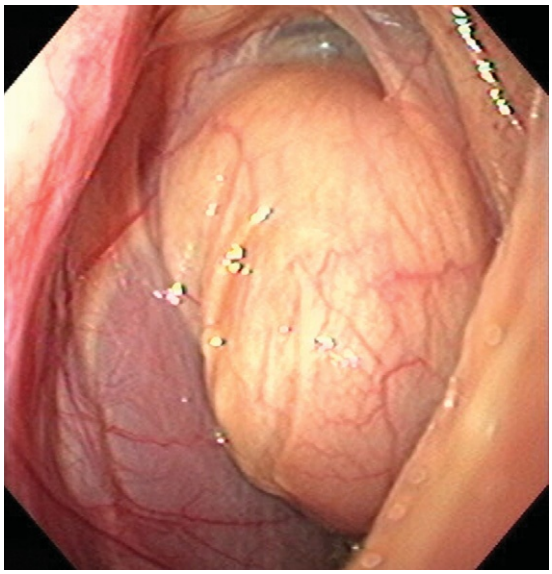

FIGURE 5-19. Enlarged retropharyngeal lymph node protruding into right guttural pouch lateral compartment.

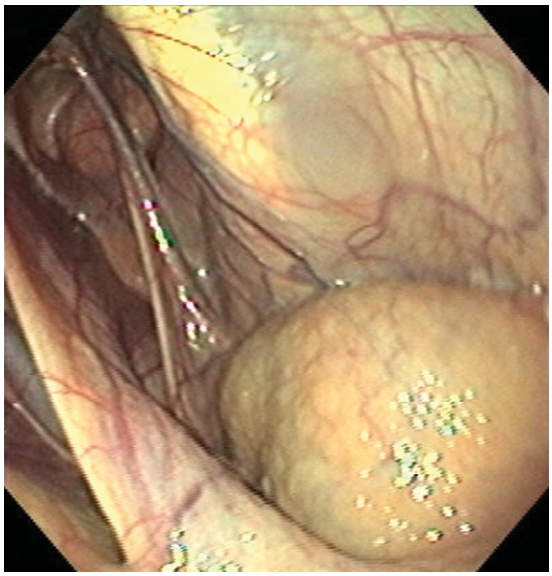

FIGURE 5-20. Additional example of enlarged retropharyngeal lymph node on floor of right medial compartment.

FIGURE 5-21. Suppurative lymph node just beginning to drain into guttural pouch.

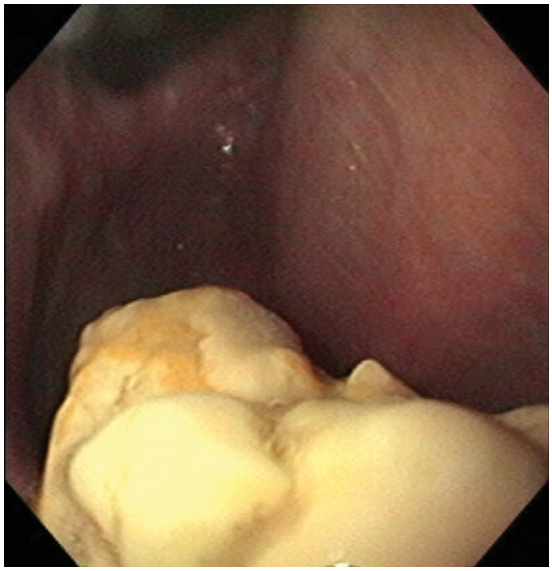

FIGURE 5-22. Chondroids in right guttural pouch.

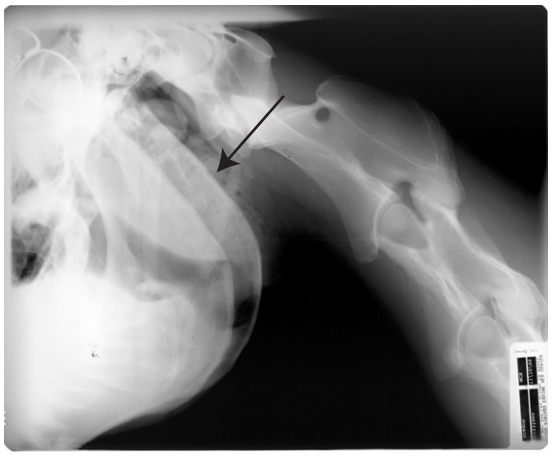

FIGURE 5-23. Radiographic image depicting chondroids within guttural pouch *(arrow).*

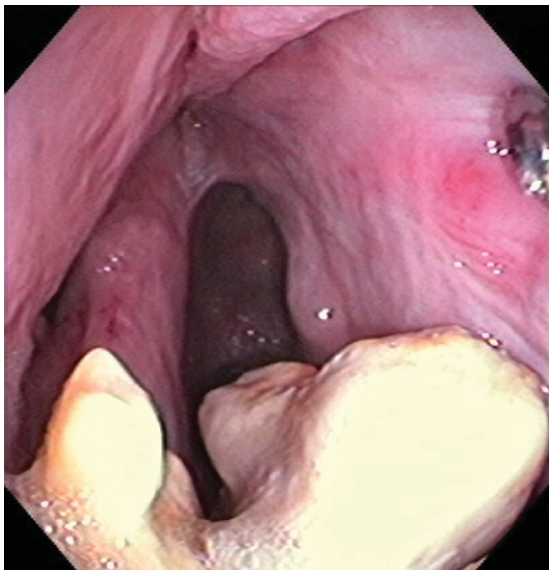

FIGURE 5-24. Fragmentation of chondroids using snare passed through biopsy port of endoscope.

A

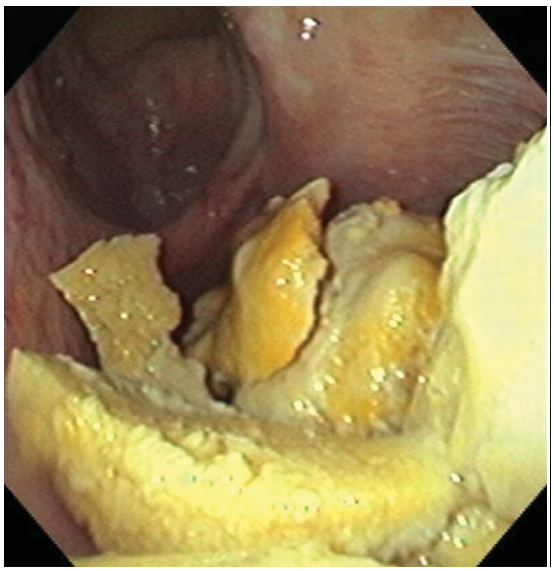

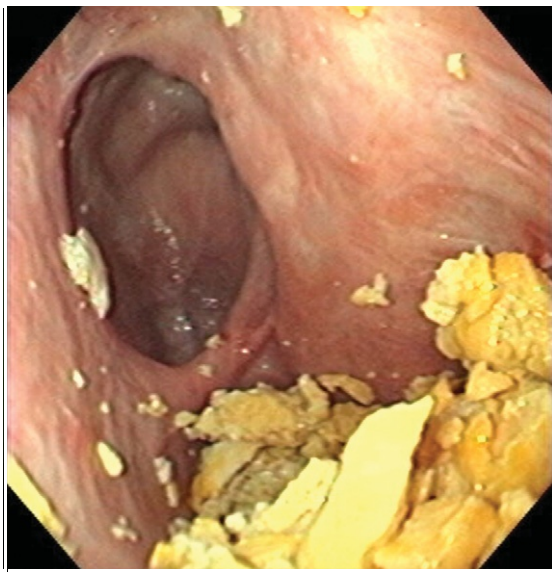

B

FIGURE 5-25. A and **B,** Chondroids after several cuts using endoscopic snare. Note fibrous adhesions within right guttural pouch.

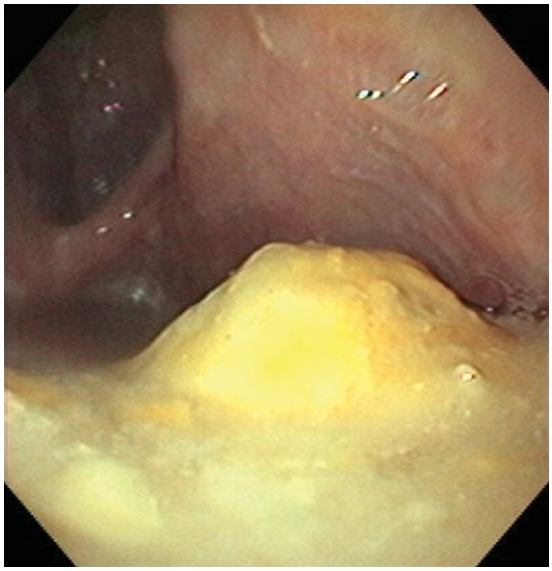

FIGURE 5-26. Chondroids after soaking in solution of 20% acetylcysteine for 12 hours.

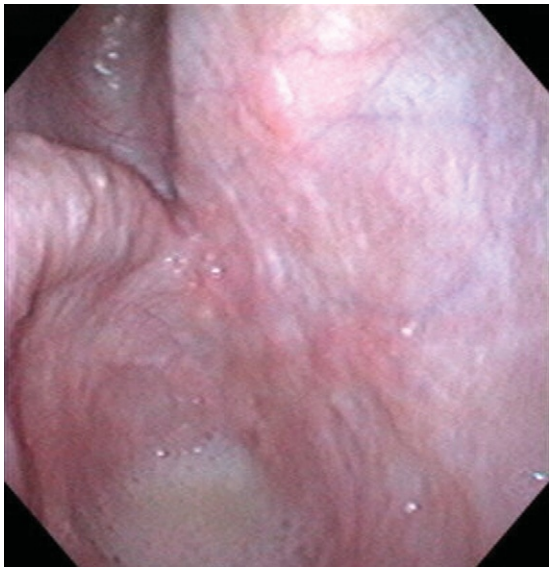

FIGURE 5-27. Empty guttural pouch after weeks of chondroid fragmentation using snare and intermittent administration of 20% acetylcysteine followed by lavage.

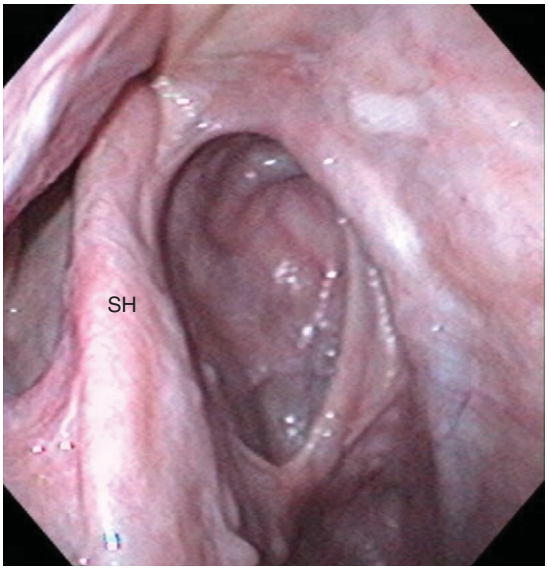

FIGURE 5-28. Empty guttural pouch after chondroid removal. Notice thickened lining of medial compartment and stylohyoid bone *(SH)* caused by chronic inflammation resulting from presence of chondroids.

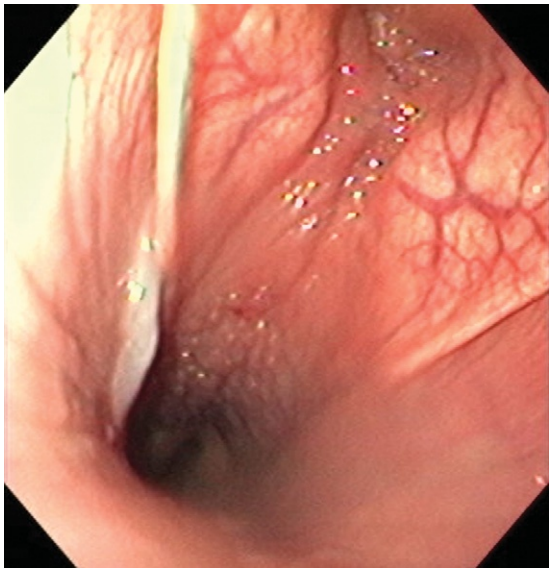

FIGURE 5-29. Mucopurulent exudates draining from nasopharyngeal opening of right guttural pouch associated with guttural pouch empyema.

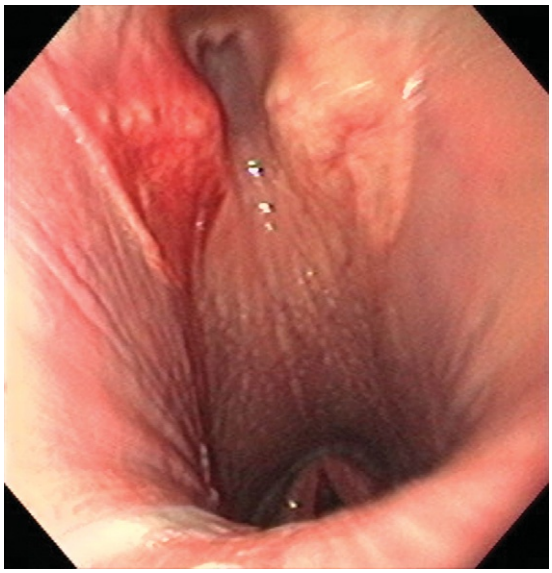

FIGURE 5-30. Note hyperemic mucus covering right guttural pouch pharyngeal opening due to *Streptococcus equi* infection of guttural pouch. Some hemorrhage could also be noted exiting pouch.

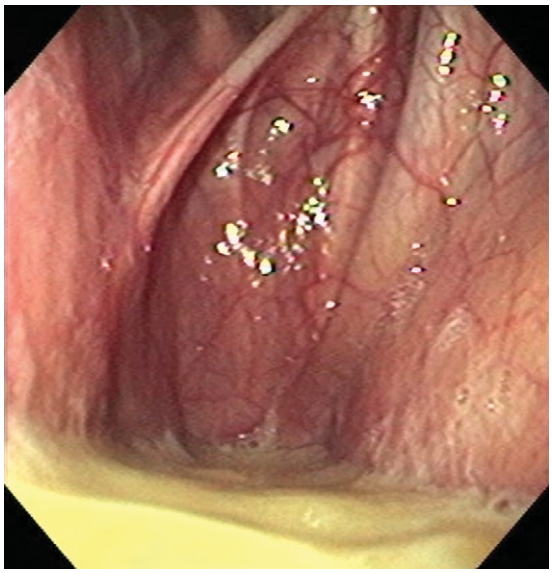

FIGURE 5-31. Guttural pouch empyema generally results from upper airway infection involving *Streptococcus* spp.

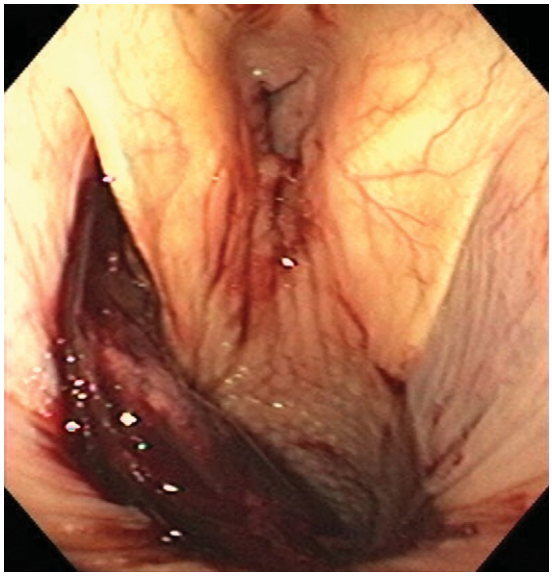

FIGURE 5-32. Hemorrhage from right guttural pouch opening. In this case, hemorrhage is caused by fungal erosion adjacent to right internal carotid artery.

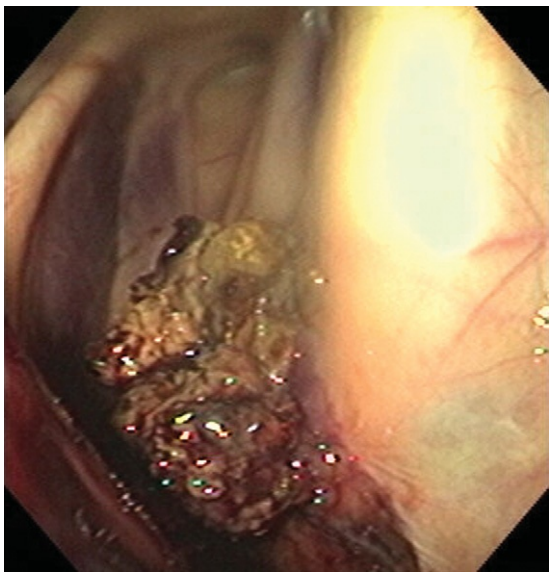

FIGURE 5-33. Guttural pouch mycosis. This isolated plaque is caused by *Aspergillus* spp. and is located on longus capitis muscle near internal carotid artery.

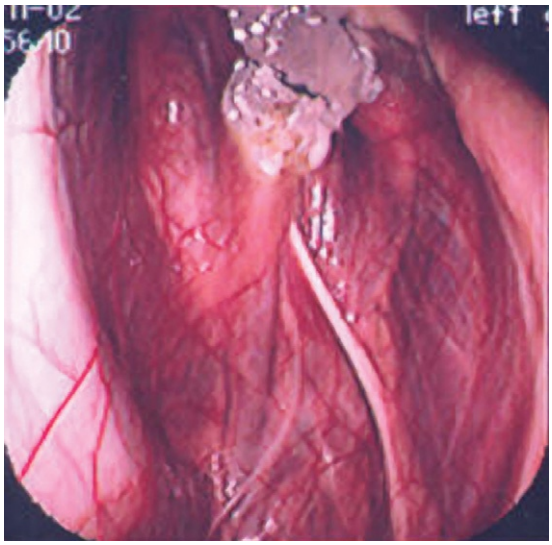

FIGURE 5-34. Additional example of guttural pouch mycosis. This lesion is located on the internal carotid artery.

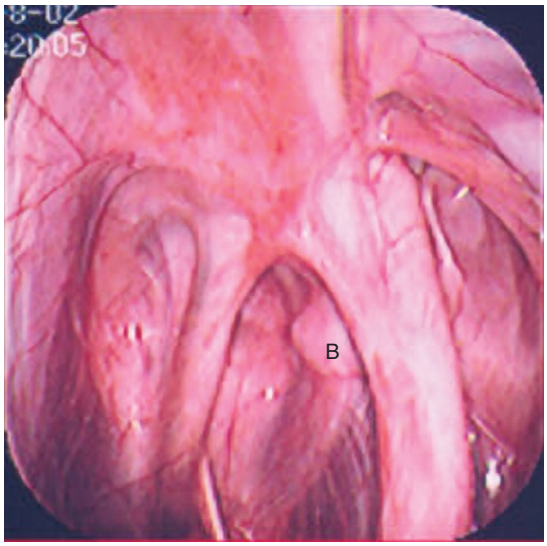

FIGURE 5-35. Guttural pouch mycosis (Figure 5-34) 1 month after treatment using arterial balloon occlusion *(B)*.

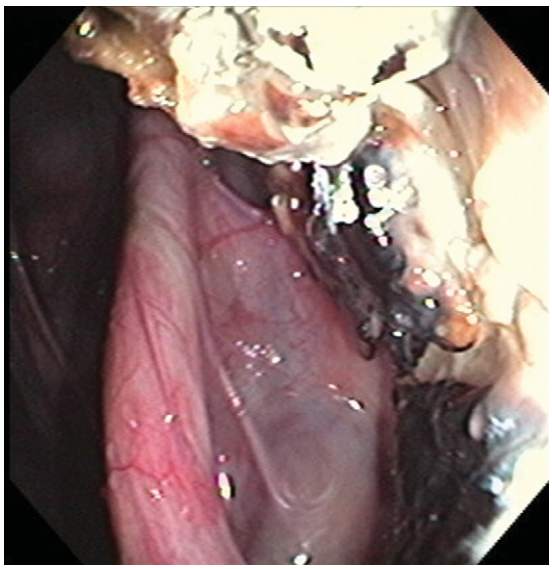

FIGURE 5-36. Left guttural pouch mycosis associated with chronic left nasal discharge. Note fungal plaques.

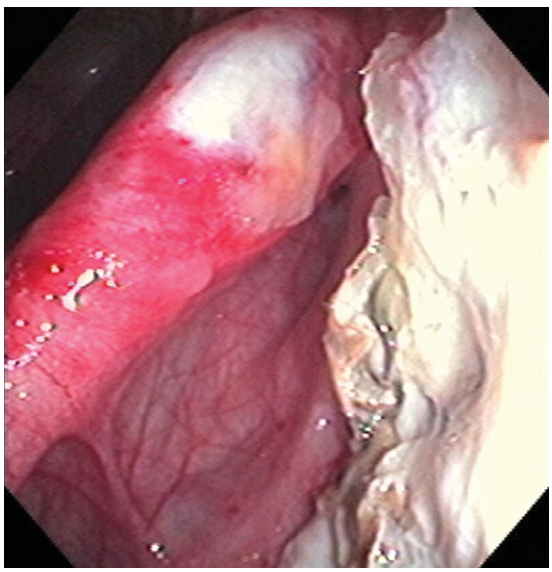

FIGURE 5-37. Additional view of left guttural pouch mycosis caused by *Aspergillus* spp.

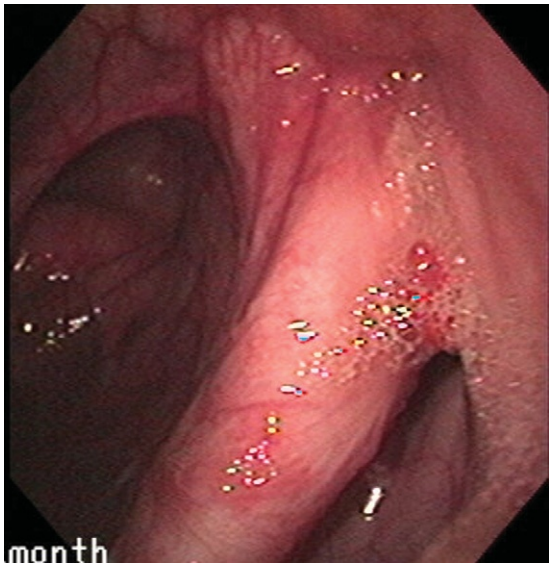

FIGURE 5-38. Guttural pouch mycosis (Figures 5-36 and 5-37) 1 month after coil embolization.

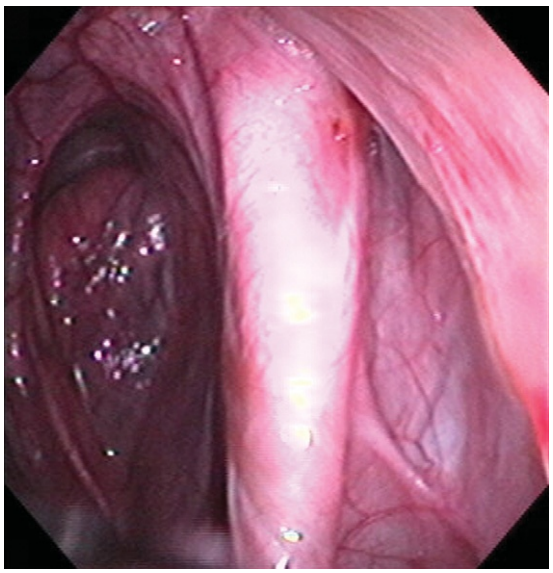

FIGURE 5-39. Guttural pouch mycosis (Figures 5-36–5-38) 2 months after coil embolization.

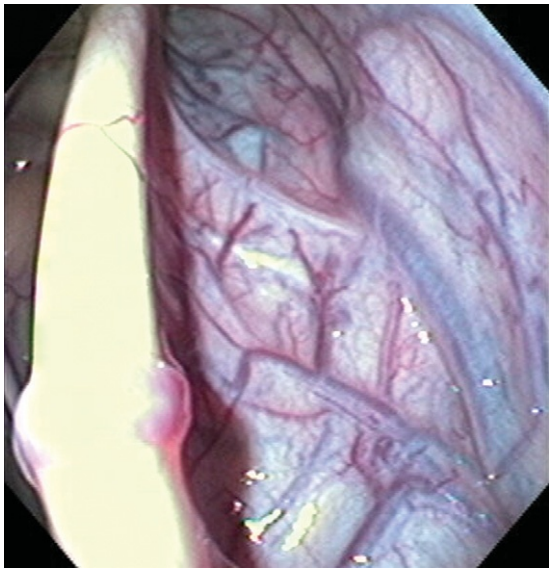

FIGURE 5-40. Congested vessels within guttural pouch due to jugular vein abscess formation.

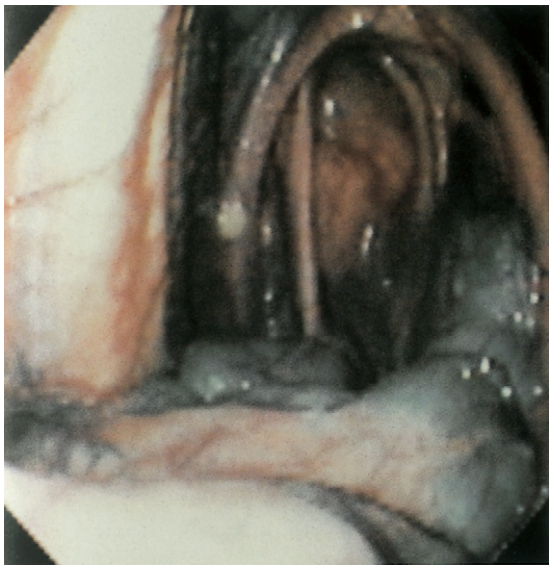

FIGURE 5-41. Melanomas on floor of medial compartment of left guttural pouch. (From Traub-Dargatz JL, Brown CM: *Equine endoscopy,* ed 2, St Louis, 1997, Mosby.)

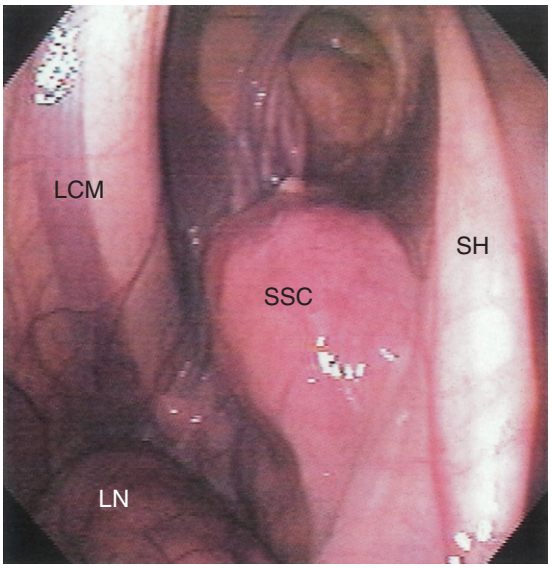

FIGURE 5-42. Squamous cell carcinoma *(SCC)* on floor of medial compartment of left guttural pouch. *LN,* Enlarged retropharyngeal lymph node; *LCM,* longus capitis muscle; *SH,* stylohyoid bone. (From Traub-Dargatz JL, Brown CM: *Equine endoscopy,* ed 2, St Louis, 1997, Mosby.)

CHAPTER 6

Tracheobronchoscopy

EDWARD VOSS • THOMAS SEAHORN

NORMAL ANATOMY

The dorsal view of the equine bronchial tree is seen in Figure 6-1; Figure 6-2 shows the lateral view. The equine trachea is the flexible air conduit between the larynx and carina. Four layers comprise the wall of the trachea (adventitia, musculocartilaginous, submucosa, and mucosa). The outermost layer is adventitia, a connective tissue layer that blends with the underlying musculocartilaginous layer. This musculocartilaginous layer consists of 40 to 60 dorsally incomplete, fibrocartilaginous rings connected at their open ends by smooth tracheal muscle. The elastic submucosa may contain tracheal glands and some fat cells whereas the inner ciliated mucosa lines the tracheal lumen.

As the direct continuation of the larynx, the trachea begins at the infraglottic region of the larynx (Figure 6-3) where subtle longitudinal folding of the mucosa can be seen

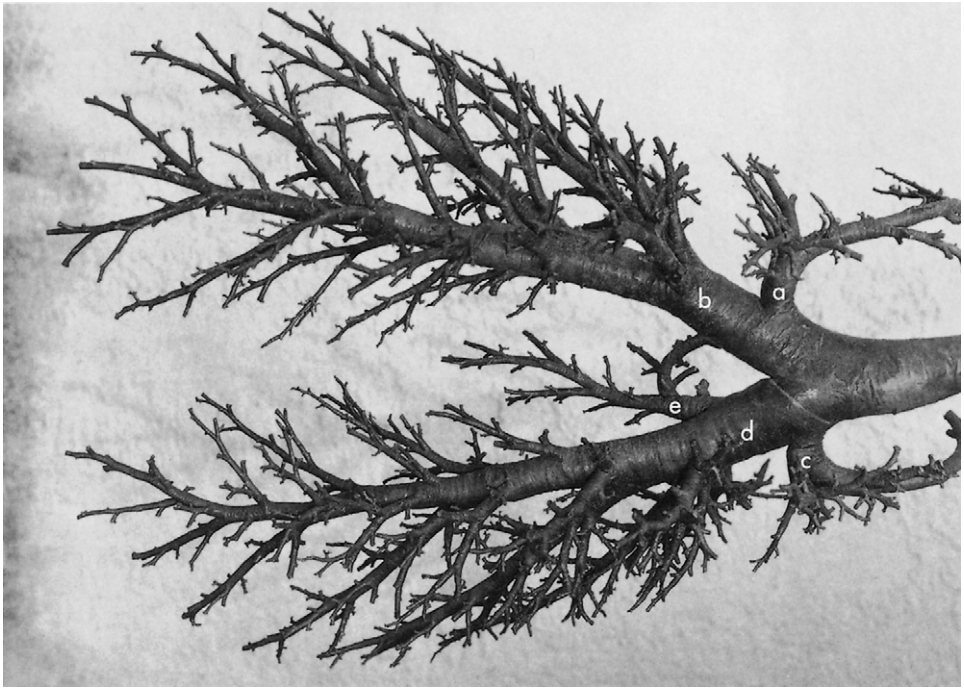

FIGURE 6-1. Plastic mold of equine bronchial tree, dorsal view. *a,* Left cranial lobar bronchus (LB1); *b,* left caudal lobar bronchus (LB2); *c,* right cranial lobar bronchus (RB1); *d,* right caudal lobar bronchus (RB2); *e,* right accessory lobar bronchus (RB3). (From Traub-Dargatz JL, Brown CM: *Equine endoscopy,* ed 2, St Louis, 1997, Mosby.)

FIGURE 6-2. Plastic mold of equine bronchial tree, right lateral view. *a,* Right cranial lobar bronchus, first segmental bronchus (RB1, 1D); *b,* right caudal lobar bronchus, first segmental bronchus (RB2, 1V); *c,* right caudal lobar bronchus, second segmental bronchus (RB2, 2D); *d,* right caudal bronchus, third segmental bronchus (RB2, 3V); *e,* right caudal lobar bronchus, fourth segmental bronchus (RB2, 4D). (From Traub-Dargatz JL, Brown CM: *Equine endoscopy,* ed 2, St Louis, 1997, Mosby.)

FIGURE 6-3. Endoscope is within larynx looking into infraglottic region with vocal folds framing view.

(Figure 6-4). At the origin, the tracheal lumen is relatively circular (Figure 6-5) with an average diameter of 5 to 6 cm but becomes progressively more dorsoventrally flattened. The fine lateral and dorsal vascular pattern of the tracheal wall becomes more noticeable (Figure 6-6). There is some variation in the dorsoventral luminal flattening with the phase of respiration especially in the cervical region (Figures 6-7 and 6-8). The thoracic trachea tends to become less dorsoventrally flattened (Figure 6-9), and the distal dorsoventral tracheal lumen diameter may actually become greater than the transverse diameter.

FIGURE 6-4. Visualization of infraglottic region and very slight longitudinal folding of mucosa.

FIGURE 6-5. Five centimeters distal to infraglottic region, tracheal lumen is nearly circular. Individual cartilaginous rings are visible.

FIGURE 6-6. Tracheal lumen shape transitions from circular to dorsoventrally flattened in proximal cervical trachea. Note more visible vascular pattern on dorsal and ventral wall of trachea.

FIGURE 6-7. Midcervical trachea during inspiration showing more dorsoventral flattening.

FIGURE 6-8. Decreased dorsoventral diameter during expiration in same midcervical location as in Figure 6-7.

FIGURE 6-9. Thoracic tracheal lumen returns to near circular in shape. Note carina in background.

At the carina the trachea bifurcates into the right and left principle bronchi (Figures 6-10 and 6-11). The right principal bronchus gives off the right cranial lobar bronchus from its lateral aspect (Figure 6-12), then continues to give off the right accessory lobar bronchus from its ventromedial aspect, the right caudal lobar first segmental bronchus from its ventrolateral aspect, and the right caudal lobar second segmental bronchus from the dorsolateral aspect, and continues as the right caudal lobar bronchus (Figure 6-13). Further advancement down the right caudal lobar bronchus reveals smaller segmental bronchi (Figures 6-14 and 6-15). The left principal bronchus has no accessory lobar bronchus but otherwise is similar to the right bronchus in that the left cranial lobar bronchus branches from the lateral aspect, the caudal lobar first ventral segmental bronchus arises from the ventral aspect, and the left caudal lobar bronchus continues distally (Figures 6-16 and 6-17). Further segmental bronchi are observed with scope advancement within the caudal lobar bronchus (Figure 6-18).

FIGURE 6-10. Very distal trachea is often narrowed transversely and wider dorsoventrally.

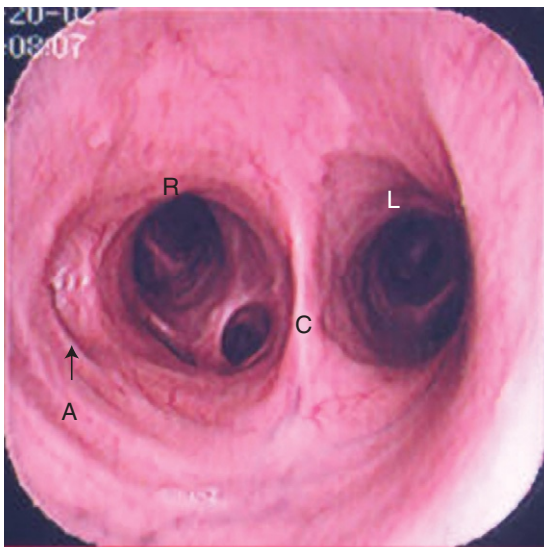

FIGURE 6-11. Carina *(C)* showing right *(R)* and left *(L)* principal bronchi and cranial lobar bronchus *(A)*.

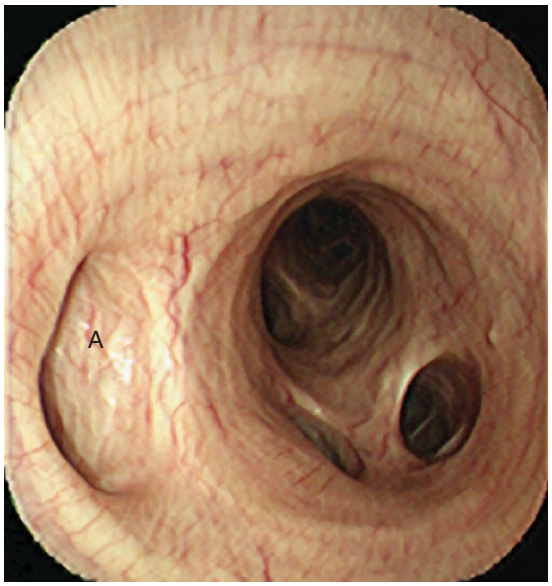

FIGURE 6-12. Looking down right principal bronchus. Cranial lobar bronchus *(A)* can be observed exiting lateral wall.

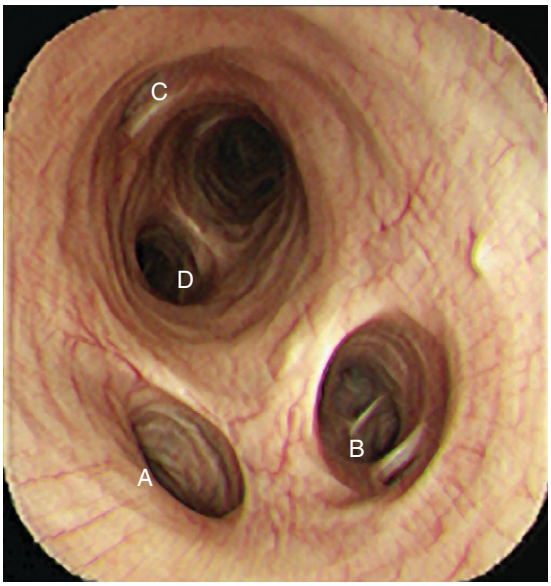

FIGURE 6-13. Advancing down right principal bronchus, principal bronchus gives off first segmental caudal lobar bronchus *(A),* accessory lobar bronchus *(B),* second segmental caudal lobar bronchus *(C),* and continues as caudal lobar bronchus *(D).*

FIGURE 6-14. Advancement down right caudal lobar bronchus allows visualization of bifurcating segmental bronchi.

FIGURE 6-15. Advancement of endoscope down these segmental bronchi allows visualization of small segmental bronchi within right caudal lung lobe.

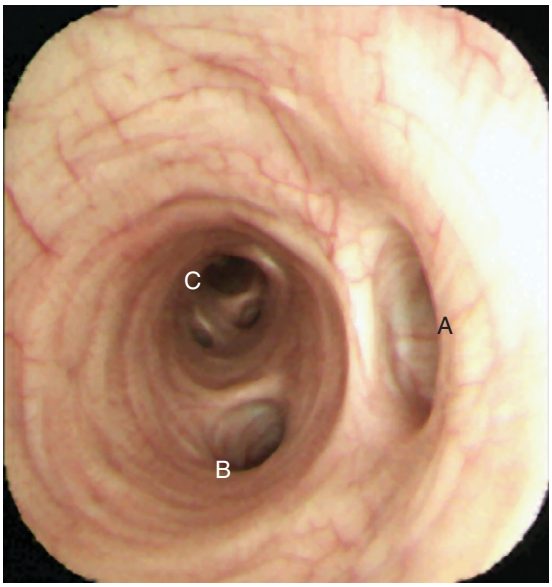

FIGURE 6-16. Looking down left principal bronchus. Left cranial lobar bronchus *(A)* is seen exiting lateral wall, first ventral caudal lobar segmental bronchus exits ventrally *(B)*, and caudal lobar bronchus *(C)* continues.

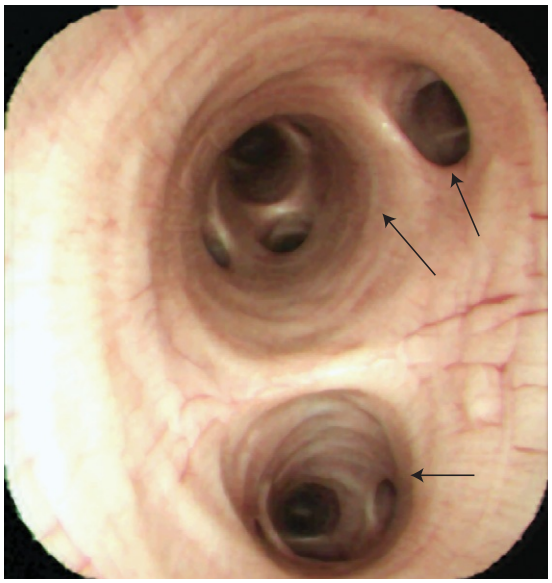

FIGURE 6-17. Advancement of endoscope into left caudal lobar bronchus. Segmental bronchi divide bronchus.

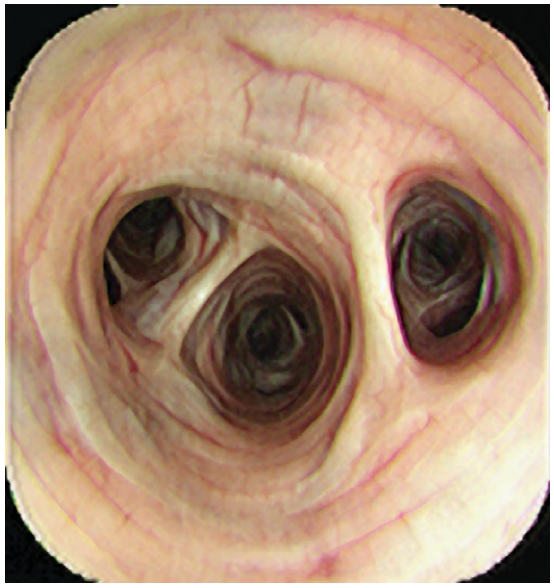

FIGURE 6-18. Deeper down left caudal segmental bronchus. Lumen of airways is rapidly tapering at this level.

EXUDATE

When normal mucociliary clearance of the tracheobronchial tree is insufficient, mucus and exudative products accumulate, and tracheal exudate is observed. Mild tracheal exudate can be seen throughout the tracheobronchial tree (Figures 6-19 to 6-21). More moderate amounts of mucus often are accompanied by mucosal hyperemia, and the pooling is greatest in the caudal cervical/thoracic tracheal segment due to gravity (Figures 6-22 to 6-25). Endoscopic evaluation while a cough occurs results in tenacious pooled mucus being "sprayed" onto the tracheal walls (Figure 6-26). In contrast to the tenacious cream/tan color of exudate, saliva in the tracheobronchial tree is less viscous, easily foamed, and nearly pure white (Figure 6-27).

Collection of tracheal exudate (transtracheal wash) can be obtained through the endoscope using a guarded aspiration catheter (Mila International, Florence, KY) (Figure 6-28).

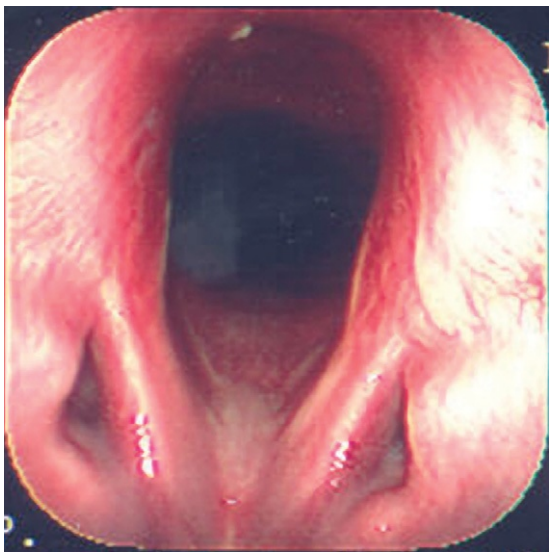

FIGURE 6-19. Mild exudate is noted in ventral rima glottidis.

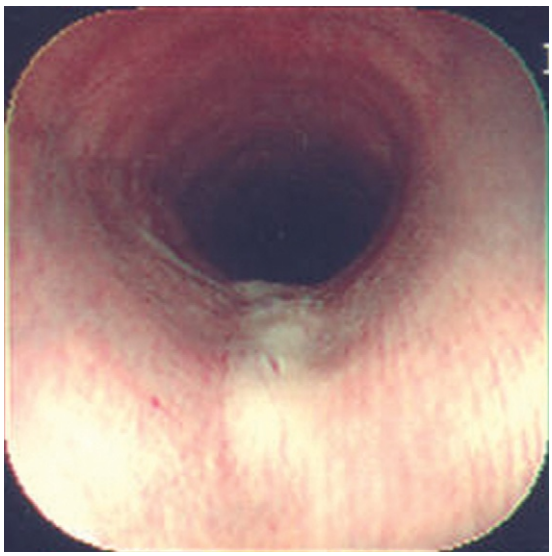

FIGURE 6-20. Mild mucopurulent exudate in ventral aspect of proximal cervical trachea.

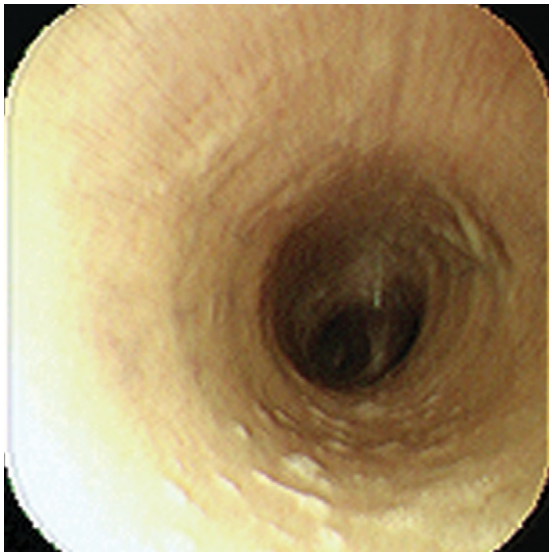

FIGURE 6-21. Mucopurulent exudate in distal trachea. Note exudate is in most ventral aspect of trachea.

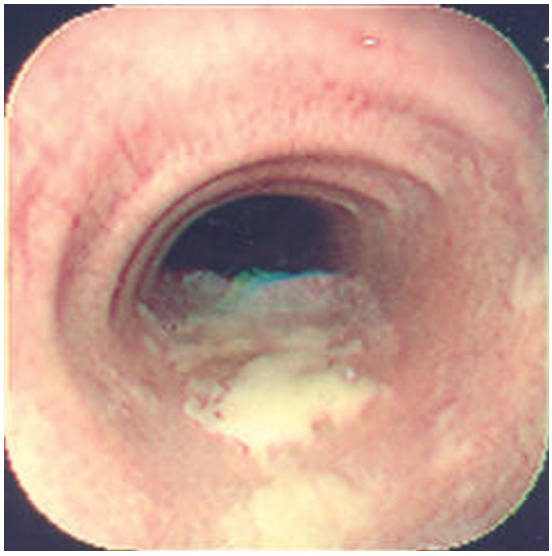

FIGURE 6-22. Moderate amount of mucopurulent exudate in cervical trachea.

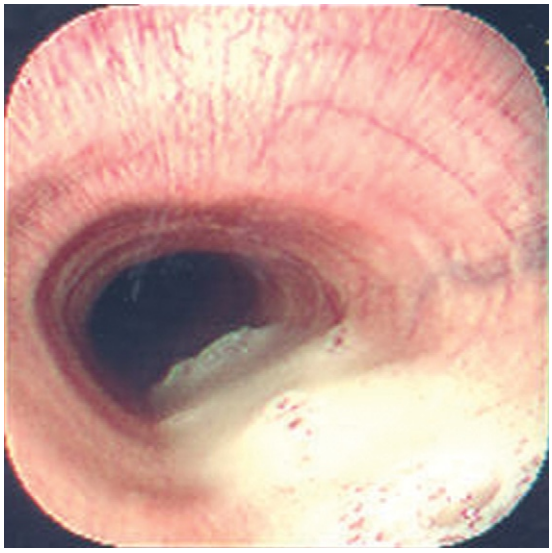

FIGURE 6-23. Moderate mucopurulent exudate in thoracic trachea. Very mild hyperemia is evident.

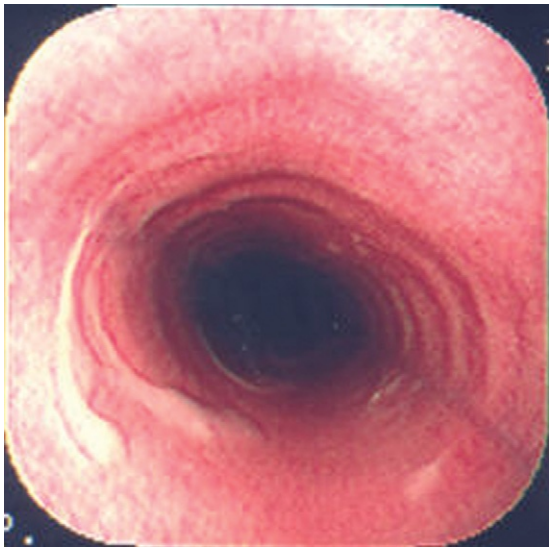

FIGURE 6-24. Cervical tracheal hyperemia and inflammation with tenacious exudate attached to lateral walls of trachea.

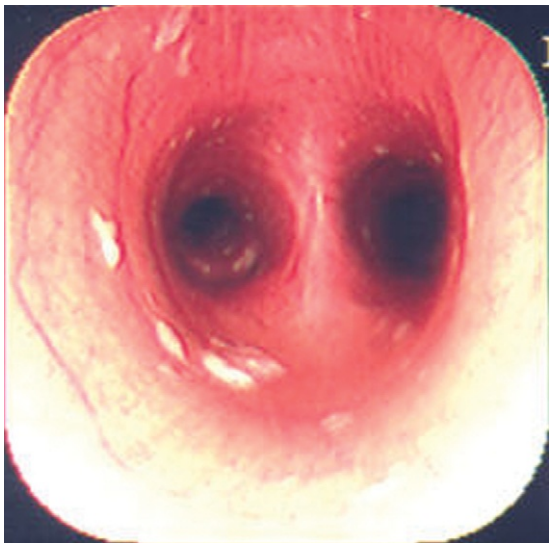

FIGURE 6-25. Tracheitis of distal trachea/carina with tenacious exudate and marked hyperemia.

FIGURE 6-26. Tenacious mucopurulent exudate sprayed onto walls of proximal trachea during coughing.

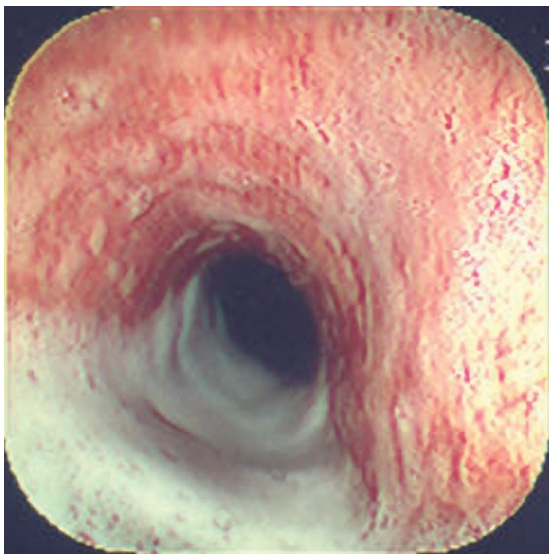

FIGURE 6-27. Saliva aspirated into tracheal lumen. Notice foamy character and true white hue of fluid within trachea.

FIGURE 6-28. Transtracheal wash being performed through endoscope with use of guarded aspiration catheter. Endoscope is passed to level approximately 90 cm from nose (in adult) and catheter is passed beyond tip of endoscope. Animal is sedated with combination of xylazine and butorphanol (antitussive) and 60 ml of saline is then infused and aspirated from pool at level of thoracic inlet. *NOTE:* If animal coughs during procedure then your sample will be contaminated (because the infused fluid would have "splashed" onto unsterile scope).

CHRONIC OBSTRUCTIVE PULMONARY DISEASE

Chronic obstructive pulmonary disease (COPD) is a chronic, noninfectious respiratory disease characterized by increased mucus production and bronchoconstriction. The disease is insidious in onset and progressive. Although there is debate about the primary cause, the most commonly recognized cause is exposure to dust, molds, or other air pollutants. Other triggering agents include respiratory tract infections and hereditary factors (Figures 6-29 and 6-30).

FIGURE 6-29. Increased mucus production in distal airways in horse with 2-month history of increased respiratory effort and abdominal lift during summer months. Bronchoalveolar lavage was performed, and results of cytologic examination were consistent with those of horse suffering from severe small airway inflammation (commonly known as COPD).

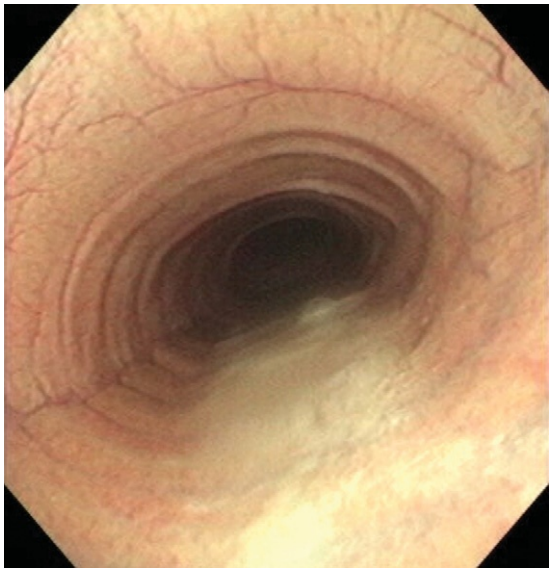

FIGURE 6-30. Note extensive mucus in proximal trachea of adult horse with COPD.

EXERCISE-INDUCED PULMONARY HEMORRHAGE

Exercise-induced pulmonary hemorrhage (EIPH) is a common occurrence in racehorses. Some experts believe that every racehorse has some degree of pulmonary hemorrhage during strenuous exercise.

The etiopathogenesis of EIPH is unknown, but currently four hypotheses appear to be tenable:

1. Chronic lower airway inflammation that results in bronchial neovascularization
2. Stress-induced rupture of the pulmonary capillaries resulting from increased cardiac output
3. Platelet dysfunction leading to predisposition to hemorrhage
4. Trauma induced by locomotory impact through wave propagation

Diagnosis consists of the following:

- Gross epistaxis
- Evidence of blood in the trachea via an endoscope (Figures 6-31 to 6-33)
- Hemosiderophages in the bronchial alveolar fluid

Treatment/prevention of the disorder may include the following:

- Furosemide: a loop diuretic that causes plasma volume depletion and decreases the pulmonary and circulatory pressures
- Proper training: a fit horse (conditioned heart)
- Suspicion of a lower airway bacterial disease: perform a transtracheal wash (TTW) and give the patient appropriate antibiotics
- Proper rest period: allow lung parenchyma to heal (6 to 8 weeks if severe)
- Fix any upper respiratory tract anatomic anomalies
- Reduce small airway inflammation (inhaled bronchodilators ± inhaled glucocorticoids)

FIGURE 6-31. Tracheal hyperemia immediately after strenuous exercise and associated with EIPH.

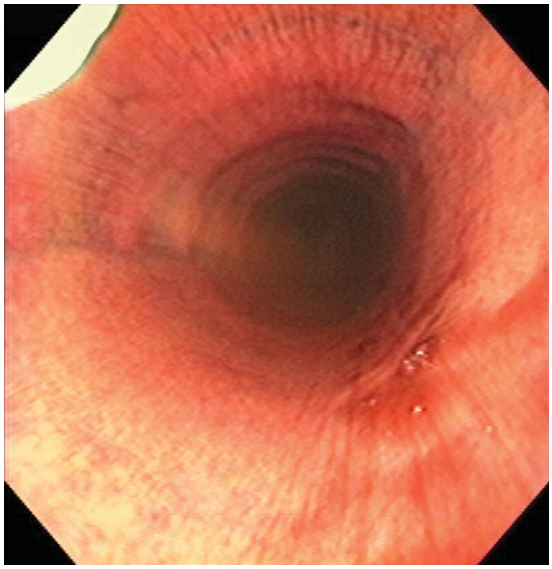

FIGURE 6-32. Small amount of serosangenous fluid in ventral trachea several hours after exercise and clinical episode of EIPH.

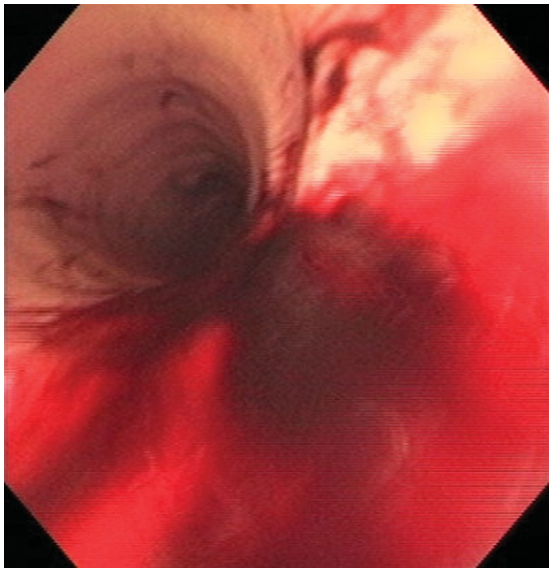

FIGURE 6-33. Large amount of blood in ventral trachea after race and clinical episode of EIPH. This horse pulled up after race with severe epistaxis from both nares and was in respiratory distress.

GRANULATION TISSUE

Generally, injury to the tracheal mucosa and submucosa (i.e., tracheal puncture or tracheostomy tube) heals remarkably well (Figure 6-34). However, substantial surface area compromise, placement of an inappropriately sized tracheostomy tube, or individual variation in wound healing can lead to proliferation of granulation tissue within the tracheal lumen (Figure 6-35). Near-complete occlusion of the tracheal lumen can result, and stenosis may be a long-term sequela (Figures 6-36 to 6-38). Small abscesses can also develop in areas of tracheal injury (Figures 6-39 and 6-40).

FIGURE 6-34. Tracheotomy tube placement as viewed from proximal to distal within tracheal lumen. Note tube has adequate clearance with far wall such that no contact with it should elicit proliferative response.

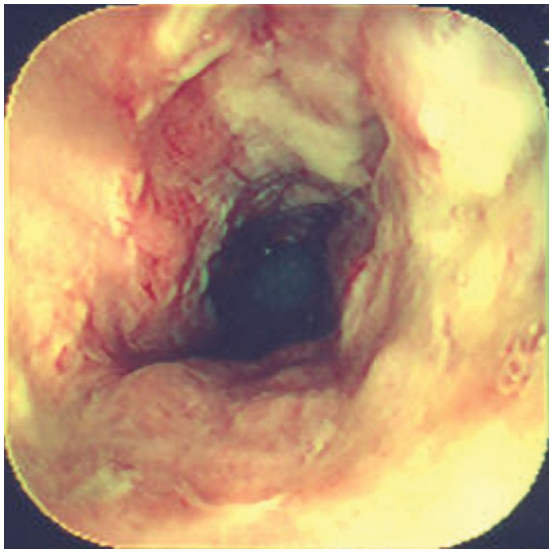

FIGURE 6-35. Moderate granulation tissue forming within tracheal lumen. Inappropriately sized tracheostomy tube caused proliferative reaction observed.

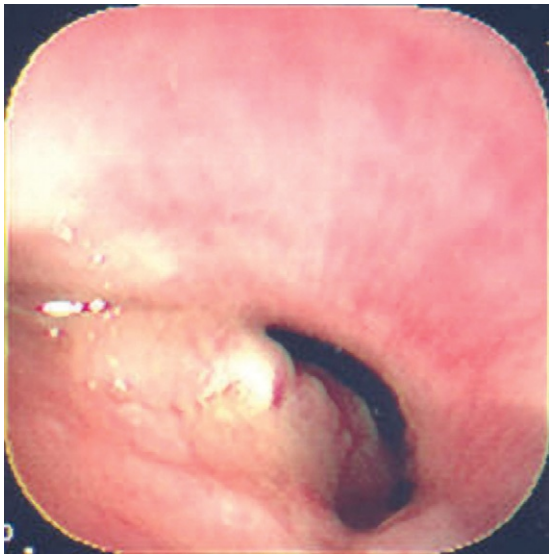

FIGURE 6-36. Near complete occlusion of tracheal lumen by proliferative granulation tissue.

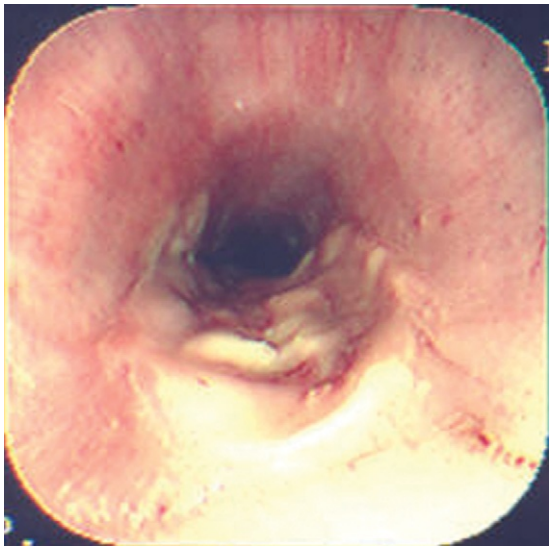

FIGURE 6-37. Early stenotic narrowing of tracheal lumen from chronic mucosal inflammation.

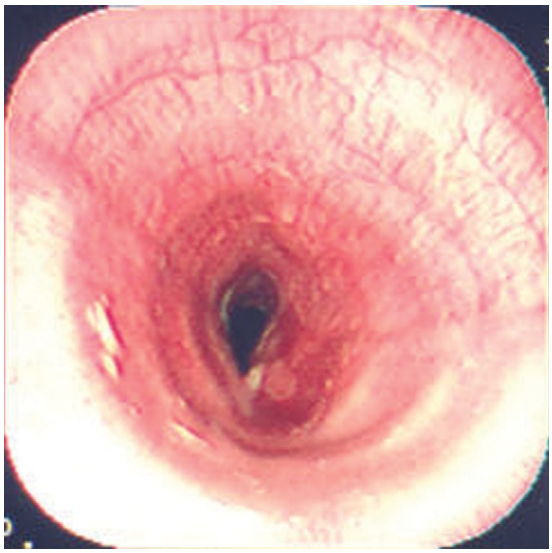

FIGURE 6-38. Severe stenosis of tracheal lumen. Note severe limitation of air flow.

FIGURE 6-39. Mare presented with chronic cough and severe respiratory stridor. A small abscess and granulation tissue just behind and distal to the corniculate process was noted in the proximal trachea. The only way to examine this area was by passing the endoscope through a tracheostomy site.

FIGURE 6-40. A snare (looping around abscess located just distal to corniculate process in proximal trachea) was used to remove abscess noted in Figure 6-39.

RUPTURE/PERFORATION

Tracheal rupture/perforation can occur from blunt or sharp trauma, but generally subcutaneous emphysema is evident (Figure 6-41).

TRACHEAL COLLAPSE

The trachea is inherently flexible, and some slight luminal "collapse" occurs naturally during the respiratory cycle (Figure 6-42). However, chronic airway disease, malformation of the hyaline cartilage rings, or trauma can result in abnormal collapse of the tracheal lumen. Generally, the trachea deforms dorsoventrally with collapse, whereas circumferential or lateral luminal narrowing occurs with stenosis. Tracheal collapse can be mild (Figure 6-43), moderate (Figures 6-44 and 6-45) or severe (Figures 6-46 to 6-49), often due to ring malformations.

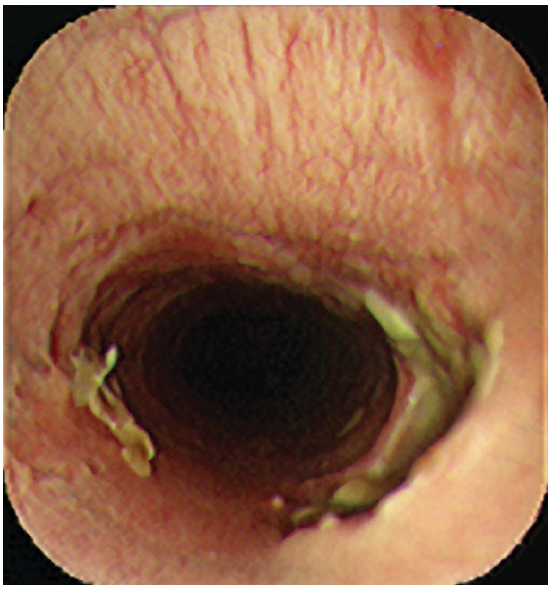

FIGURE 6-41. Traumatic perforation of trachea.

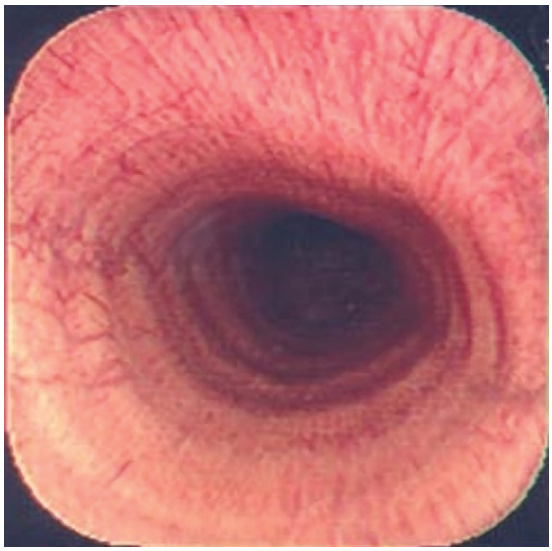

FIGURE 6-42. Minimal tracheal dorsoventral flattening with phases of respiration.

FIGURE 6-43. Mild tracheal collapse. Note increased dorsoventral flattening of tracheal lumen.

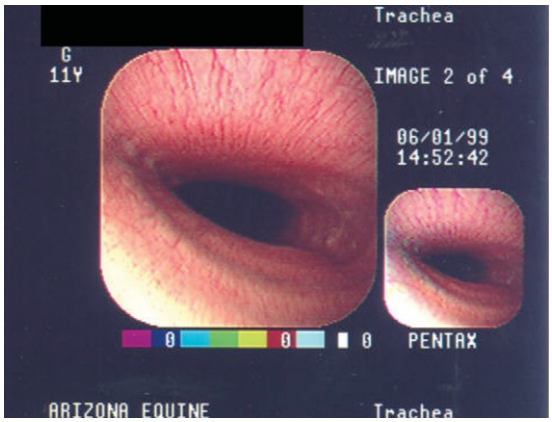

FIGURE 6-44. More pronounced collapse of distal cervical trachea.

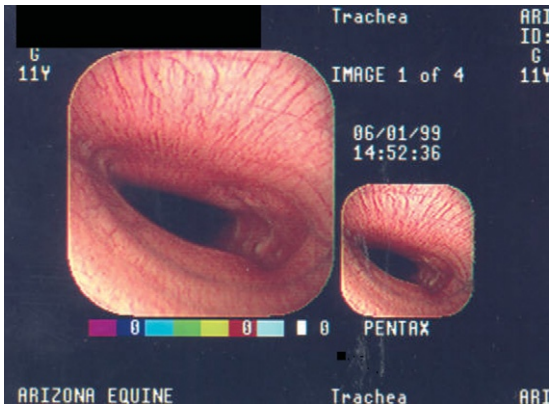

FIGURE 6-45. Moderate collapse of cervical trachea.

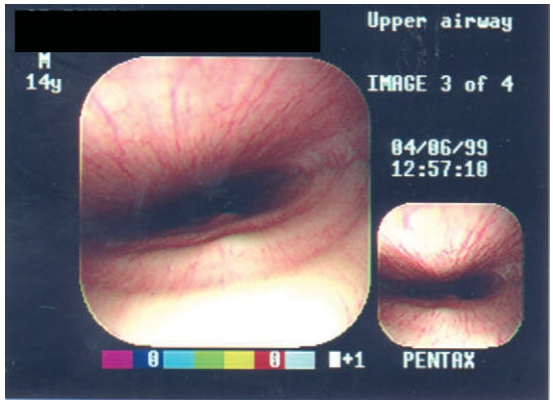

FIGURE 6-46. Severe tracheal collapse. Note sharp angulation of rings in lateral walls.

FIGURE 6-47. Severe tracheal collapse. Note hyperemia and tracheitis often present.

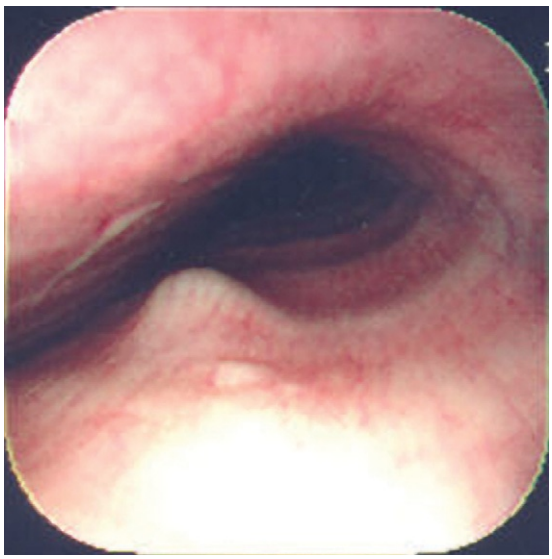

FIGURE 6-48. Severe collapse of trachea and ring malformation in miniature horse.

FIGURE 6-49. Severe tracheal collapse due to ring malformation. Note spiraling of fibrocartilaginous ring further narrowing lumen.

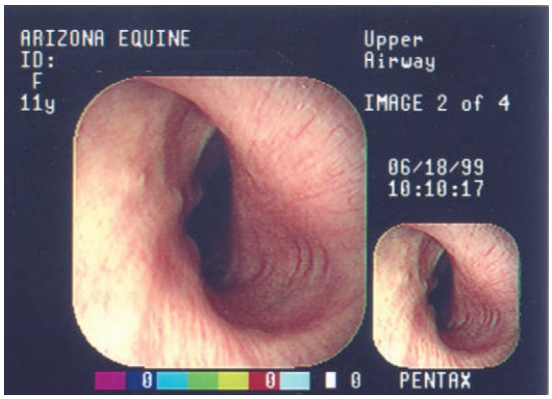

FOREIGN BODY

The tracheobronchial tree is susceptible to lodgment by foreign objects/materials. Plant material can lodge in the larynx and proximal trachea, necessitating removal via tracheotomy (Figures 6-50 and 6-51). Healing with fibrosis of laryngeal structures and tracheal lumen may result in chronic occurrences (Figures 6-52 to 6-54).

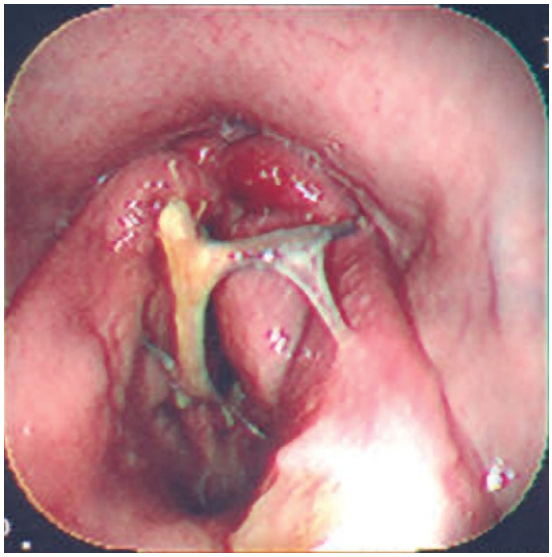

FIGURE 6-50. Pharyngeal view of mesquite branch lodged through rima glottidis into proximal trachea. Note arytenoiditis and inflammation of vocal folds. Owner reported cough, malodorous breath, and exercise intolerance 6 weeks before presentation.

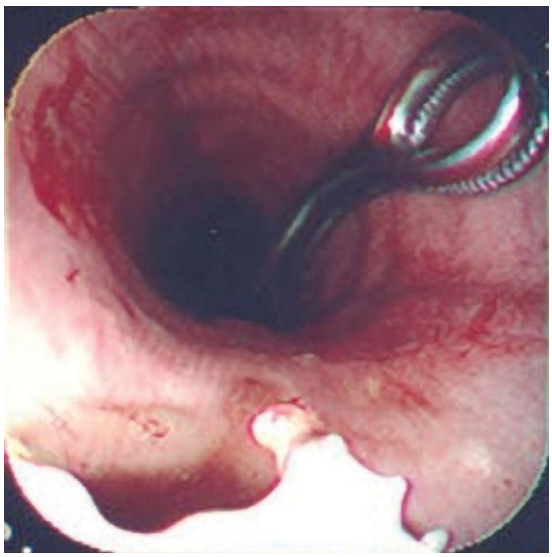

FIGURE 6-51. Endoscope placed in infraglottic region looking distally. Mesquite branch is in foreground; towel forcep is being advanced from distal to proximal through tracheotomy.

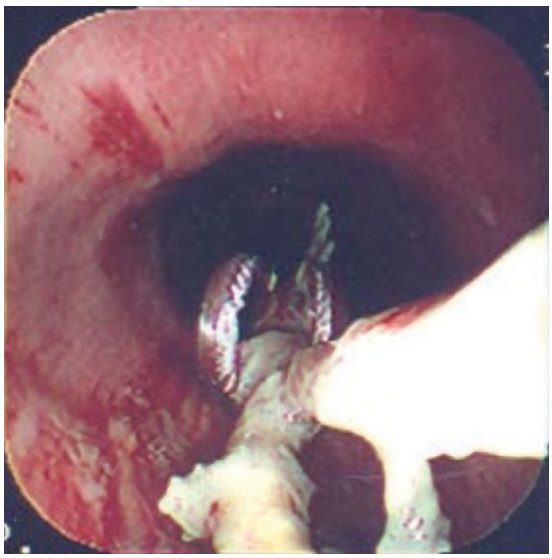

FIGURE 6-52. Towel forcep grasping mesquite branch and removing through distal tracheotomy incision.

FIGURE 6-53. Larynx of horse in Figures 6-50, 6-51, and 6-52. Seven months after mesquite branch retrieval.

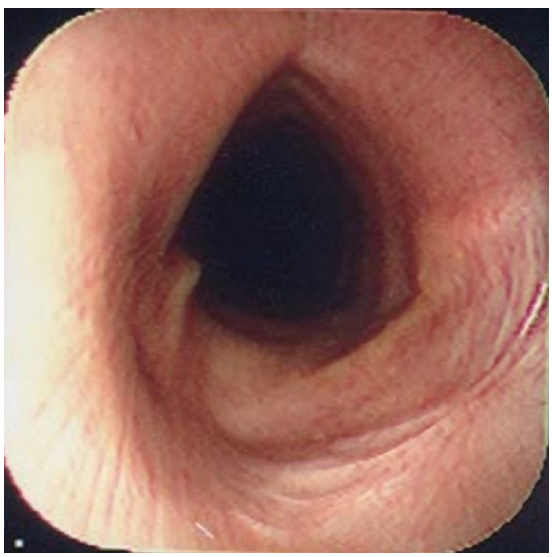

FIGURE 6-54. Tracheal scarring secondary to tracheotomy and foreign body removal 7 months postoperatively.

TUMORS

A 7-year-old Warmblood gelding was seen with a 4-month history of coughing without exercise intolerance. A large nodule protruding into the trachea was noted. The biopsy of the mass revealed a granular cell tumor of the trachea. Pulmonary granular cell tumor is a locally invasive but a rare type of tumor with low metastatic potential (Figure 6-55).

FIGURE 6-55. Granular cell tumor in mid trachea of 7-year-old Warmblood with chronic cough (Dr. Gary Magdesian).

CHAPTER 7

Esophagoscopy

EDWARD VOSS

NORMAL ANATOMY

The equine musculomembranous esophagus averages 125 to 150 cm in length, is divided into three segments (cervical, thoracic, and abdominal), and is the direct continuation of the laryngopharynx. The wall of the esophagus is composed of four tissue layers or coats. The outer fibrous sheath (tunica adventitia) loosely attaches the esophagus to surrounding structures. This permits freedom of movement and expansion during swallowing and cervical positioning. The muscular coat (tunica muscularis) is chiefly arranged in two layers of fibers oriented spirally or elliptically, which intercross dorsally and ventrally. The muscular layers are striated-type muscle in the proximal two-thirds which transitions to smooth-type muscle fibers in the distal one-third near the base of the heart. Distally, the two muscular layers form an outer longitudinal and an inner circular layer. Additionally, this distal muscular layer is thicker than the less pronounced proximal musculature, and this tends to decrease the luminal diameter of the distal esophagus. Beneath the muscular coat lies the submucosal layer (tela submucosa) and lining the esophageal lumen is the mucosal layer (tunica mucosa). This mucosa is glistening, is pale pink to whitish gray in color, and lies in longitudinal folds when not dilated.

The esophageal opening lies dorsal to the arytenoid cartilages (Figure 7-1) and continues on the median plane just dorsal to the cricoid cartilage of the larynx. The lumen of the pharyngeal-esophageal junction is flattened dorsoventrally and the submucosal mucus glands may be seen (Figure 7-2). Just distal to the pharyngeal-esophageal junction, the region of the upper esophageal sphincter is encountered (Figure 7-3). At approximately the fourth cervical vertebra, the esophagus deviates from the median plane to the left lateral aspect of the trachea. In this region a stomach tube, endoscope, or food/water can be visualized moving down the esophageal lumen due to the close proximity to the skin. The lumen of the esophagus in this region is relatively less folded, and the mucosa is less thick in appearance (Figure 7-4). The thoracic portion of the esophagus begins at the thoracic inlet where, after passing through the inlet on the left of the trachea, the esophagus deviates back to median, dorsal to the trachea. In this region, the mucosa lies in deeper longitudinal folds (Figure 7-5) that dilate easily and dissipate with air insufflation (Figure 7-6). As the esophagus is moved to the right of median in the midthoracic region by the great vessels (aortic arch), a slight bulging of the lumen may be seen (Figure 7-7). Terminally, the longitudinal folds of the mucosa become quite pronounced because of the thickened muscularis distally (Figure 7-8). This area can be insufflated gradually with air to visualize the lumen more clearly (Figure 7-9) to become fairly distended (Figure 7-10). The short abdominal portion of the esophagus terminates at the lower esophageal sphincter where it enters

Text continued on p. 123

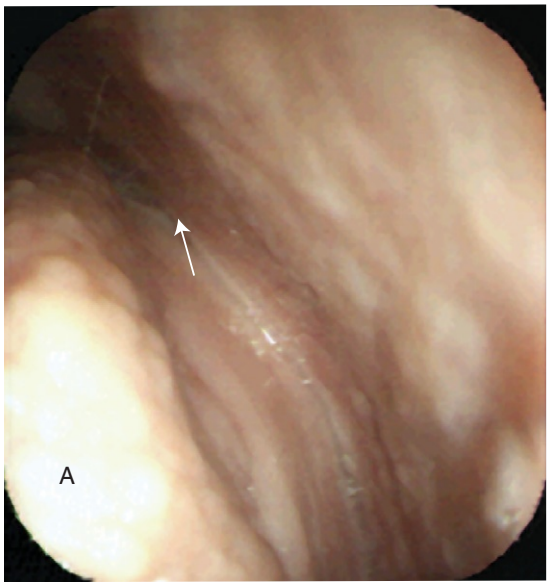

FIGURE 7-1. Pharyngeal view of left lateral food channel showing esophageal opening *(arrow)* dorsal to left arytenoids cartilage *(A)*.

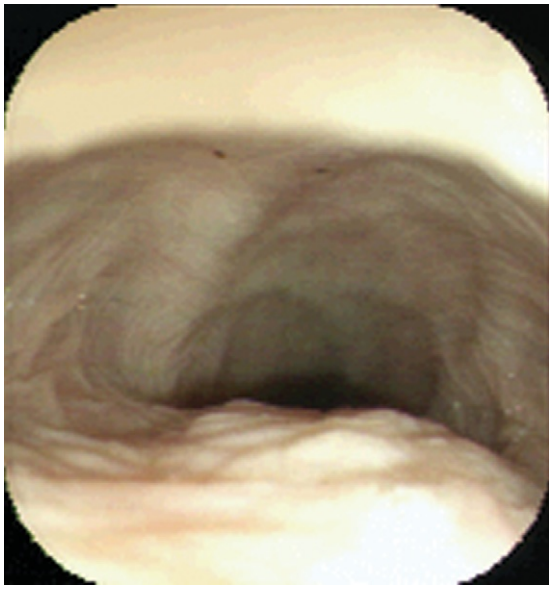

FIGURE 7-2. Pharyngoesophageal junction. Luminal view of pharyngoesophageal junction. Note obvious flattening of lumen and submucosal glands.

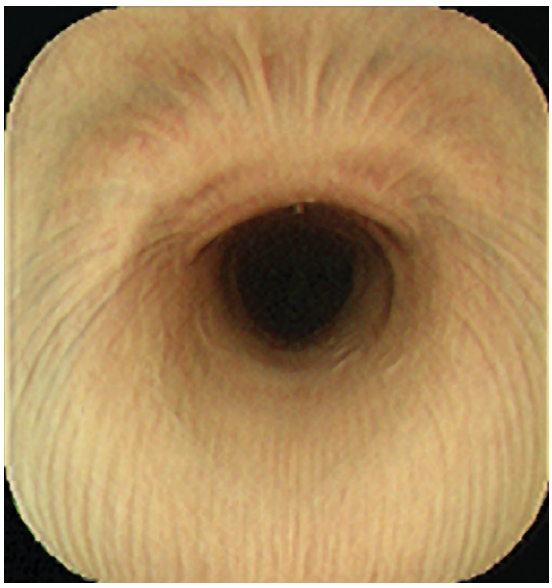

FIGURE 7-3. View of proximal esophagus just distal to pharyngoesophageal junction. Note petite longitudinal folding and area of upper esophageal sphincter.

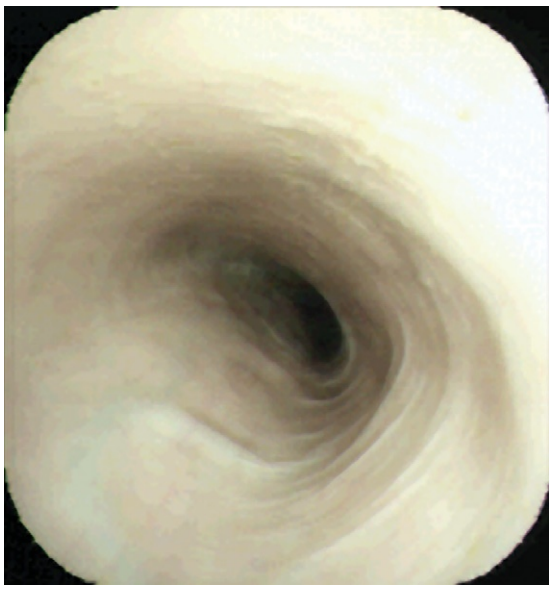

FIGURE 7-4. Proximal cervical esophagus. Note the relatively thin, whitish gray mucosa lacking deep longitudinal folds.

FIGURE 7-5. Midcervical esophagus with increasingly deeper longitudinal mucosal folds.

FIGURE 7-6. Insufflation of midcervical esophagus. Note how longitudinal mucosal folds attenuate easily.

FIGURE 7-7. Thoracic esophagus. Note indentation of esophageal wall by great vessels at heart base.

FIGURE 7-8. Distal esophagus with longitudinal and transverse mucosal folds. Note normal increasingly thick-appearing mucosa.

FIGURE 7-9. Modest insufflation of distal esophagus. Note gradual disappearance of folding.

FIGURE 7-10. Increasing insufflation within distal esophagus and near-complete ablation of mucosal folds.

the cardia of the stomach (Figure 7-11). Both longitudinal and transverse folding of the mucosa are appreciable in this region. The lower esophageal sphincter is normally closed to minimize gastroesophageal reflux but can easily be dilated by normal peristaltic waves or insufflation of the distal esophagus (Figure 7-12).

FIGURE 7-11. Lower esophageal sphincter. Note closure even with marked insufflation.

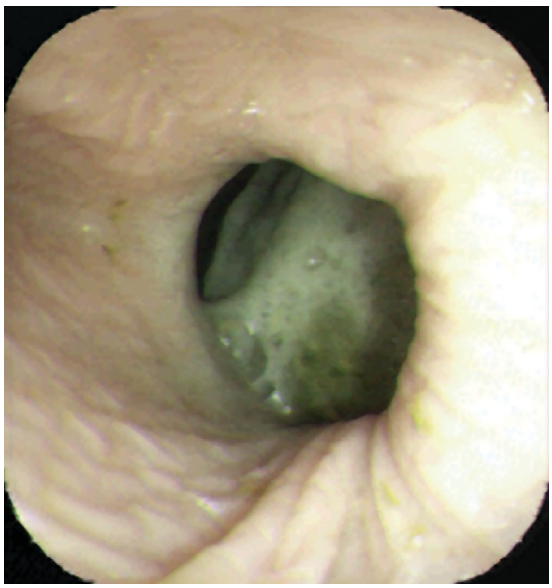

FIGURE 7-12. Normal lower esophageal sphincter during peristaltic wave- or insufflation-induced dilation. Food material can be seen in cardia of stomach.

OBSTRUCTIONS/FOREIGN BODIES

Obstructive luminal esophageal disease, "choke," is common in equine practice. Food material or foreign object lodgment often necessitates esophageal video endoscopic evaluation. Adequate sedation may reduce the anxiety of the patient and lower the head and cervical region, minimizing the potential for aspiration (Figure 7-13) during endoscope or nasogastric tube passage. Topical anesthesia of the nasal/pharyngeal mucosa (4 to 6 ml of 2% lidocaine) can reduce the retching/gagging behavior frequently encountered due to pharyngeal irritation (Figure 7-14) and facilitate entry into the pharyngoesophageal opening. A large proportion of mechanical luminal obstructions occur in the cervical esophagus although obstruction at the thoracic inlet may occur due to the reduced expandability of the esophagus as it passes between the trachea and first rib.

FIGURE 7-13. Food and saliva in pharynx due to esophageal obstruction. Note high risk of aspiration into trachea.

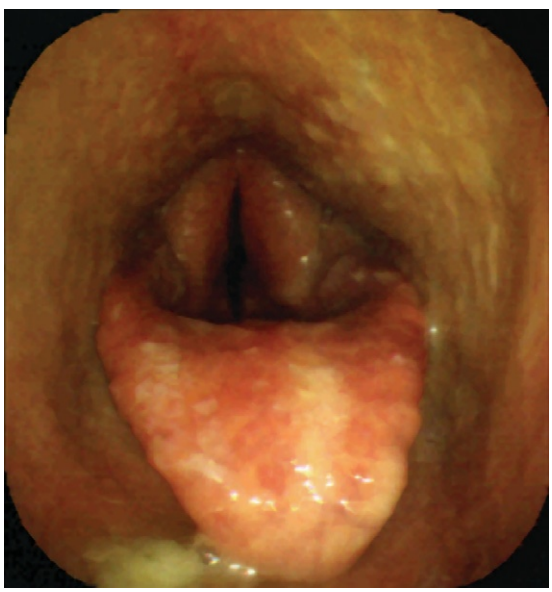

FIGURE 7-14. Severe pharyngeal inflammation resulting from esophageal obstruction.

Video endoscopy can be used to determine nasogastric tube placement in the pharyngoesophageal opening (Figure 7-15) when very proximal cervical obstructions preclude "blind" passage of tube into esophagus. Material, location, and treatment options for an esophageal obstruction can be determined readily via endoscopy. Feed material–type (Figure 7-16) obstructions may be gently advanced into the stomach (Figure 7-17) or broken into fragments with endoscopic biopsy instruments (Figure 7-18). Some obstructions resist advancement to the stomach or to do so may be undesirable. Thus endoscopic snares or loops can be used to retrieve objects occluding the esophageal lumen (Figure 7-19). This pony had eaten a large number of oranges as seen when the orange fragments in the esophagus were retrieved with a loop snare, and the stomach contents could be inspected (Figure 7-20).

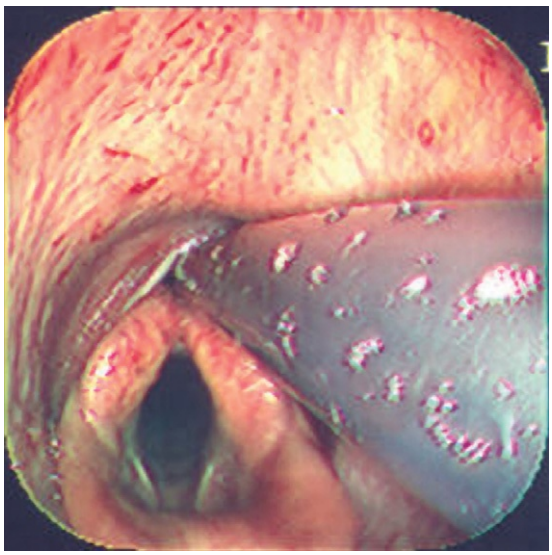

FIGURE 7-15. Endoscopic confirmation of nasogastric tube within esophagus.

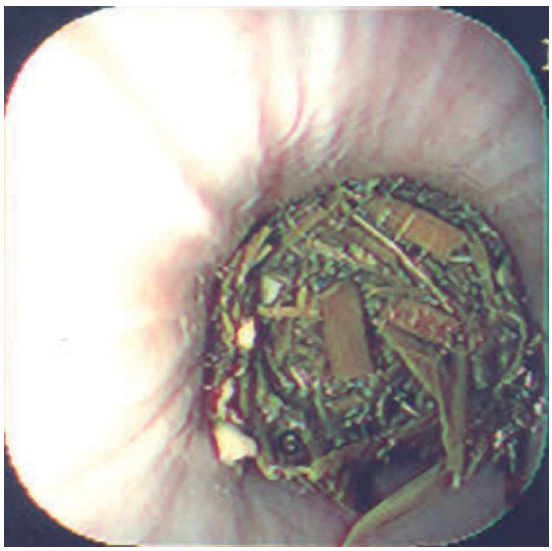

FIGURE 7-16. Coarse plant material–type obstruction of esophageal lumen.

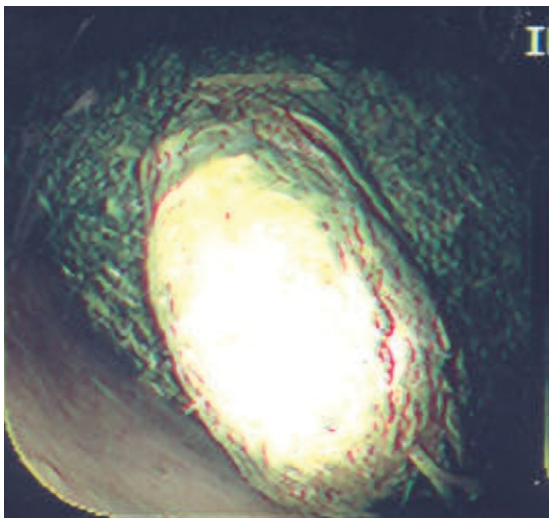

FIGURE 7-17. Esophageal obstruction passed into stomach. Note smooth, tubular contour to bolus.

FIGURE 7-18. Guided disruption of food material–type esophageal obstruction with endoscopic biopsy forceps.

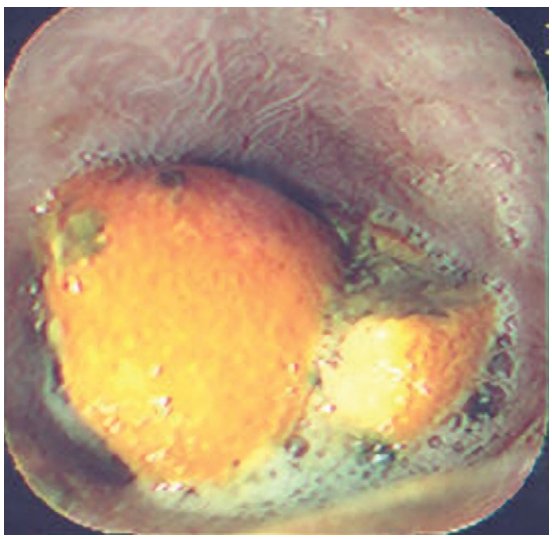

FIGURE 7-19. Orange fruit obstruction in cervical esophagus. "D" type snare was used to retrieve orange fragments and relieve obstruction.

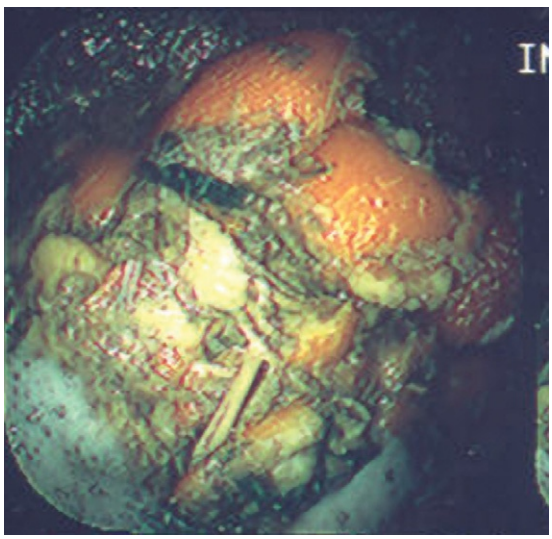

FIGURE 7-20. Passage of endoscope after relief of obstruction revealed large volume of citrus in stomach.

MUCOSAL/SUBMUCOSAL DEFECTS

After relief of esophageal obstruction, mucosal and submucosal damage can be observed. If the obstruction is of relatively short duration and easily dislodged, variable discoloration or bruising of the mucosa may be seen (Figures 7-21 to 7-24). Longer-standing, more severe obstructions may cause mucosal sloughing (Figure 7-25) or deeper defects in the esophageal wall (Figures 7-26 and 7-27). Aggressive nasogastric tube pressure or passage of obstructions of firmer character (e.g., carrots or medicinal boluses) may damage the esophageal mucosa and submucosa as seen in the series of three photos at 1-week intervals (Figures 7-28 to 7-30).

FIGURE 7-21. Mild bruising of esophageal mucosa after relief of obstruction.

FIGURE 7-22. Moderate bruising of mucosa postobstruction. Note "horse cookie" distally advanced down esophagus.

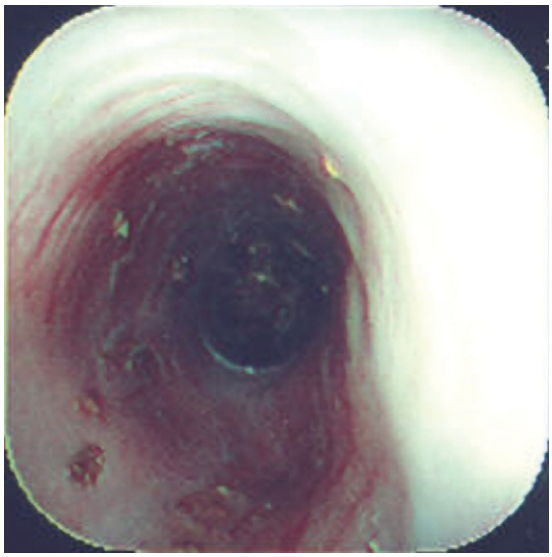

FIGURE 7-23. More severe, focal bruising of mucosa postobstruction.

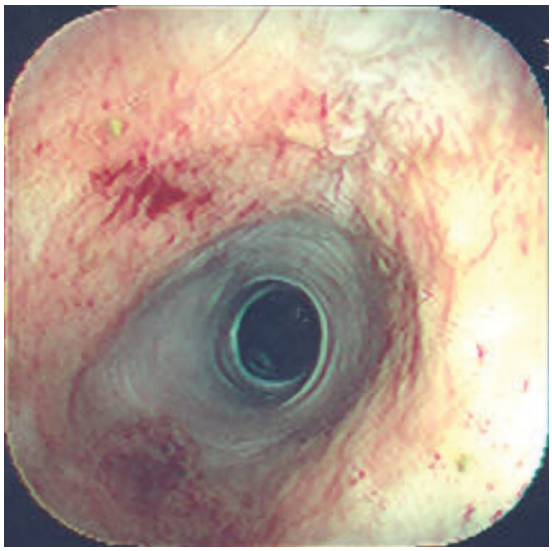

FIGURE 7-24. Mucosal and submucosal bruising with ecchymotic hemorrhages postobstruction.

FIGURE 7-25. Mucosa stripped off the submucosa in a sheet postobstruction.

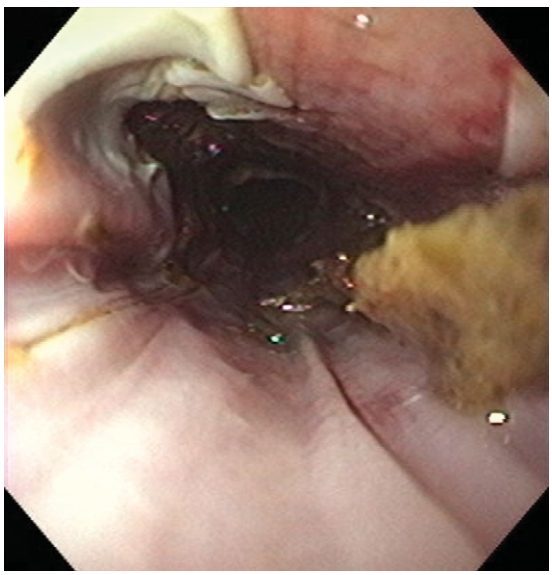

FIGURE 7-26. Deeper, more severe stripping of esophageal mucosa postobstruction.

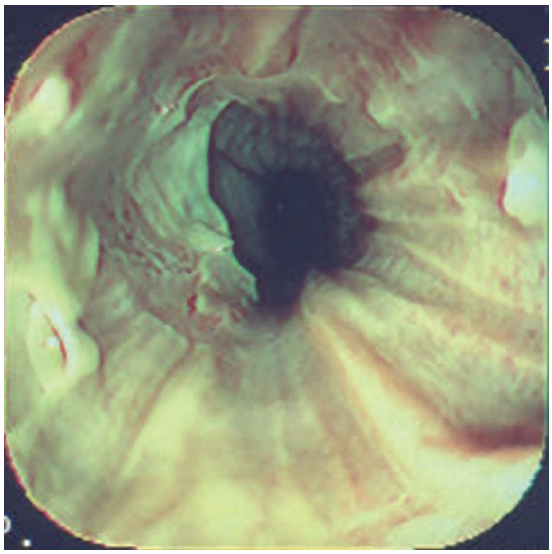

FIGURE 7-27. Circumferential mucosal sloughing after relief of esophageal obstruction.

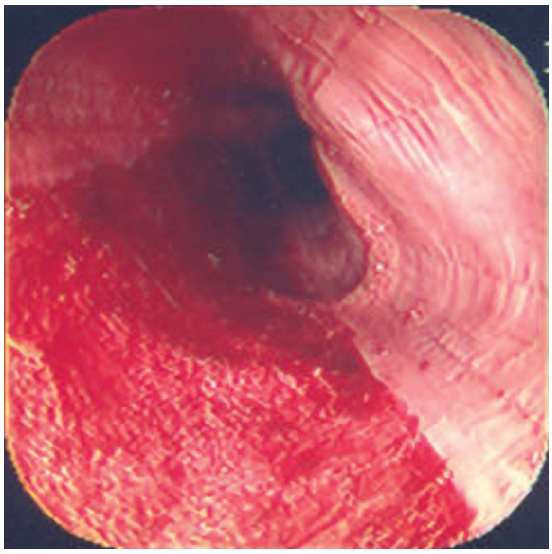

FIGURE 7-28. Substantial injury to mucosa and submucosa after advancement of carrot portion. Note longitudinal nature of defect.

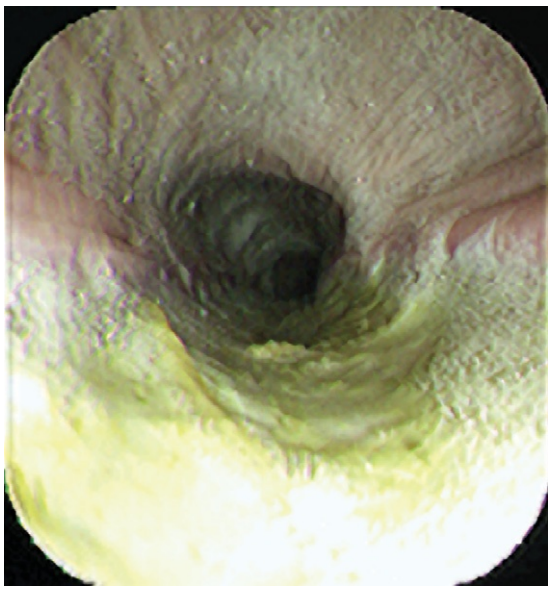

FIGURE 7-29. Esophageal trauma seen in Figure 7-28 7 days after incident. Note slight contracture of wound edges.

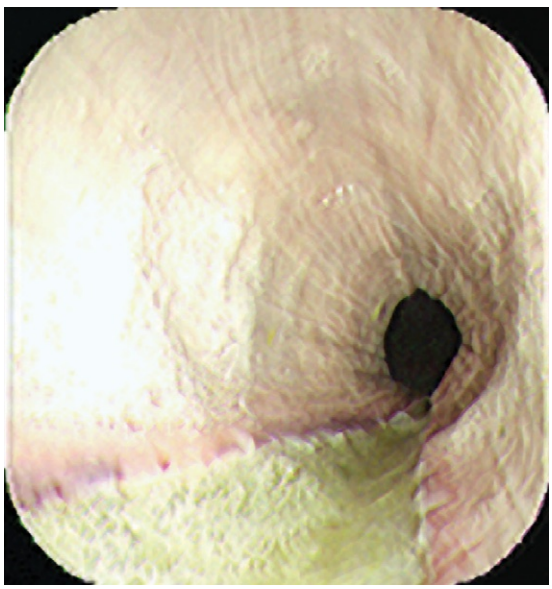

FIGURE 7-30. Esophageal trauma seen in Figure 7-28 14 days after trauma. Defect is contracting without decrease in lumen diameter.

STRICTURE

Longitudinal mucosal and submucosal defects generally heal without incident, but if circumferential injury to the mucosa, submucosa, or muscularis occurs (Figure 7-31), a stricture may form (Figure 7-32). As seen at 14 days after choke relief (Figure 7-33), a circumferential fibrous stricture is forming in the midesophageal region. At 30 days after choke relief (Figure 7-34), the stricture is more fibrous and not easily dilated via insufflation (Figure 7-35). By 70 days after choke relief, the stricture has remodeled and its diameter has increased to near normal (Figure 7-36). Commercially available polyethylene balloon catheters (Rigiflex Balloon Dilator, Microinvasive, Watertown, MA) can be used for dilation of severe esophageal strictures. When inflated the

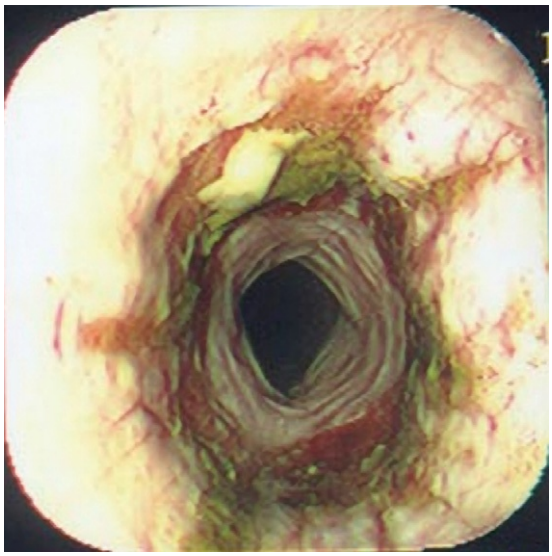

FIGURE 7-31. Circumferential injury to esophageal mucosa and submucosa.

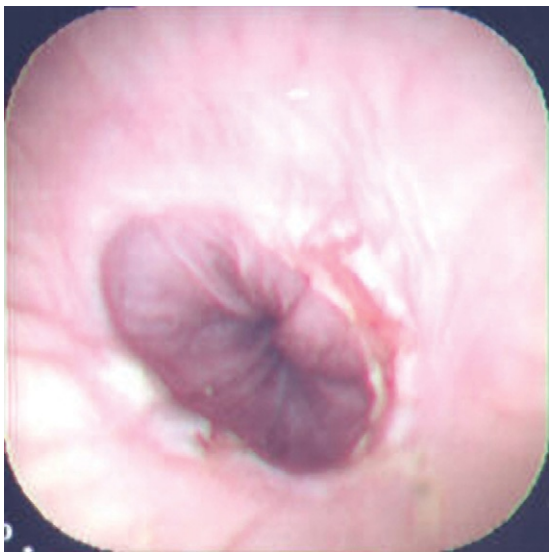

FIGURE 7-32. Early stricture forming as result of circumferential injury to esophageal mucosa/submucosa.

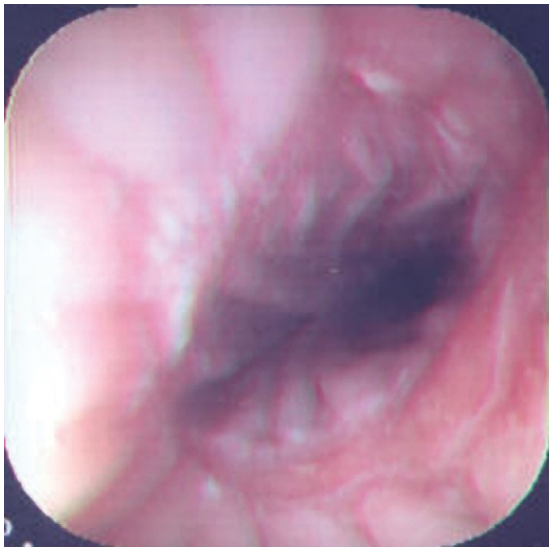

FIGURE 7-33. Stricture forming 14 days postobstruction.

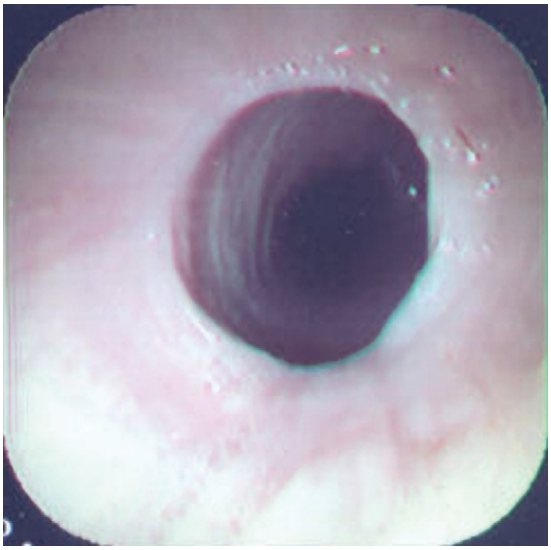

FIGURE 7-34. Stricture contracture at 30 days postobstruction. Note smooth edges of stricture and luminal narrowing.

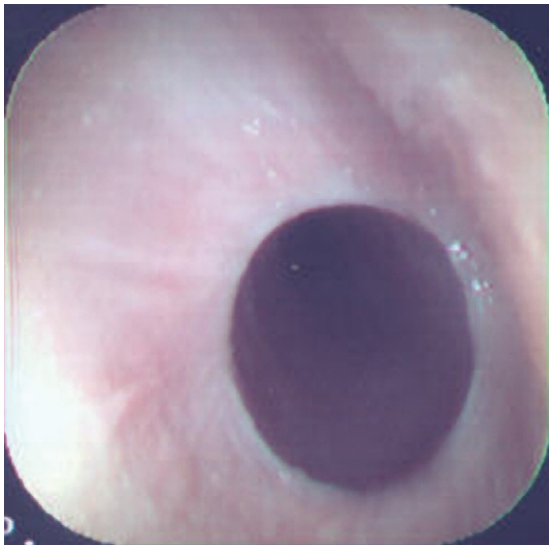

FIGURE 7-35. Stricture seen in Figure 7-34 with esophagus insufflation to maximum. Note inability to widen luminal diameter at stricture.

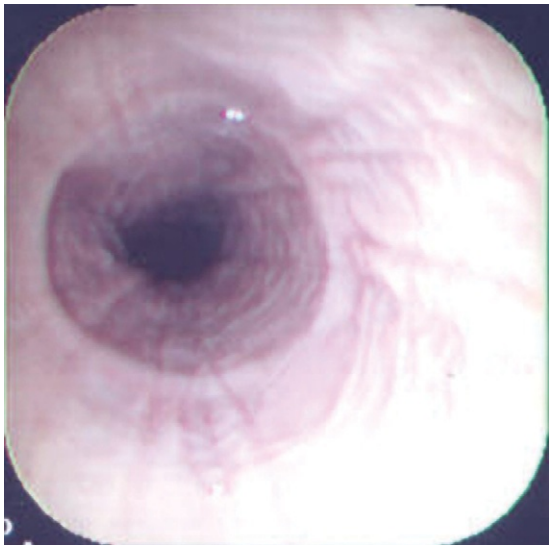

FIGURE 7-36. Stricture in Figures 7-33 and 7-34 at 70 days postinjury. Note remodeling of fibrous annulus such that luminal diameter is near normal.

catheters can have a diameter ranging from 4 to 20 mm and a length of 8 cm (Figure 7-37). A conservative approach is recommended (start off with a small balloon size, e.g., 12 to 14 mm), which greatly reduces the chance of esophageal perforation. After the initial procedure a 15- to 18-mm catheter may be used next, followed by a 20-mm balloon. A standard disposable syringe is used to inflate the balloon with sterile water to the manufacturer-recommended pressure (usually 45 to 50 psi). A pressure monitor is attached between the catheter and syringe to ensure that the pressure in the balloon does not exceed 50 psi and cause inadvertent balloon rupture (Figures 7-38 and 7-39). Endoscopic-guided balloon dilation of esophageal strictures may be attempted if conservative management is not warranted (Figures 7-40 to 7-44).

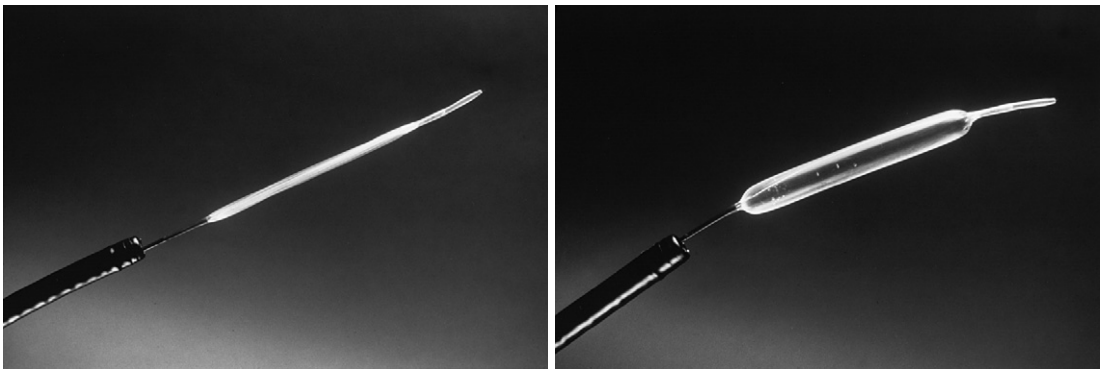

FIGURE 7-37. Rigiflex Balloon Dilator catheter (Microvasive) for esophageal stricture dilation. **A,** Appearance of 10-mm by 8-cm balloon when it is deflated for passage through 2.8-mm channel of flexible endoscope and into esophageal stricture. **B,** Appearance of balloon when it is inflated with distilled water to 50 psi, used in endoscopic dilation of esophageal stricture. Balloon now has diameter of 10 mm and length of 8 cm. (From Tams TR: *Small animal endoscopy,* ed 2, St Louis, 1999, Mosby.)

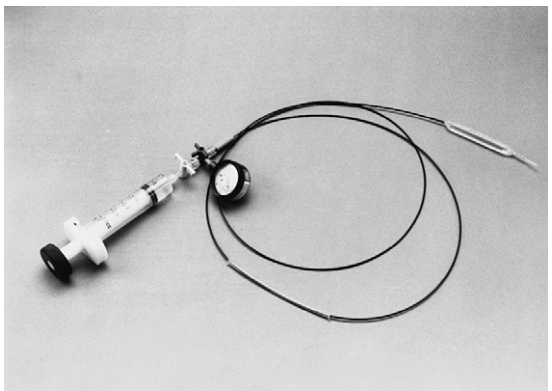

FIGURE 7-38. Coiled Rigiflex Balloon Dilator catheter with balloon inflated and pressure gauge and LeVeen Inflator (Meditech) attached. (From Tams TR: *Small animal endoscopy,* ed 2, St Louis, 1999, Mosby.)

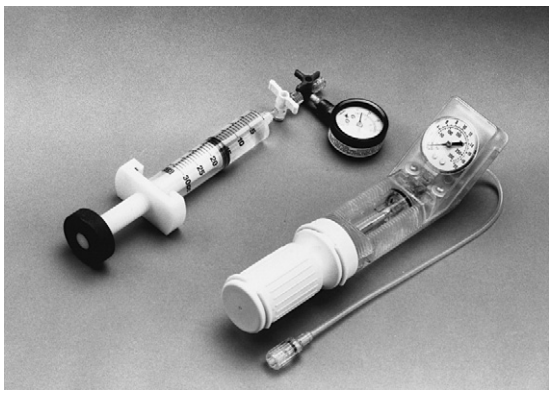

FIGURE 7-39. Two types of inflation devices that can be used for endoscopic balloon dilation of esophageal strictures. On left is LeVeen Inflator, screw-press device that compresses syringe plunger to ensure that adequate dilation pressures are achieved and maintained. Syringe and Marsh pressure gauge for monitoring inflation pressure are attached. On right is Indeflator (Advanced Cardiovascular Systems), inflation device with built-in pressure gauge. (From Tams TR: *Small animal endoscopy,* ed 2, St Louis, 1999, Mosby.)

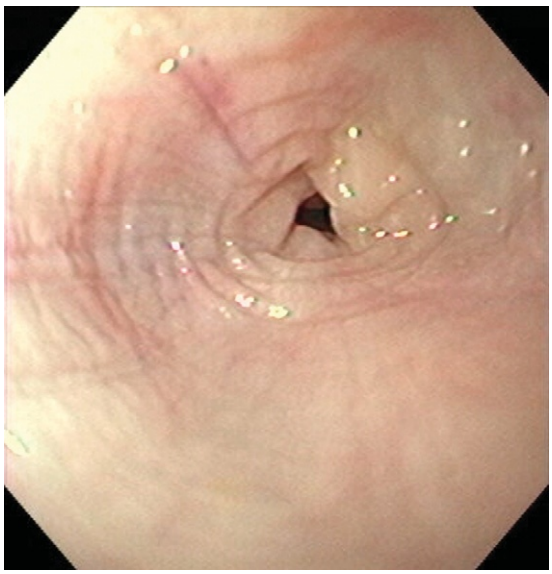

FIGURE 7-40. A mucosal/submucosal stricture of esophagus that formed 30 days after luminal obstruction.

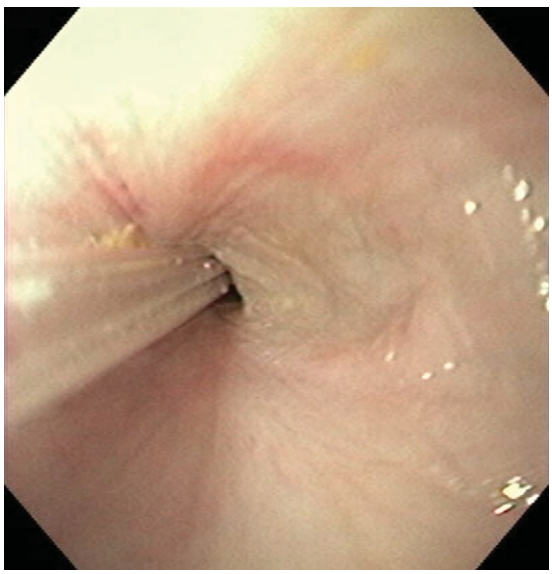

FIGURE 7-41. Advancement of balloon dilator into stricture with initiation of dilation.

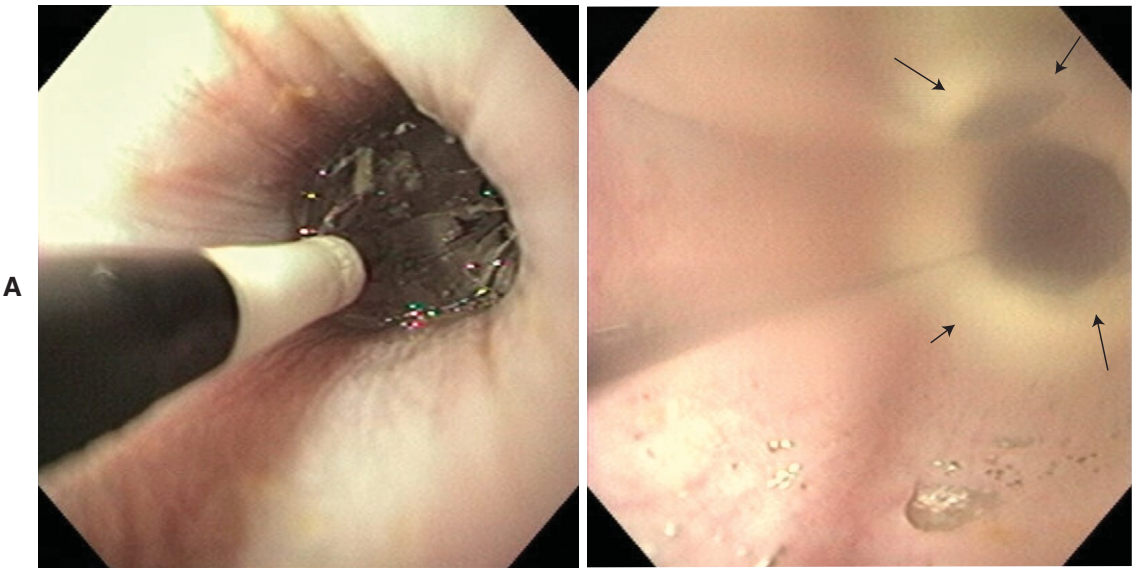

FIGURE 7-42. **A,** Dilation time of 1 to 2 minutes at maximum inflation pressure of 45 to 50 psi is adequate for treating most strictures; 20-mm balloon catheter was used for this foal. **B,** Stricture ring *(arrows).*

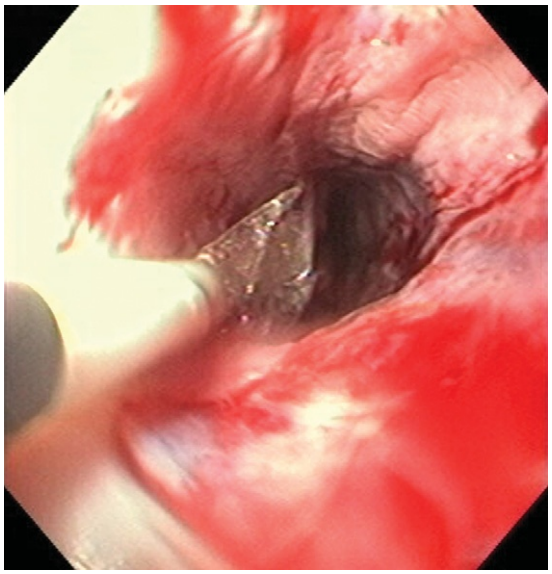

FIGURE 7-43. Immediate deflation of balloon showing residual dilation of stricture. Note mucosal tearing and mild hemorrhage from distention of strictured region. This balloon dilation procedure is typically repeated every 5 to 7 days for a total of three to five treatments.

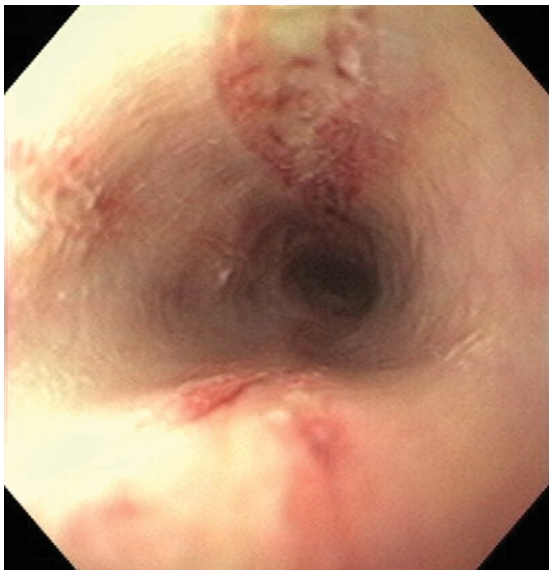

FIGURE 7-44. Forty-eight hours after balloon dilation procedure. Note healing of mucosal defects.

RUPTURE/PERFORATIONS

If trauma to the esophageal wall is substantial or a luminal obstruction erodes through the four coats of the esophageal wall, a perforation or rupture occurs. Proximal perforations or lacerations (Figures 7-45 and 7-46) can be managed via esophagotomy distal to the lesion or sutured primarily (Figures 7-47 to 7-49). Perforations that occur more distally can be life-threatening because of deep septic cellulitis or gross contamination of body cavities with feed and saliva. When a perforation of the esophagus is present, insufflation attempts are often unsuccessful because of air escaping through the rent (Figures 7-50 to 7-52).

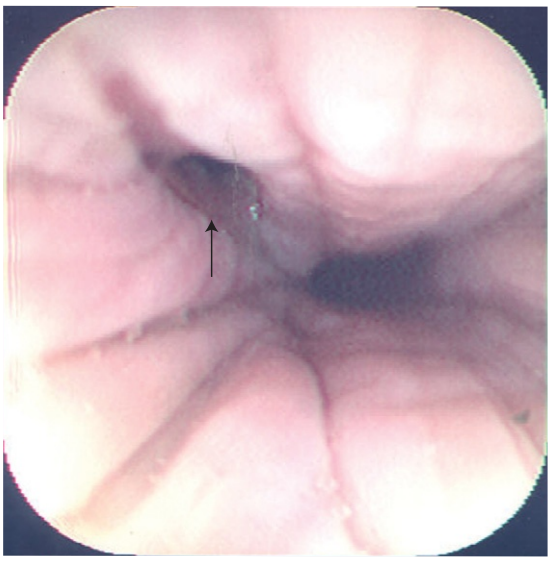

FIGURE 7-45. Perforation of 15 mm in esophageal wall *(arrow).*

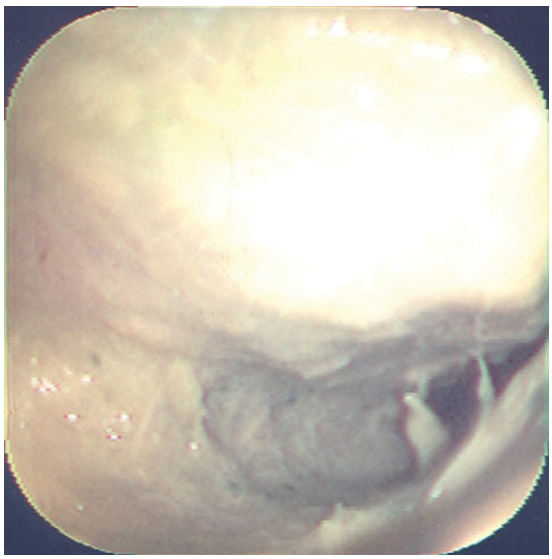

FIGURE 7-46. Passage of endoscope into perforation in Figure 7-45 reveals dissecting tract into fascia lined with green feed material.

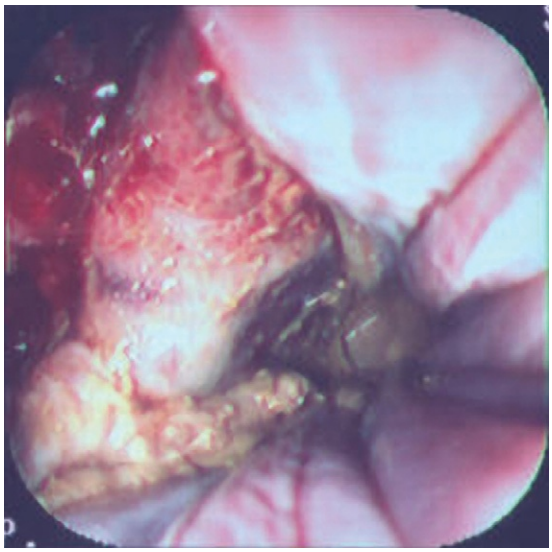

FIGURE 7-47. Large, full-thickness, lateral perforation of esophageal wall. Note mucosal, submucosal, and muscular layers penetrated.

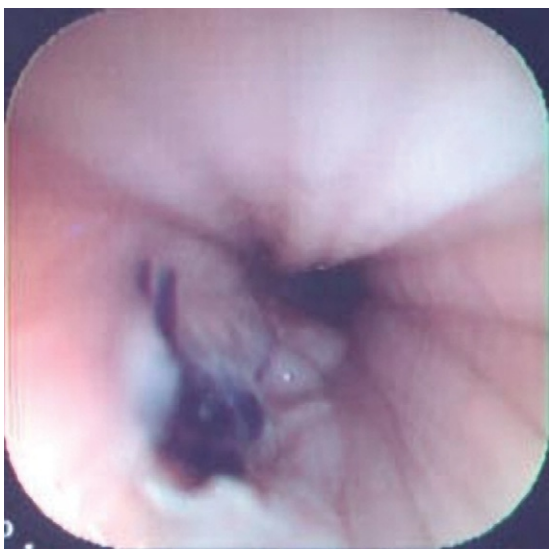

FIGURE 7-48. Perforation in Figure 7-47, 7 days after surgical repair. Note suture is visible in submucosa and mucosa is not yet healed.

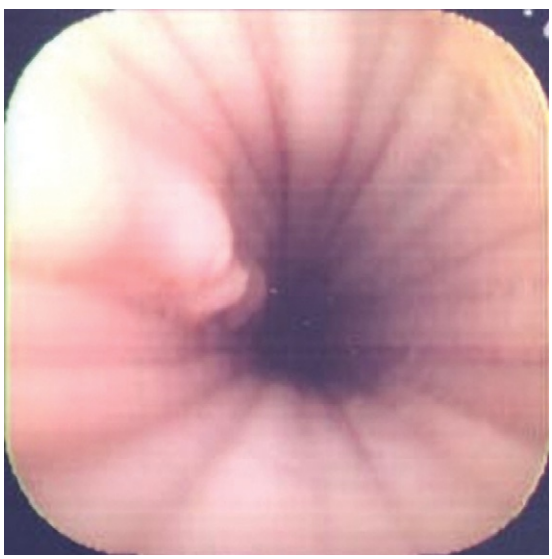

FIGURE 7-49. Fourteen days after surgery, mucosal defect in Figures 7-47 and 7-48 is completely healed.

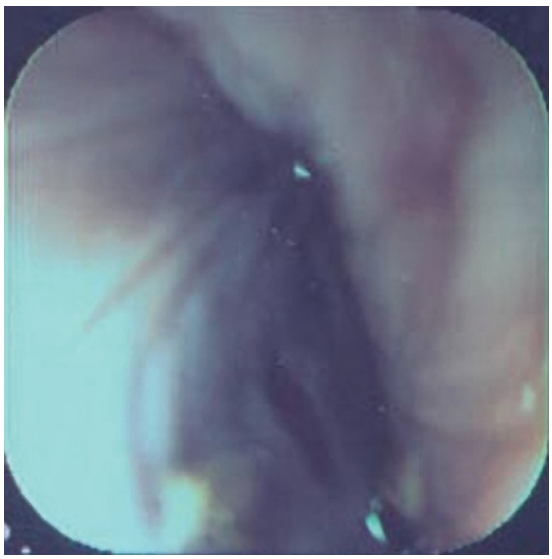

FIGURE 7-50. Perforation of distal esophageal wall. Note inability to distend esophagus via insufflation.

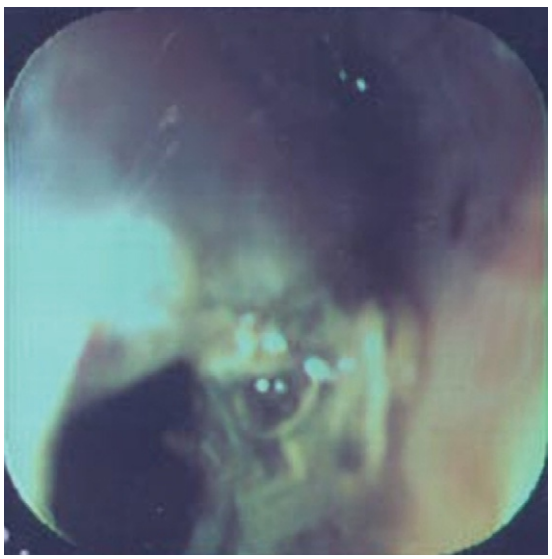

FIGURE 7-51. Close-up view of perforation in Figure 7-50 as endoscope is advanced into defect.

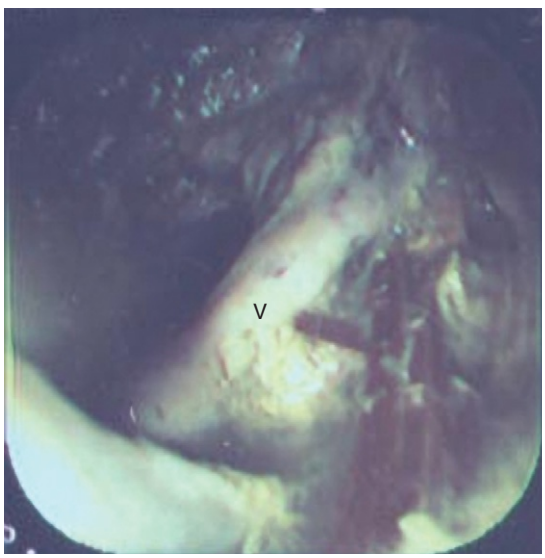

FIGURE 7-52. Passage of endoscope into defect seen in Figures 7-50 and 7-51 allows direct visualization of thoracic cavity. Note food material on thoracic organs and great vessels *(V)*.

FISTULA

Esophagitis/Ulceration

Inflammatory conditions of the equine esophagus, once thought infrequent, are not an uncommon observation. Gastric esophageal reflux disorder (GERD) causes esophagitis typically in the distal portion of the esophagus whereas caustic chemical-type injury may involve the entire oropharyngeal and esophageal tracts. Gastric acid reflux into the distal esophagus is generally a failure of the lower esophageal sphincter to adequately seal the gastroesophageal junction (Figure 7-53). Mild esophageal hyperemia and erosion initially occurs within the deep folds of the esophageal mucosa and is only readily apparent with insufflation (Figures 7-54 and 7-55), whereas moderate-type changes involve more surface area and deeper erosions (Figures 7-56 to 7-59) evident without esophageal distention. Severe esophagitis often entails ulcerative and diffuse erosive pathologic changes (Figures 7-60 to 7-63).

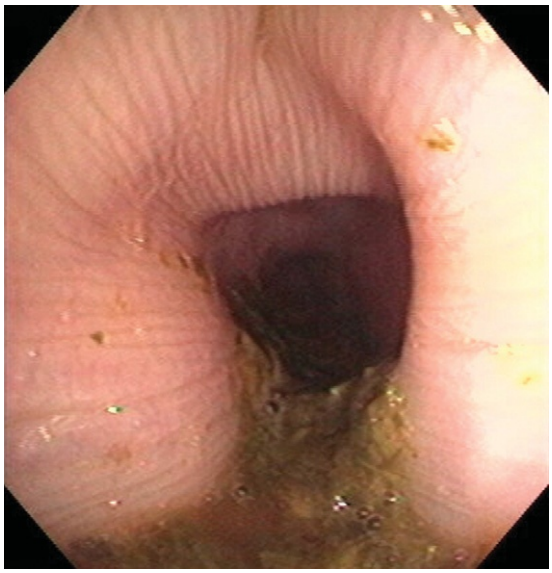

FIGURE 7-53. Reflux of gastric contents into distal esophagus through lower esophageal sphincter.

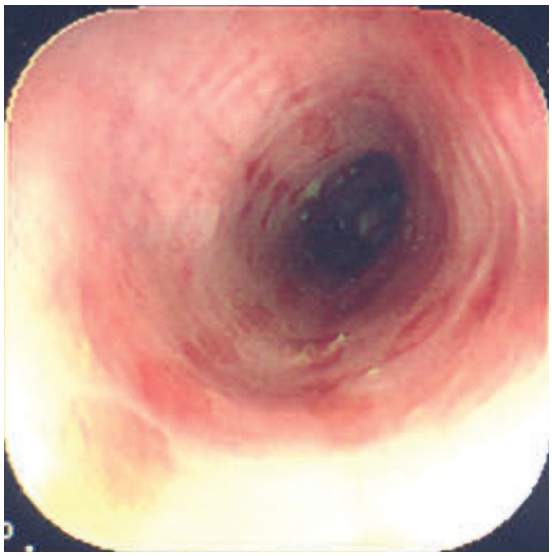

FIGURE 7-54. Diffuse mild esophagitis due to gastroesophageal reflux. Note focal superficial mucosal erosions.

FIGURE 7-55. Esophagitis due to gastroesophageal reflux. Note that mild, thin, linear erosions are visible after insufflation with air.

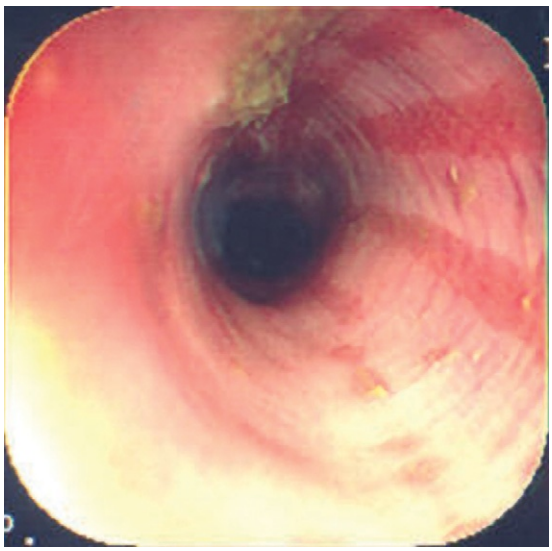

FIGURE 7-56. Moderate esophagitis and linear erosions due to equine gastric ulceration syndrome (EGUS) and gastroesophageal reflux.

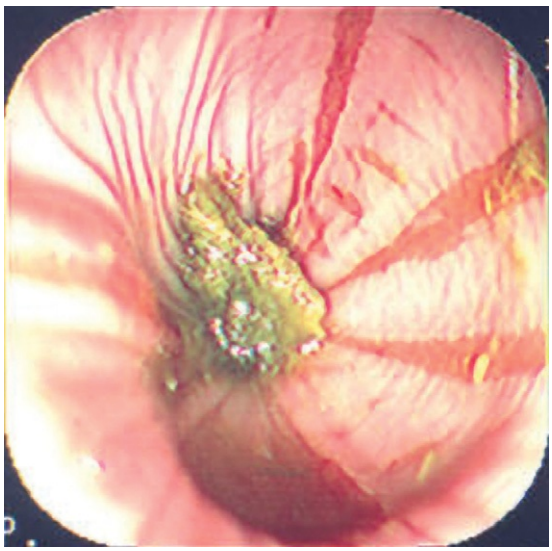

FIGURE 7-57. Moderate esophagitis with deeper linear ulceration of mucosa secondary to gastroesophageal reflux.

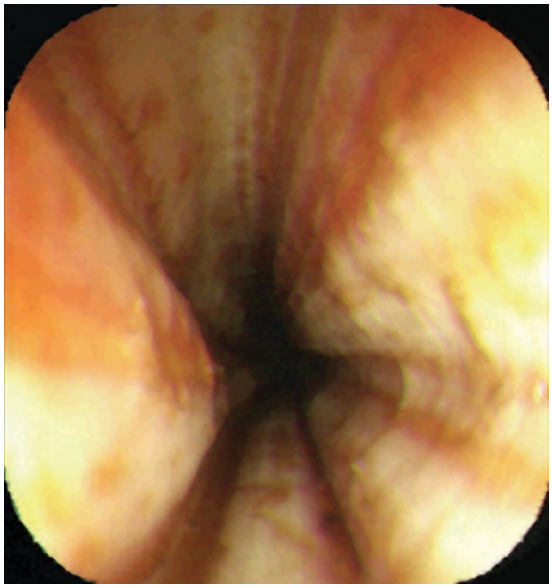

FIGURE 7-58. Moderate gastroesophageal–induced distal esophagitis evident without insufflation.

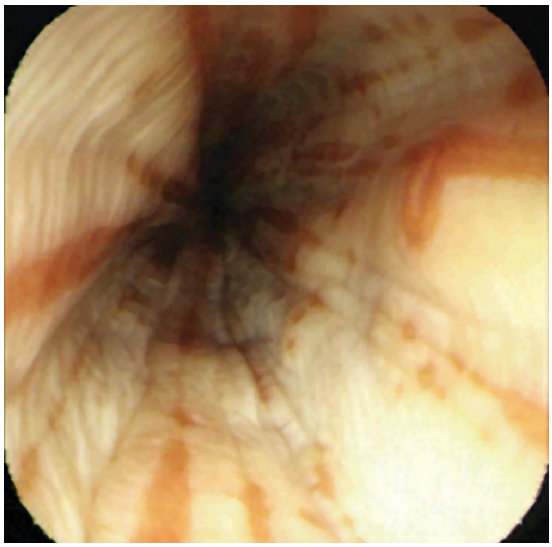

FIGURE 7-59. With insufflation, visibility of entire surface area esophageal lumen allows for more accurate interpretation of lesions.

FIGURE 7-60. Severe, diffuse, ulcerative esophagitis due to ingestion of "soda lime" (calcium oxide/sodium hydroxide) used to disinfect stalls.

FIGURE 7-61. Deeper focal ulceration in wall of esophagus.

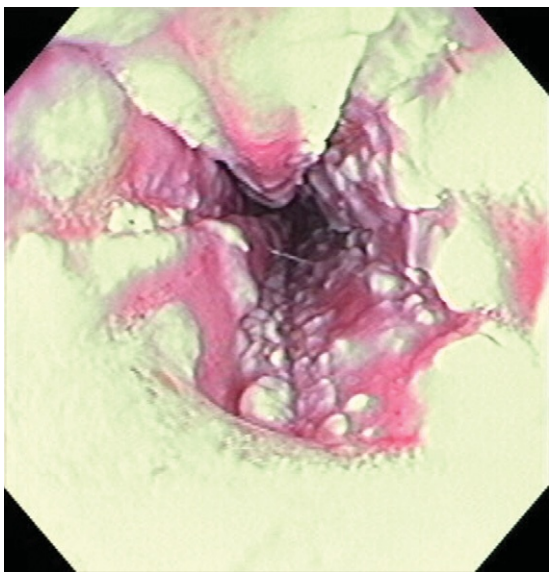

FIGURE 7-62. Severe diffuse ulcerative esophagitis from severe EGUS and gastroesophageal reflux.

FIGURE 7-63. Close-up view of severe ulcerative esophagitis seen in Figure 7-62.

Megaesophagus

Motor disturbances, dilation, and megaesophagus are infrequent and not well described in the horse. In obvious cases, food and saliva run from nares with lowering of the head and a palpable, persistently fluid-filled esophagus may be observed. Primary muscle, neurologic, autoimmune, endocrine, or idiopathic disease may be responsible. Commonly used sedatives (xylazine, detomidine, or acepromazine) can profoundly alter esophageal motility, making interpretation of the "flaccid" esophagus difficult. Evaluation without chemical restraint, using nasopharyngeal topical anesthesia may allow for a more accurate inspection of esophageal motility. Retention of fluid, food, or both within the esophageal lumen may be minimal (Figures 7-64 and 7-65), moderate (Figure 7-66), or marked (Figure 7-67), requiring lavage for adequate inspection. Insufflation often results in pronounced, misshapen, dorsoventral oriented dilation (Figures 7-68 to 7-70) compared with the normal, nearly symmetrical, insufflated esophagus.

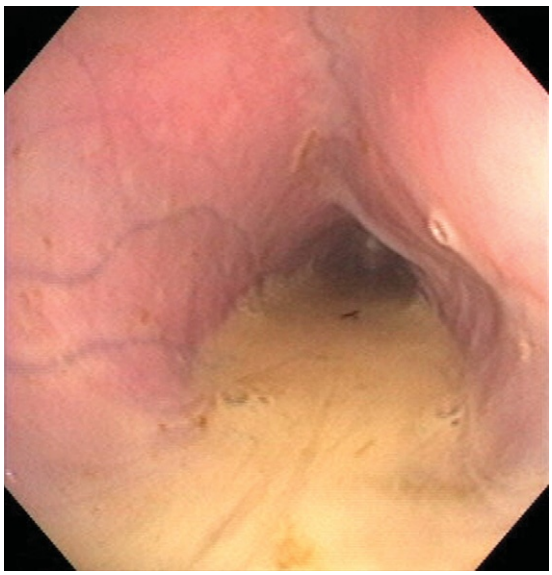

FIGURE 7-64. Megaesophagus with fluid pooling on ventral wall of esophagus. Normal clearance of material from esophagus via peristaltic waves does not occur.

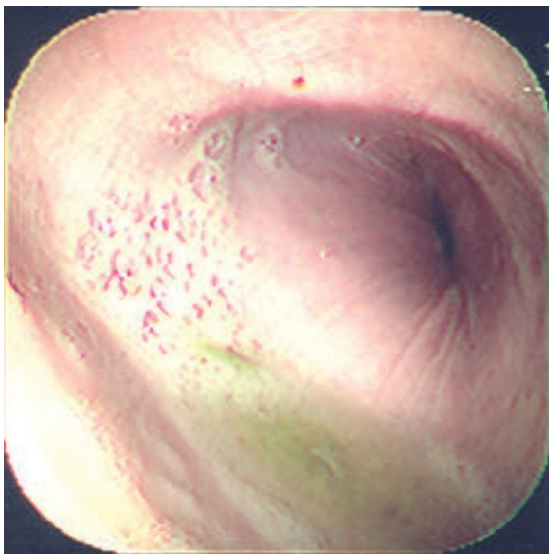

FIGURE 7-65. Enlarged distal esophagus with misshapen lumen dorsoventrally. Fluid pooling on floor is not cleared spontaneously.

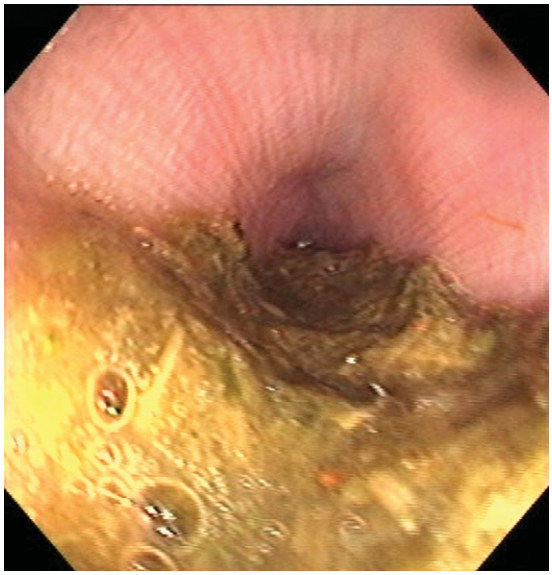

FIGURE 7-66. Moderate amount of retained feed material in distal esophagus compatible with esophageal motor disturbance.

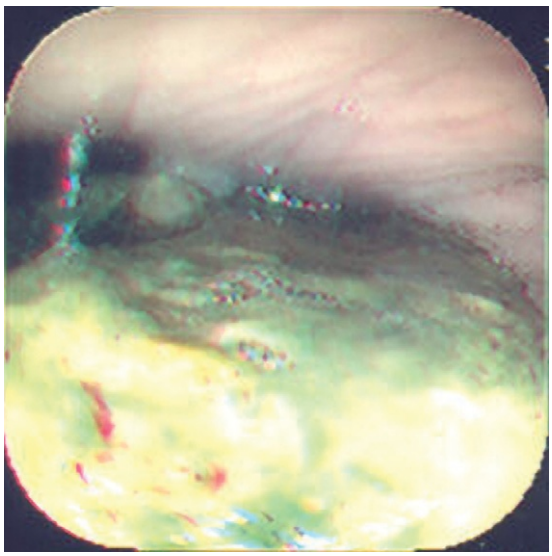

FIGURE 7-67. Marked amount of dilation and food retention within distal esophagus due to megaesophagus.

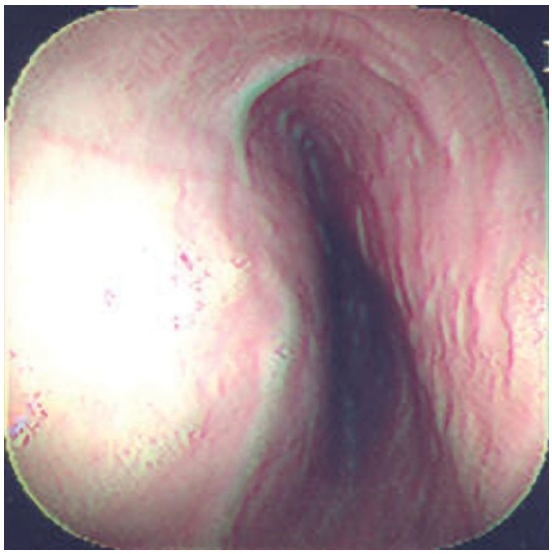

FIGURE 7-68. Insufflation of megaesophagus often results in pronounced dorsoventral elongation and dilation.

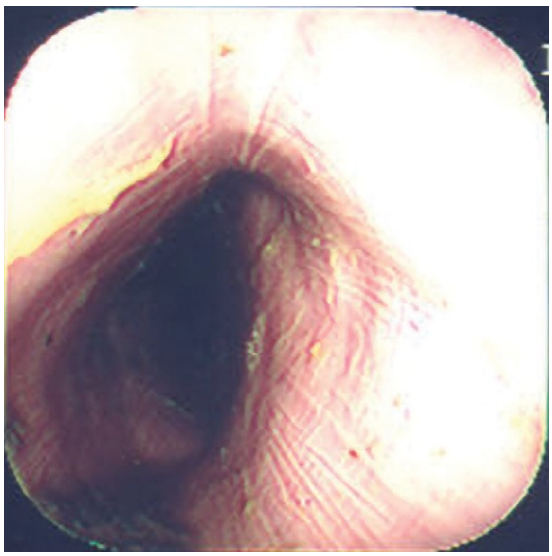

FIGURE 7-69. Example of dorsoventral misshapen dilation when distal esophagus of 8-year-old Thoroughbred mare with suspected megaesophagus was insufflated.

FIGURE 7-70. Marked elongation and dilation of megaesophagus after lavage to clear retained food and fluid material.

BIBLIOGRAPHY

Green EM: Esophagus. In Traub-Dargatz J, Brown CM, editors: *Equine endoscopy*, ed 2, St Louis, 1997, Mosby.

Sisson S: Equine digestive system. In Getty R, editor: *Sisson and Grossman's the anatomy of the domestic animals*, ed 5, Philadelphia, 1975, WB Saunders.

CHAPTER 8

Gastroscopy and Duodenoscopy

FAIRFIELD T. BAIN • LUCIO PETRIZZI • LUCA VALBONETTI • AURELIO MUTTINI

GASTROSCOPY

Indications for gastroscopy include the following:

- Colic
- Persistent gastric reflux
- Chronic weight loss

Equipment required for endoscopic examination of the esophagus is readily available and includes flexible endoscopes of at least 120 cm in length. For foals, endoscopes with smaller diameters of 9 mm or less may be needed for ease of passage past the nasal turbinates. These relatively shorter endoscopes may be satisfactory for gastroscopy in foals; however, for gastroscopy in adult horses, a minimum length of 220 cm is necessary. Care and maintenance of endoscopes are beyond the scope of this chapter; however, caution is required in passage of a flexible endoscope into the esophagus and stomach. A common problem is retroflexion or folding of the endoscope in the caudal pharynx and inadvertent passage into the oral cavity where the tip may be crushed or damaged by the teeth.

On passage of the endoscope into the stomach, inflation with a moderate volume of air may be needed to allow for adequate observation of the gastric mucosa. On some occasions, it is valuable to pass the endoscope inwardly enough for retroflexion and observation of the cardia region (Figures 8-1 and 8-2).

NORMAL ADULT STOMACH

The endoscopic appearance of the normal adult equine stomach may vary with the degree of gas distention, extent of gastric emptying, and amount of remaining fluid or adherent feed material on the mucosal surfaces (Figures 8-3 to 8-8).

GASTRIC ULCERS (Figures 8-9 and 8-10)

Grading Ulcers

The endoscopic appearance of gastric ulcers can be described according to location within the stomach as well as pattern, distribution, and depth of lesions. A subjective grading scheme has been reported.[1] Grades 0 through 3 have been described in the literature. Grade 0 is given for stomach with a normal mucosal surface. Grade 1 ulcers are those with single or multiple small erosions or ulcerations (Figure 8-11). Grade 2 ulcers include those with single or multiple ulcers with larger surface area involved (Figure 8-12). Grade 3 ulcers include those ulcers involving extensive surface area; sometimes these are multifocal coalescing ulcers with more extensive depth of ulceration (Figure 8-13).

Text continued on p. 159

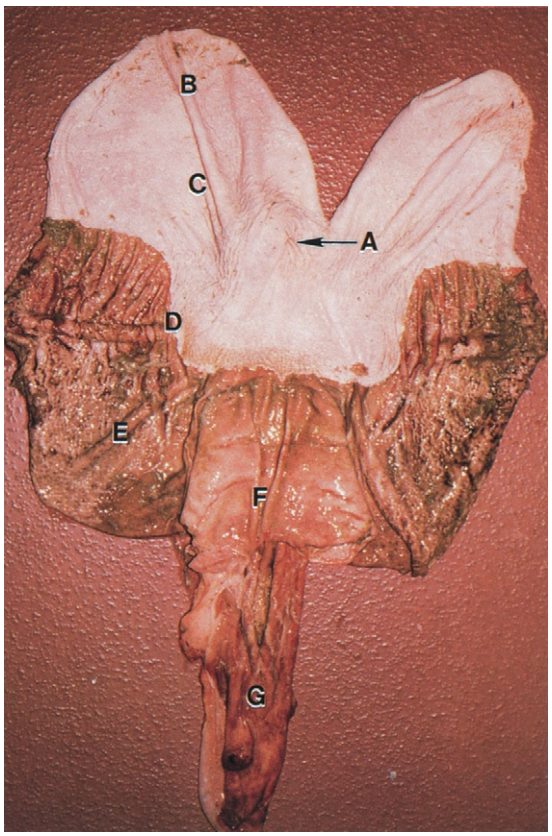

FIGURE 8-1. Necropsy specimen of stomach of an adult horse incised along greater curvature. *A,* Cardiac orifice; *B,* saccus cecus; *C,* squamous epithelium; *D,* margo plicatus; *E,* glandular mucosa; *F,* pyloric region; *G,* duodenum. (From Traub-Dargatz JL, Brown CM: *Equine endoscopy,* ed 2, St Louis, 1997, Mosby.)

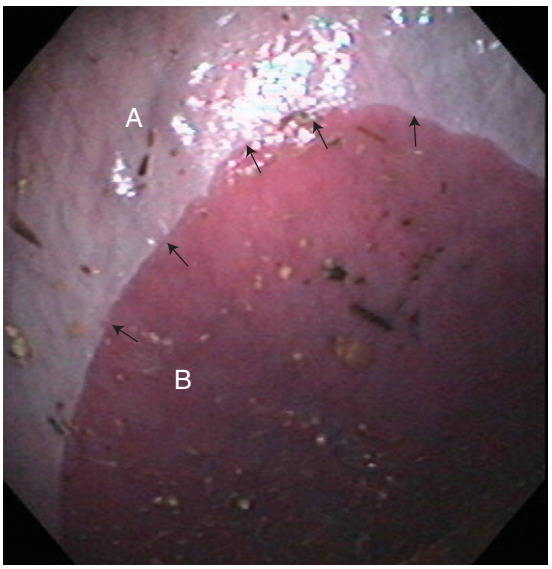

FIGURE 8-2. Normal neonatal stomach. Neonatal gastric mucosa has a thinner, pale-pink squamous region *(A)* in which underlying vasculature is sometimes visible, and a pink-red glandular region *(B).* These regions are demarcated by margo plicatus *(arrows),* which is observed as a distinct line of separation.

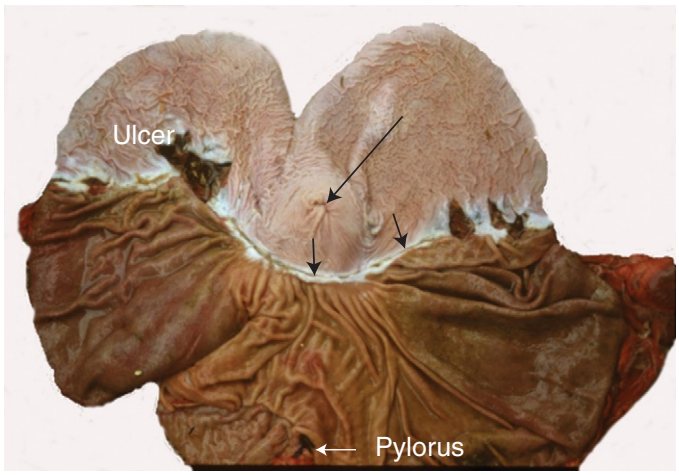

FIGURE 8-3. Postmortem sample showing stomach opened along greater curvature with squamous mucosa on top and margo plicatus *(short black arrows),* separating it from glandular region below. Cardia *(thin long arrow)* is seen just above lesser curvature with pylorus directly below *(white arrow).* There are multiple large angular ulcers (one of which is perforated) as well as a linear ulcer along margo plicatus with thick, raised epithelial margins. Remaining squamous mucosa and glandular mucosa are normal in appearance.

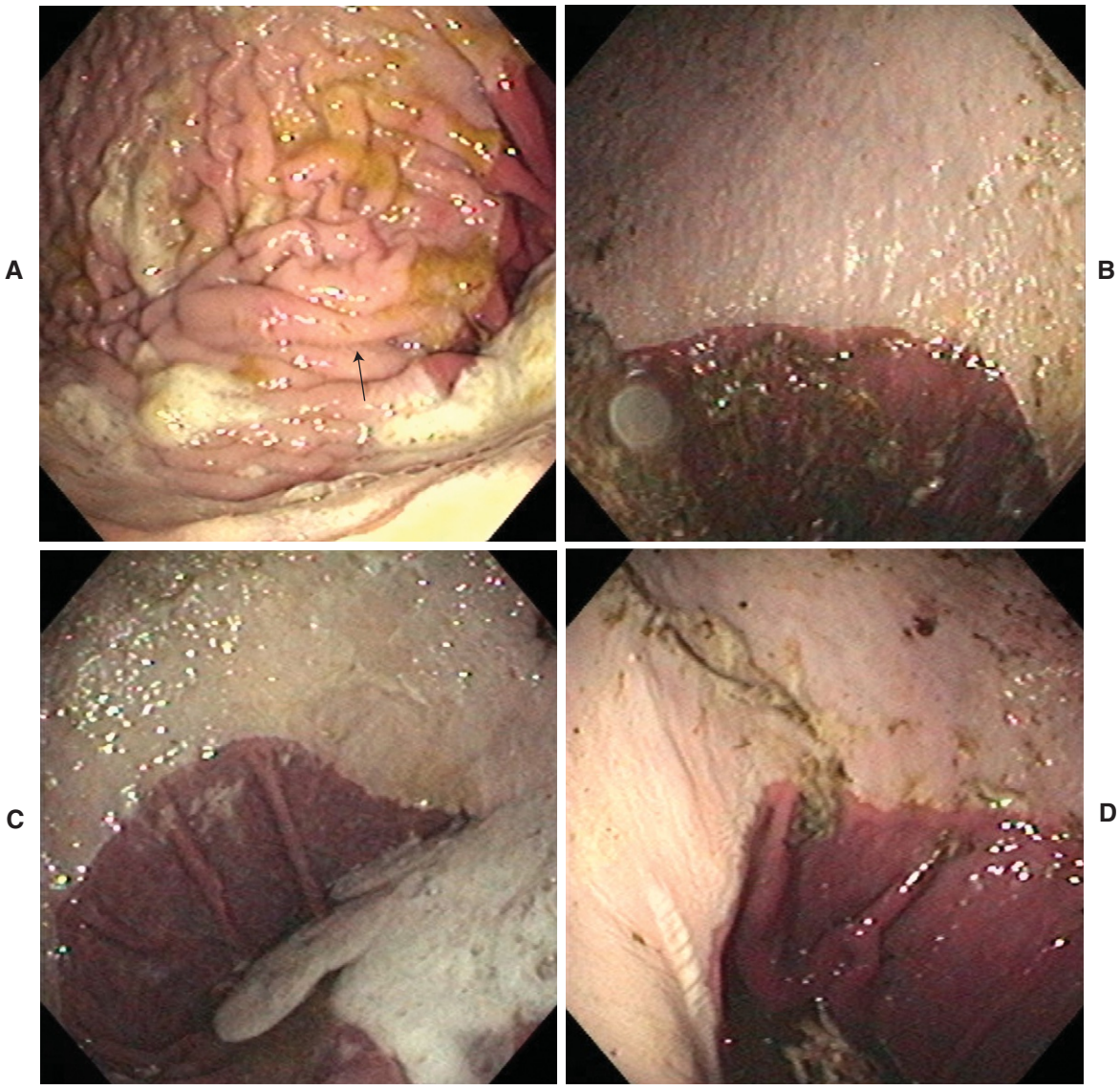

FIGURE 8-4. **A,** Lesser gas distention allows for observation of gastric folds *(arrow).* Margo plicatus is visible along right margin of image. **B** to **H,** Normal gastric mucosal images. All of these demonstrate a relatively smooth, pale-pink to white squamous region with a well-demarcated margo plicatus along separation with darker pink-red glandular region. Differing degrees of residual fluid are present with foamy surface commonly present. Small amounts of green feed material are occasionally adhering to mucosal surface. **B,** View from cardia toward greater curvature of stomach. Normal squamous mucosa above margo plicatus and normal glandular region below. There is a small amount of feed material adherent to glandular mucosa. **C,** Similar view from cardia toward greater curvature with a small volume of liquid material covered with foamy white saliva on surface. **D,** View from cardia with lesser curvature in near lower left foreground. Normal mucosa and margo plicatus.

Continued

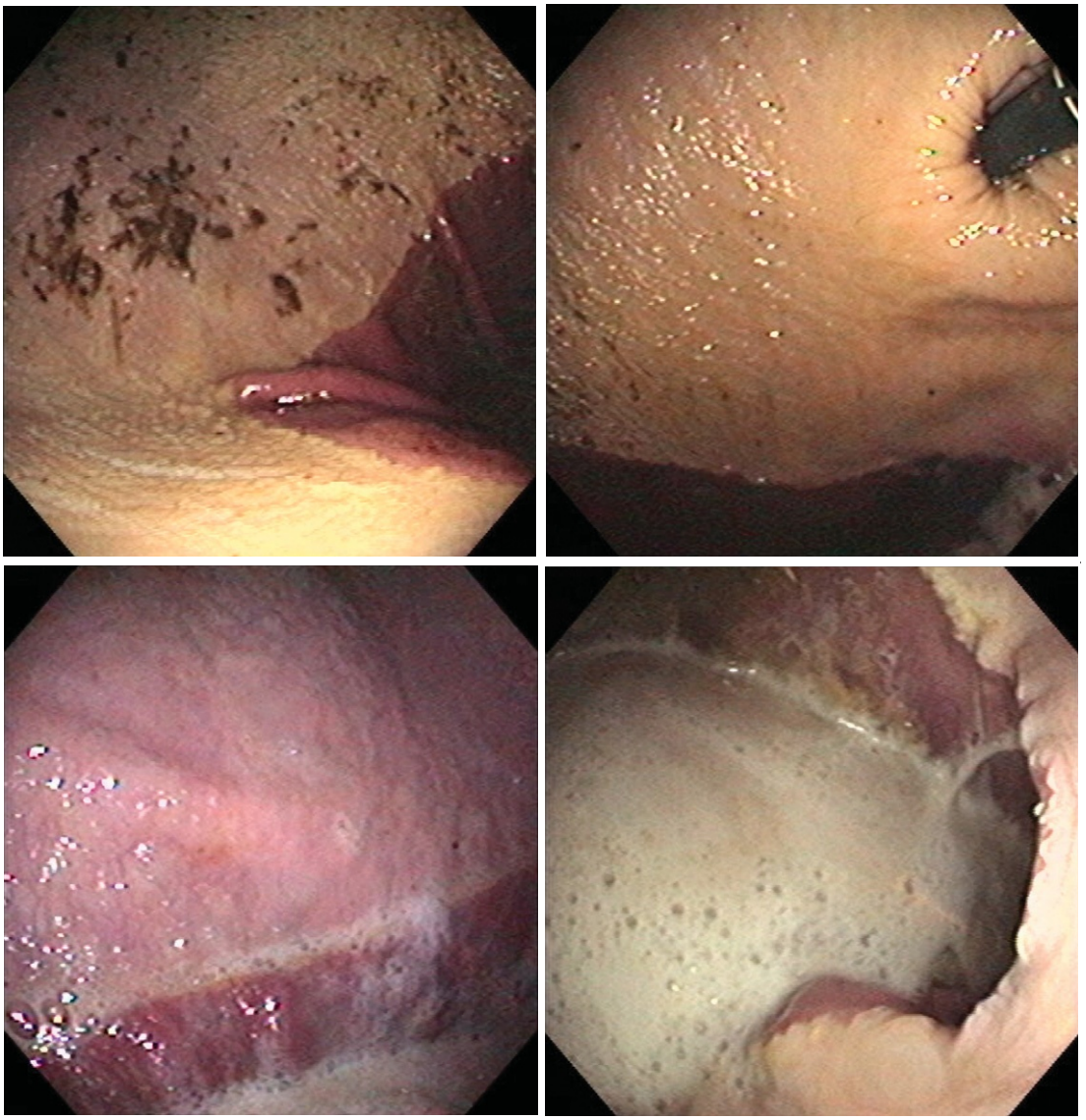

FIGURE 8-4, cont'd **E,** View from cardia with endoscope slightly rotated showing lesser curvature in near lower left foreground extending toward greater curvature in upper right. Normal mucosa and margo plicatus. Small amounts of green feed material adhere to squamous mucosa. **F,** Endoscope has been retroflexed such that it can be seen entering from cardia in upper right. Mucosa is normal and margo plicatus can be seen in lower aspect of image. **G,** View from cardia showing margo plicatus and normal mucosa along greater curvature. There is a small amount of saliva adherent to mucosa. **H,** View of lesser curvature with endoscope positioned just inside cardia. Mucosa is normal with moderate amount of fluid content covered with foamy saliva present in ventral aspect.

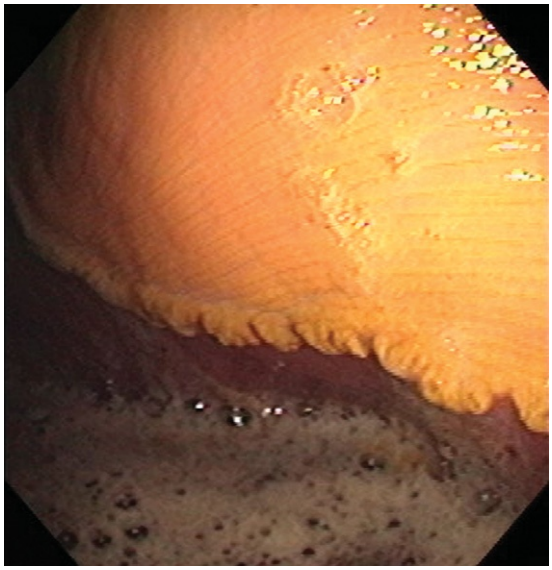

FIGURE 8-5. Margo plicatus. Margo plicatus is generally a distinct line as seen in images of Figure 8-4, but occasionally can be observed as a wavy, irregular line as seen here.

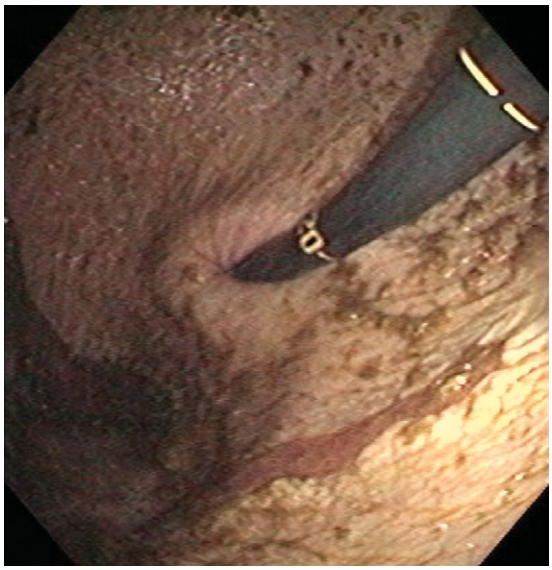

FIGURE 8-6. Cardia. Retroflexion of endoscope will allow observation of region of cardia. In this image, it is surrounded by normal squamous mucosa contiguous with that of esophagus.

A

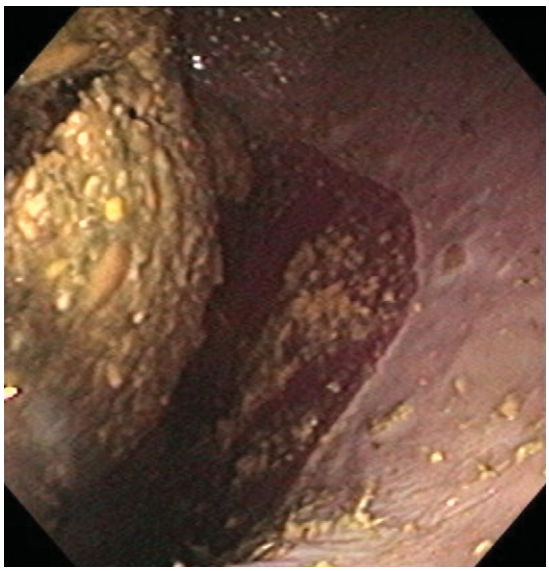

B

FIGURE 8-7. Failure of gastric emptying. **A,** Bolus of compacted feed material is observed protruding through cardia. This can be seen with failure to appropriately fast horse as well as with gastric impaction. **B,** If horse was inappropriately fasted, many times endoscope can still be advanced between feed material and gastric wall and with some degree of inflation, some gastric mucosa (usually only squamous portion) can be observed as in this image.

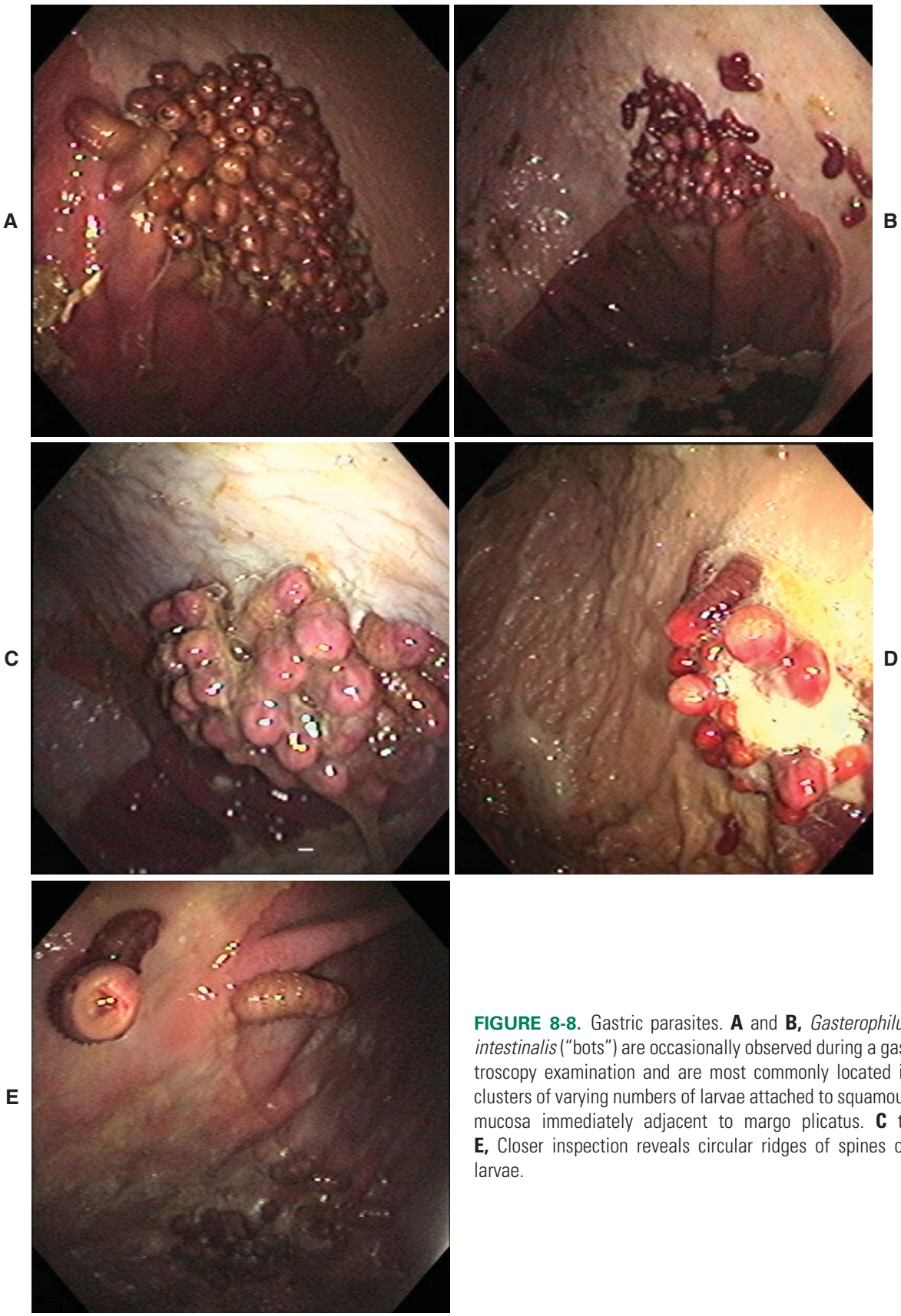

FIGURE 8-8. Gastric parasites. **A** and **B,** *Gasterophilus intestinalis* ("bots") are occasionally observed during a gastroscopy examination and are most commonly located in clusters of varying numbers of larvae attached to squamous mucosa immediately adjacent to margo plicatus. **C** to **E,** Closer inspection reveals circular ridges of spines on larvae.

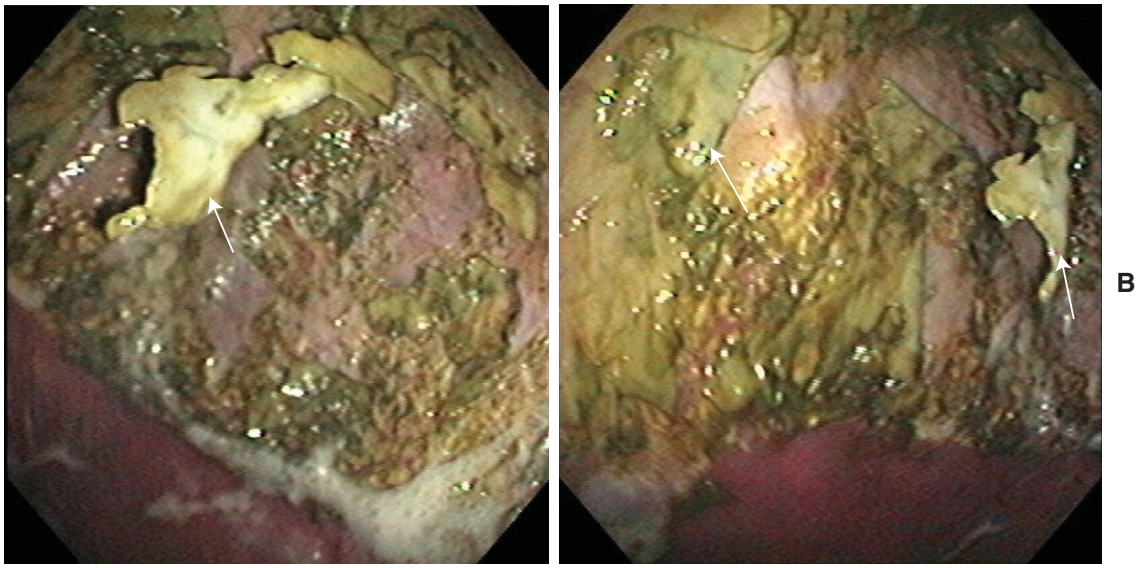

FIGURE 8-9. **A** and **B,** Neonatal gastric ulcers. Gastric ulceration is a common finding in neonates with a variety of illnesses. Squamous epithelium is seen detaching in large sheets *(arrows).*

FIGURE 8-10. Neonatal gastric ulceration. Occasionally, squamous epithelium thickens over focal regions and sometimes separates leaving an exposed pink-red submucosal area as seen in center of this image.

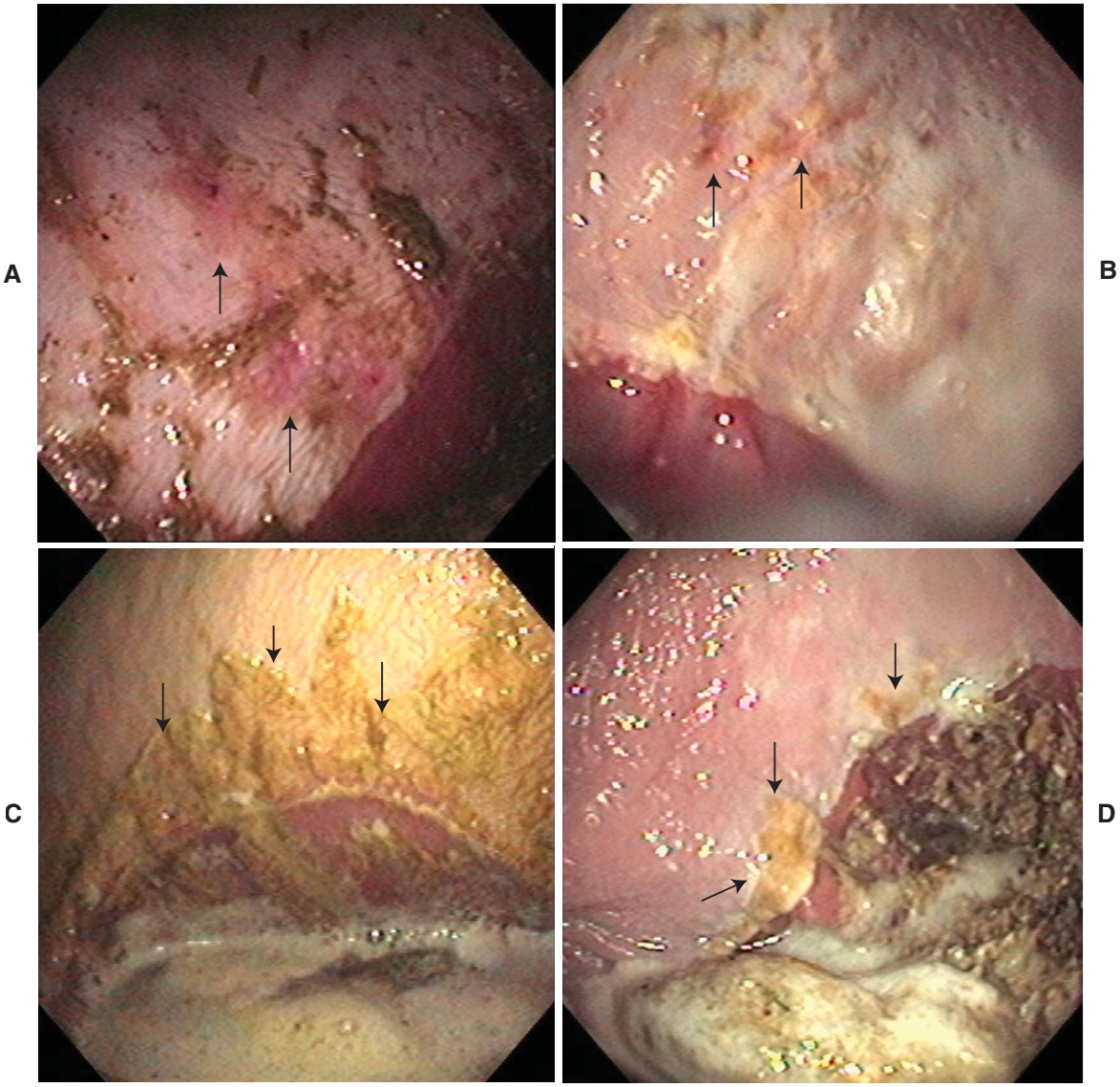

FIGURE 8-11. Grade 1 gastric ulcers. **A,** Scattered red erosions *(arrows)* on squamous mucosa characteristic of a grade 1 ulceration. **B,** Few small erosions *(arrows)* are present on squamous mucosa. **C,** Focally extensive area of epithelial separation and ulceration of squamous mucosa (delineated by *arrows*) along margo plicatus. **D,** Smaller focal regions of ulceration *(arrows)* along margo plicatus. Thicker white margins are consistent with epithelial hyperplasia suggestive of a healing response.

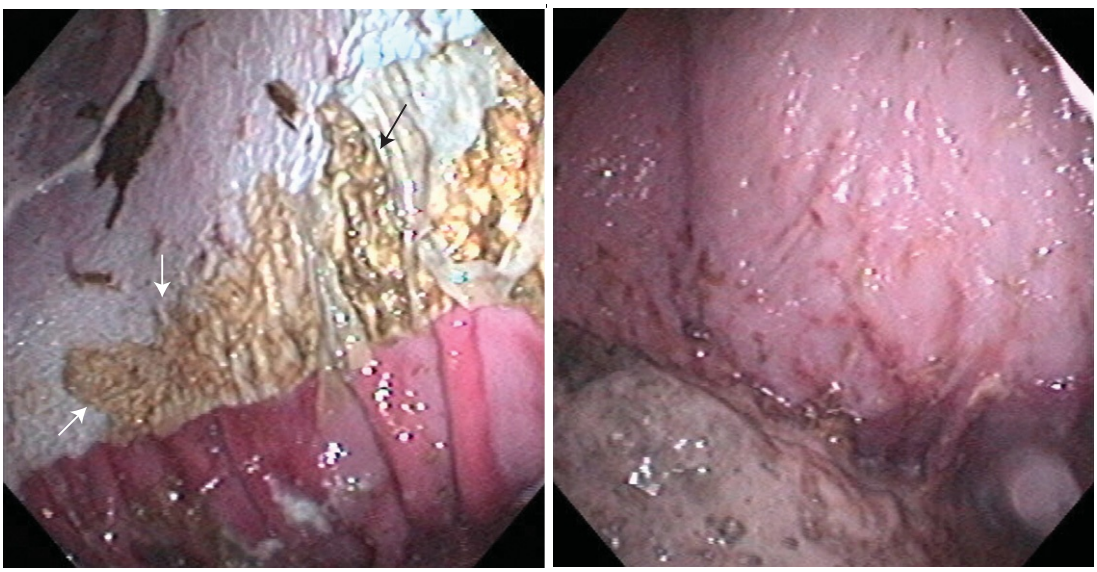

FIGURE 8-11, cont'd **E,** Large region of superficial ulceration and epithelial separation (delineated by *arrows*) in squamous mucosa just above margo plicatus in a neonatal foal. **F,** Multiple small foci of ulceration scattered across squamous mucosa.

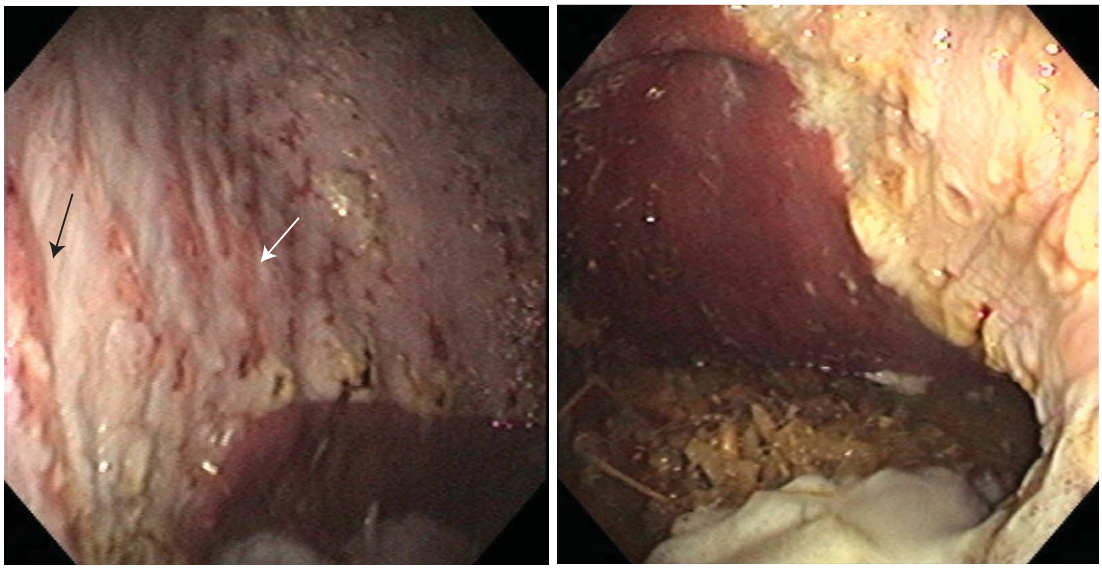

FIGURE 8-12. Grade 2 gastric ulcers. **A,** Extensive reddened linear erosions *(arrows)* are present in squamous mucosa. **B,** Multiple crater like ulcerations in squamous mucosa consistent with healing grade 2 gastric ulcers. *Continued*

C

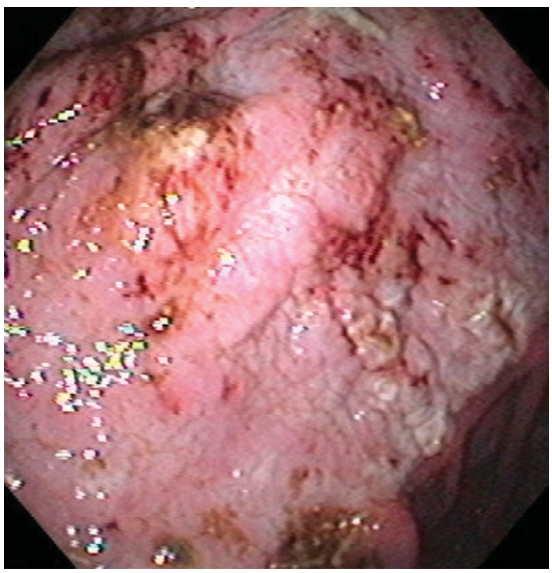

D

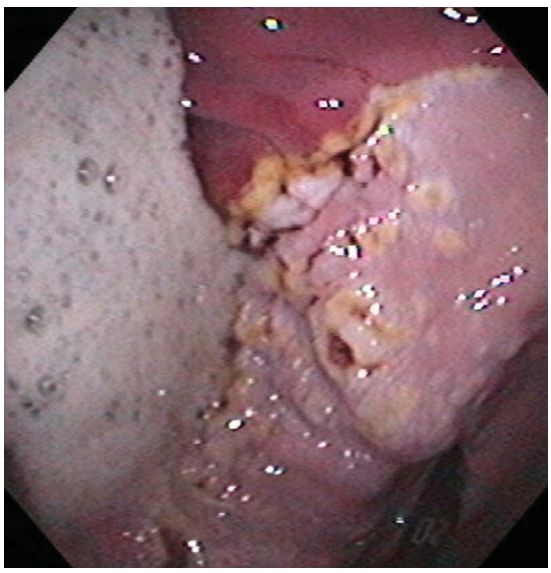

E

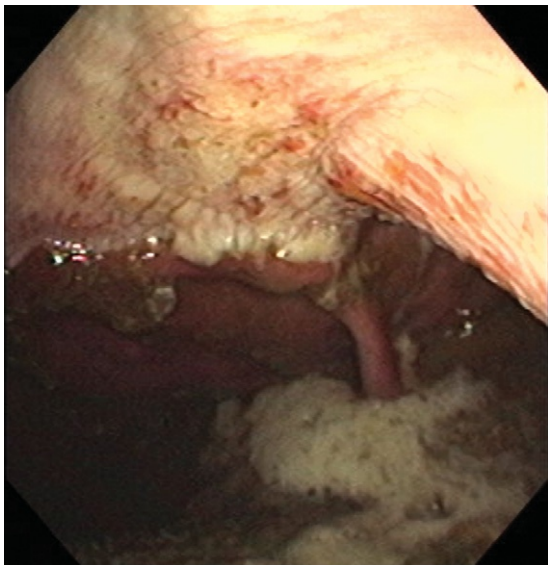

FIGURE 8-12, cont'd **C,** Multiple ulcerations of medium depth in squamous mucosa. **D,** Multifocal ulcers in squamous mucosa with raised borders. **E,** Multifocal coalescing ulcerations in squamous mucosa.

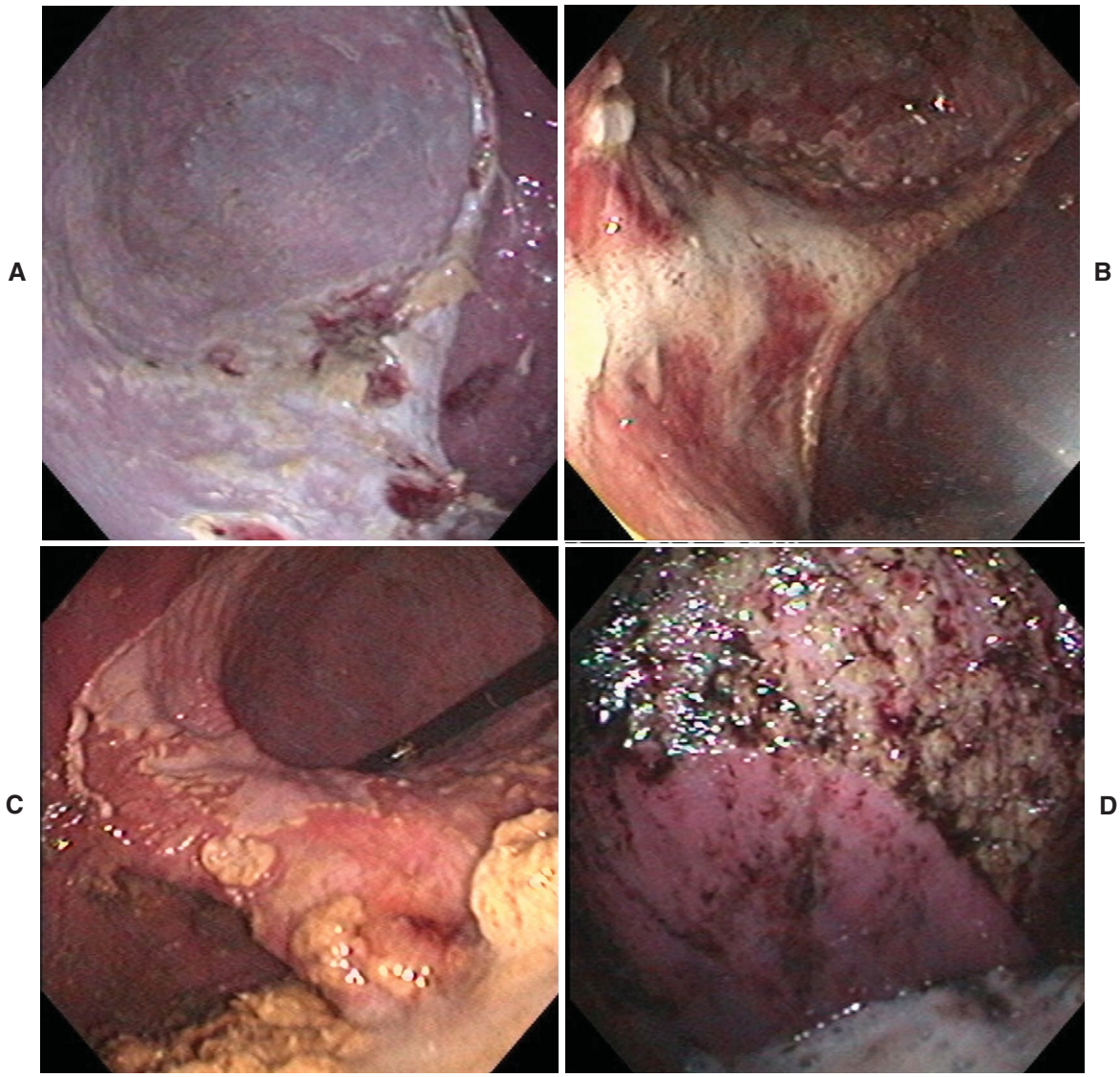

FIGURE 8-13. Grade 3 gastric ulcers. **A,** Multiple deep ulcerations in squamous mucosa. Thick, raised margins suggest some epithelial regenerative response. **B,** More extensive ulceration of squamous mucosa along lesser curvature. **C,** Extensive, coalescing region of ulceration along lesser curvature. **D,** Large percentage of squamous mucosa is ulcerated with remnants of squamous epithelium remaining.

Continued

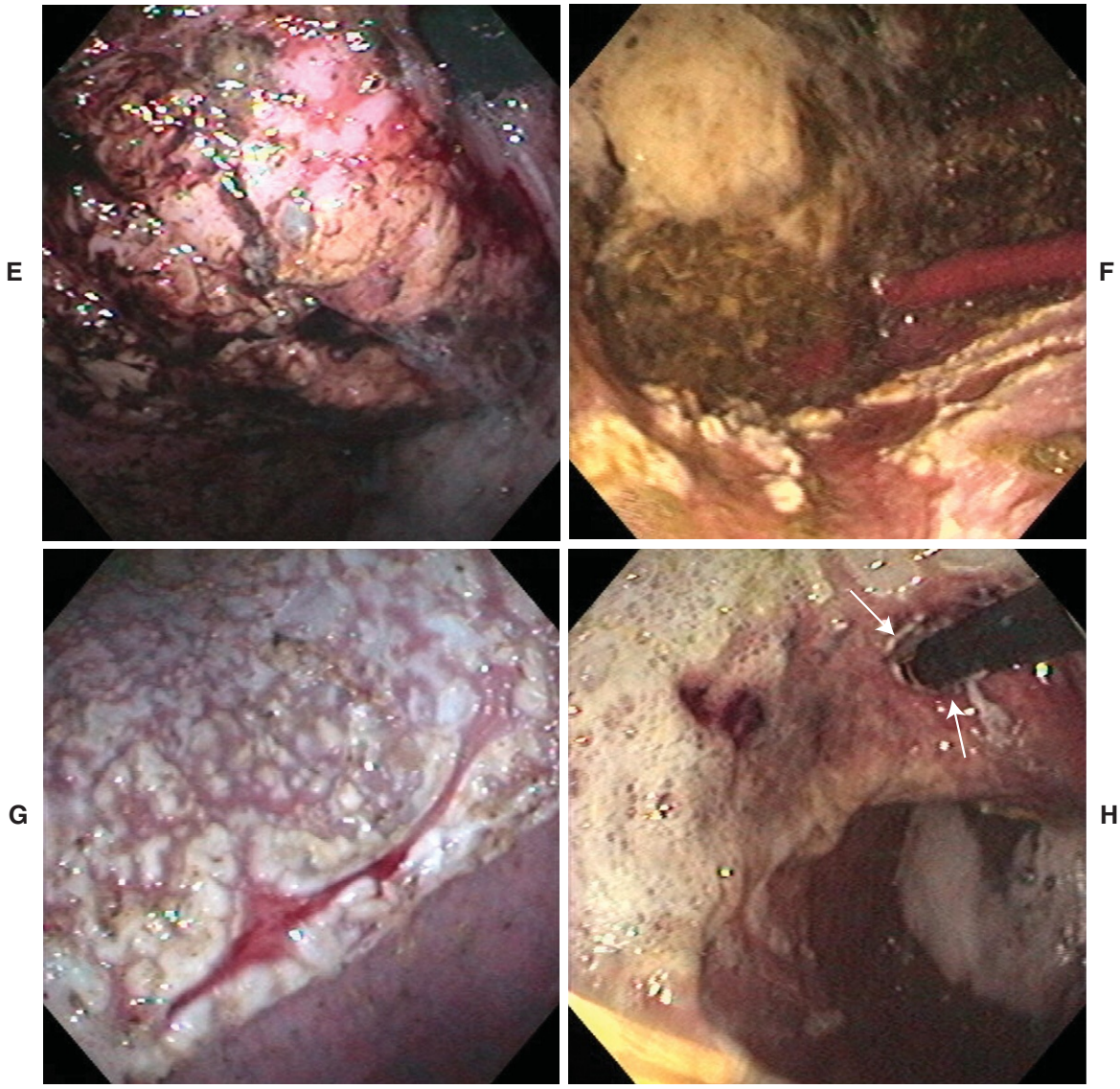

FIGURE 8-13, cont'd **E,** Closer view of mucosa from Figure 8-28, *D*. **F,** Extensive area of ulceration with raised epithelial margins in squamous mucosa. **G,** Extensive diffuse regions of ulceration with larger, linear region of ulceration along margo plicatus. **H,** Focally extensive squamous mucosal ulceration surrounding cardia (*arrow* indicates entrance of endoscope from esophagus).

Healing of Gastric Ulcers

Serial endoscopic examination is often performed to assess whether satisfactory healing of gastric ulcers has occurred to determine when to discontinue medical therapy (Figures 8-14 and 8-15). No reference exists for accurate determination of healing rates; however, most conditions have been observed to be repaired over 1 to 4 weeks. The extent and depth of the initial ulcer process is most likely the main determinant of time to resolution.

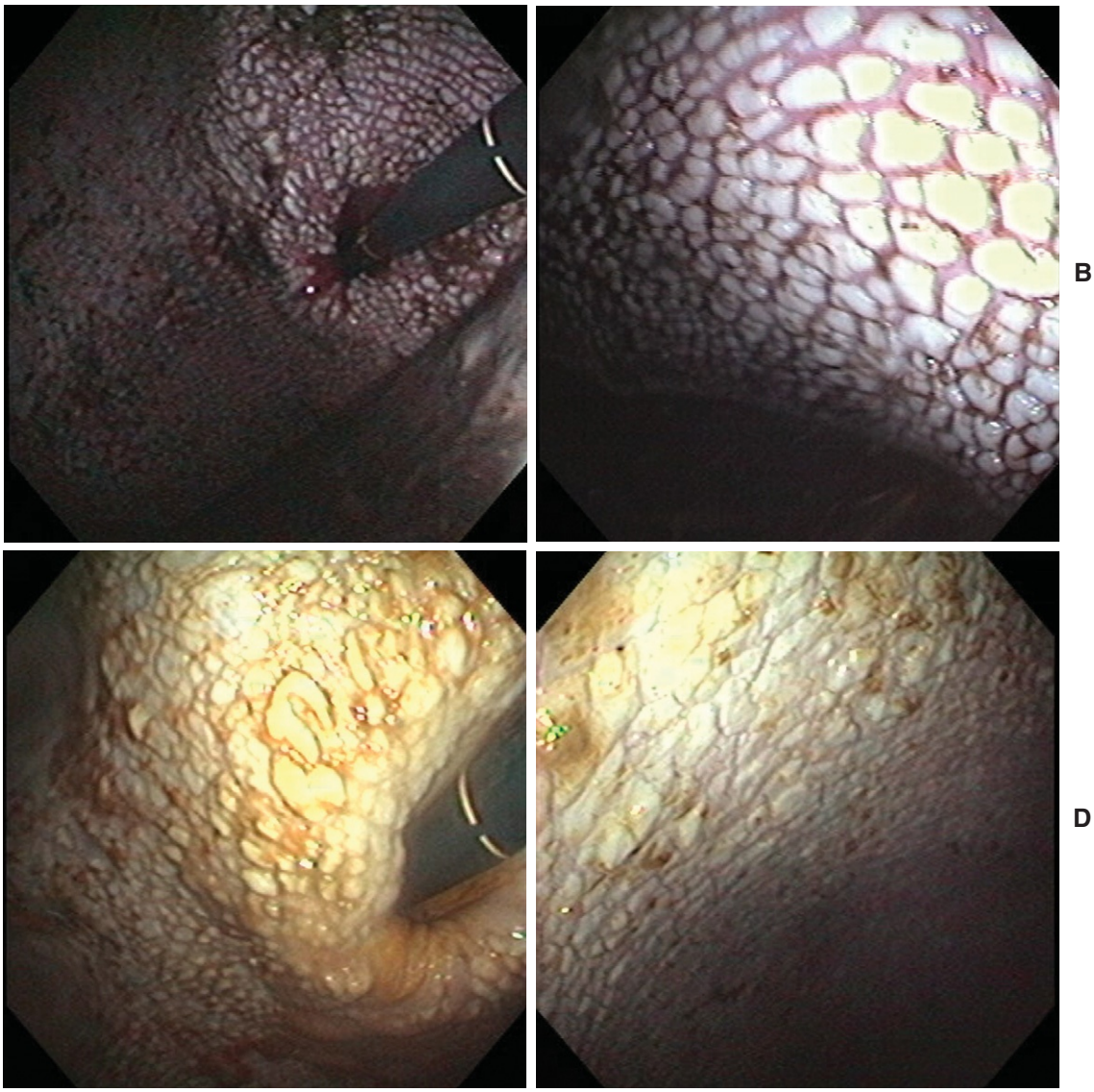

FIGURES 8-14. Gastritis. **A,** 10-year-old Warmblood was seen with a history of melena and anorexia. Diffuse grade 3 ulceration of squamous mucosa, resulting in "cobblestone" mounds of epithelium in squamous mucosa, was present in cardia. **B,** Same horse demonstrating similar cobblestone appearance of squamous mucosa. **C,** Same horse after 3 days of treatment with oral metoclopramide, sucralfate (Carafate), and omeprazole. Note decreased depth of ulceration. **D,** Same horse as in Figure 8-14, *B,* after 10 days of treatment showing marked healing of grade 3 ulceration.

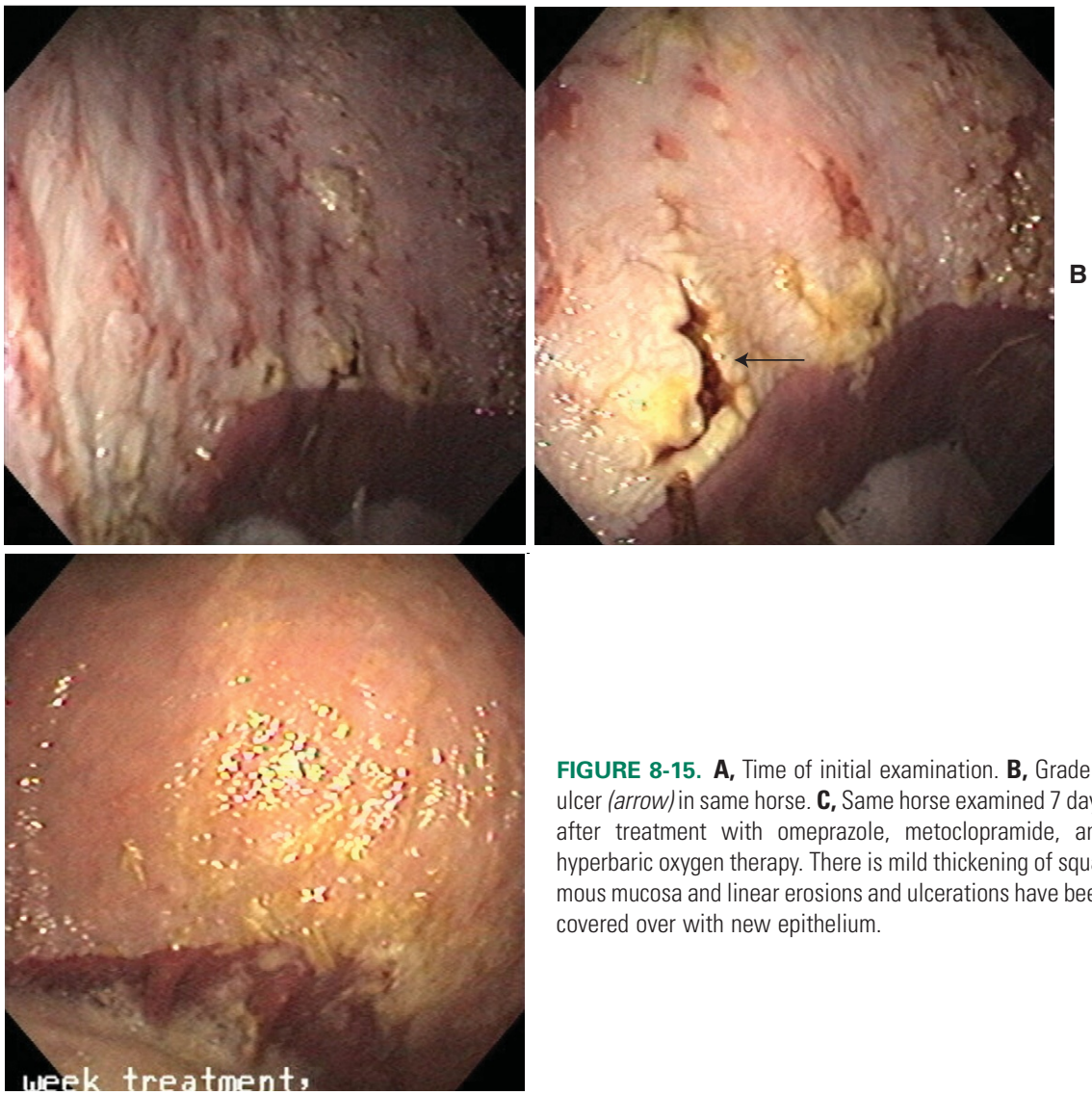

FIGURE 8-15. **A,** Time of initial examination. **B,** Grade 3 ulcer *(arrow)* in same horse. **C,** Same horse examined 7 days after treatment with omeprazole, metoclopramide, and hyperbaric oxygen therapy. There is mild thickening of squamous mucosa and linear erosions and ulcerations have been covered over with new epithelium.

NEOPLASIA (Figure 8-16)

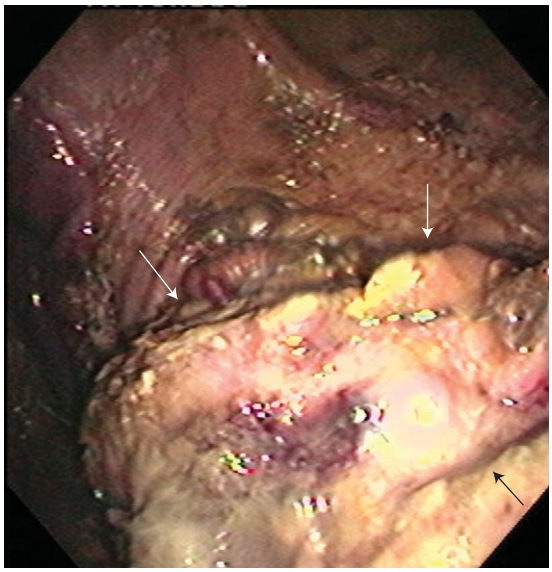

FIGURE 8-16. Squamous cell carcinoma is seen as a raised mound of white-to-pink mucosa *(arrows)* with a focal area of ulceration due to proliferation, invasion, and thickening of gastric wall by neoplasm. This is the most common form of neoplasm in the stomach, which can sometimes be seen endoscopically.

EXAMINATION OF THE DUODENUM

Duodenum

An increasing number of diseases involving proximal small intestine have been reported in the horse, including gastroduodenal ulceration,[2] duodenal stenosis,[3] and duodenitis-proximal jejunitis.[4-6] Clinical signs of diseases involving the proximal small intestine are sometimes vague and unspecific, and distinction between these conditions and others can be difficult. Standing laparoscopy,[7] gastroscopy,[7–9] and gastroduodenoscopy[10] have been described as useful diagnostic tools for abdominal disorders of the horse.

The availability of proper instrumentation has contributed to the development of duodenoscopy for the inspection of normal and pathologic features of the duodenum.[11] This is a safe technique to obtain direct insight into the status of this part of the bowel.

Preparation and Restraining

Food has to be withheld for 12 hours before the examination and water for 8 hours. Horses are sedated and contained in suitable stocks; twitch is applied if necessary. At least three people are needed to perform the examination: one to restrain the horse, one to move the scope, and one to manipulate the handle of the scope and adjust all the regulations of the equipment.

Equipment

A 3 m endoscope (see Chapter 1) should be used to reach the duodenum in adult horses weighing 400 kg or more. For the small foal or weanling weighing 250 kg or less, the use of a 2.2 m endoscope would be adequate to reach the pylorus and the proximal duodenum.

One of the authors (L.P.) currently uses a 3.3-m length, 1.3-cm wide video endoscope with a 0.3-cm wide working channel to perform duodenoscopies. Flexible bioptic endoscopic forceps and a 350-cm length aspiration catheter of a suitable diameter (0.25 cm) are also required for a complete examination.

A 300-watt cold light source must be connected to the scope to provide enough power to illuminate the inside of the duodenum. A digital processing device (see Chapter 2) is also very useful for recording images.

Technique

The first part of the examination is exactly the same as that for gastroscopy. Once the cardia has been reached, the tip of the scope must be directed towards the margo plicatus at the level of the greater curvature of the stomach (Figures 8-17 and 8-18). Then the scope is moved downward along the greater curvature. Some amount of fluid often lies in the lower part of the stomach, but this does not interfere with the procedure. The progression of the scope must be slow and continue until the image of the *pylorus* can be seen as a black hole in the middle of the monitor (Figure 8-19, *A* and *B*). The

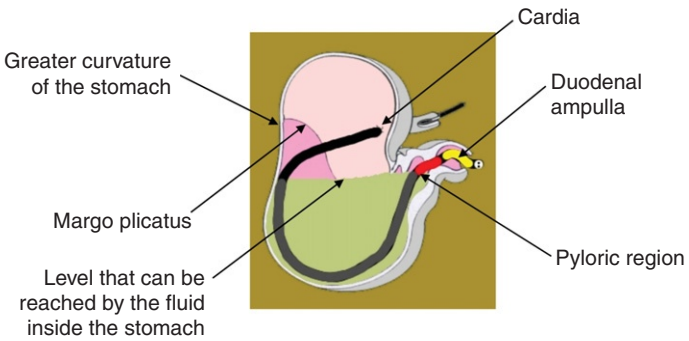

FIGURE 8-17. Schematic of stomach and duodenum.

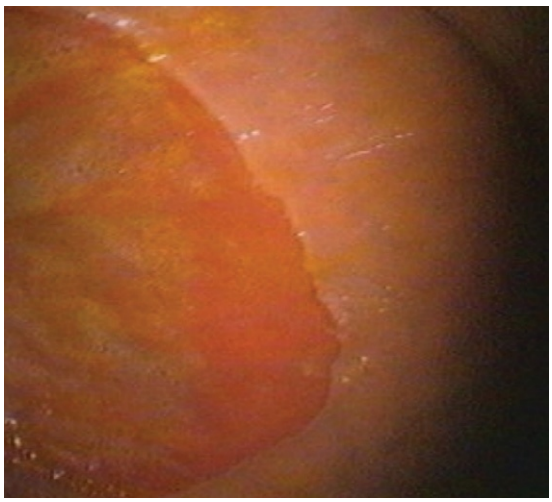

FIGURE 8-18. Margo plicatus at level of greater curvature is the landmark for reaching antrum and lower parts of stomach.

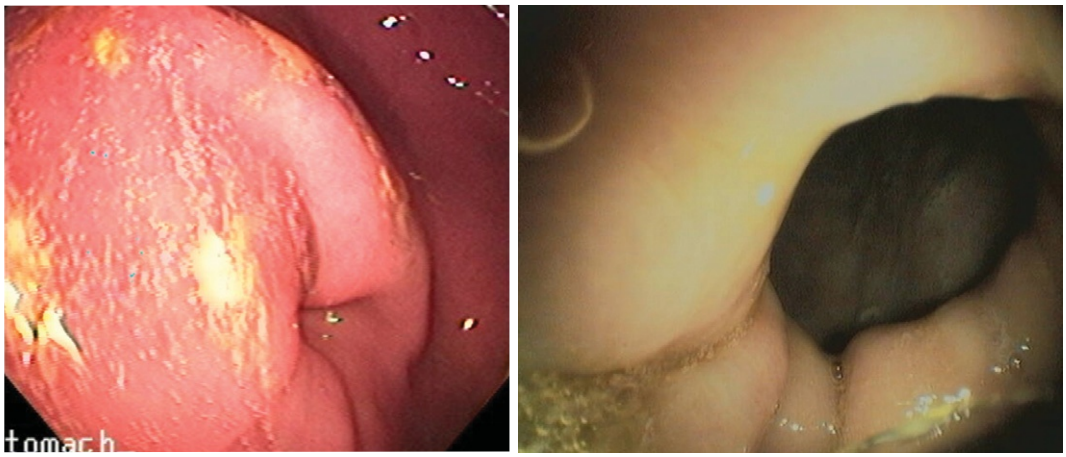

FIGURE 8-19. **A** and **B,** Pylorus can be seen as a black hole in middle of monitor. Visualization and progression through pyloric orifice can be enhanced by inflating air in stomach once in pyloric region.

tip of the scope has to pass through the pyloric orifice. Once the scope is inside the duodenal ampulla the progression has to be particularly slow and is enhanced by the peristalsis of the gastroenteric tract. With the scope inside the duodenum the appearance of the mucosa can be evaluated, biopsy specimens can be taken (Figure 8-20, *A* to *C*), and duodenal fluid can be obtained (Figure 8-21).

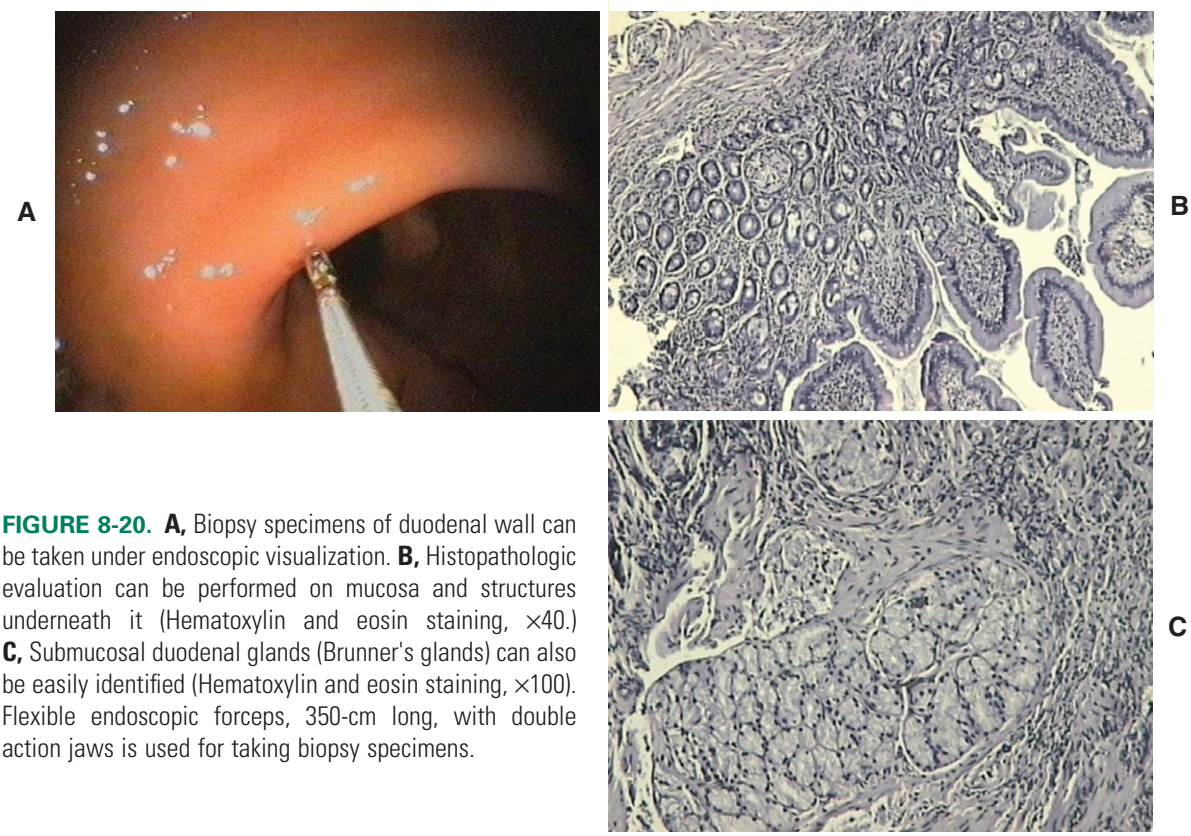

FIGURE 8-20. **A,** Biopsy specimens of duodenal wall can be taken under endoscopic visualization. **B,** Histopathologic evaluation can be performed on mucosa and structures underneath it (Hematoxylin and eosin staining, ×40.) **C,** Submucosal duodenal glands (Brunner's glands) can also be easily identified (Hematoxylin and eosin staining, ×100). Flexible endoscopic forceps, 350-cm long, with double action jaws is used for taking biopsy specimens.

Duodenal fluid can be used for microbiologic evaluation, but in this case a sterile collection procedure is required to avoid contamination by bacteria of the first respiratory and digestive tracts (Figure 8-22). For duodenal fluid specimens one should measure pH and perform aerobic, anaerobic, and microaerophilic cultures.

The anatomic structures of the duodenum that can be easily inspected in almost any adult horse are the duodenal ampulla and the proximal duodenum.

FIGURE 8-21. Aspiration of duodenal contents through a Teflon cannula enhances collection of fluid specimens for biochemical and microbiologic evaluation. Teflon cannula, 350-cm long and 0.25-cm wide, is used, connected to a 20-ml sterile syringe.

FIGURE 8-22. To avoid risk of bacterial contamination of duodenal fluid specimens, a small amount of sterile agar gel can be aspirated into cannula before examination. This plug must be flushed off when the cannula is in duodenum before collecting fluid.

NORMAL DUODENUM

The passage from the pylorus to the duodenum (Figure 8-23) is matched with the change of color and aspect of the mucosa (Figure 8-24). The healthy duodenal mucosa has a red-brownish color and a velvety appearance (Figure 8-25) due to the presence of the intestinal villi.

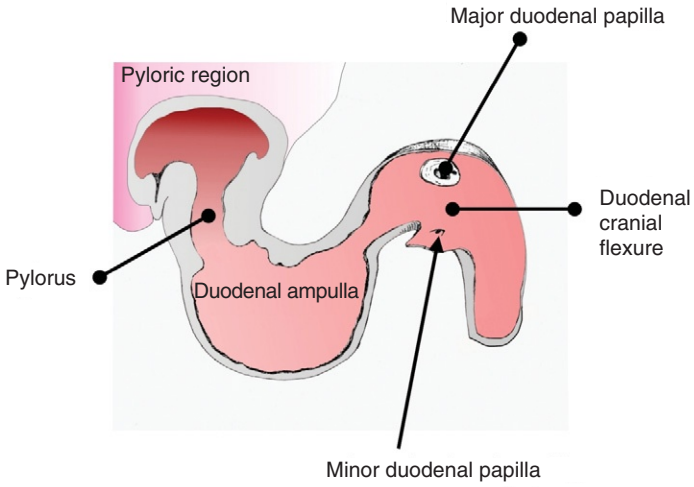

FIGURE 8-23. Proximal duodenum.

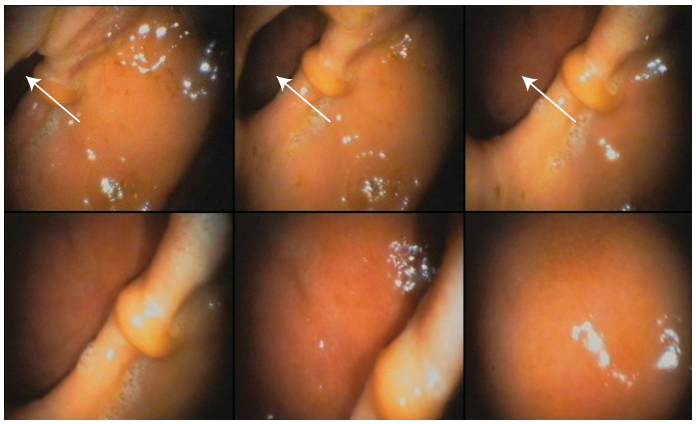

FIGURE 8-24. Sequence of images showing passage of endoscope through pyloric orifice. Passage from pylorus *(arrows)* to duodenum is matched with change of color and aspect of mucosa.

FIGURE 8-25. Close-up view of healthy duodenal mucosa enhances visualization of velvety appearance due to presence of villi.

The proximal duodenum begins from the pylorus with a sharp bend to the right of the animal (Figure 8-26). Its diameter is uniform except at the duodenal ampulla where it is widened for a short distance. Many circular mucosal folds that move together with duodenal peristalsis characterize the endoscopic appearance of the proximal duodenum (Figure 8-27).

The major duodenal papilla is the common outlet of the hepatic and the pancreatic ducts (Figure 8-28) and lies about 10 cm from the pylorus at the end of the ampulla. On the opposite side a little farther along is the outlet of the accessory pancreatic duct (minor duodenal papilla) (Figure 8-29).

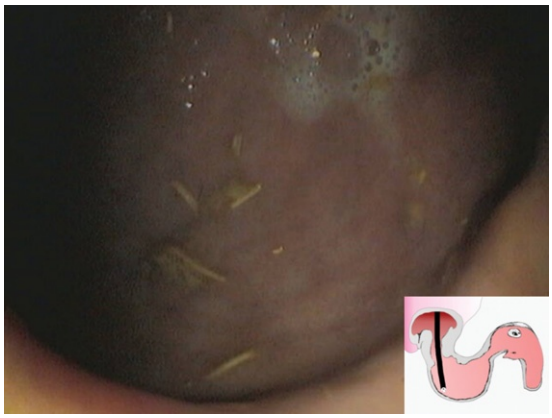

FIGURE 8-26. Proximal duodenum begins from pylorus with sharp bend to right of animal *(left in image)*.

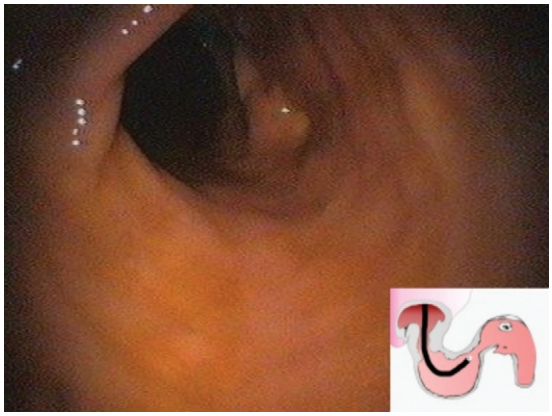

FIGURE 8-27. Many circular mucosal folds moving together with duodenal peristalsis characterize proximal duodenum.

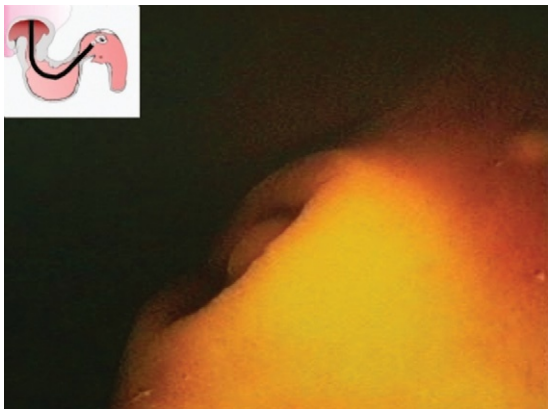

FIGURE 8-28. Close-up view of major duodenal papilla soaking in duodenal fluid.

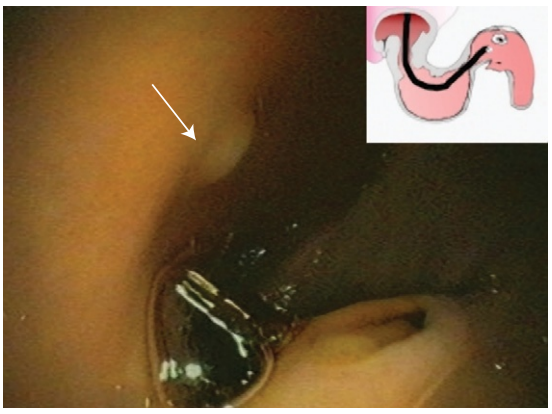

FIGURE 8-29. Minor duodenal papilla *(arrow)* lies a little farther on opposite side.

The normal duodenal content mixed with hepatic and pancreatic secretions can be seen as a clear amber fluid inside the lumen of the duodenum (Figure 8-30).

In healthy adult horses, duodenal fluid pH is about 7.4 (±0.4), and its bacterial content is mainly represented by *Escherichia coli* spp., *Enterococcus* spp., and *Streptococcus* spp. *Staphylococcus* spp. and *Bacillus* spp. have also been isolated.[11]

DISEASES OF DUODENUM

Reports on diagnosis of duodenal ulcers and parasites with duodenoscopy are available in literature.[10] Duodenal ulcers usually involve the pyloric region (Figure 8-31, *A* and *B*) and should be called gastroduodenal ulcers. Duodenal diverticula and stenosis have also been reported.[3] Proximal enteritis is a clinical concern in the horse, but endoscopic findings have not been described.

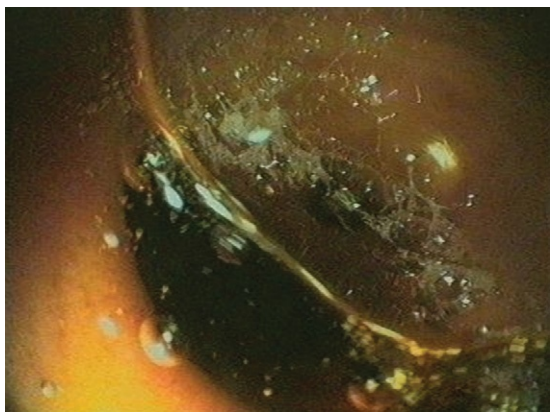

FIGURE 8-30. Normal duodenal content looks like clear amber fluid inside lumen.

A

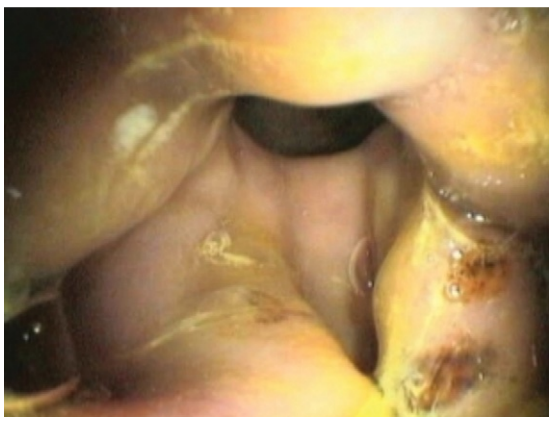

B

FIGURE 8-31. Duodenal ulceration often involve the pyloric region also. **A,** 3-year-old Thoroughbred stallion with poor racing performance, at end of very intense racing season. For 2 months horse had poor appetite and poor body condition. No other clinical abnormalities were detected. Laboratory findings were all within normal range. Duodenoscopic examination revealed a wide ulcer of proximal duodenum. Therapy consisted of rest and oral administration of 2 mg/kg of omeprazole twice a day. After 15 days, endoscopy confirmed complete resolution of ulcer. **B,** 2-year-old Thoroughbred filly with history of recurrent colic and poor appetite. Because of a tendinitis horse had been at stall rest and was treated with nonsteroidal antiinflammatory drugs for 10 days. Results of rectal examination were negative, and laboratory findings did not suggest any particular alteration. Gastroduodenoscopy permitted diagnosis of deep ulcer of pyloric orifice.

The collection of histopathologic samples and fluid from the duodenum could be very useful in understanding the pathogenesis of diseases involving the proximal intestine and possibly identifying their clinical or subclinical patterns. Duodenal neoplasms, although rare, have also been described.[12]

REFERENCES

1. *Equine gastric ulcers (equine gastric ulcer syndrome): prevalence, pathophysiology, and veterinary practice,* 1999, Merial Limited. Available at http://www.egus.org.
2. Murray MJ: Gastroduodenal ulceration. In Robinson NE: *Current therapy in equine medicine,* ed 4, pp 191-197, Philadelphia, 1997, WB Saunders.
3. Ettinger JJ, Ford T, Palmer E: Ulcerative duodenitis with luminal constriction in two horses, *J Am Vet Med Assoc* 196:1628-1630, 1990.
4. Allen D Jr, Clark ES: Duodenitis-proximal jejunitis. In Robinson NE: *Current therapy in equine medicine,* ed 3, pp 211-214, Philadelphia, 1991, WB Saunders.
5. Freeman DE: Duodenitis-proximal jejunitis, *Equine Vet Educ* 12:322-332, 2000.
6. White NA, Tyler DE, Blackwell RB, Allen D: Hemorrhagic fibronecrotic duodenitis-proximal jejunitis in horses: 20 cases (1977-1984), *J Am Vet Med Assoc* 190:311-315, 1987.
7. Fischer AT, Kent Lloyd KC, Carlsson GP, Madigan JE: Diagnostic laparoscopy in the horse, *J Am Vet Med Assoc* 189:289, 1986.
8. Valbonetti L, Castellano G, De Leo P et al: Indagine gastroscopia in 83 cavalli sportivi, XIV Congresso Nazionale SIDI Parma, *Rivista SIDI*, Vol 5, No 3, pp 29-39, 1999.
9. Murray MJ, Grodinsky C, Anderson CW et al: Gastric ulcers in horses: a comparison of endoscopic findings in horses with and without clinical sings, *Equine Vet J Suppl* 7:68-72, 1989.
10. Brown CM, Slocombe RF, Derksen FJ: Fiberoptic gastroduodenoscopy in the horse, *J Am Vet Med Assoc* 186: 965-968, 1985.
11. Petrizzi L, Valbonetti L, Varasano V: Endoscopic examination of duodenum in adult horses, *Proceedings of the 7th WEVA Congress*, p 290, 2001.
12. Kasper C, Doran R: Duodenal leiomyoma associated with colic in a two year old horse, *J Am Vet Med Assoc* 202:769-770, 1993.

CHAPTER 9

Cystoscopy

KIM SPRAYBERRY

NORMAL ANATOMY

Multiple views of the normal anatomic appearance of the bladder can be seen from the neck (Figure 9-1). The ureters *(arrows)* enter the dorsal surface of the bladder and course through the wall to enter the lumen dorsally at an acute angle. The normal configuration of the ureteral orifices is slitlike (Figure 9-2). Insufflation of the bladder with air quickly causes the vasculature to become prominent, a normal finding.

In urinary tract endoscopy, examination is performed with the endoscope facing in the same direction as the horse, unlike when the respiratory tract is visualized. When viewing the bladder, the right side of the image is the right side of the horse and vice versa.

Visualization of the urethra in the male horse is best done by insufflating while simultaneously withdrawing the endoscope from the neck of the bladder to the prepuce.

SABULOUS CYSTITIS

An adult mare had chronic urinary incontinence and severe urine scalding on the caudal aspect of the hindquarters. Yellowish greasy sediment was splashed onto the lower hind limbs and tail. The bladder was easily expressed per rectum. The mare was a successful broodmare and was seen with a healthy weanling at her side. Her body condition was excellent, and the mare appeared in excellent health other than the severe urine-scald dermatitis. Results of blood tests showed mild azotemia and an inflammatory hemogram (Figures 9-3 to 9-9).

Chronic Urinary Incontinence

An adult Thoroughbred mare was seen for chronic urinary incontinence (Figures 9-10 to 9-15).

HEMATURIA

An aged adult mare was seen with acute onset of urine discoloration, noted by farm staff. The mare had been losing weight over the past 6 months, an observation that had been attributed to lactational demands, although weaning and provision of an increased nutritional plane had not improved the mare's body condition. Results of blood tests from the referring practitioner demonstrated no significant alterations from normal. The urine stream was uniformly discolored, from beginning to end of voiding (Figures 9-16).

Text continued on p. 176

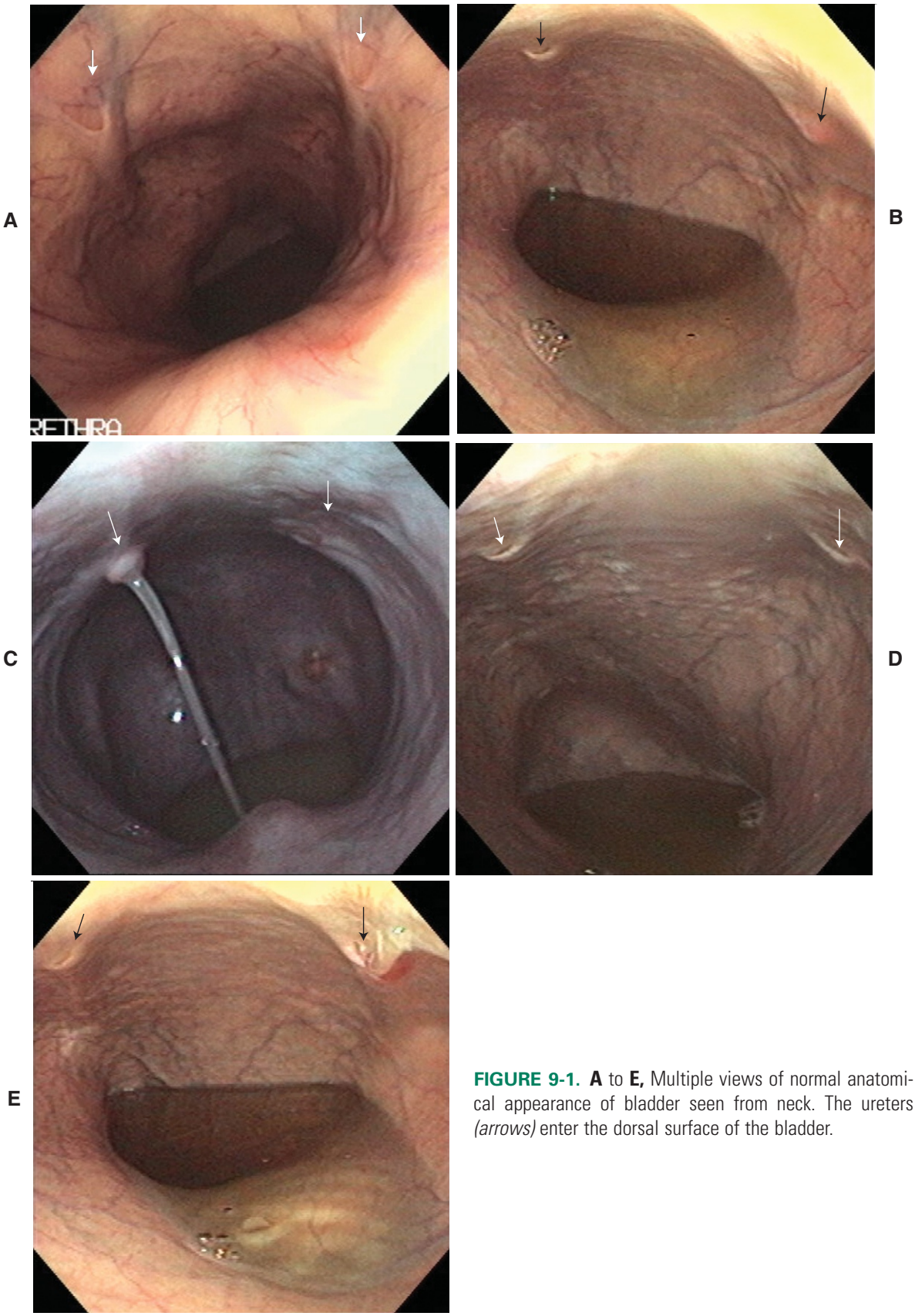

FIGURE 9-1. **A** to **E,** Multiple views of normal anatomical appearance of bladder seen from neck. The ureters *(arrows)* enter the dorsal surface of the bladder.

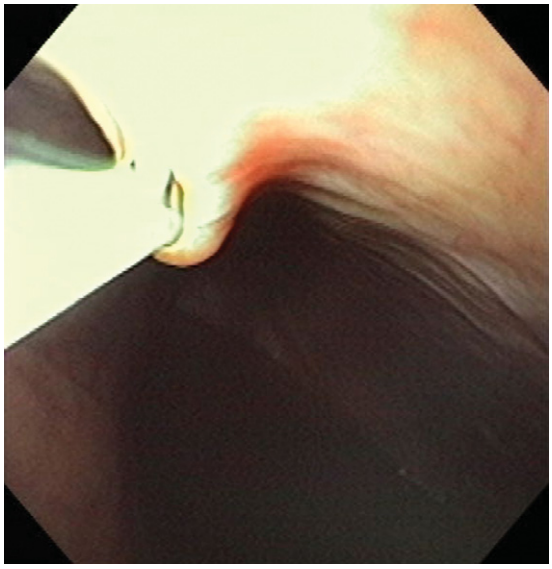

FIGURE 9-2. An 8-French polypropylene catheter is seen placed through right ureteral orifice into ureter.

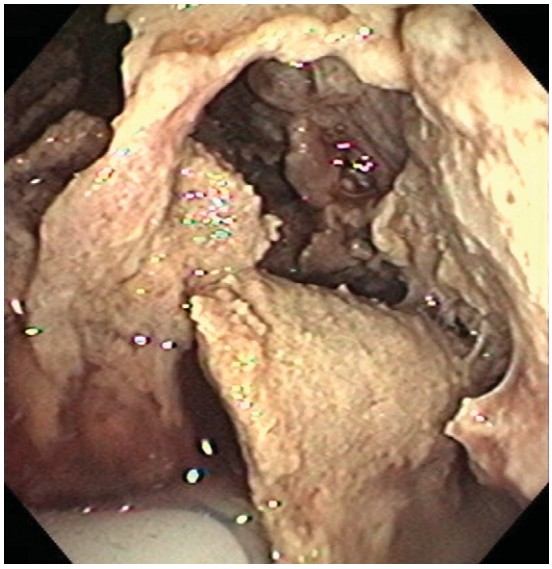

FIGURE 9-3. Endoscopic view of bladder lumen showing severe cystitis, with formation of pseudomembranous layer of fibrin and epithelial debris. Ureteral openings could not be visualized.

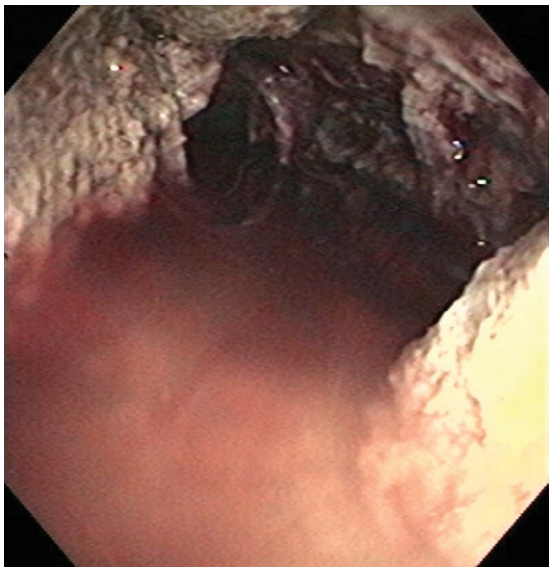

FIGURE 9-4. Image taken after manual removal of some pseudomembranous material. It can now be recognized that urine is blood-tinged, and a layer of gritty yellow sediment on bladder floor is slightly visible through urine.

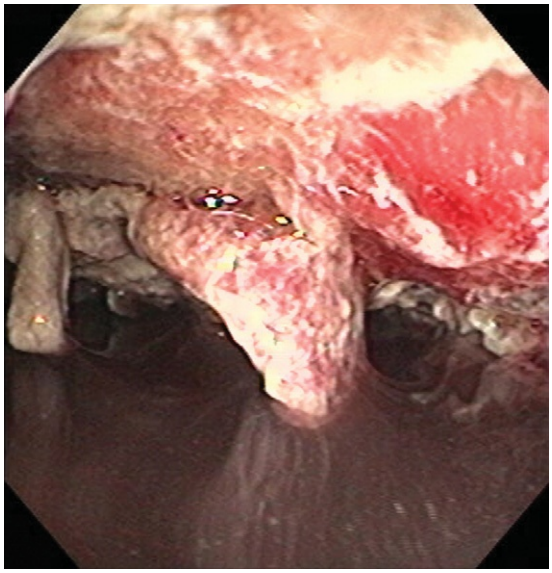

FIGURE 9-5. Luminal view after further removal of pseudomembrane. Short, distensible urethra of mare allows entry of hand into bladder, which in this mare was facilitated by very poor urethral and sphincteral tone. Some thick crusts are still adherent dorsally, but irritated mucosa is finally visible.

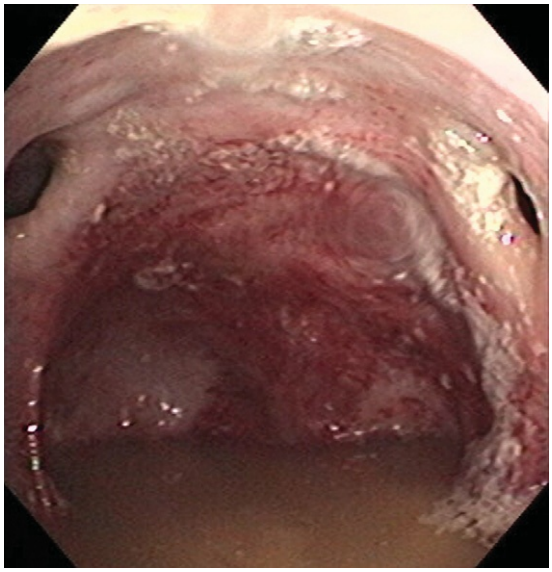

FIGURE 9-6. View of bladder lumen after 4 days of antibiotic therapy and daily lavage. Ureteral openings, located dorsally on extreme left and right of image, are grossly dilated, flaccid, and adynamic, reflective of absence of normal smooth muscle tone in remainder of lower urinary tract. This image conveys a large, atonic, and cavernous bladder, typical of neurologic syndrome of deficient innervation that usually underlies this condition. Patient's inability to voluntarily void bladder results in prolonged contact between urine and mucosa, culminating in bacterial infection and chemical injury to bladder. Dilated ureteral openings are typical of most cases of sabulous cystitis, but appearance of bladder interior in this mare was more extreme than is typical and is related to chronic time course.

FIGURE 9-7. Luminal view after catheterization and removal of urine, leaving sabulous sediment clearly visible on bladder floor.

FIGURE 9-8. Luminal view of right ureter. Endoscope (9-mm outside diameter) could be advanced approximately 6 cm proximally up ureter. Aside from adynamic, dilated anatomic structures, ureteral mucosa appears normal.

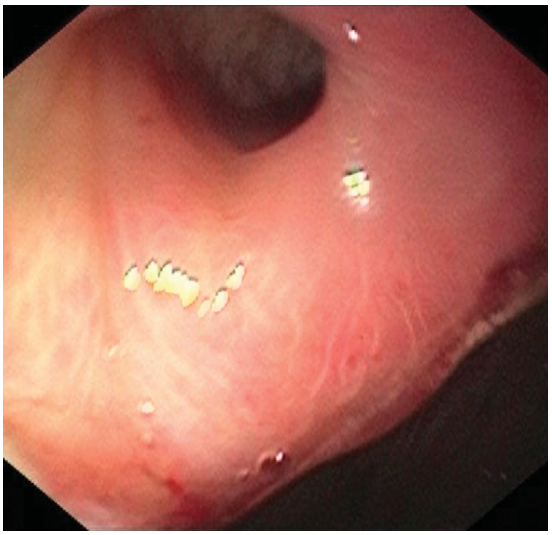

FIGURE 9-9. Close-up perspective of entrance to left ureter, showing dilation and absence of smooth muscle tone.

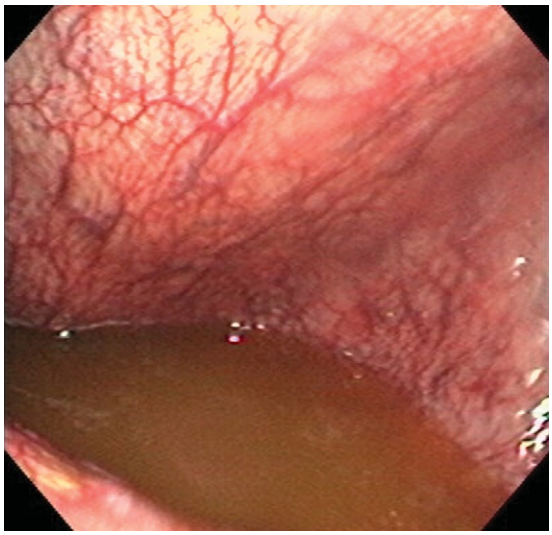

FIGURE 9-10. Severe cystitis. Note the hyperemic mucosa.

FIGURE 9-11. Luminal view of bladder from which urine has been removed via catheterization. Extreme mucosal irritation and hemorrhage are seen at apex of bladder. Diagnosis: Sabulous cystitis with overflow incontinence.

FIGURE 9-12. View of opening to right ureter showing poor smooth muscle tone.

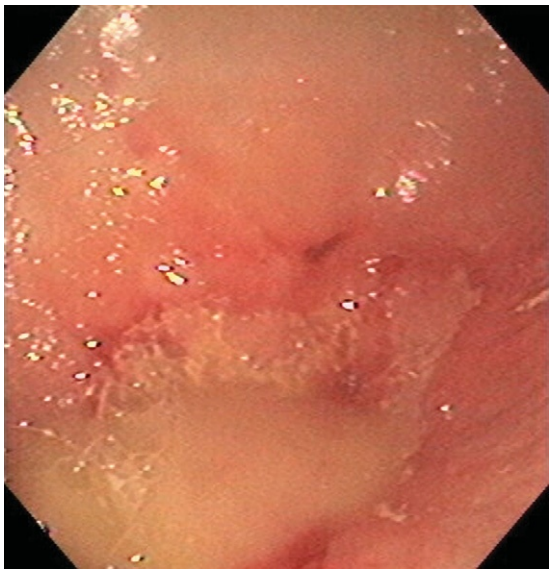

FIGURE 9-13. Same mare 14 days after initial assessment. A resistant strain of *Escherichia coli* was cultured from urine. Bladder apex remains ulcerated, with delineation between normal and involved mucosa easily distinguishable.

FIGURE 9-14. Left ureter *(arrow)* opening on this recheck visit was more normal in appearance. When viewed in real time, waves of smooth muscle contraction deposited normal peristaltic deposition of urine in bladder lumen.

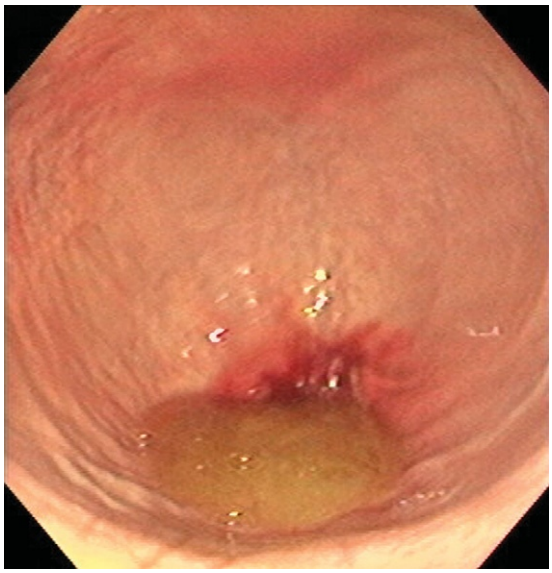

FIGURE 9-15. View of bladder after 5 weeks of systemic antibiotic administration. Affected area of mucosa at apex is confined to focal, more discrete lesion by aggressive medical management, but ongoing urine stasis is preventing resolution of cystitis in this mare.

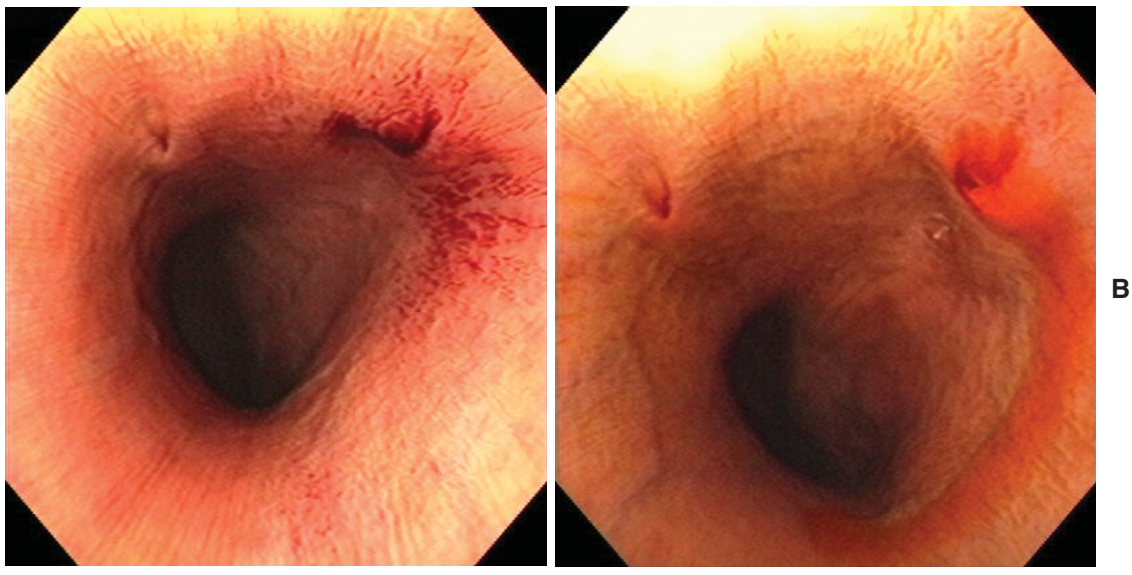

FIGURE 9-16. **A** and **B,** Hematuria. Endoscopic view from bladder neck looking cranially. Urine exiting right ureter is hematuric whereas that from left ureter appears grossly normal. This finding indicates damage or injury to right kidney or ureter. Patient with urine discoloration due to hemoglobinuria or myoglobinuria would produce dark urine from both ureteral orifices. Diagnosis: Renal carcinoma involving caudal pole of right kidney.

Idiopathic Hematuria (Figures 9-17 and 9-18)

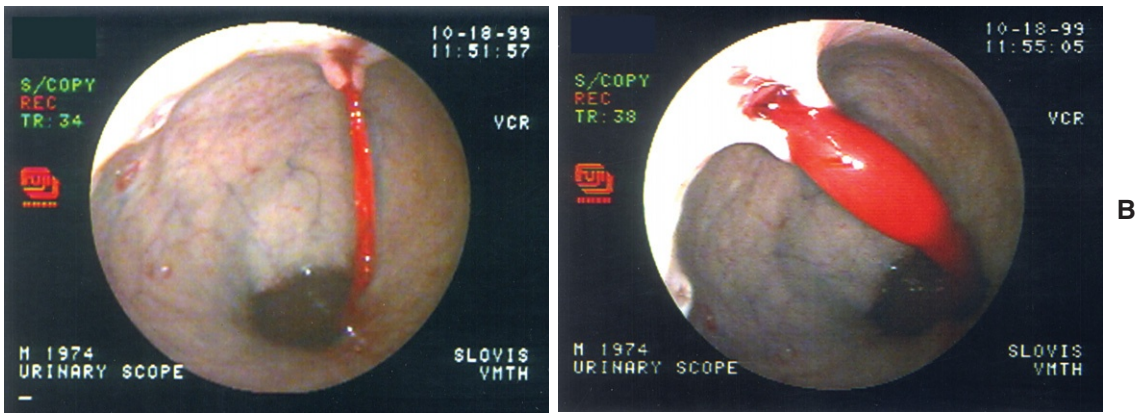

FIGURE 9-17. **A** and **B,** Adult Arabian stallion was seen with a chronic history of intermittent hematuria with blood clots. Stallion's hematocrit on presentation was 12%. Cytoscopy revealed a large blood clot exiting right ureter.

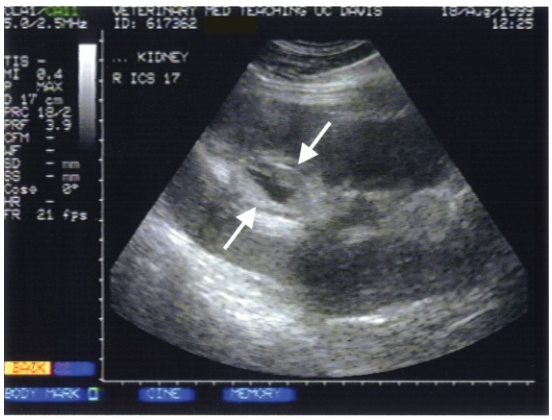

FIGURE 9-18. Ultrasonographic examination of right kidney revealed a large blood clot within renal pelvis *(arrows).* Diagnosis: Idiopathic hematuria of renal origin.

UROLITHIASIS

Cystic Calculus, Case 1

An adult Thoroughbred broodmare was seen for stranguria, polyuria, and intermittent hematuria. The owner reported a strong, acrid smell to the urine and noted that the mare had lost weight (Figures 9-19 and 9-20).

Treatment included destruction of a stone via lithotripsy and manual removal of fragments through the urethra and administration of systemic antibiotics and anti-inflammatory drugs. Analysis of the stone revealed it to be calcium carbonate, and the owners were given instructions for altering the diet in favor of grass hays rather than alfalfa, as well as the addition of salt to drive water intake and promote diuresis.

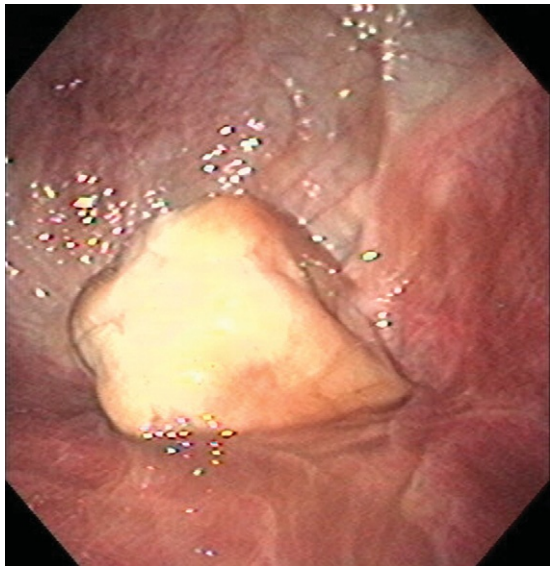

FIGURE 9-19. Cystoscopy revealed a cystic calculus resting at apex of bladder. Spiculated surface is typical of calcium carbonate uroliths, most common form of calculus produced in horses. Other forms, such as struvite, also occur. All stones should be submitted for analysis and determination of their mineral composition. Diagnosis: Cystic calculus, calcium carbonate.

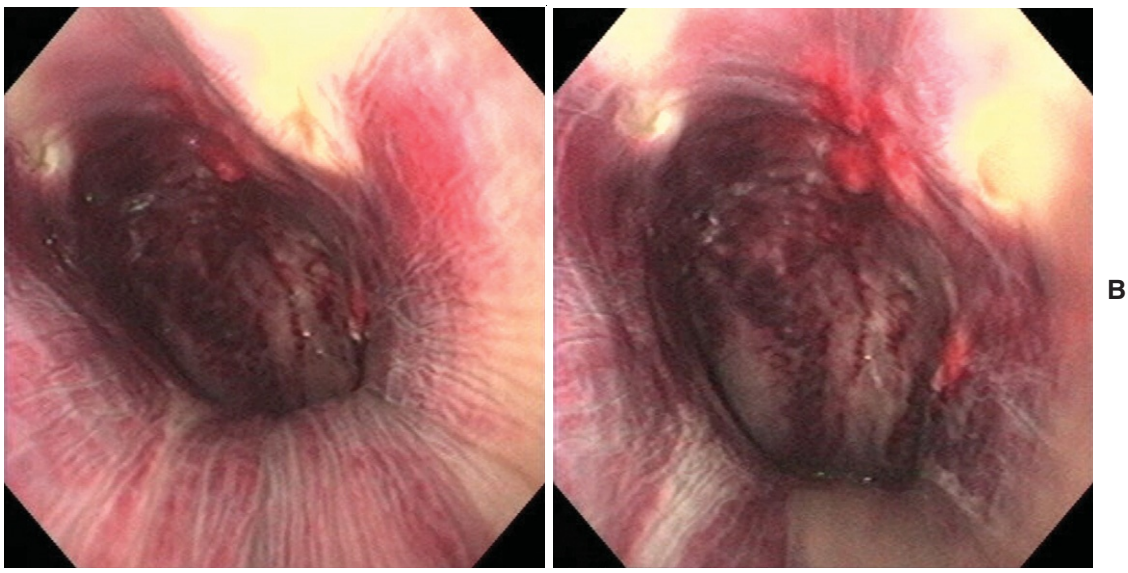

FIGURE 9-20. **A** and **B,** Linear streaks of inflammation and intramural hemorrhage, more easily visualized after removal of calculus.

Cystic Calculus, Case 2

An adult mare was seen with urinary incontinence, stranguria, and intermittent hematuria (Figures 9-21 and 9-22).

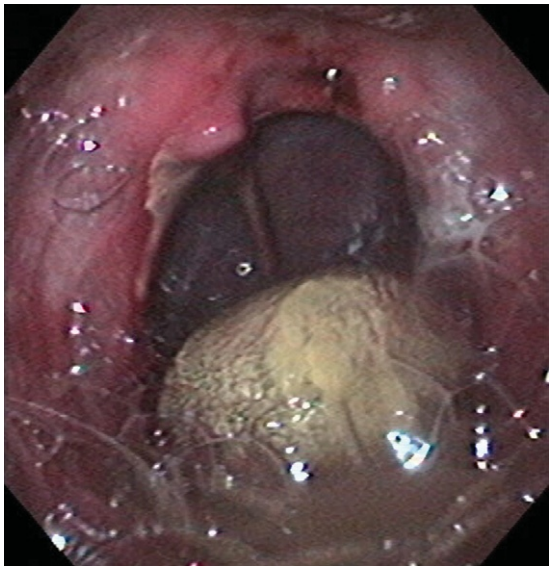

FIGURE 9-21. Round calculus resting on bladder floor, with inflammation and thickening of bladder wall. Diagnosis: Cystic calculus, calcium carbonate.

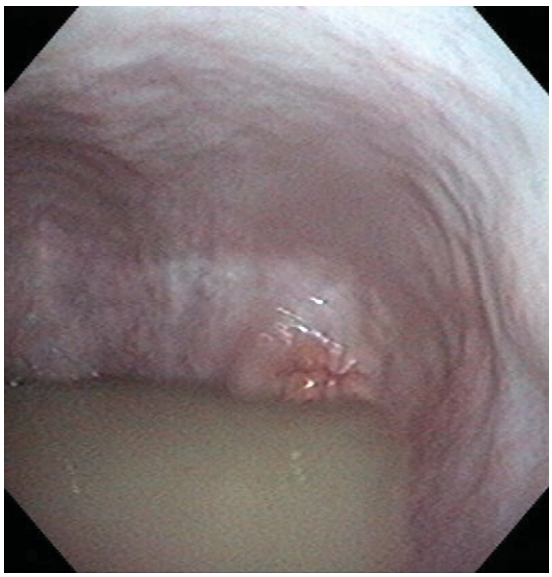

FIGURE 9-22. View at 3-week recheck shows improved, more quiescent appearance of bladder wall after surgical removal of stone.

Cystic Calculus, Case 3

An adult horse was seen with incontinence, stranguria, and intermittent hematuria, associated with chronic weight loss (Figures 9-23).

A

B

C

FIGURE 9-23. A to **C,** Endoscopic views demonstrating presence of calcium carbonate calculus on bladder floor. Spiculated surface can be easily recognized, as well as formation of cicatricial pillars that are due to chronic inflammation. This complication permanently alters bladder distensibility and impairs normal function. Diagnosis: Cystic calculus, calcium carbonate.

BLADDER TRAUMA

Trauma to Bladder During Parturition

A mare had suffered dystocia while foaling in a standing position. During efforts to reduce the dystocia, the mare fell. Extraction of the foal proceeded uneventfully, but in the following days, the mare developed fever, grew depressed, and demonstrated mild azotemia as seen on a blood profiles. Sonographic imaging of the abdomen showed free peritoneal fluid, which was sampled and determined to be urine.

The diagnosis was traumatic injury to the bladder during parturition with eventual rupture (Figures 9-24 and 9-25).

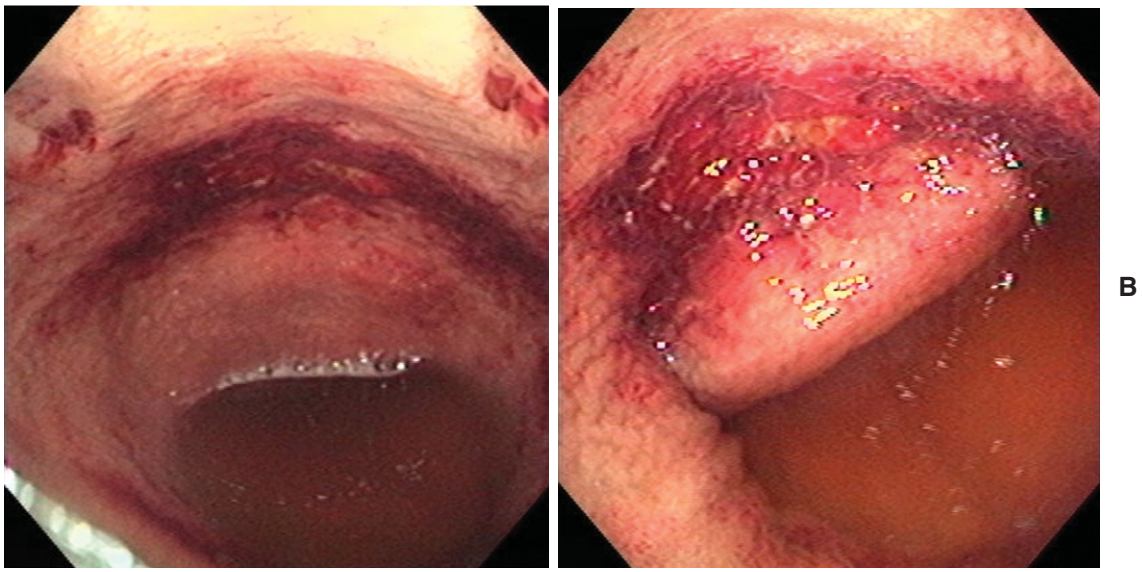

FIGURE 9-24. **A** and **B,** Endoscopic views demonstrating bladder trauma incurred during parturition. Images show hemorrhagic appearance of mucosa due to severe transmural bruising.

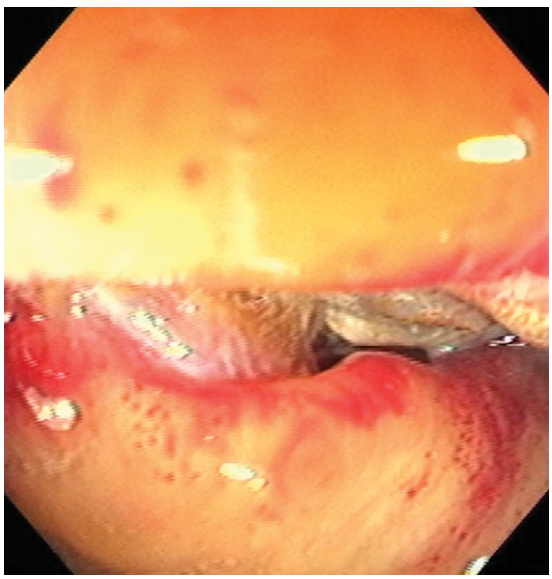

FIGURE 9-25. Most severely affected portion of bladder wall has undergone full-thickness necrosis and pathologic rupture.

Bladder Wall Necrosis

An adult mare was seen 7 days postpartum with colic, fever, toxic mucous membranes, and pollakiuria. There was no history of dystocia or assisted delivery (Figure 9-26).

Prolapsed Bladder

An adult Thoroughbred mare was seen with a prolapsed bladder after severe dystocia and forced fetal extraction (Figure 9-27).

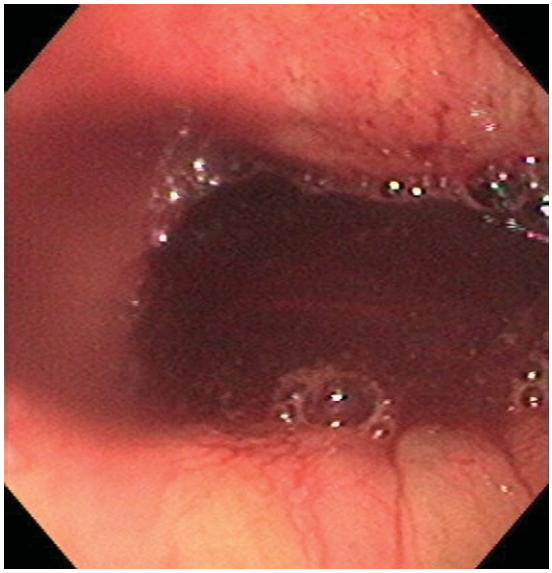

FIGURE 9-26. Luminal view of bladder containing hematuric urine due to parturition trauma. Dark red-brown hue of urine can be seen. Bladder ruptured several days after endoscopic examination. Diagnosis: Bladder wall necrosis after injury during parturition.

A

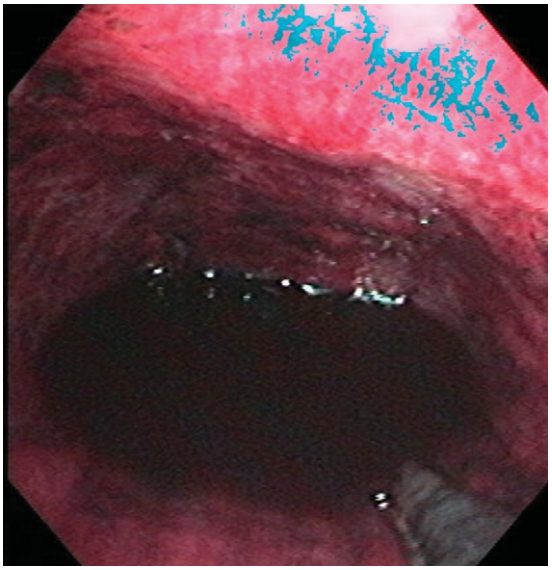

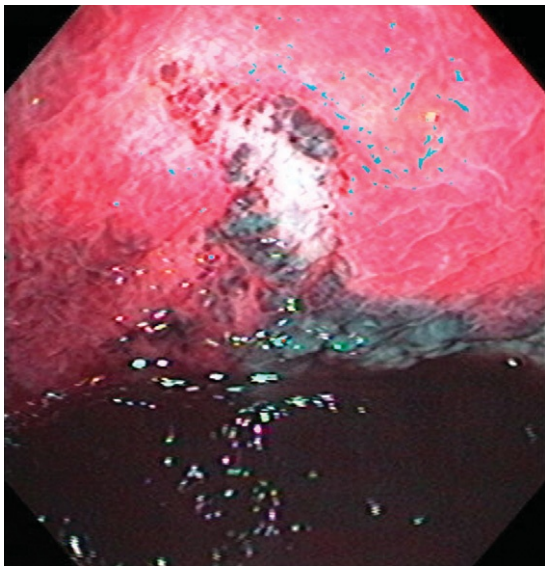

B

FIGURE 9-27. **A,** Luminal view showing dark hemorrhagic urine contained in bladder undergoing well-demarcated zone of necrosis after complete prolapse as a complication of dystocia. Gray-green tract in lower right aspect of image is seam of necrosis. **B,** View showing darkly discolored urine up to level of seam of necrosis and partial-thickness mural tear. Diagnosis: Prolapsed bladder after foaling, with eventual full-thickness necrosis and rupture.

NEOPLASIA (Figures 9-28 and 9-29)

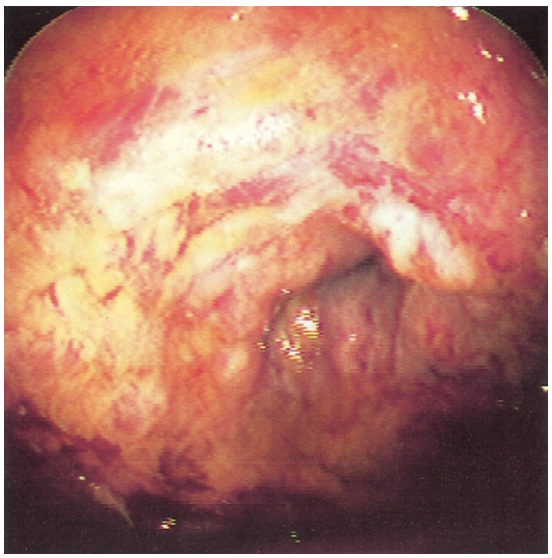

FIGURE 9-28. View of thickened, irregular bladder wall affected by squamous cell carcinoma. Diagnosis established with biopsy sample. (From Traub-Dargatz JL, Brown CM: *Equine endoscopy,* ed 2, St Louis, 1997, Mosby.)

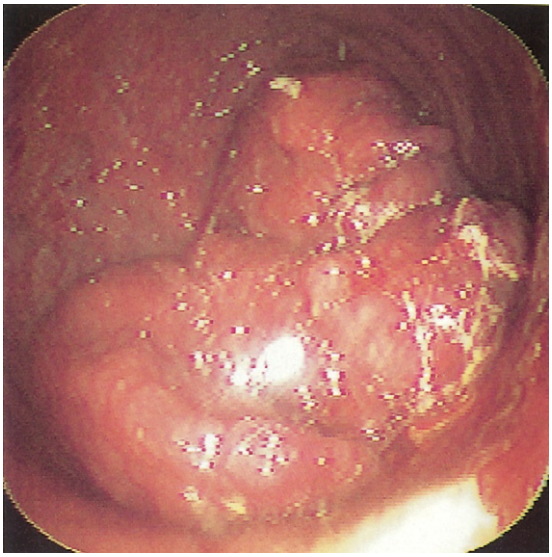

FIGURE 9-29. Leiomyosarcoma of urinary bladder that resulted in hematuria. (From Traub-Dargatz JL, Brown CM: *Equine endoscopy,* ed 2, St Louis, 1997, Mosby.)

CHAPTER 10

Mare Reproductive Tract

JOHN STEINER

MATERIALS AND METHODS

A flexible fiberoptic endoscope can be useful in diagnostic procedures. In general, the procedure should be considered when unidentified uterine abnormalities are detected by rectal palpation or ultrasonography. In addition, this technique can be of value when the cause of infertility cannot be determined by all other diagnostic procedures.

For this procedure to be useful, the mare to be examined should be in diestrus and the cervix should be closed. During diestrus, the uterine lumen will distend more readily than during estrus when the cervix is more relaxed and open. However, when endoscopy is performed during diestrus, the uterus is under the influence of progesterone, and therefore bactericidal activity and neutrophil activity are decreased. Thus potential inflammation of the uterus may be increased at this time, and therapeutic measures should be taken to minimize this inflammatory process.

The endoscope (if a fiberoptic endoscope is used, then preferably it should be equipped with a camera and video monitor) should be no larger than 13 mm in diameter and 100 to 130 cm in length. The light source should be suitable for illuminating the uterine lumen.

The mare should be properly restrained (e.g., stocks or tranquilizer). The tail should be wrapped and tied out of the way and the perineal area carefully washed and dried. The examination should be carried out in an aseptic manner.

The endoscope should be prepared by sterilization in glutaraldehyde solution, thoroughly rinsed with copious amounts of sterile water (including the internal biopsy channels), and placed within a sterile sleeve until used. It should be noted that only disinfectants approved by the manufacturer of the endoscope being used should be employed because endoscopes can be damaged by the use of certain harsh chemicals.

To visualize the uterine lumen, it must be distended. This can be accomplished by the use of sterile saline or lactated Ringer's solution or by the use of an inert gas such as carbon dioxide or air. The use of air appears to be more irritating to the endometrium. The drawback to the use of fluid to distend the uterus is the presence of mucopurulent material or exudates in the uterus. These may cause the fluid to become quite cloudy and make viewing of the uterus very difficult. An advantage to the use of fluid is that it has some therapeutic value after the procedure is over and the fluid is evacuated from the uterus.

Generally, fluid (1 to 2 liters) is infused into the uterus using an equine embryo-flushing catheter (Bivona Inc., Gary, IN) with an 80-ml inflatable cuff to seal up the cervix and keep the fluid from leaking out. The fluid is instilled by gravity flow.

When the uterus is distended, the operator, wearing a sterile sleeve, passes the endoscope into the distended uterus. If the uterus is not sufficiently distended, more

fluid can be infused. In addition, if the fluid is cloudy, it can be expelled and new fluid infused.

After the procedure is completed, the fluid or air is evacuated. A luteolytic agent (prostaglandin) is administered to return the mare to estrus. In addition, uterine lavage is encouraged for the next 1 to 2 days to minimize any inflammation or contamination of the uterus. Antibiotics given either systemically or intrauterine are used as deemed necessary by the practitioner but are generally not needed.

REPRODUCTIVE EVALUATION

The common observations within the uterine lumen when viewed endoscopically are cystic structures, adhesions, scarring, endometrial color, texture changes, and exudate. More infrequently seen are neoplasms, foreign bodies, lacerations, and endometrial cups.

When the endoscope is first introduced vaginally, the vaginal vault and cervix can be visualized (Figures 10-1 to 10-7). Vaginal abnormalities may be viewed at this time (Figure 10-8).

The endoscope is passed through the cervix and the previously dilated uterus can now be viewed (Figures 10-9 to 10-11). If there is evidence of endometritis or other inflammatory change, the fluid used to distend the uterus may be clouded by flocculent material (Figures 10-12 to 10-14).

The horns of the uterus may be visualized by passing the scope anteriorly down each distended horn (Figures 10-15 to 10-17). The distal portion of the uterine horn can be visualized with the uterotubal junction (oviductal papilla) (Figures 10-18 and 10-19).

When the uterus is viewed endoscopically, one of the most common findings, especially in older mares, is the presence of endometrial cysts. These cysts originate from lymphatic tissue or glandular tissue. Lymphatic cysts are caused by obstruction

Text continued on p. 190

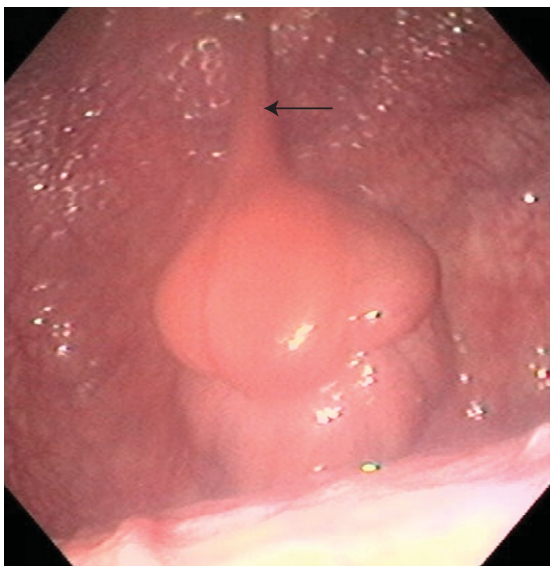

FIGURE 10-1. Normal external os of cervix in early estrus. Note frenulum of cervix *(arrow),* which is located dorsally and lesser ventrally.

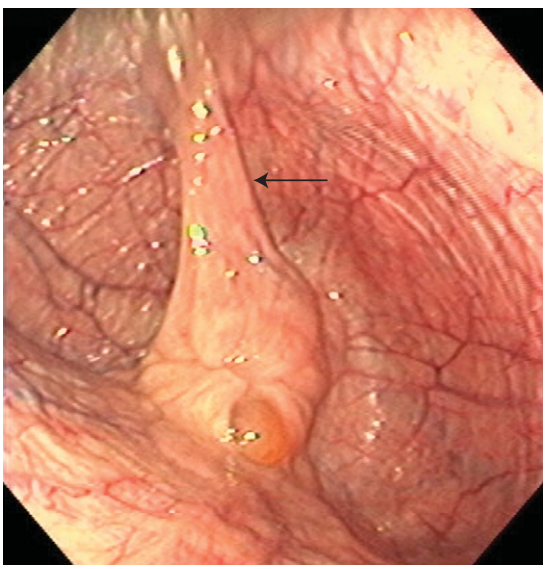

FIGURE 10-2. Normal external os of cervix. *Arrow* is pointing to frenulum.

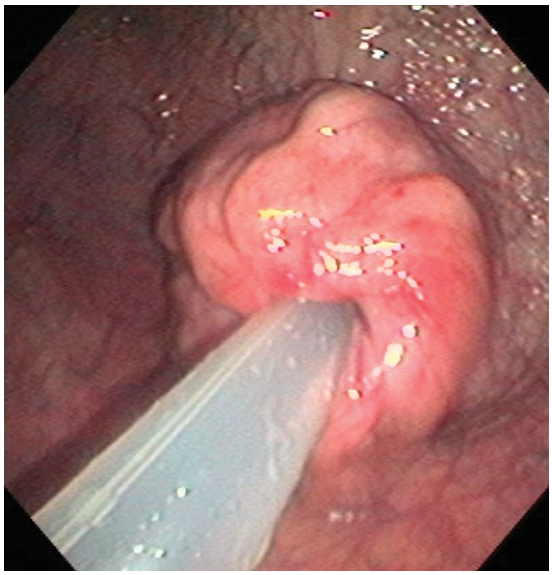

FIGURE 10-3. Infusion of sterile saline into uterus before endoscopic examination.

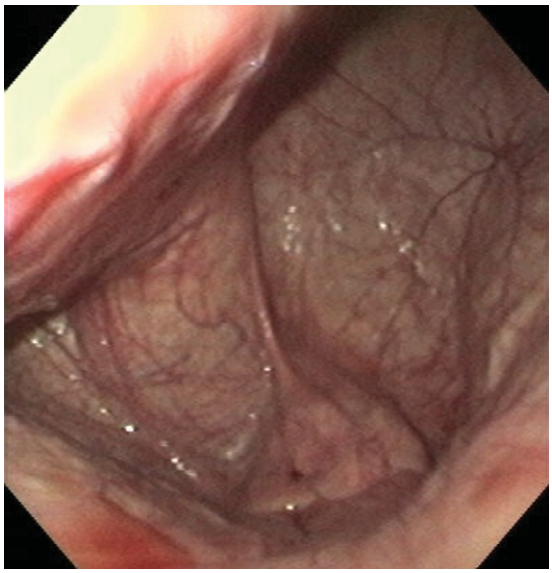

FIGURE 10-4. Normal external os of cervix of mare in estrus. External os protrudes less and becomes more dependent on floor of vagina.

FIGURE 10-5. Normal pregnant cervix. Cervix is elevated from vaginal floor and protrudes posteriorly.

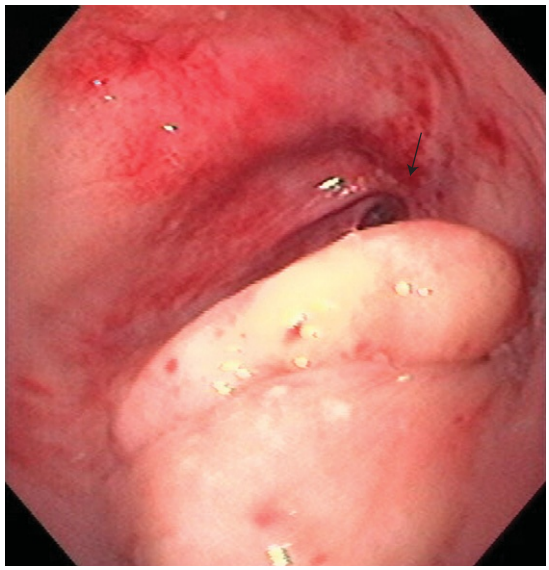

FIGURE 10-6. Ten-year-old miniature horse was seen with pyometra. Severe scarring of cervix due to dystocia 10 months before presentation. External os was only 3 mm in diameter *(arrow)*.

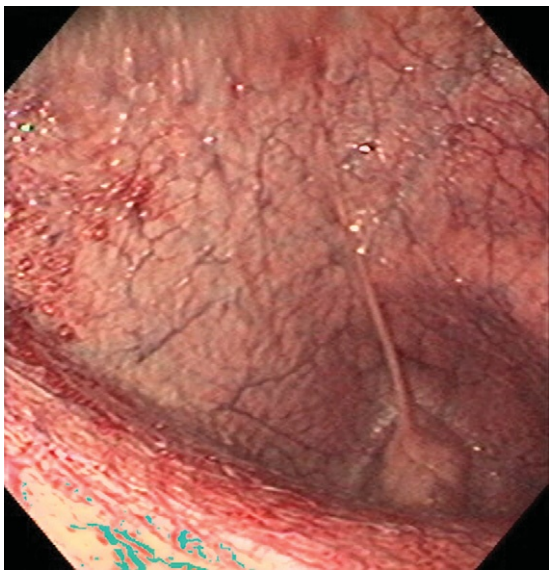

FIGURE 10-7. Mare that had chronic vaginal discharge. This mare was noted to be pooling urine in vagina vault. Note hyperemic mucosa.

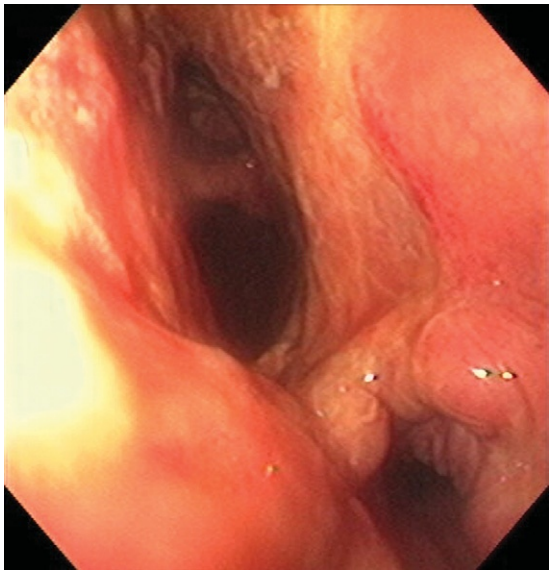

FIGURE 10-8. Mare had severe dystocia and was noted to be febrile and depressed 3 days postpartum. Endoscopic examination revealed a dorsal vaginal tear that communicated with the abdomen.

FIGURE 10-9. Uterine horn of mare with cysts.

FIGURE 10-10. Uterine horn not fully distended with cysts.

FIGURE 10-11. Both uterine horns dilated at bifurcation.

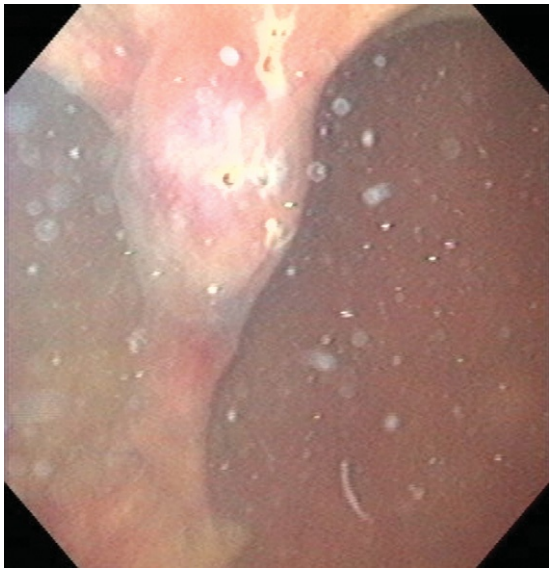

FIGURE 10-12. Flocculent debris in uterus.

FIGURE 10-13. Mucopurulent material noted in uterus with normal endometrial folds.

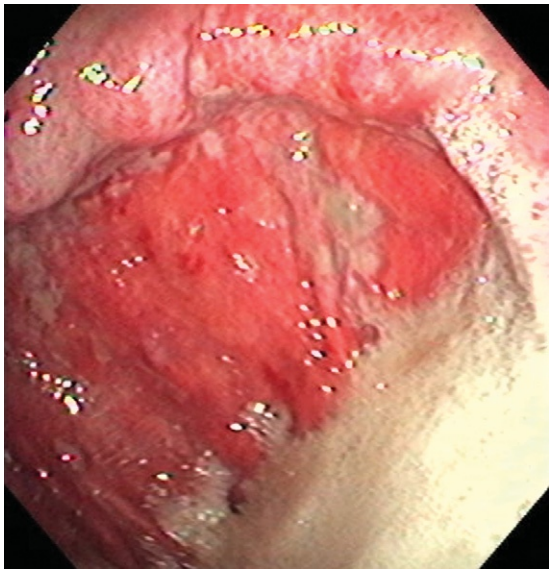

FIGURE 10-14. Metritis with septic exudate 3 days postpartum.

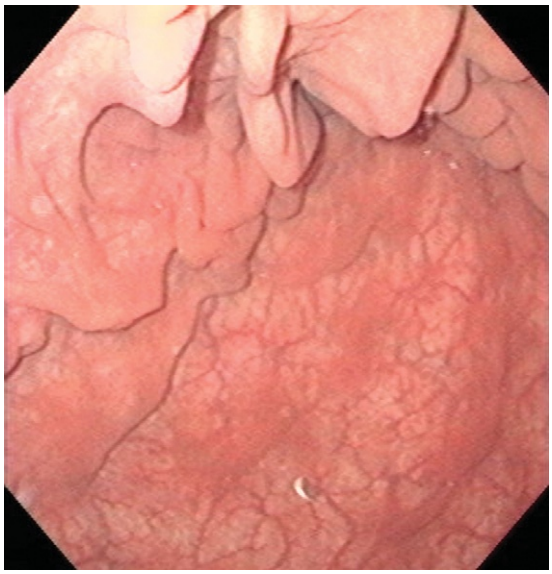

FIGURE 10-15. Normal uterine horn with endometrial folds.

FIGURE 10-16. Traveling anteriorly down the horn.

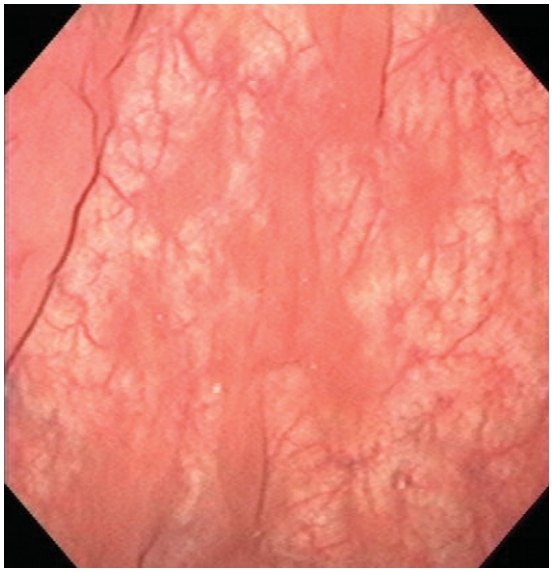

FIGURE 10-17. Normal uterine mucosal vasculature.

FIGURE 10-18. Normal uterotubal junction *(arrow)* at distal portion of uterine horn.

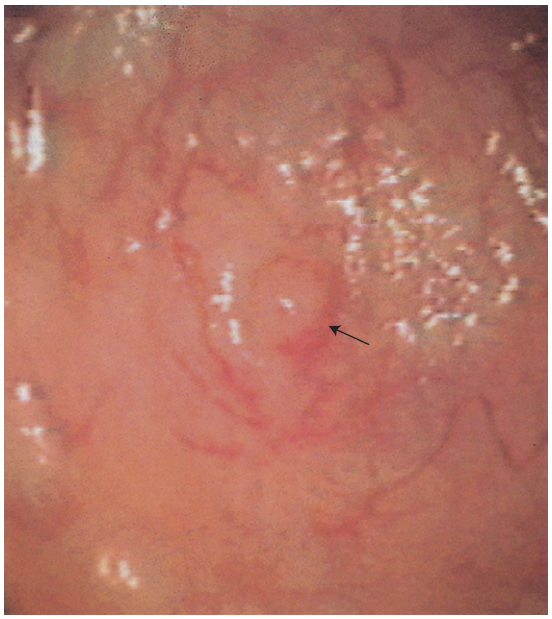

FIGURE 10-19. Normal uterine ostium of oviduct shown as slightly elevated area in center of image *(arrow)*. (From Traub-Dargatz JL, Brown CM: *Equine endoscopy,* ed 2, St Louis, 1997, Mosby.)

to lymphatic channels and appear as single or multilobulated structures, which may be pedunculated or more tightly adhered to the endometrium (Figures 10-20 to 10-28). Most lymphatic cysts are located in the body of the uterus, at the bifurcation of the uterus or just within the uterine horn itself. Less commonly, these cysts are located midhorn or further anteriorly.

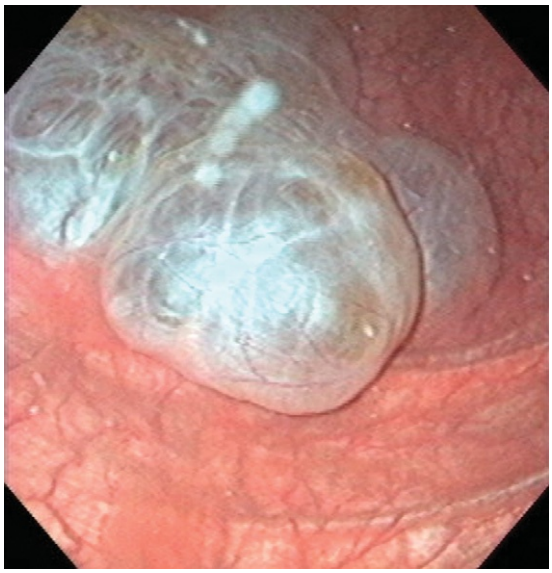

FIGURE 10-20. Large uterine cysts.

FIGURE 10-21. Multiple large cysts.

FIGURE 10-22. Cysts noted at bifurcation.

FIGURE 10-23. Small pedunculated cyst.

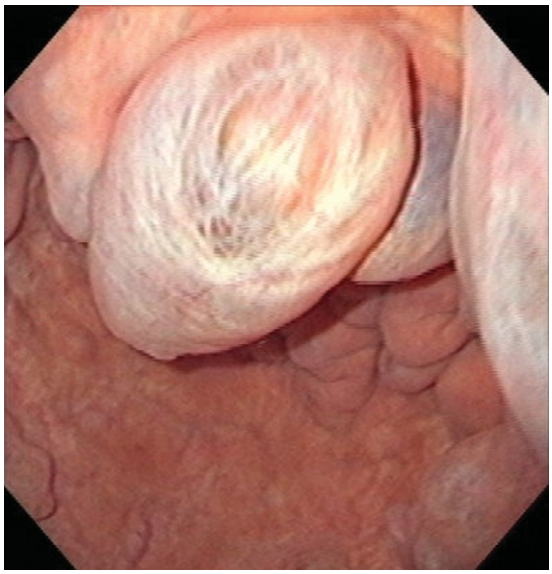

FIGURE 10-24. Large multilobular endometrial cyst.

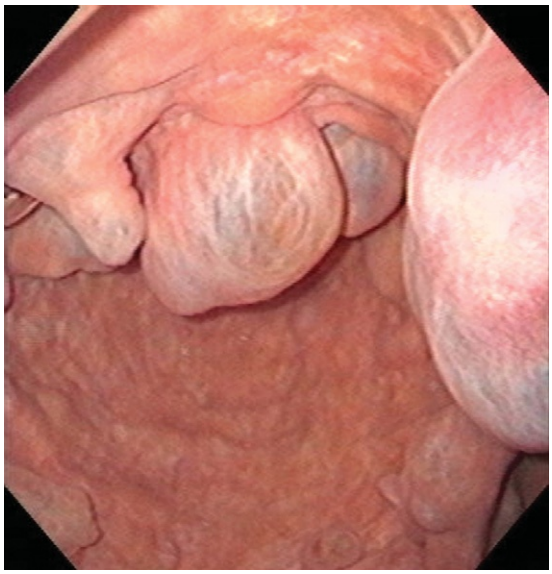

FIGURE 10-25. Multiple endometrial cysts.

FIGURE 10-26. Multiple endometrial cysts.

FIGURE 10-27. Multiple endometrial cysts.

FIGURE 10-28. Dilated uterine horn with small endometrial cysts.

Endometrial glandular cysts are derived from endometrial glands. They tend to be quite small, are located within the endometrium, and are not visualized with the endoscope because of their location.

If it is determined that endometrial cysts may be a problem in the reproductive performance of a particular mare, several methods of removal are available. One method of cyst removal, particularly if there are multiple cysts, is the use of a laser. A diode laser set at 14 to 18 watts of power is generally used. The larger and more lobulated the cyst, the more power needed. The laser fiber is passed through a port of the fiberoptic endoscope. One or more areas of the cyst are burned so that fluid drains from the cyst (Figures 10-29 to 10-32).

FIGURE 10-29. Diode laser treatment of uterine cysts.

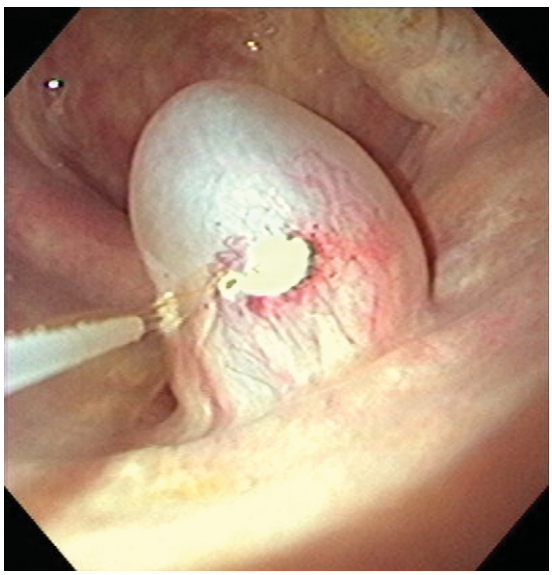

FIGURE 10-30. Lymphatic fluid draining from cyst after laser treatment.

FIGURE 10-31. Region of laser penetration.

FIGURE 10-32. Close-up of laser penetration points.

OTHER UTERINE VISUALIZATIONS USING THE ENDOSCOPE

Scar From Previous Cesarean Section (Figure 10-33)

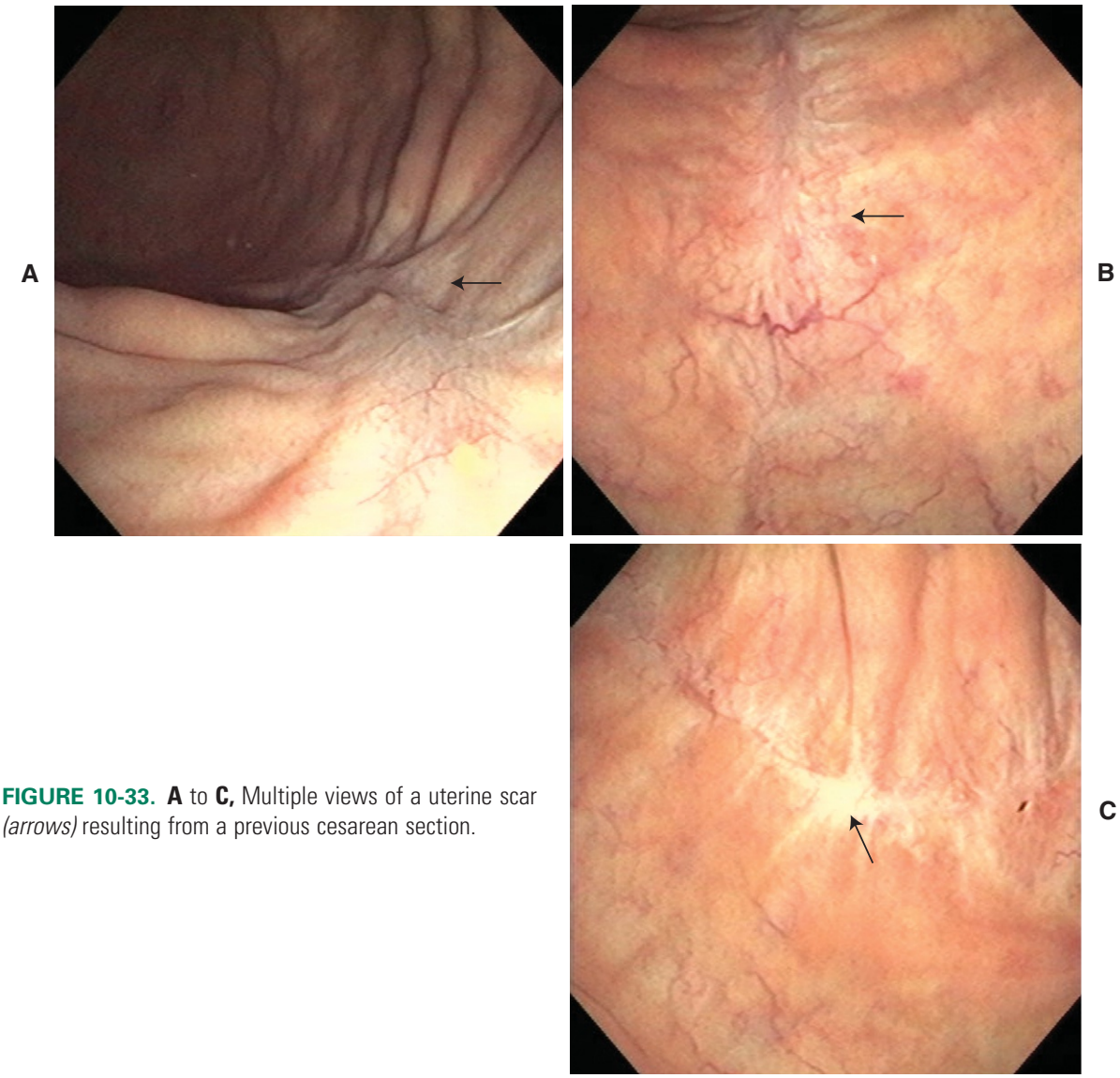

FIGURE 10-33. **A** to **C,** Multiple views of a uterine scar *(arrows)* resulting from a previous cesarean section.

Foreign Body in the Uterus (Figure 10-34)

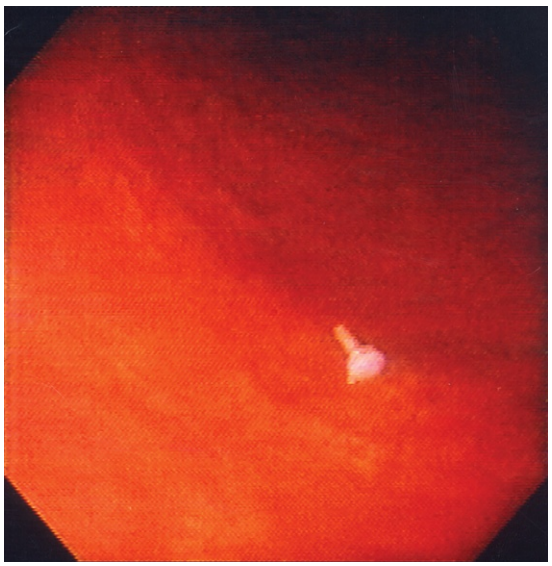

FIGURE 10-34. Foreign body (culture swab) in uterus (Courtesy Dr. C. Schweizer.)

Mummified Fetus (Figures 10-35 to 10-39)

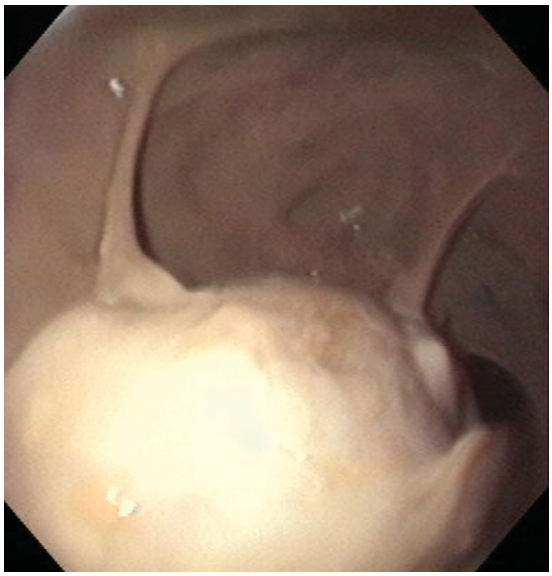

FIGURE 10-35. Uterine adhesions with mummified fetus.

FIGURE 10-36. Mummified fetus.

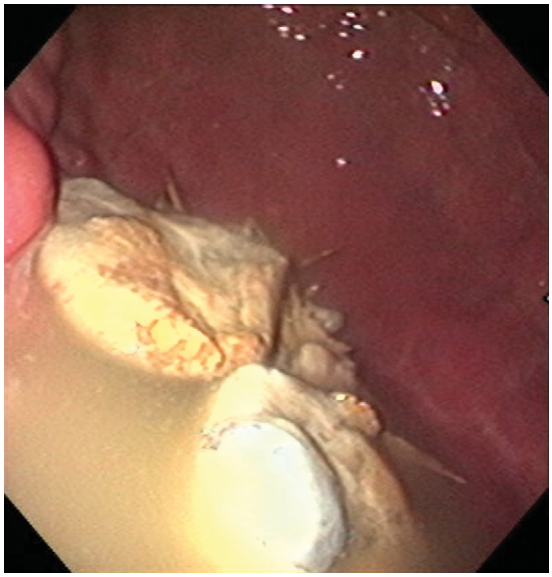

FIGURE 10-37. Metritis and mummified fetus.

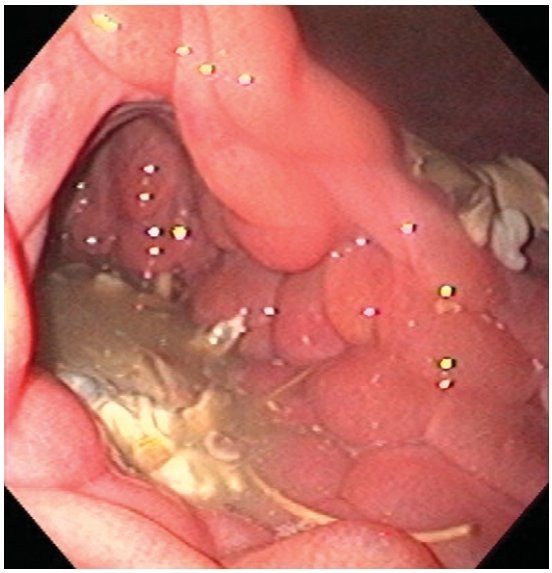

FIGURE 10-38. Endometrium in estrus with ribs from mummified fetus.

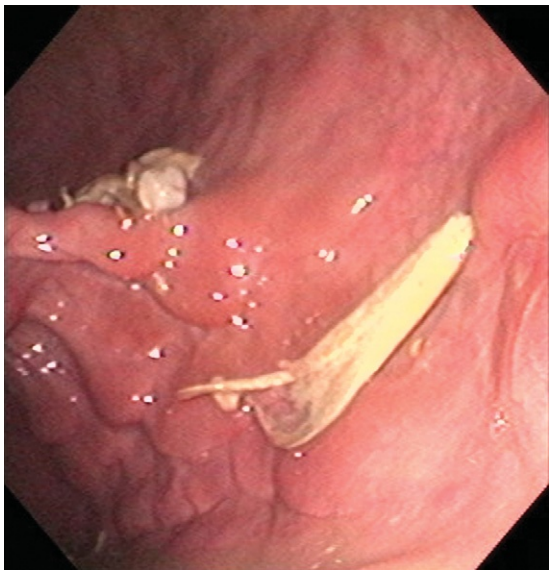

FIGURE 10-39. Scapula of mummified fetus.

Endometrial Cups (Figures 10-40 and 10-41)

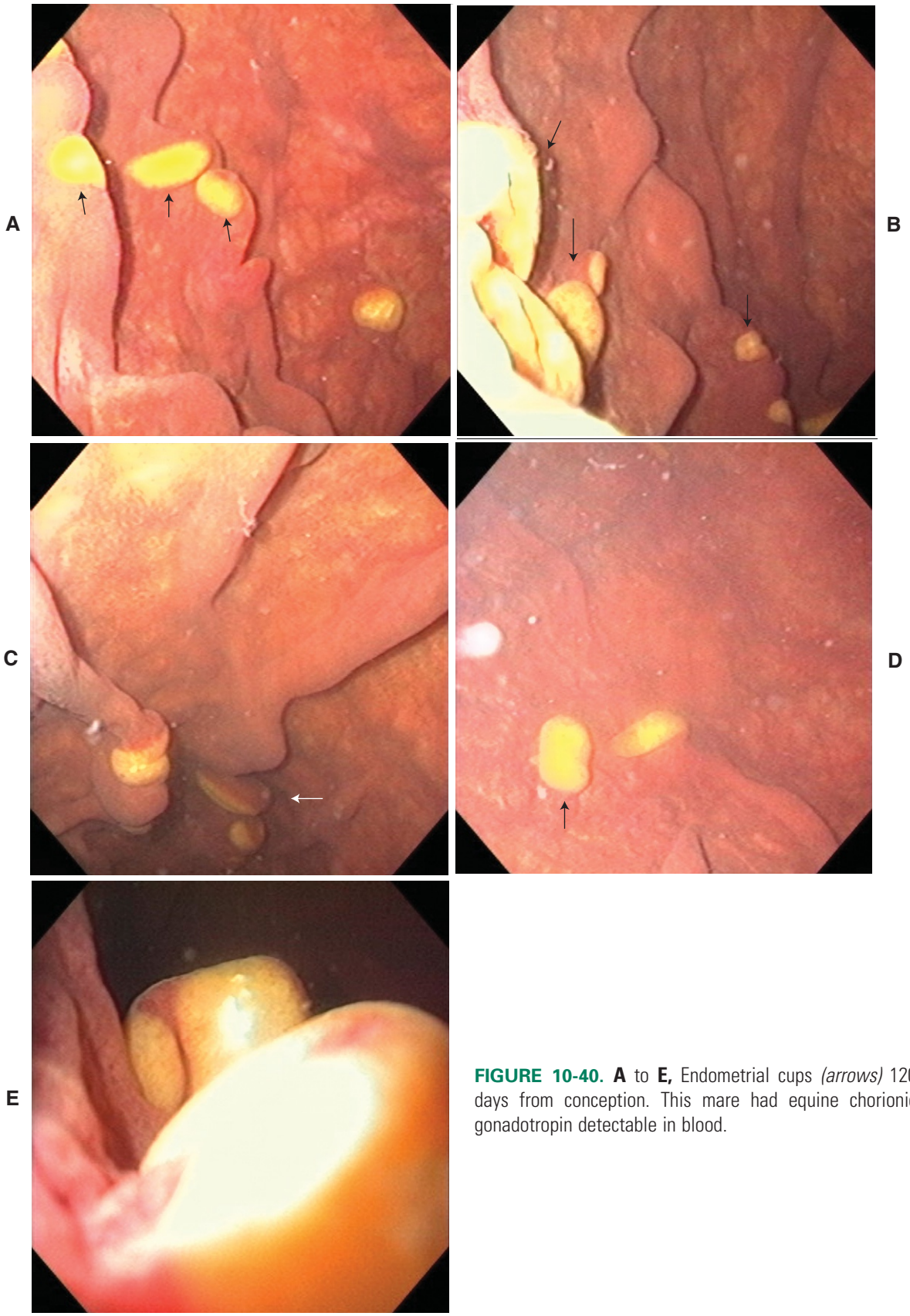

FIGURE 10-40. A to **E,** Endometrial cups *(arrows)* 120 days from conception. This mare had equine chorionic gonadotropin detectable in blood.

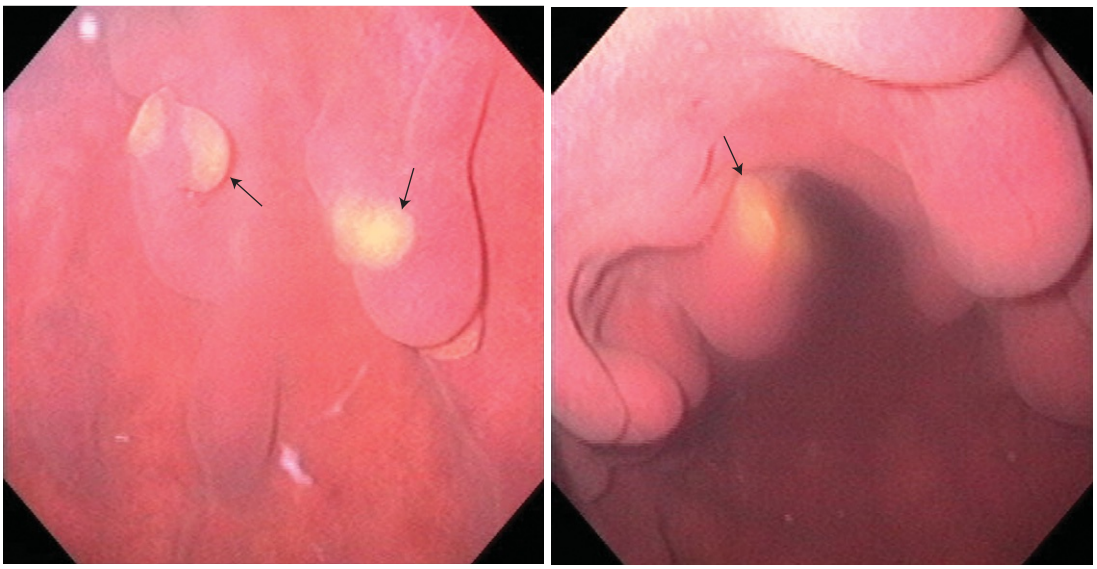

FIGURE 10-41. **A** and **B,** Endometrial cups 172 days from conception. Equine chorionic gonadotropin was not present in blood.

Remnant of Trophoblastic Vesicle (Figure 10-42)

FIGURE 10-42. Trophoblastic vesicle 120 days from conception.

Leiomyoma (Figure 10-43)

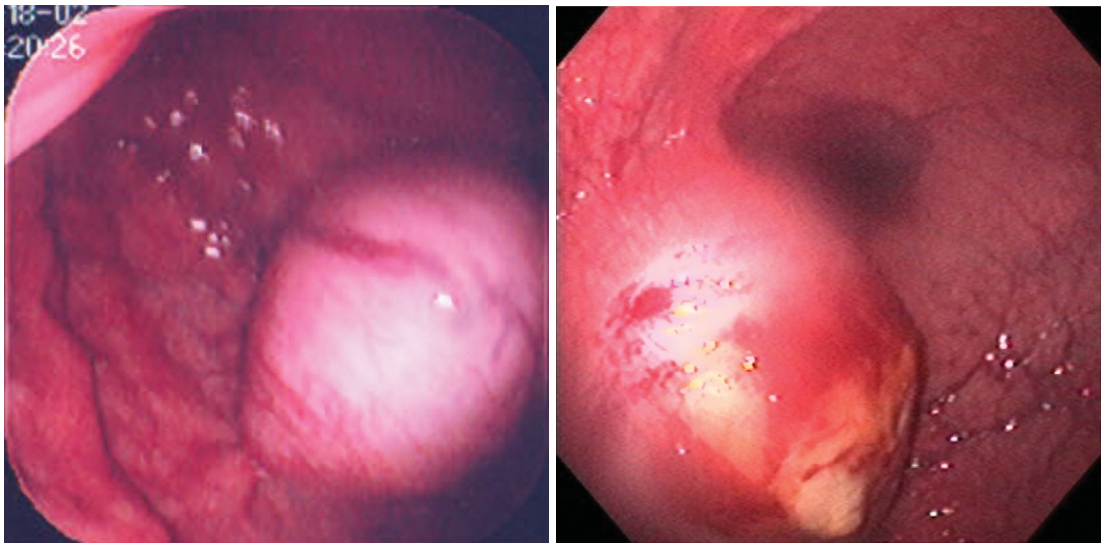

FIGURE 10-43. **A** and **B,** Leiomyosarcoma in uterus.

Gangrenous Cervical Tear (Figures 10-44 and 10-45)

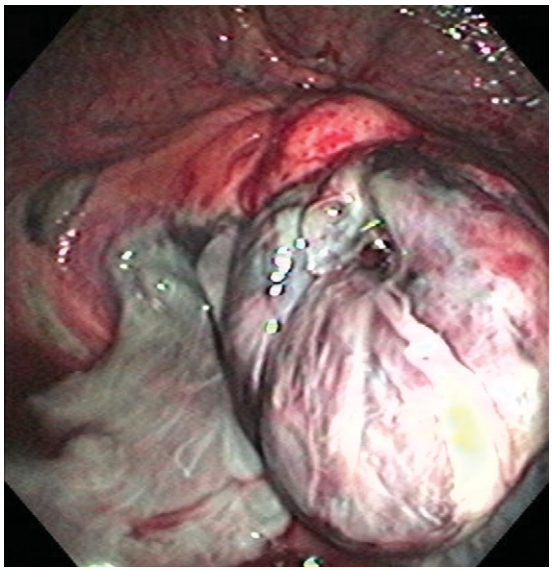

FIGURE 10-44. Dystocia resulting in severe cervical trauma causing necrosis.

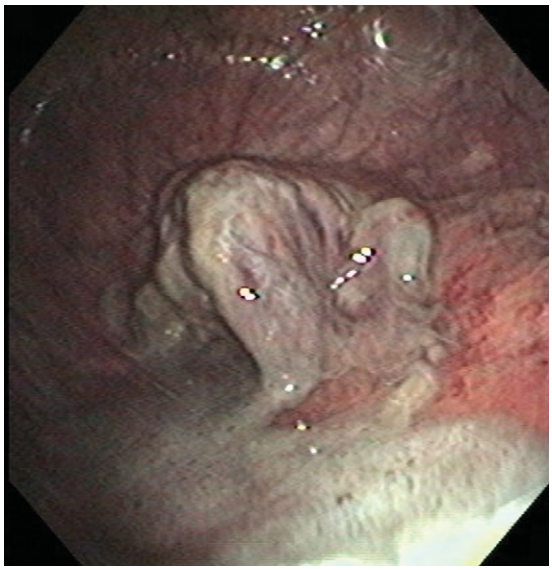

FIGURE 10-45. Another view of necrotic cervix in Figure 10-44.

Necrosis of the Endometrium (Figure 10-46)

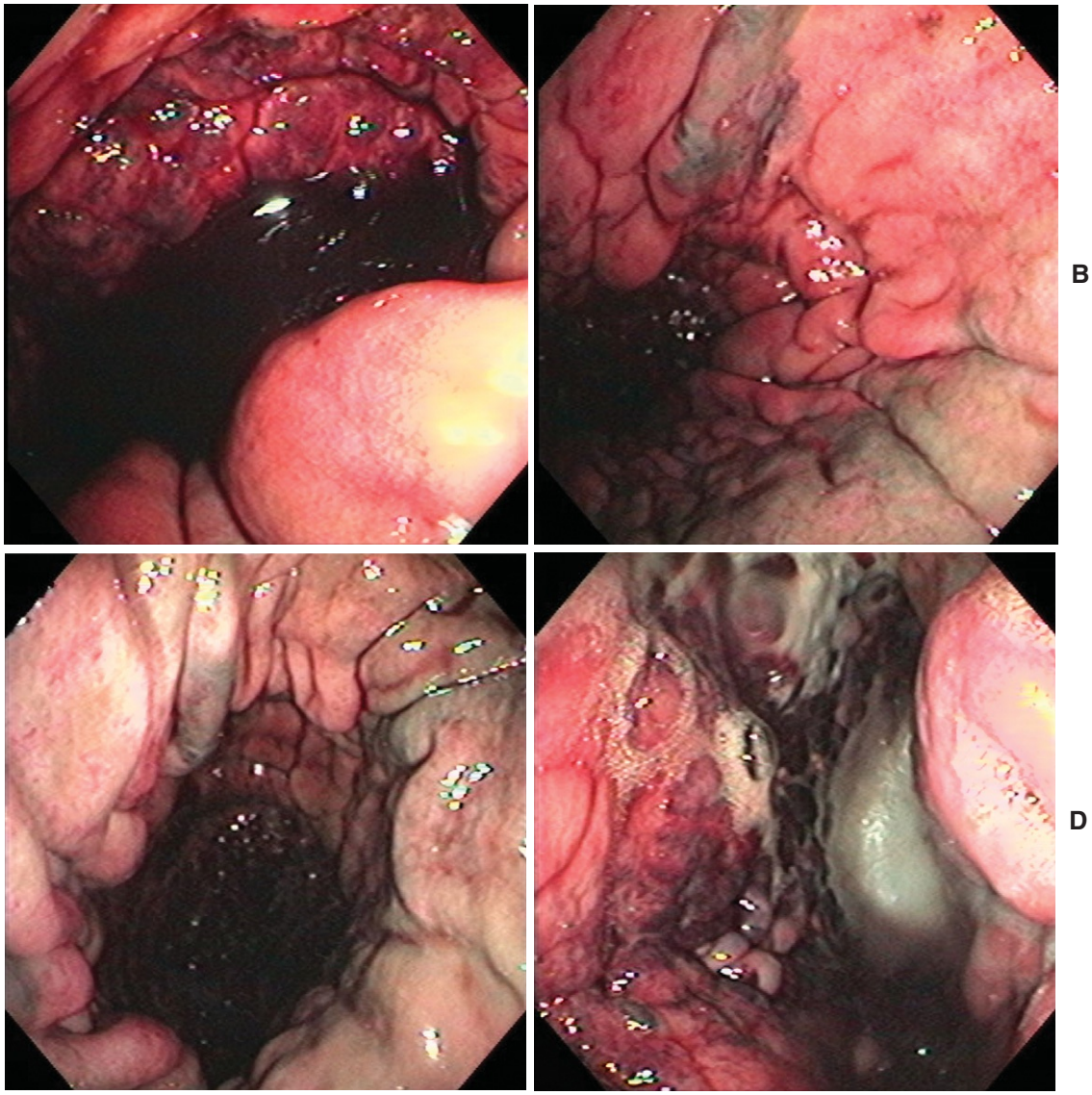

FIGURE 10-46. **A** to **D,** Infarcted uterine horn after foaling. This mare had severe dystocia that had to be corrected with fetotomy.

Antibiotic Residue Lumen of Uterus 3 Days After Infusion of Ampicillin (Figure 10-47)

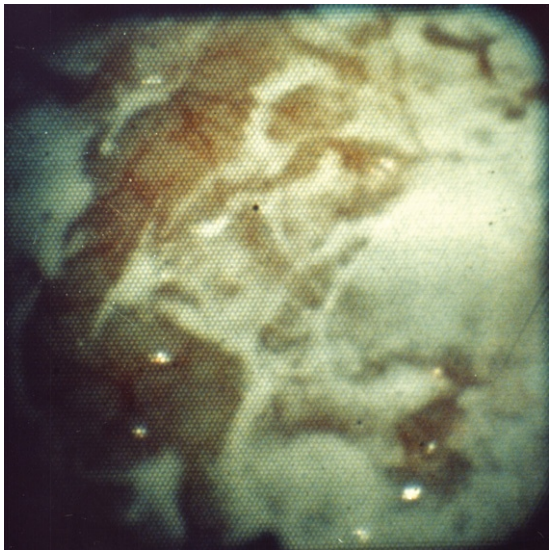

FIGURE 10-47. Ampicillin residue 3 days after infusion (Courtesy Dr. E. C. Mather.)

Uterine Adhesions Caused by Lugol's Solution (Figures 10-48 and 10-49)

FIGURE 10-48. Severe endometritis of uterus treated with Lugol's solution. (Courtesy Dr. E. C. Mather.)

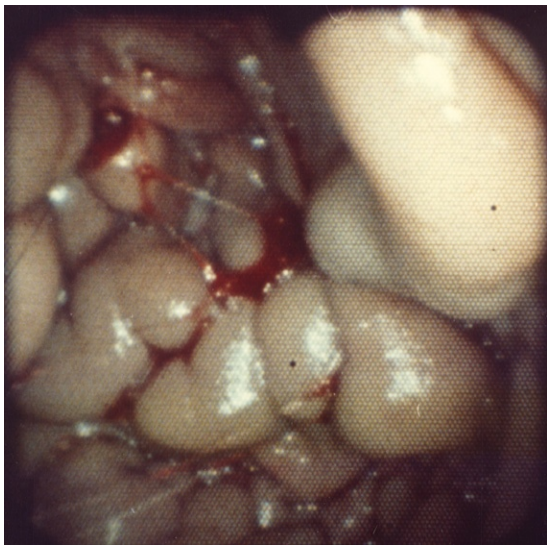

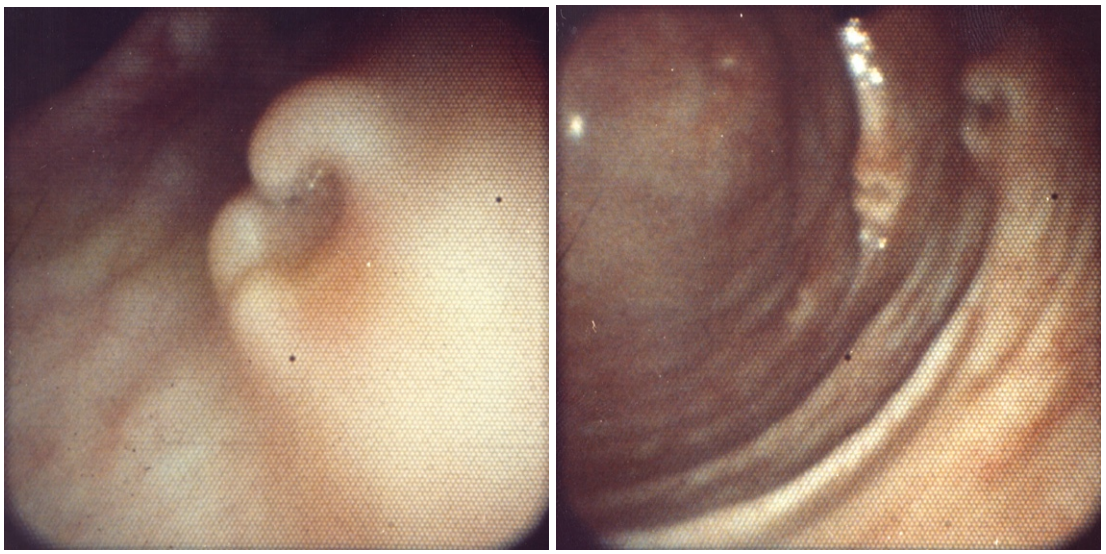

FIGURE 10-49. **A** and **B,** Uterine wall adhesions and lesions from Lugol's iodine solution infusion (Courtesy Dr. E. C. Mather.)

Urine in Uterus (Figures 10-50 to 10-52)

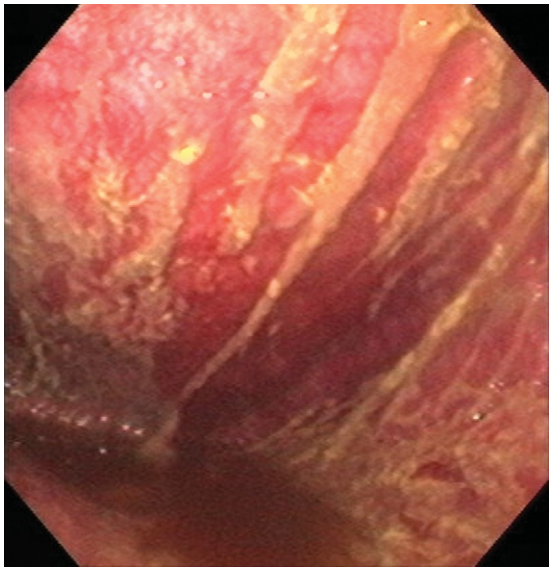

FIGURE 10-50. Urine pooling of vagina.

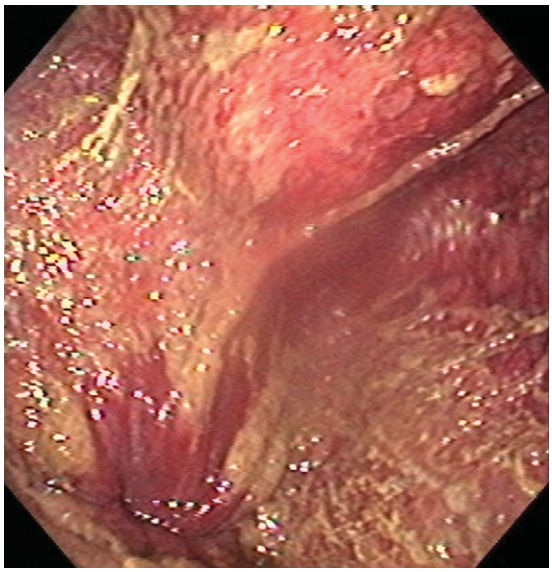

FIGURE 10-51. Urine pooling of vagina. Note calcium carbonate crystals on vagina's mucosa.

FIGURE 10-52. Urine pooling of uterus.

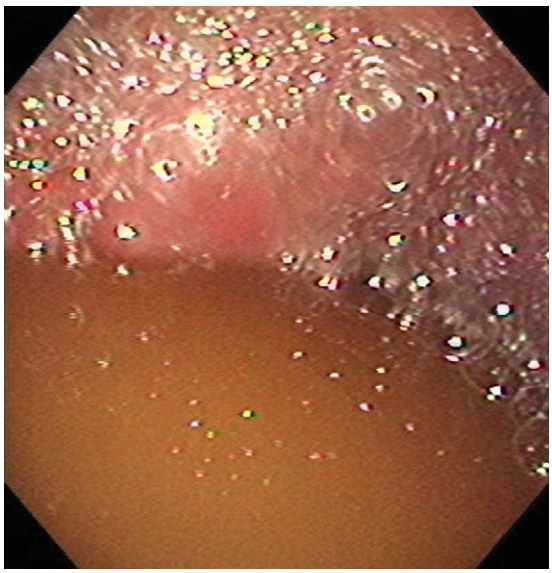

Hemangioma of the Cervix (Figure 10-53)

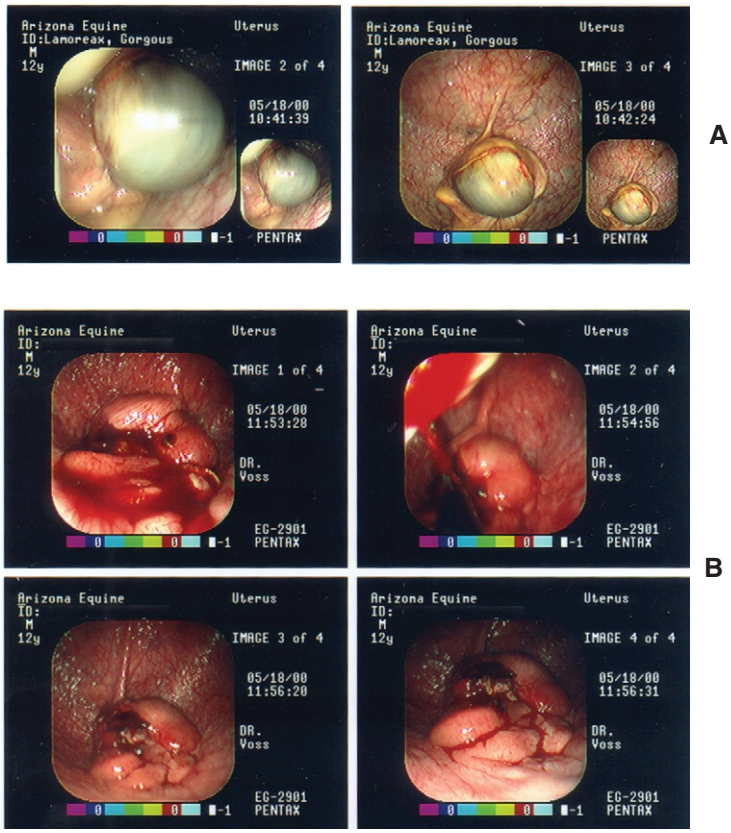

FIGURE 10-53. A, Hemangioma of cervix that was removed surgically with snare. No complications were noted. **B,** View of cervix after removal of hemangioma.

Melanoma of the Uterus (Figure 10-54)

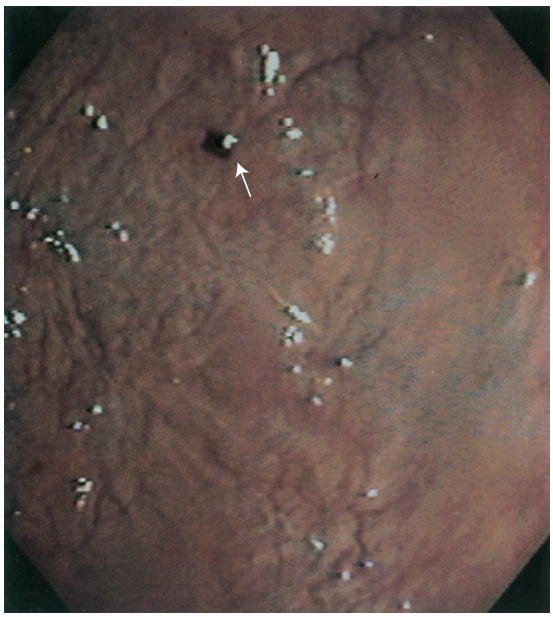

FIGURE 10-54. Small black pigmented area in upper center of image was diagnosed as a melanoma. (From Traub-Dargatz JL, Brown CM: *Equine endoscopy,* ed 2, St Louis, 1997, Mosby.)

CHAPTER 11

Stallion Reproductive Tract

JOHN STEINER

MATERIAL AND METHODS

Endoscopic examination of the stallion's urogenital tract is a useful diagnostic tool when a condition such as hemospermia or suspected disease of the accessory sex glands is encountered. Urethral defects, uroliths, neoplasia, and infectious processes can often be confirmed with the use of a flexible endoscope.

Endoscopy in the stallion can be easily performed in the sedated, standing horse that is confined in a set of suitable stocks. Restraints and sedation are necessary to protect the operator and equipment and allow exteriorization of the penis.

The endoscope used in the adult stallion should be at least 100 cm in length and 10 mm in diameter or less. A pediatric endoscope with a diameter of 7 mm would be more suitable for a foal, pony, or miniature horse.

Cold disinfection of the endoscope in 2% glutaraldehyde is usually adequate to avoid iatrogenic introduction of pathogens into the urogenital system. It is also very important to rinse the endoscope with large volumes of sterile water to remove all traces of the glutaraldehyde before starting the procedure. As an alternative, the endoscope can be sterilized with ethylene oxide.

After the stallion is sedated, the external genitalia need to be prepared before the procedure. This can be accomplished by a surgical scrub of the distal penis and prepuce followed by a thorough rinsing.

The examination requires two to three people. One person will pass the endoscope after a small amount of sterile lubricant is applied to the end of the endoscope. A second person is needed to operate the controls of the endoscope. A third person is used to help restrain the horse. As the endoscope is passed up the urethra, the urethra is dilated with air.

REPRODUCTIVE EVALUATION

In the normal stallion, the urethral mucosa is pale-pink and is arranged in longitudinal folds. However, as the urethra is distended with air when viewed endoscopically, the folds disappear, and the vasculature becomes more prominent (Figures 11-1 to 11-3). It is important not to confuse this more prominent vasculature with inflammatory change.

Passing further along the urethra, two rows of small duct openings are occasionally visible. These are the ducts of the lateral urethral glands (Figure 11-4 *arrows*).

As the endoscope reaches the ischial arch, the urethra widens and becomes more ovoid in diameter. In Figure 11-5 *arrows* point to the urethral glands. Also, two rows of multiple gland openings come into view parallel to each other near the midline.

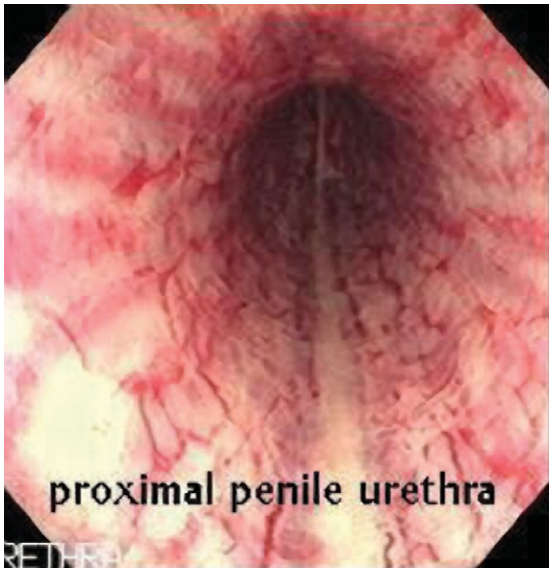

FIGURE 11-1. Normal vasculature.

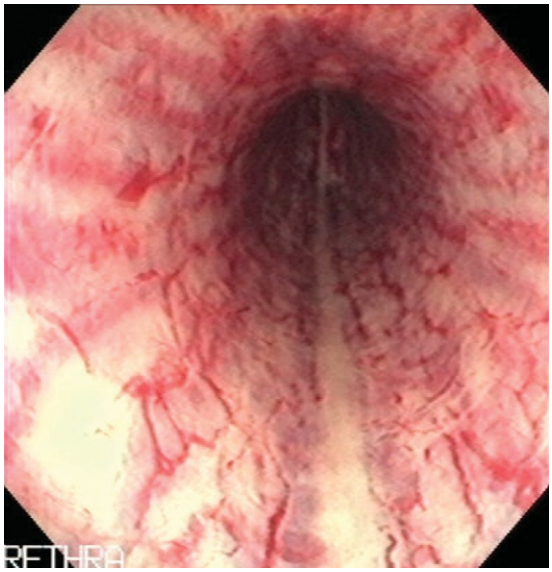

FIGURE 11-2. Normal vasculature in dilated urethra.

FIGURE 11-3. Normal urethral vasculature.

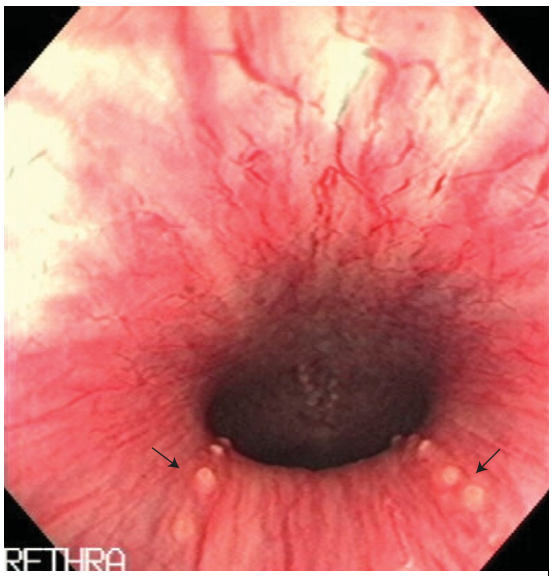

FIGURE 11-4. Note urethral glands on ventral aspect of figure.

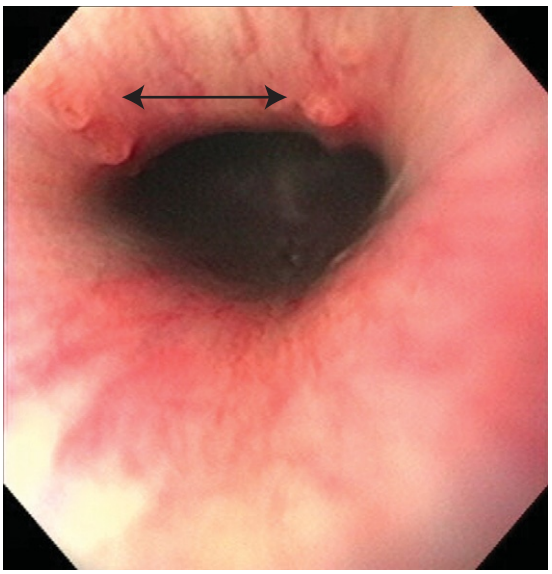

FIGURE 11-5. *Arrows* point to urethral glands. Note how urethral glands are on dorsal aspect of this image compared with their location in Figure 11-4. Urethral glands may appear either dorsal or ventral on your image, depending on position of camera lens when you pass endoscope into urethra.

These are the duct openings to the bulbourethral glands (Figure 11-6). As the endoscope bends over the urethral arch, the image will be inverted. Therefore the bulbourethral gland openings will appear ventrally but are actually located on the dorsal aspect of the urethra (Figure 11-7). Urethral defects occur at this level of the urethra where it curves over the ischial arch (Figures 11-5 to 11-9).

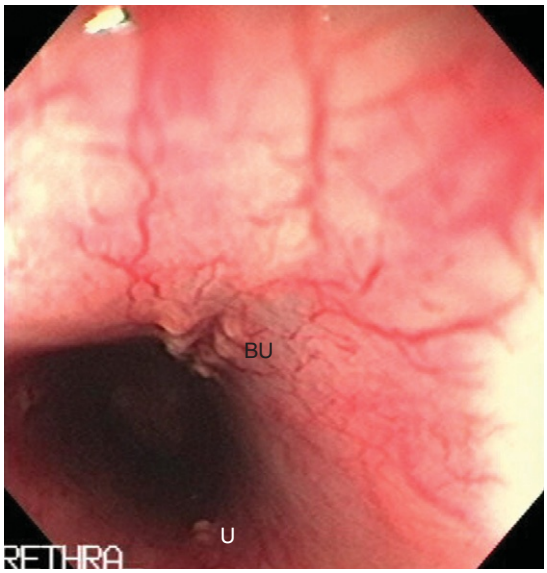

FIGURE 11-6. *BU,* Bulbourethral glands; *U,* urethral glands.

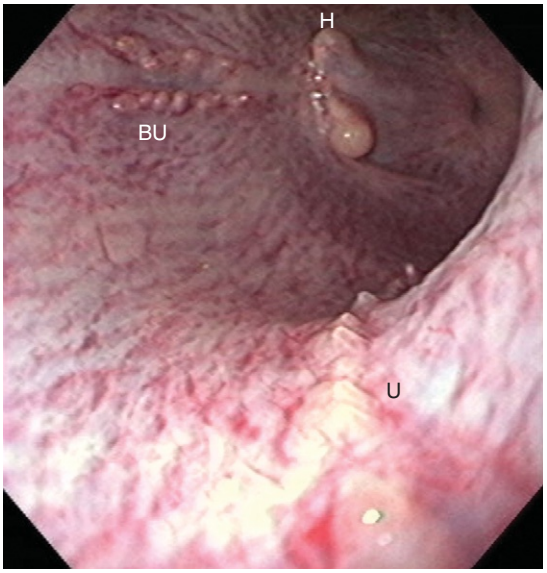

FIGURE 11-7. This examination was performed on an aged stallion. Note incidental finding of ejaculatory duct hyperplasia. *BU,* Bulbourethral glands; *H,* ejaculatory duct hyperplasia *U,* urethral ducts.

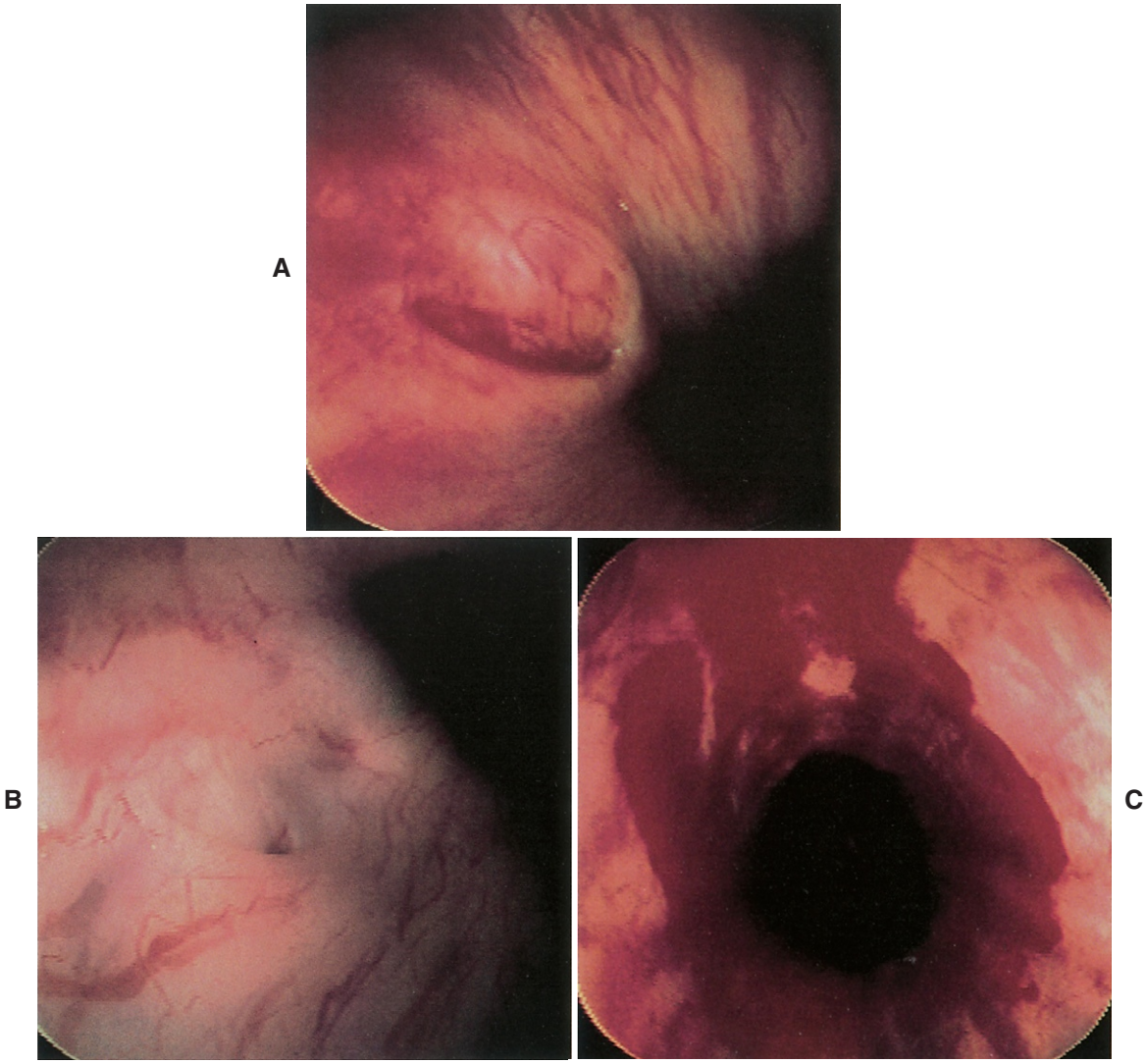

FIGURE 11-8. Proximal urethral defects at level of ischial arch in geldings brought in for occurrence of hematuria at end of urination for **A,** 3 weeks' and **B,** 8 months' duration. **C,** Shortly after a bout of hematuria, hemorrhage along the distal urethra was apparent in the gelding with hematuria of shorter duration. Both geldings responded favorable to a temporary perineal urethrotomy. (From Traub-Dargatz JL, Brown CM: *Equine endoscopy,* ed 2, St Louis, 1997, Mosby.)

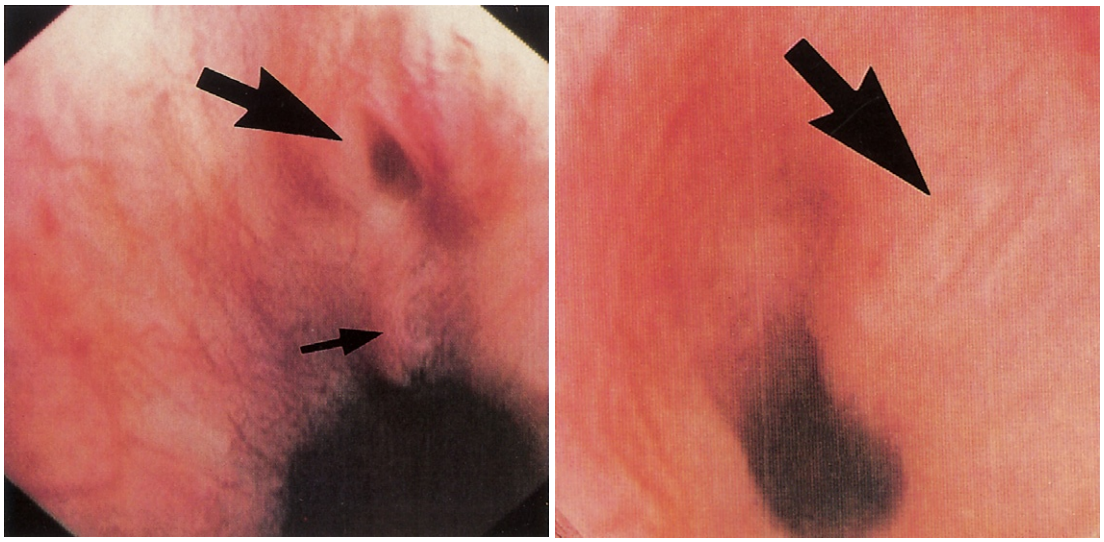

FIGURE 11-9. **A,** Two urethral mucosal defects remain 2 months after incision into corpus spongiosum penis at level of ischium to correct the condition. Proximal defect *(small arrow),* was partially healed and did not bleed when erection was induced. More distal lesion *(large arrow),* bled readily when stallion developed erection. **B,** Edges of more distal defect *(arrow),* were apposed by primary closure through ischial urethrotomy approach. (From Traub-Dargatz JL, Brown CM: *Equine endoscopy,* ed 2, St Louis, 1997, Mosby.)

Proximal to the bulbourethral gland openings is the colliculus seminalis (Figure 11-10). This structure contains the opening to the ducts of the seminal vesicles and to the ductus deferens. There may be only two distinct openings, each of which is a combined opening of the duct of the seminal vesicle and ductus deferens, which are joined together. This is called an ejaculatory duct opening (Figures 11-11 to 11-13). However, there may be four distinct openings: two for the seminal vesicles, which are "moon" shaped, and two to the ductus deferens (Figures 11-14 to 11-18).

Text continued on p. 215

FIGURE 11-10. Proximal to bulbourethral gland openings is colliculus seminalis.

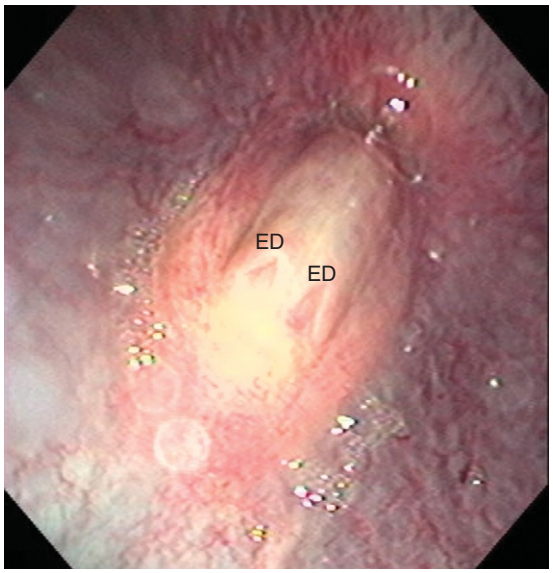

FIGURE 11-11. Ejaculatory ducts *(ED)* of colliculus seminalis.

FIGURE 11-12. Colliculus seminalis with ejaculatory ducts *(ED).*

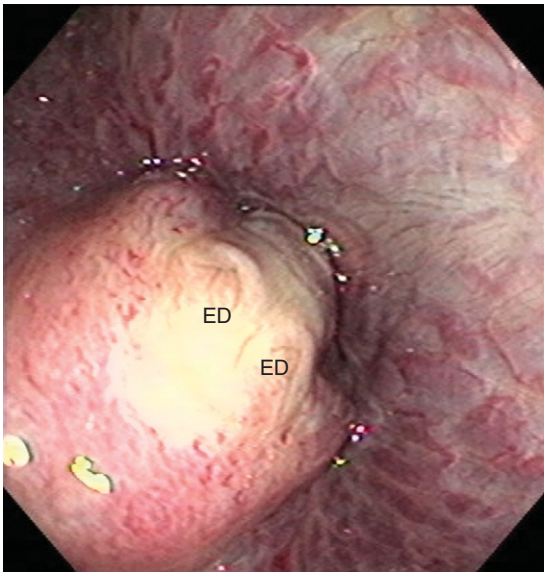

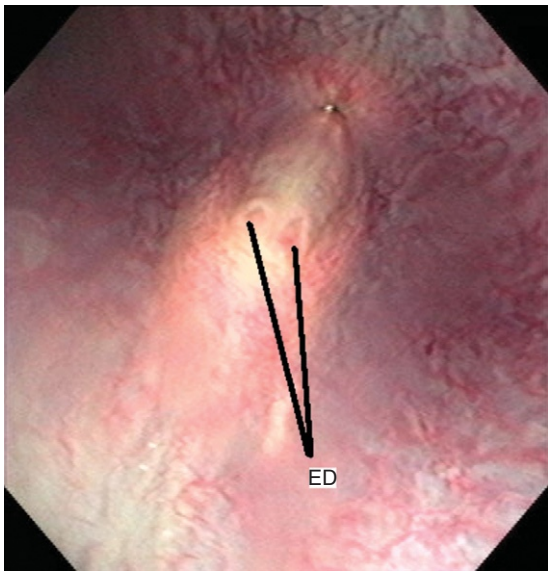

FIGURE 11-13. Normal variation of colliculus seminalis with ejaculatory ducts *(ED).*

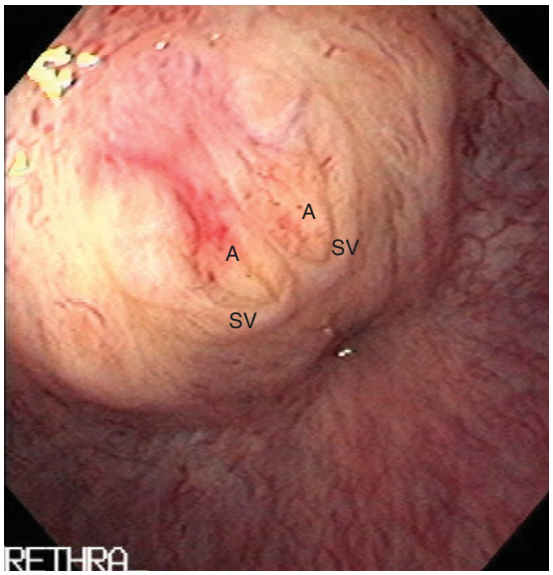

FIGURE 11-14. Colliculus seminalis with four distinct openings. Two seminal vesicle openings *(SV)* and two ductus deferens *(A)* openings.

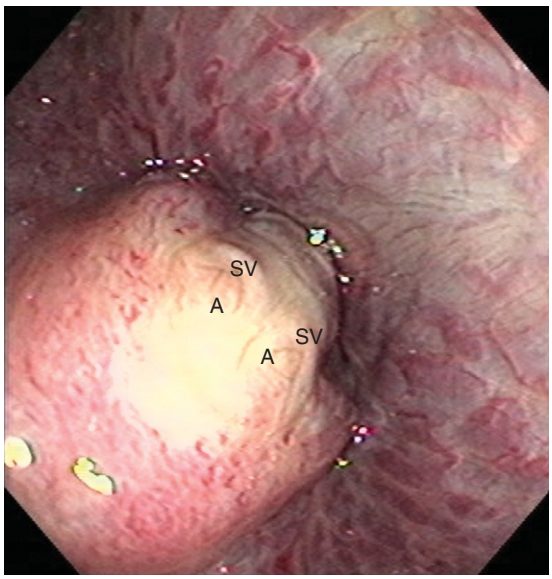

FIGURE 11-15. Colliculus seminalis. *A,* Ductus deferens openings (ampulla); *SV,* seminal vesicle.

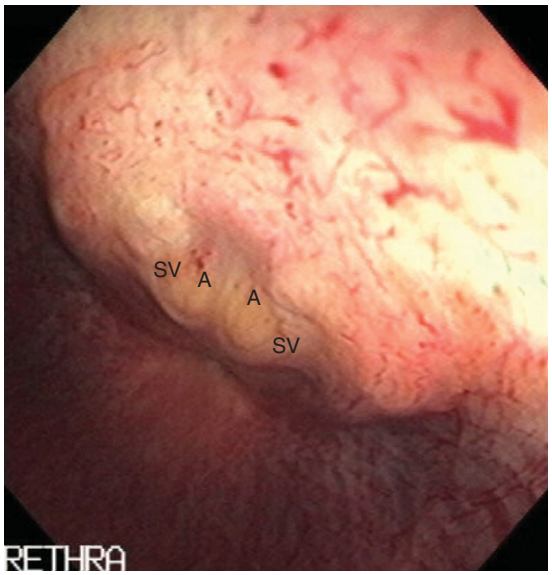

FIGURE 11-16. Colliculus seminalis of aged stallion. *A,* Ductus deferens (ampulla) openings; *SV,* seminal vesicle openings.

FIGURE 11-17. Placement of catheter into seminal vesicle opening.

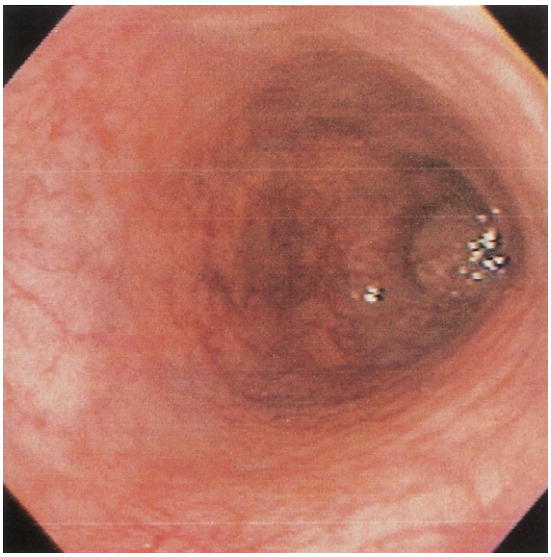

FIGURE 11-18. Seminal vesicles can be easily seen endoscopically by passing endoscope (10 mm or less in diameter) into large duct openings of colliculus seminalis and advancing endoscope while using air insufflation to expand lumina. (From Traub-Dargatz JL, Brown CM: *Equine endoscopy,* ed 2, St Louis, 1997, Mosby.)

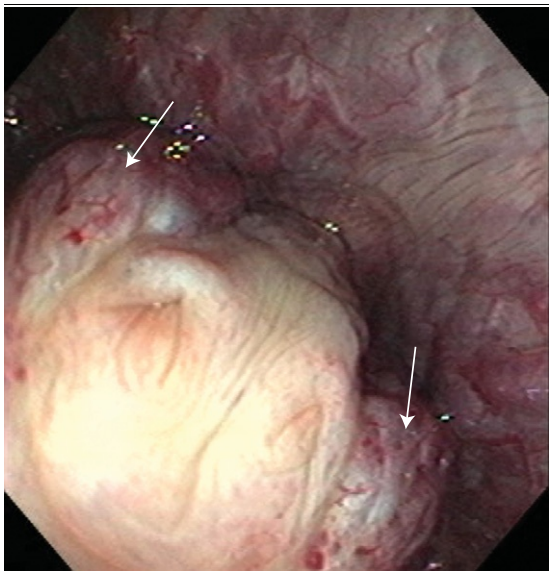

FIGURE 11-19. Prostatic ducts next to colliculus seminalis *(arrows).*

The orifices of the prostatic ducts are more difficult to visualize and lie lateral to the ejaculatory openings on the colliculus seminalis (Figure 11-19).

The openings from the bladder into the urethra is termed the internal urethral orifice and is closed except during urination (Figure 11-20).

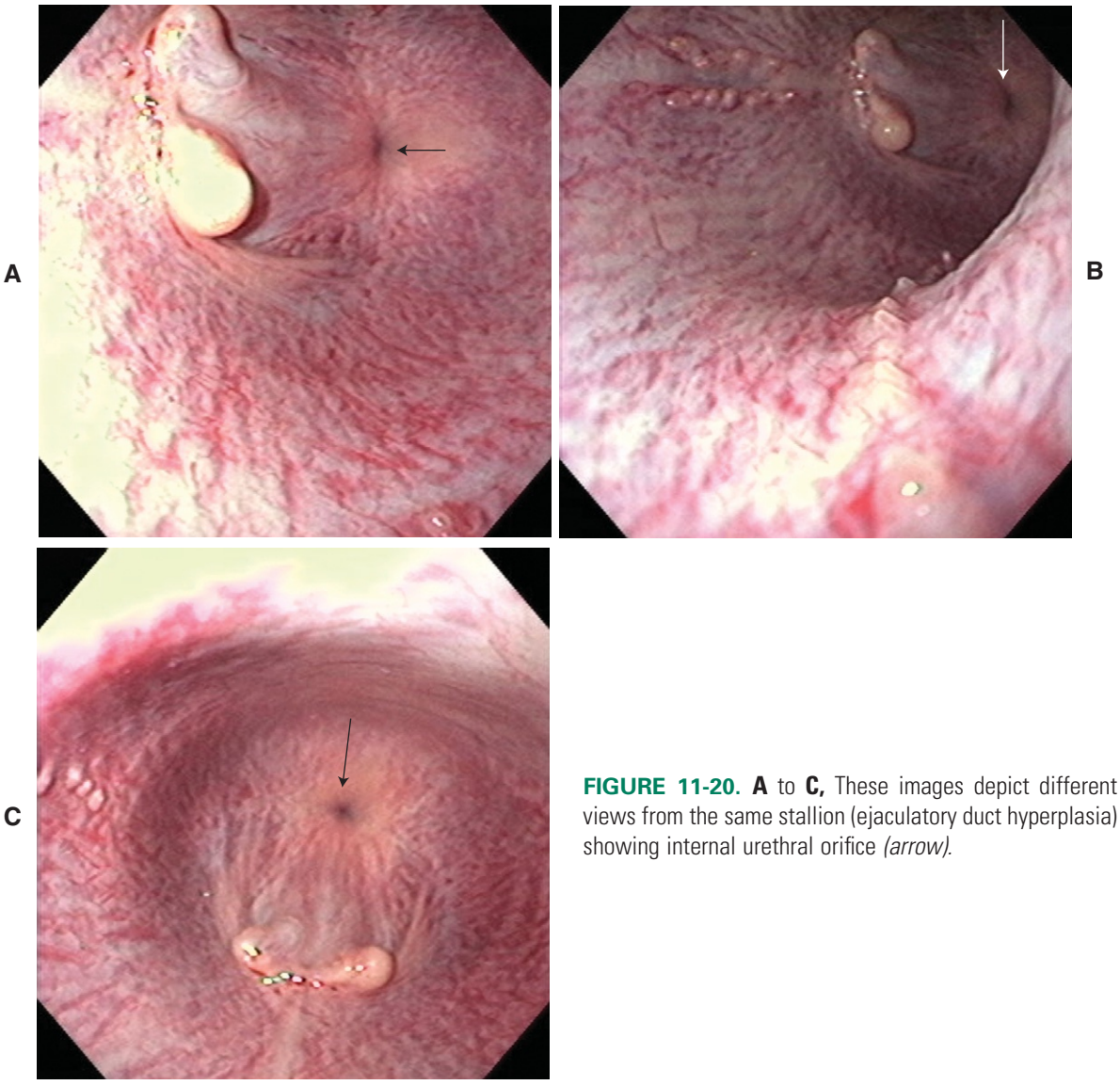

FIGURE 11-20. A to **C,** These images depict different views from the same stallion (ejaculatory duct hyperplasia) showing internal urethral orifice *(arrow).*

CHAPTER 12

Proctoscopy

NATHAN M. SLOVIS

Proctoscopy allows the veterinarian to look inside the anus and rectum to help in the diagnosis of the following:

- Inflammatory bowel disease
- Bowel obstruction
- Rectal tears
- Causes of abdominal pain (e.g., rectal abscess)
- Cancer

The rectum continues the descending colon beyond the pelvic inlet. Initially it resembles the colon in structure and in relationship to the peritoneum, but as it proceeds caudally the mesentery shortens and the peritoneal covering is gradually lost; finally the rectum is wholly retroperitoneal and embedded in fat-rich connective tissue. This terminal part loses the sacculated character and forms a wide flasklike expansion (ampulla) just before it joins the anal canal. The ampulla stores feces before evacuation (Figures 12-1 and 12-2).

FIGURE 12-1. Normal ampulla of rectum. Note pink mucosa and submucosal vasculature.

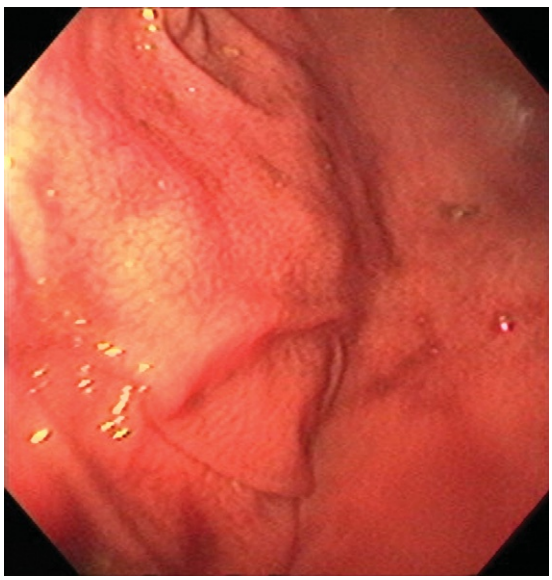

FIGURE 12-2. Magnified view of normal rectal mucosa.

The anal canal continues the rectum, but, unlike the ampulla, it is generally empty of feces. The anal canal is the distal 6 to 7 cm of the rectum, which is closed by the apposition and interdigitation of longitudinal mucosal folds and by the contraction of the internal and external anal sphincters.

MECONIUM IMPACTIONS (Figures 12-3 and 12-4)

Meconium impaction is the most common cause of colic in the newborn foal. This condition may cause foals to strain with discomfort. Some owners may confuse this straining with the inability to urinate properly, as most of these foals will squat and drip urine when attempting to pass the meconium. The meconium most commonly becomes impacted in the rectum or small colon. Occasionally, the impaction is located more proximally (large and small colon) where radiography or ultrasonography is required for diagnosis.

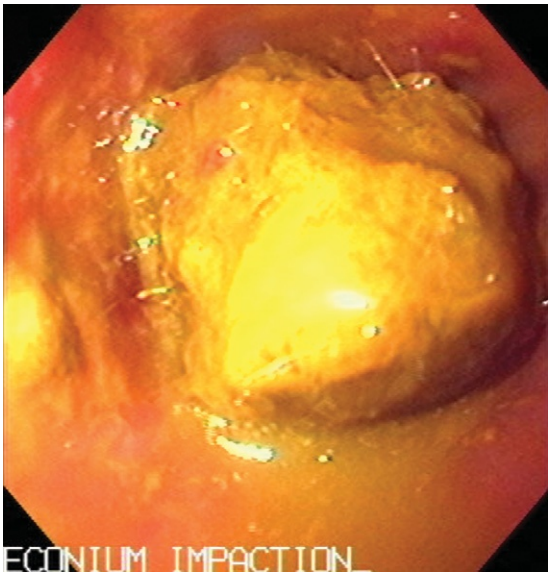

FIGURE 12-3. Twelve-hour-old thoroughbred foal was seen with marked abdominal gas distention and straining to defecate. A meconium impaction was noted 20 cm in rectum.

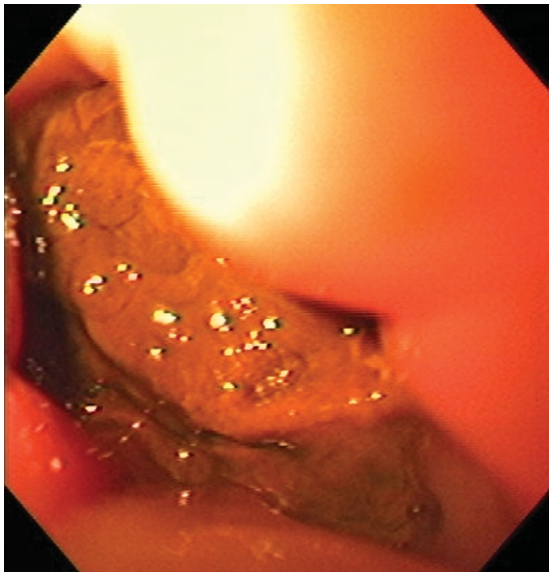

FIGURE 12-4. Twenty-four-hour-old foal was seen with colic and bloated abdomen. A meconium impaction was noted 25 cm in rectum.

DIARRHEA (Figure 12-5)

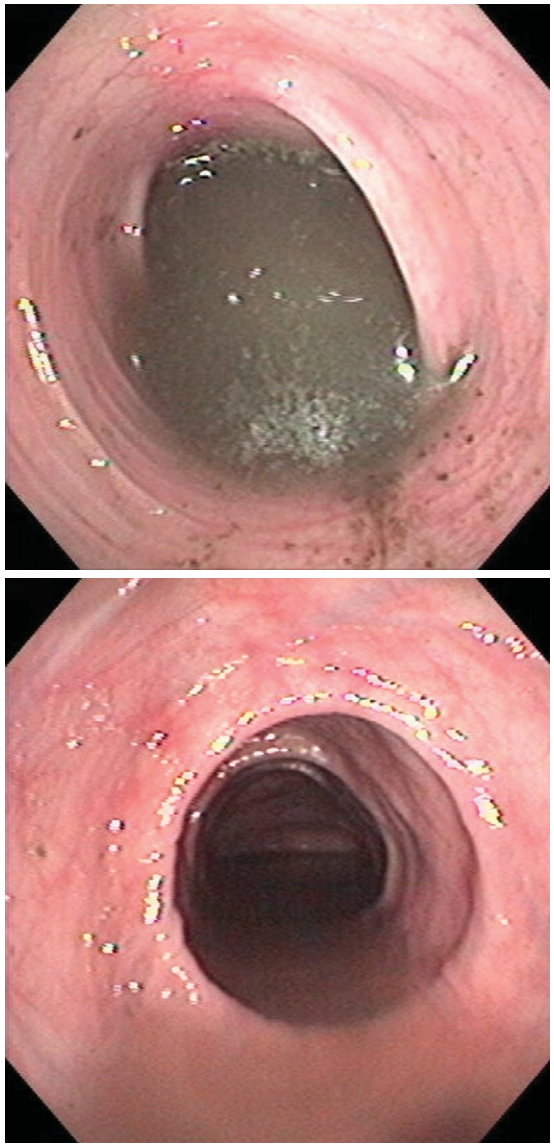

FIGURE 12-5. **A** and **B,** Yearling Arab gelding was seen with a chronic history of diarrhea and weigh loss. Proctoscopy revealed a normal rectum with normal peristaltic activity and diarrhea. Results of rectal biopsy were inconclusive. Yearling's diet was changed from alfalfa hay to a timothy mixture and no concentrates. Diarrhea was noted to have resolved 2 weeks after diet change.

RECTAL ABSCESS (Figure 12-6)

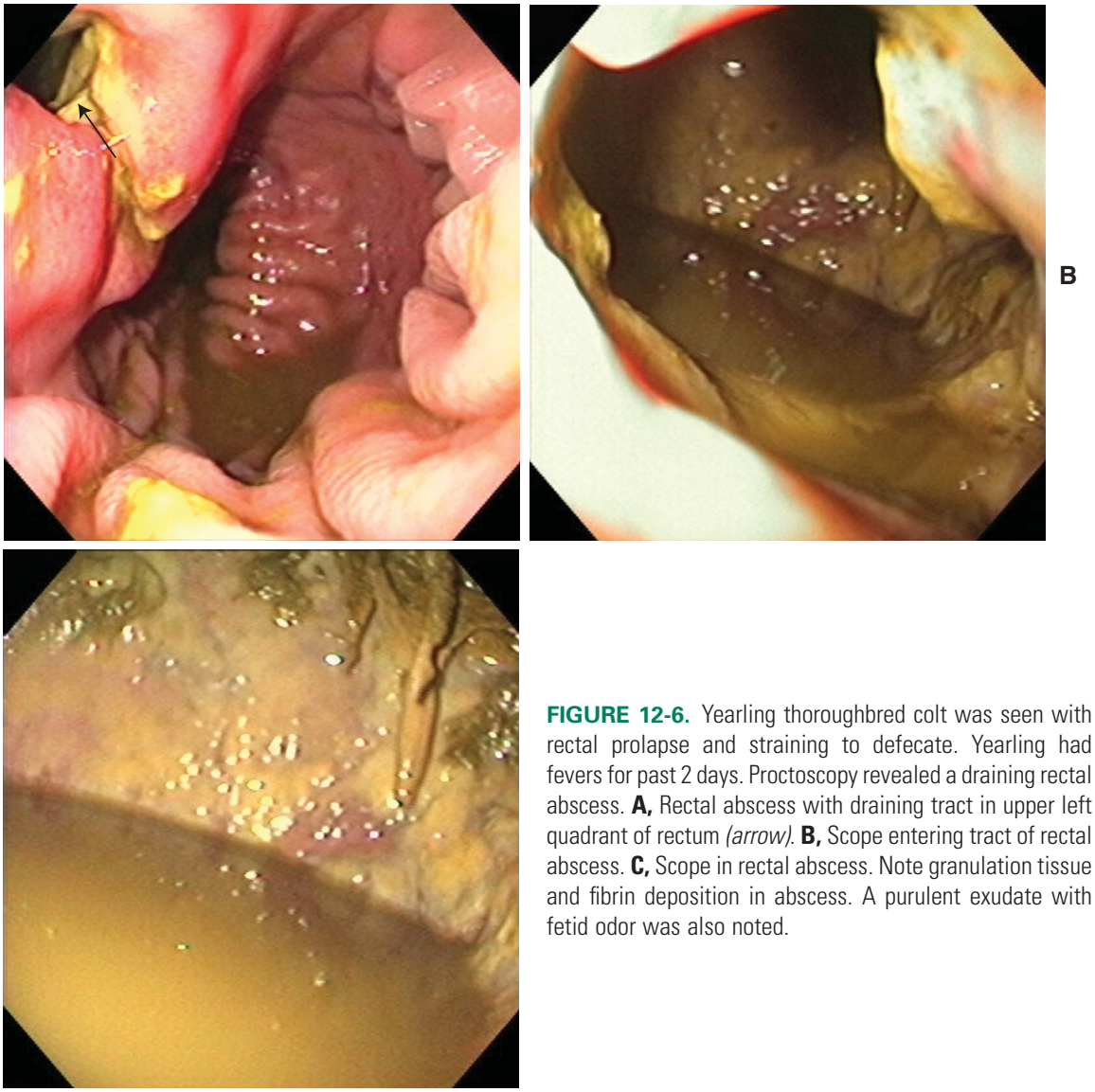

FIGURE 12-6. Yearling thoroughbred colt was seen with rectal prolapse and straining to defecate. Yearling had fevers for past 2 days. Proctoscopy revealed a draining rectal abscess. **A,** Rectal abscess with draining tract in upper left quadrant of rectum *(arrow)*. **B,** Scope entering tract of rectal abscess. **C,** Scope in rectal abscess. Note granulation tissue and fibrin deposition in abscess. A purulent exudate with fetid odor was also noted.

RECTAL TEARS

Rectal tears are classified according to the layers penetrated:

- Grade 1: Tear that involves just the mucosal and submucosa (Figure 12-7).
- Grade 2: Tear that involves only the muscular layer
- Grade 3: Subclassified into grade 3a (serosa is intact) and grade 3b (tear extends dorsally into mesorectum)
- Grade 4: Full-thickness tear that communicates with the abdomen (Figures 12-8 and 12-9)

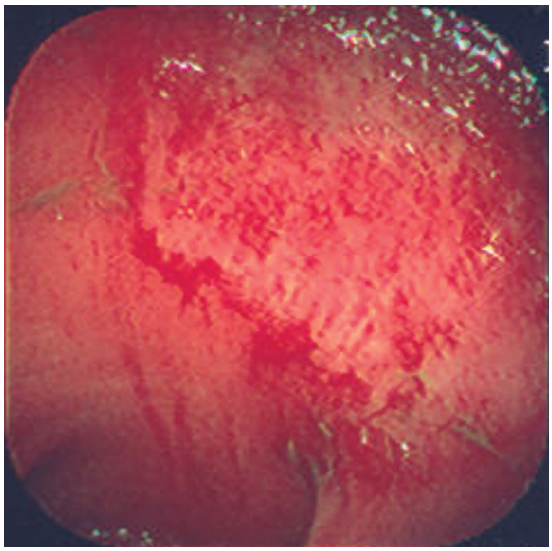

FIGURE 12-7. Mild grade 1 tear due to aggressive rectal palpation.

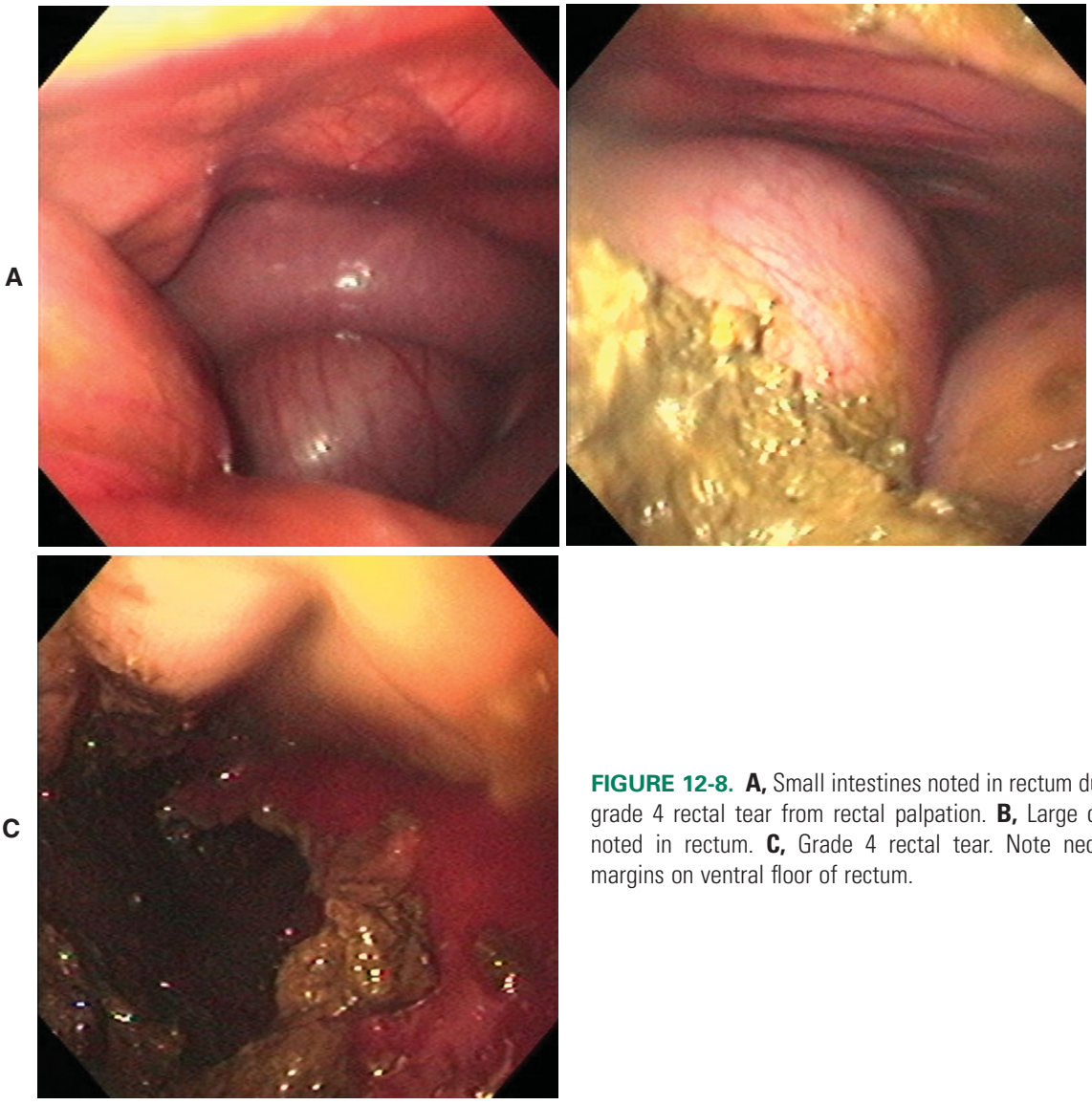

FIGURE 12-8. **A,** Small intestines noted in rectum due to grade 4 rectal tear from rectal palpation. **B,** Large colon noted in rectum. **C,** Grade 4 rectal tear. Note necrotic margins on ventral floor of rectum.

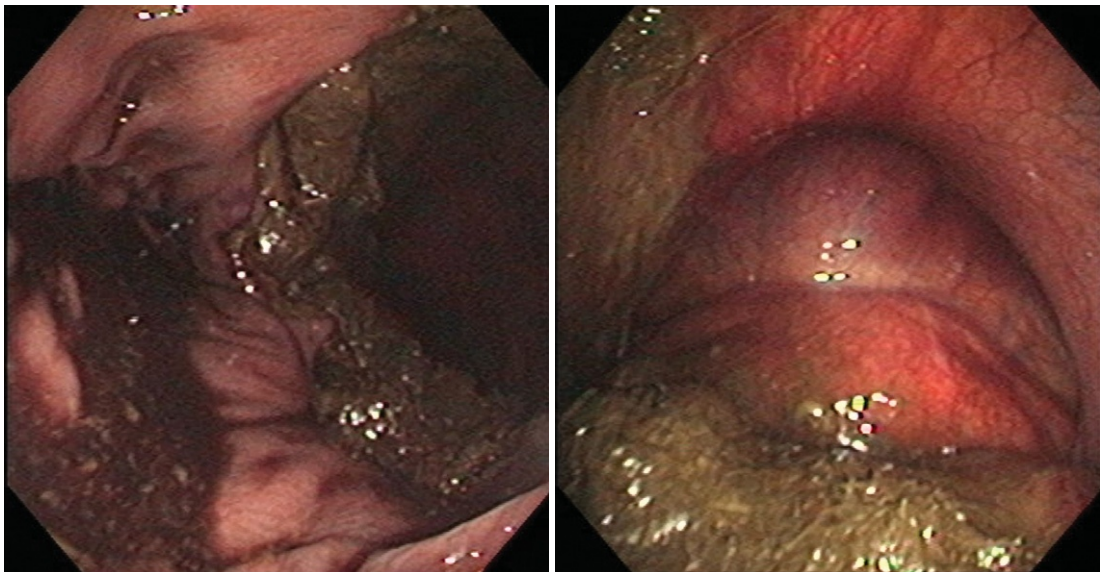

FIGURE 12-9. **A,** Necrotic mucosa of grade 4 tear in dorsal aspect of rectum. **B,** Large colon in rectum.

PROCTITIS (Figure 12-10)

FIGURE 12-10. Ten-year-old mustang was seen with history of straining to defecate. Mesquite bean rectal impaction was noted by referring veterinarian and was removed 24 hours before presentation. Severe proctitis due to mucosal injury from mesquite bean impaction was present.

CHAPTER 13

Treadmill Pharyngoscopy and Laryngoscopy

DWAYNE RODGERSON

DYNAMIC OBSTRUCTIVE DISORDERS OBSERVED ON A HIGH-SPEED TREADMILL

Endoscopic evaluation of the equine upper airway is most commonly performed at rest. Resting endoscopic examination of the upper airway is an effective diagnostic modality for identifying structural abnormalities but often is ineffective for identifying functional or dynamic obstructive abnormalities (Box 13-1). Dynamic obstructive abnormalities decrease the diameter of the airway and increase airway resistance. The increased resistance can cause respiratory noises due to air turbulence. If the degree of obstruction is severe enough, exercise intolerance or poor performance may result. With increased resistance, inspiratory pressure markedly increases within the upper airway. In some horses, multiple dynamic obstructive conditions may develop during

BOX 13-1 Structural Abnormalities Observed During Resting Endoscopic Examination and Functional Abnormalities Observed During High-Speed Treadmill Examinations

STRUCTURAL ABNORMALITIES
- Epiglottic entrapment
- Lymphoid hyperplasia
- Epiglottic hypoplasia
- Subepiglottic cysts
- Arytenoid chondritis
- Permanent dorsal displacement of the soft palate

FUNCTIONAL ABNORMALITIES
- Laryngeal hemiparesis
- Intermittent dorsal displacement of the soft palate
- Axial deviation of the aryepiglottic folds
- Pharyngeal collapse
- Epiglottic retroversion
- Axial deviation of the vocal cords
- Epiglottic entrapment
- Tracheal collapse

different levels of exercise. Obstructive upper airway abnormalities that develop during exercise present a diagnostic challenge for accurate identification.

Nasal occlusion has been shown to closely mimic upper airway pressure observed during periods of strenuous exercise; that is, nasal occlusion during endoscopic examinations at rest can potentially result in dorsal displacement of the soft palate. In one study, horses that experienced soft palate displacement during nasal occlusion were eight times more likely to displace the soft palate during exercise than horses that did not displace the palate at rest.[1] This test is an indirect method of assessing palate function, but numerous other dynamic obstructive upper airway conditions do not occur with resting nasal occlusion. Because of the differences in upper airway dynamics and neuromuscular function in horses at rest versus during periods of strenuous exercise, the results of such tests during resting examinations must be interpreted cautiously.

Another method to assess dynamic upper airway function is to evaluate horses after exercise. Endoscopic evaluation of the upper airway after exercise can demonstrate asymmetry of the corniculate process of the arytenoids and dorsal displacement of the soft palate. However, the exact cause of respiratory noises or exercise intolerance may not be accurately identified if the primary problem occurs only during periods of exercise.

Endoscopic evaluation of horses exercised on a high-speed treadmill is considered the gold standard for accurately identifying dynamic abnormalities involving the upper airway.[2] This technique has greatly enhanced our ability to evaluate the physiologic and pathophysiologic disorders of the equine upper airway. Endoscopic examination of horses on a high-speed treadmill allows evaluation of the upper airway as horses exercise at a variety of speeds in a controlled environment. The use of the high-speed treadmill has become popular in the recent years: numerous university clinics and private practices now offer endoscopic evaluation of the upper airway of horses exercising on the treadmill. Evaluation of the upper airway is typically performed using video endoscopy, which results in an easier procedure for the examiner. Videotapes of the examination may be reviewed at a slower rate to accurately assess the type and degree of dynamic obstructive abnormality.

PATIENT PREPARATION

Horses delivered for upper airway examinations using the high-speed treadmill typically arrive the morning of the examination. Physical examination is performed before the horses are moved to the treadmill room where they are trained by experienced personnel. When a horse has become accustomed to the treadmill, the video endoscope is passed through a flexible plastic tube inserted in the right or left nostril (Figure 13-1). The endoscope is positioned so that its tip is rostral to the epiglottis, and the external portion of the endoscope is then secured to the horse's halter. The horse is placed on the treadmill and stimulated to walk and then trot. The treadmill speed is gradually increased to encourage horses to canter and accelerate into a gallop (Figure 13-2). The treadmill is then progressively elevated to a 3% incline. An exercise program described for Thoroughbreds has been reported.[3] In this program, horses start at 9 m/sec for 800 m, and then the treadmill is elevated to 3%. The speed is increased to 11 m/sec for 800 m, 12 m/sec for an additional 800 m, 14 m/sec for 1600 m, and 12 m/sec for a final 800 m. The total distance on the treadmill is approximately 4000 m.[2] However, differences in the speed, distance, and time on the treadmill can occur between horses, depending on the degree of conditioning, identification of

FIGURE 13-1. **A,** Flexible plastic tube with three Velcro straps used to secure endoscope to halter and within horse's nostril. Plastic tube is passed into right or left nostril and then secured to special halter using Velcro straps. **B,** Endoscope passed through plastic tube in right nostril and secured using Velcro straps. Endoscope has a Velcro attachment to keep it secured within flexible plastic tube.

FIGURE 13-2. Horse galloping on a high-speed treadmill. Treadmill has been placed at incline and video endoscopy is being performed while horse is exercising.

an abnormality, or the particular function of the horse. Shoes are not pulled for the examination.

POSTEXERCISE PROTOCOL

After completion of the examination, horses are cooled down and washed. Examination results (including videotape) are kept as hospital records, and a copy is sent to the owner/trainer. Horses are typically discharged on the same day unless they are hospitalized for surgical correction of a disorder found during the examination.

FUNCTIONAL ABNORMALITIES OF THE UPPER AIRWAY

In the normal horse exercising on a high-speed treadmill, the corniculate process of the arytenoids should be fully abducted and the rima glottidis should be at its maximum diameter (Figure 13-3). However, numerous dynamic obstructive disorders can occur in exercising horses. In some horses, multiple abnormalities may be observed. Common dynamic obstructive abnormalities observed include laryngeal hemiparesis, intermittent dorsal displacement of the soft palate, axial deviation of the aryepiglottic folds, pharyngeal collapse, and epiglottic retroversion.

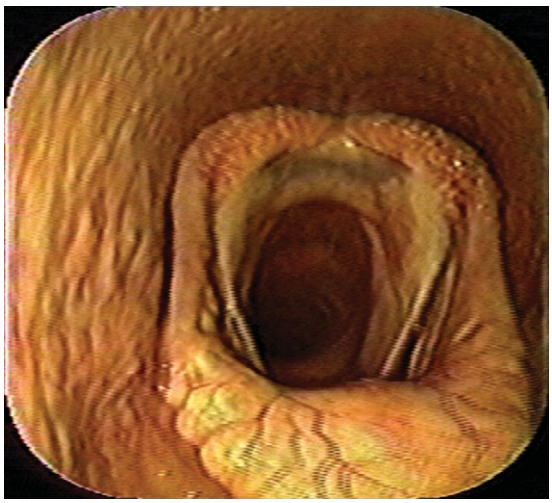

FIGURE 13-3. Normal upper airway of horse on high-speed treadmill. Corniculate processes of arytenoids are fully abducted and rima glottidis is at its maximum diameter.

Laryngeal Hemiparesis

Abnormalities in resting laryngeal function involving the corniculate process of the arytenoid have been classically categorized into four grades. Grades I and IV represent normal laryngeal function and laryngeal hemiplegia, respectively. Grades II and III both refer to asymmetry in the movement of the corniculate process of the arytenoids, but with Grade III horses cannot fully abduct the corniculate process of the arytenoid after nasal occlusion or after swallowing.

This grading system has been found to be inadequate for the description of horses exercised on the treadmill. With increases in inspiratory pressure during exercise, horses with grade III laryngeal hemiparesis have been found to experience varying degrees of dynamic axial collapse of the arytenoid. Based on this finding, three subclasses were proposed to more accurately describe this variation (Box 13-2 and Figure 13-4).[3] In one report, 77% of horses with laryngeal hemiparesis categorized as having grade III at rest had grade IIIC after evaluation on a high-speed treadmill.[3] Because of the dynamic nature of the equine larynx, variations can still potentially exist for grading individual horses. The author has seen several horses with laryngeal hemiparesis characterized as grade II at rest that become grade IIIC when exercised to fatigue on the treadmill. This observation emphasizes that the horse's level of fatigue can cause variations in grading laryngeal hemiparesis (Figures 13-5 to 13-7).

Clinically, horses affected with laryngeal hemiplegia often make a roaring to whistling noise on inspiration. The degree of laryngeal obstruction may vary based on the level of fatigue and in many horses, axial deviation of the aryepiglottic folds can be observed before or in conjunction with dynamic collapse of the corniculate process.

Treatment of horses exhibiting dynamic collapse of the corniculate process of the arytenoid involves performing a prosthetic laryngoplasty (Figure 13-8). Prognosis for successful return to previous level of work after laryngoplasty is reported to be 50% to 70%. Laser resection of the aryepiglottic folds or vocal cords may also be performed to help enlarge the rima glottidis during exercise.

Dorsal Displacement of the Soft Palate

Intermittent dorsal displacement of the soft palate is a common dynamic upper airway abnormality (Figure 13-9 and 13-10). Affected horses often are seen with a history of exercise intolerance and a loud gurgling noise on expiration. The gurgling noise is related to the soft palate billowing into the caudal aspect of the nasopharynx on expiration.

Horses that intermittently displace their soft palate often appear to be clinically normal at rest, and this displacement may be very difficult to accurately identify during resting endoscopy. In horses that displace their soft palate during resting examination,

Text continued on p. 233

BOX 13-2 Subclasses of Grade III Laryngeal Hemiparesis Used to Characterize Laryngeal Function During High-Speed Treadmill Examinations

Grade IIIA: Able to maintain full abduction during exercise

Grade IIIB: Able to maintain left arytenoid and vocal fold in fixed position but incompletely abducted

Grade IIIC: Severe collapse of left arytenoid and vocal fold during exercise and arytenoid assumed position axial to its position at rest

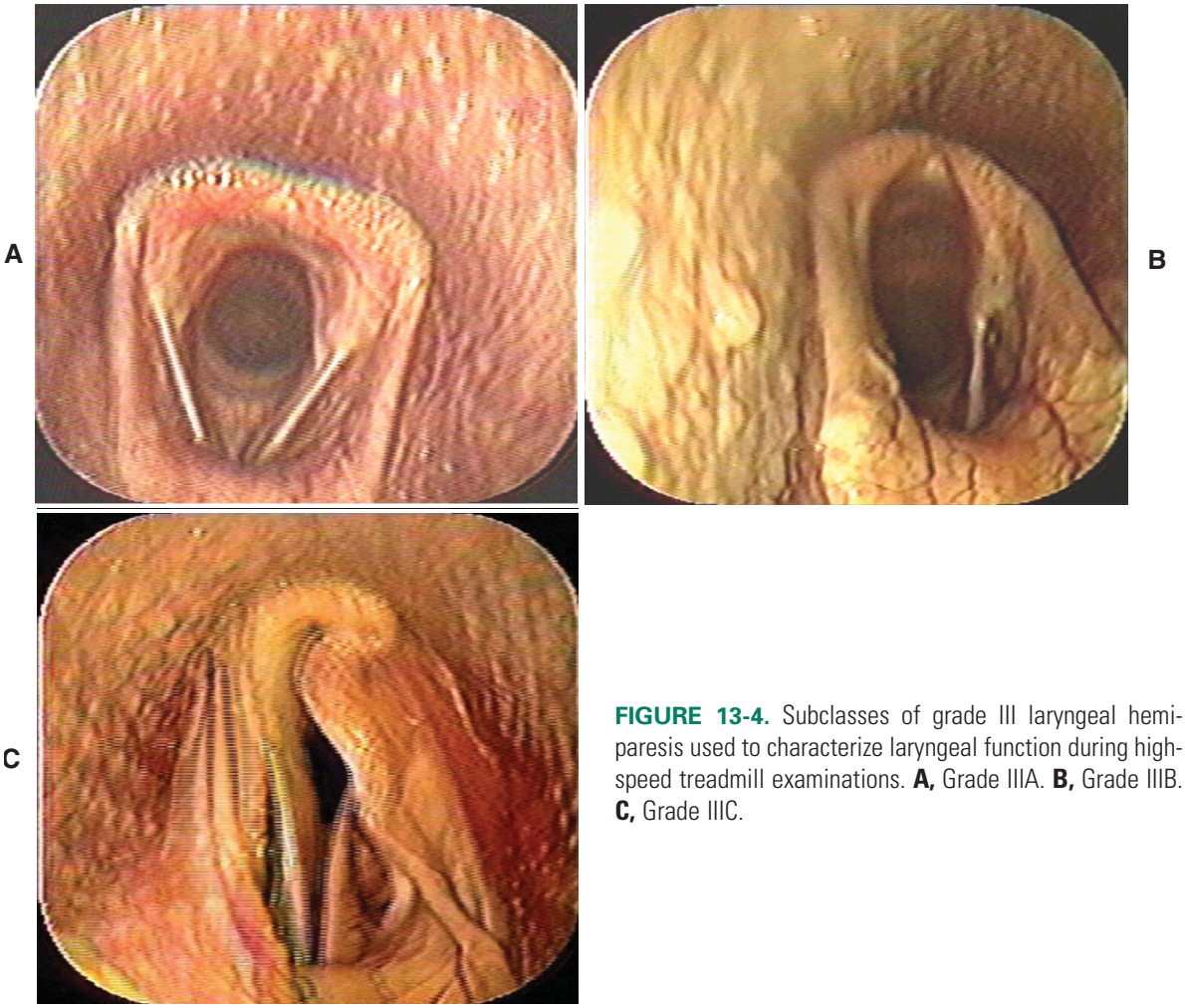

FIGURE 13-4. Subclasses of grade III laryngeal hemiparesis used to characterize laryngeal function during high-speed treadmill examinations. **A,** Grade IIIA. **B,** Grade IIIB. **C,** Grade IIIC.

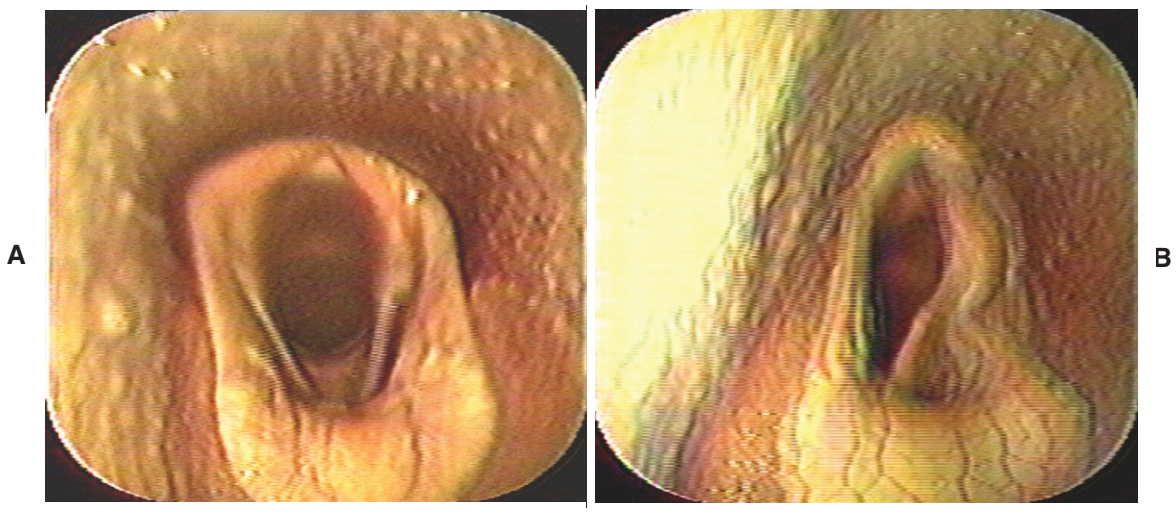

FIGURE 13-5. Dynamic collapse of left corniculate process in racehorse while exercising on a high-speed treadmill. **A,** Horse begins to gallop. Left corniculate process is abducted but not fully (grade IIIB). **B,** Horse is now later in stage of examination, and laryngeal function can now be graded as grade IIIC.

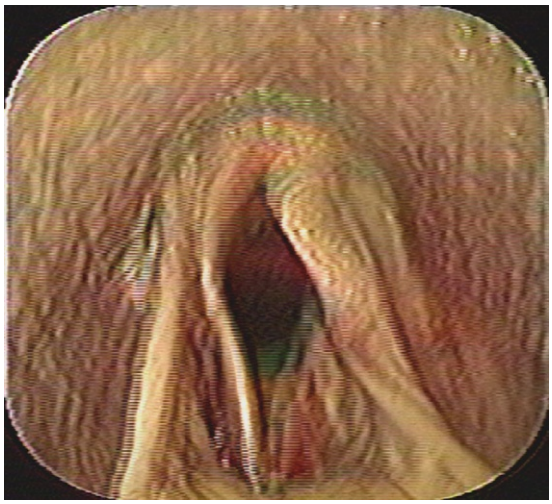

FIGURE 13-6. Horse that had a prosthetic laryngoplasty and left-side ventriculocordectomy performed about 18 months before this examination. Horse had returned to racing, but started making a respiratory noise. Collapse of left arytenoid is seen. Left aryepiglottic fold shows mild to moderate axial deviation.

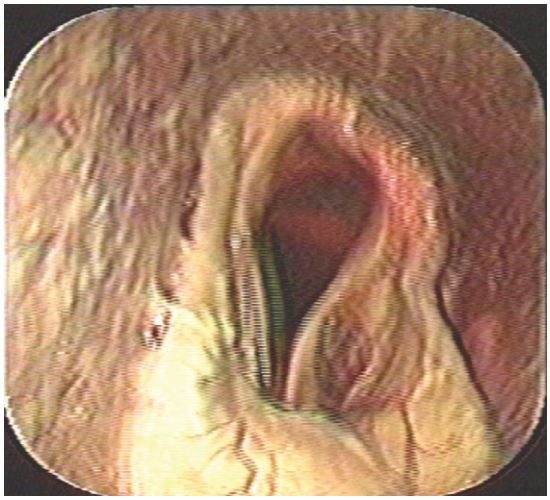

FIGURE 13-7. Discoloration of left arytenoid. Continued axial deviation of left arytenoid caused corniculate process to become red or hemorrhagic during high-speed treadmill examination.

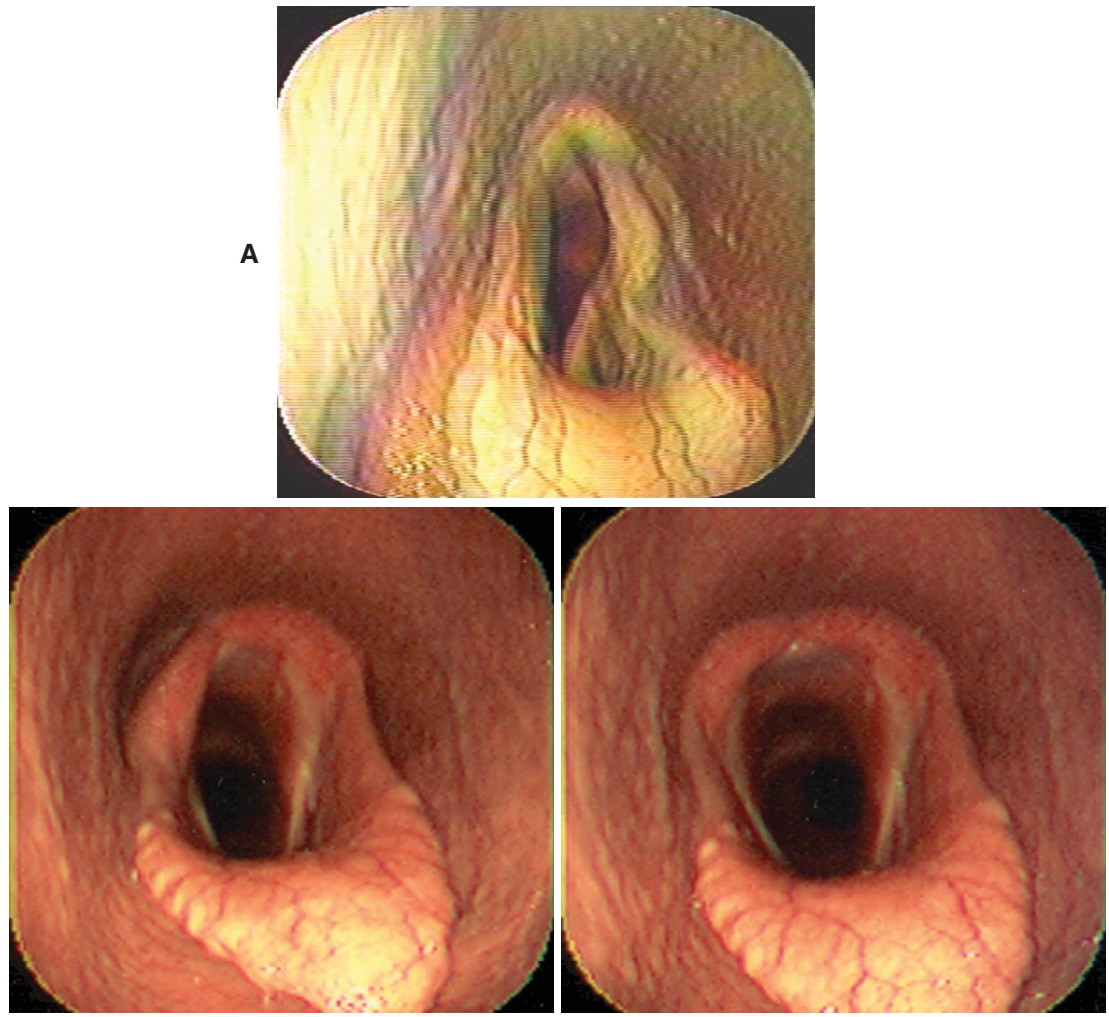

FIGURE 13-8. **A,** Horse shows dynamic collapse of left corniculate process (grade IIIC). **B,** Images taken postoperatively after prosthetic laryngoplasty has been performed. Abduction of left arytenoid can be seen on both expiration and inspiration.

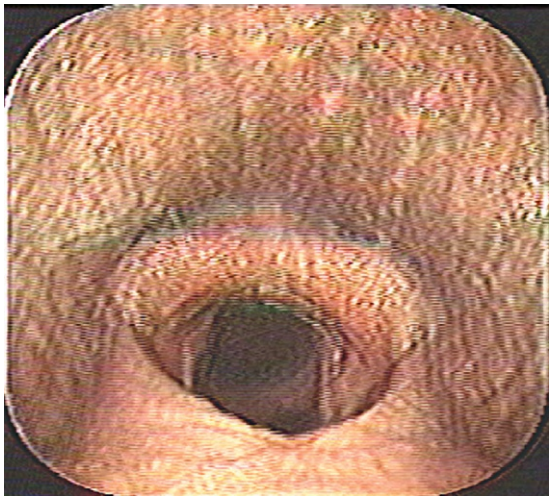

FIGURE 13-9. Dorsal displacement of soft palate observed on high-speed treadmill.

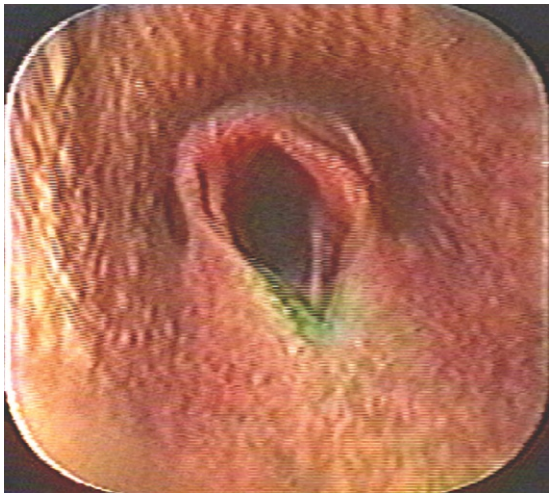

FIGURE 13-10. Multiple abnormalities: dynamic collapse of left arytenoid and dorsal displacement of soft palate.

an ulcer involving the caudal soft palate may be observed that indirectly indicates a history of displacement during exercise. As stated earlier, nasal occlusion has been found to mimic pressures observed during periods of strenuous exercise. Horses that displace their palate during nasal occlusion are more likely to do so during a high-speed treadmill examination. However, many horses that displace their palate during nasal occlusion may not do so during a treadmill examination.

During treadmill examinations, horses that displace their palate can often replace it in a normal position and continue without displacing it. The period of the examination in which horses displace their soft palate is typically near the end of the exercise, but this is not always the case. Horses with a very flaccid or small epiglottis may displace the palate earlier in the course of the treadmill examination, but conversely, some horses with a small epiglottis never displace their soft palate.

Soft palate displacement is considered significant in horses that do not immediately replace it. In general, the treadmill is slowed down when horses experience displacement of the soft palate if they do not replace it immediately. The author often immediately resumes the treadmill examination after the horse replaces the soft palate to determine if the displacement reoccurs. In some horses, axial deviation of the aryepiglottic folds seems to precede dorsal displacement of the soft palate.

Medical and surgical treatment options have been described for horses with intermittent soft palate displacement. Common medical treatment options include changing the horse's head position, tongue-tie, figure-eight noseband, and bit changes. The author strongly supports recent work by Holcombe and associates,[4] who aimed to control upper airway inflammation, if present, with antiinflammatory agents. Inflammation of the upper airway is typically associated with lymphoid hyperplasia. The use of both systemic and local antiinflammatory agents within the nasopharynx is based on the theory that inflammation in the nasopharynx could affect the neuromuscular function of the soft plate (controlled in part by the pharyngeal branch of the vagus nerve).[4] Inflammation and subsequent neuritis in the nasopharynx could result in intermittent dorsal displacement of the soft palate.

Surgical management of dorsal displacement of the soft palate includes myectomy, staphylectomy, combined staphylectomy and myectomy, and epiglottic augmentation. The myectomy is aimed at eliminating caudal retraction forces on the larynx. Various procedures are described. Presently, the method most commonly performed involves taking a small section of the sternothyroideus muscles/tendons at the level of attachment on the thyroid cartilage of the larynx. The success rate for this procedure is close to 60%. The success rate is reported to be similar for the staphylectomy, but the author performs this procedure less commonly because some horses may persistently displace their soft plate after surgery.

Epiglottic augmentation is only used in horses with a small or flaccid epiglottis. The augmentation procedure may improve the degree of flaccidity by increasing the stiffness of the epiglottis. A success rate of 66% has been reported for this procedure.

Axial Deviation of the Aryepiglottic Folds

This anomaly has been recently noted to occur during high-speed treadmill examinations.[5] The axial deviation occurs on inspiration, and the degree of deviation can be mild, moderate, or severe (Figure 13-11). Mild deviation of the fold is characterized by the fold staying abaxial to the vocal cord. Moderate deviation refers to collapse of the fold beyond the vocal cord but less than halfway between the vocal cord and the midline. In severe cases of axial deviation of the aryepiglottic folds, the fold actually

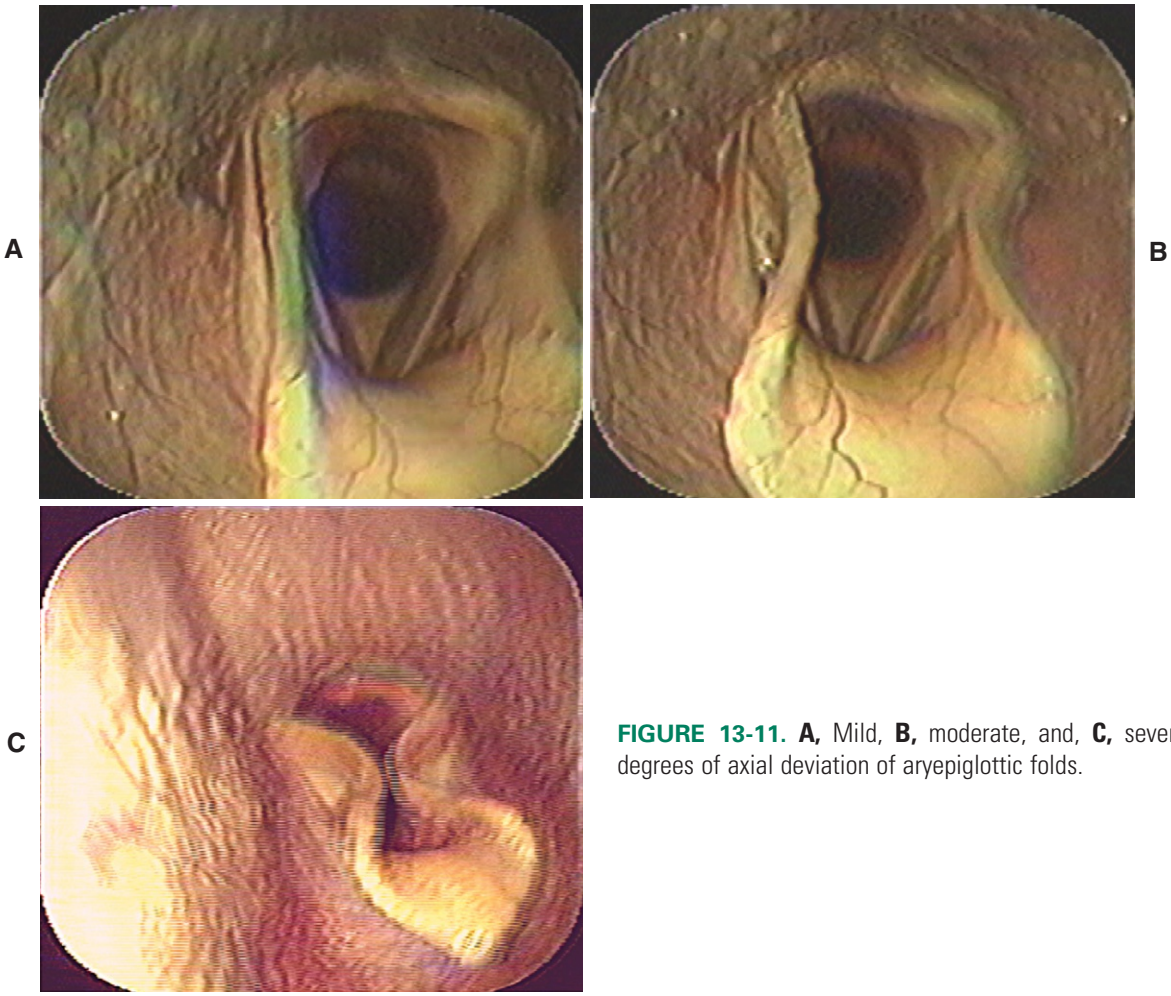

FIGURE 13-11. A, Mild, **B,** moderate, and, **C,** severe degrees of axial deviation of aryepiglottic folds.

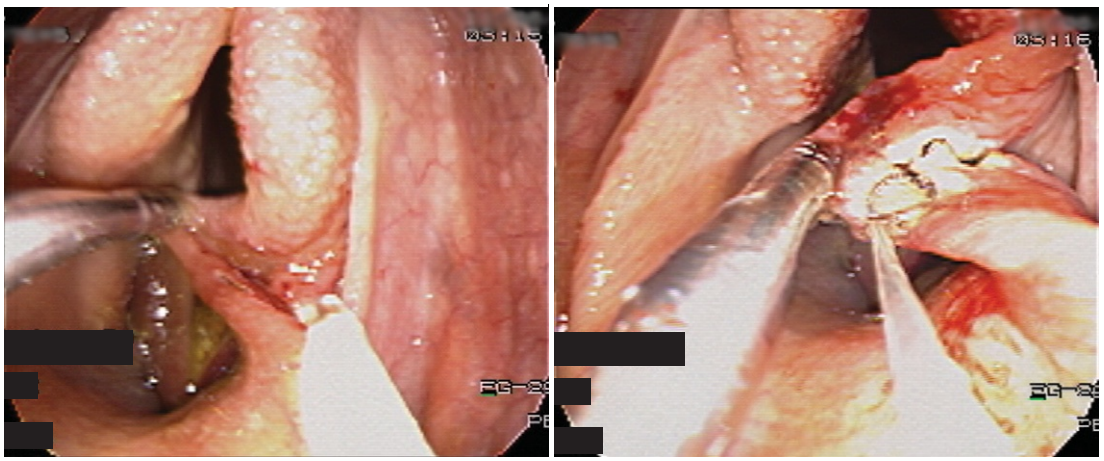

FIGURE 13-12. Transendoscopic laser resection of left aryepiglottic fold. **A,** Fold is grasped and maintained using long handled forceps. **B,** Laser fiber is then used to cut a 1- to 2-cm triangular section of aryepiglottic fold.

reaches the midline of the rima glottidis. Horses with mild, moderate, and severe deviation of the aryepiglottic folds have been reported to have less than 20%, 21% to 40%, and 41% to 63% obstruction of the glottis, respectively.[6] However, the degree of deviation in some horses can progress through all degrees, depending on the level of fatigue.

Axial deviation of the aryepiglottic folds can place tension on the corniculate process of the arytenoids, leading to laryngeal hemiparesis. Axial deviation of the aryepiglottic folds often precedes dorsal displacement of the soft palate. This may be related to the increased inspiratory pressure that forces the aryepiglottic folds axially and then the soft palate dorsally.

Surgical resection of a portion of these folds has been described, but few numbers preclude drawing accurate conclusions on the effectiveness of this therapy.[5,7] However, future data may indicate that resection of the aryepiglottic folds improves laryngeal hemiparesis in horses and may be an option in minimizing dorsal displacement of the soft palate. The aryepiglottic folds are usually resected using either a neodymium : yttrium-aluminum-garnet (Nd : YAG) or diode laser (Figure 13-12) or via sharp dissection through a laryngotomy approach. In conditions that also involve dorsal displacement of the soft palate or laryngeal hemiparesis, other surgical procedures to correct these conditions may be indicated.

Other Abnormalities

Pharyngeal Collapse Pharyngeal collapse is sometimes observed during high-speed treadmill examinations (Figures 13-13 and 13-14). The collapse may be related to a neuromuscular disorder of the nasopharynx. The condition can be so severe during exercise that the nasopharynx completely collapses during inspiration. Therapy for pharyngeal collapse is aimed at controlling upper airway inflammation if present. Systemic and topical antiinflammatory drugs may help reduce the degree of nasopharyngeal collapse.

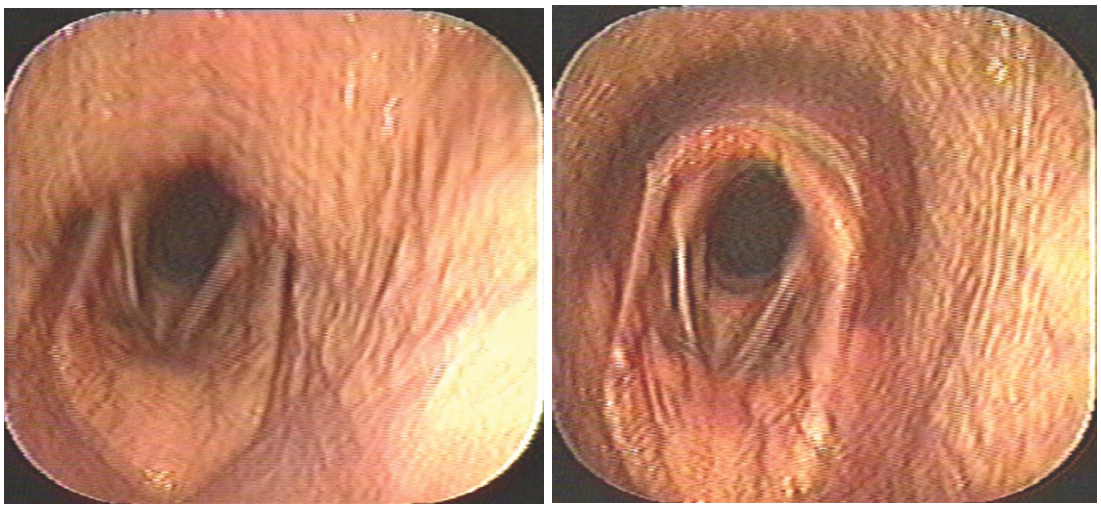

FIGURE 13-13. **A,** Dorsal pharyngeal collapse on inspiration. **B,** On expiration dorsal pharyngeal collapse is no longer present.

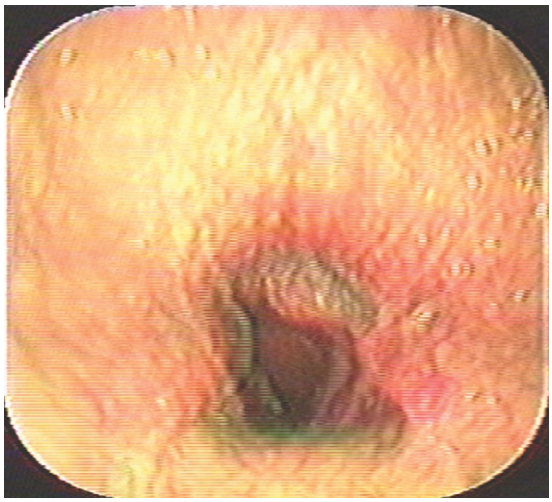

FIGURE 13-14. Dorsal and lateral collapse of pharyngeal wall around larynx.

Epiglottic Retroversion Epiglottic retroversion is a rare condition that may cause a gurgling sound during inspiration (Figure 13-15). This endoscopic finding is not observed at rest or during nasal occlusion. With inspiration the epiglottis is retroflexed caudally and obstructs the rima glottidis. Epiglottic augmentation using Teflon has been suggested, but the prognosis for successful racing is unknown due to the infrequency of this condition.[8]

Axial Deviation of the Vocal Cords Axial deviation of the vocal cords can decrease the diameter of the rima glottidis (Figure 13-16). This condition is often associated with laryngeal hemiplegia. Surgical resection of the vocal cords using a laser (Figure 13-17) or via sharp dissection through a laryngotomy approach is recommended.

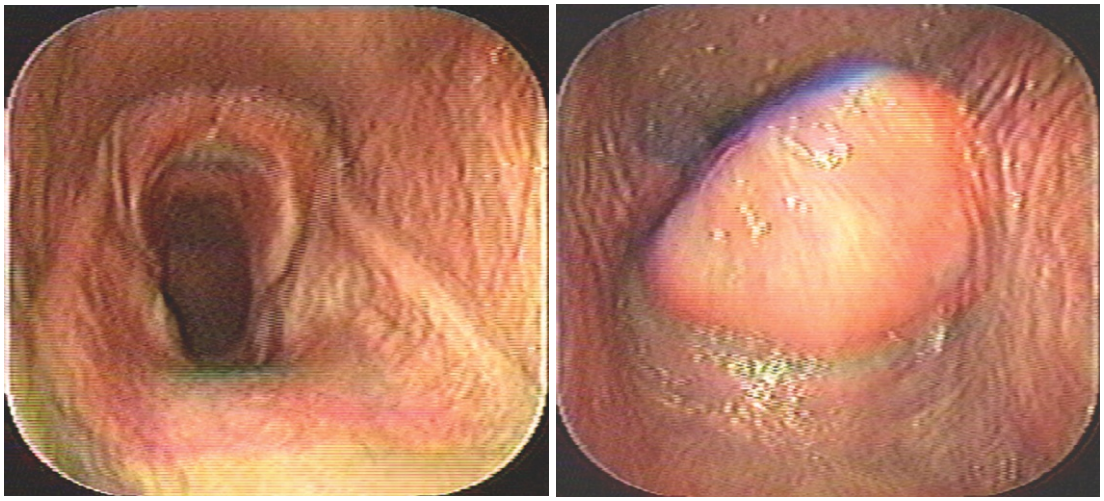

FIGURE 13-15. Epiglottic retroversion in a horse exercising on a high-speed treadmill. **A,** Normal position of epiglottis. **B,** Epiglottic retroversion. Epiglottis can be seen obstructing rima glottidis. Epiglottic retroversion occurs on inspiration.

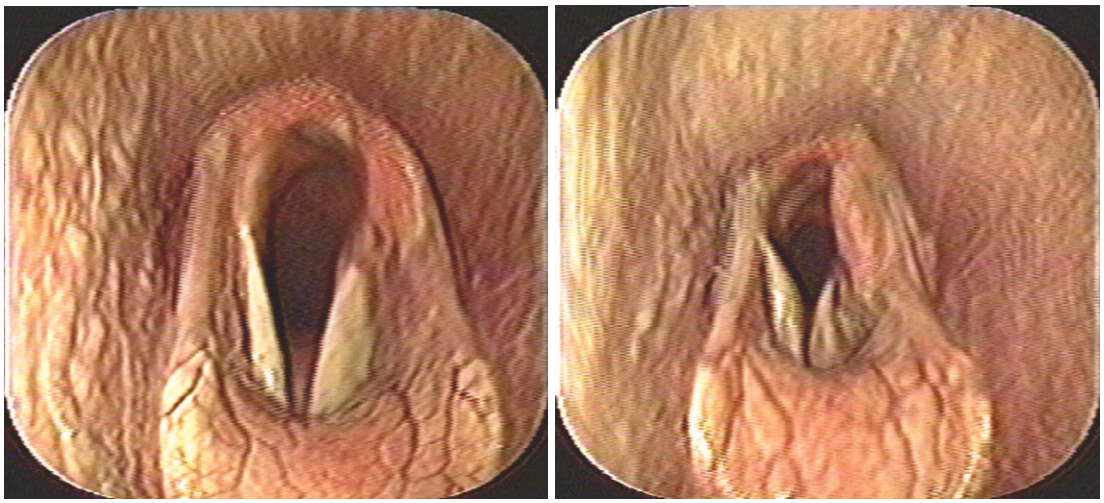

FIGURE 13-16. Axial deviation of vocal cords. **A,** Vocal cords are slightly separated, and there is mild asymmetry between right and left arytenoids. **B,** Multiple abnormalities: dynamic collapse of left arytenoid and axial deviation of vocal cords.

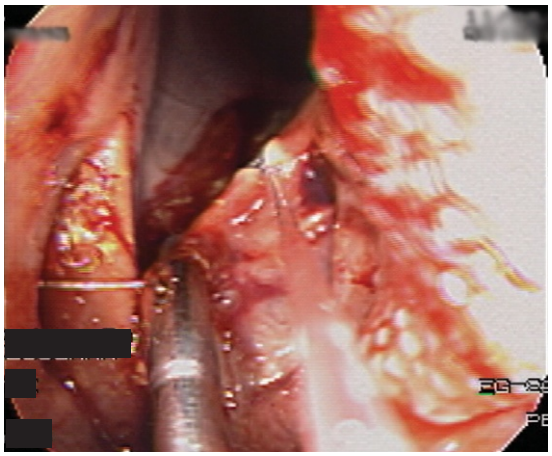

FIGURE 13-17. Transendoscopic laser cordectomy. Long-handled forceps are securing and maintaining left vocal cord in axial position while laser is used to resect axial free portion of vocal cord.

Epiglottic Entrapment Epiglottic entrapment can occur during high-speed treadmill examinations. This condition can be very hard to detect while the video monitor is viewed at normal speed. Reviewing the recorded endoscopic examination at slower speeds can help identify horses entrapping their epiglottis while they exercise on the high-speed treadmill. Tracheal collapse is also rare in horses, but this condition has been observed in miniature horses.

If the endoscopic examination does not reveal any significant findings, further diagnostic tests for poor performance should be done to evaluate the lower airway. Transtracheal washes, bronchoalveolar lavage, and chest radiographs may be performed after the treadmill examination. Cardiac examinations should also be included in the evaluation of horses seen for poor performance. Examinations of horses using echocardiography before and after exercise and electrocardiography before, during, and after exercise may provide useful information.

REFERENCES

1. Parente EJ, Martin BB: Correlation between standing endoscopic examinations and those made during high-speed exercise in horses: 150 cases, *Am J Vet Res* 41:170-175, 1995.
2. Parente EJ: Treadmill endoscopy. In Traub-Dargatz J, Brown C, editors: *Equine endoscopy,* ed 2, pp 107-116, St Louis, 1997, Mosby.
3. Hammer EJ, Tulleners EP, Parente EJ et al: Videoendoscopic assessment of dynamic laryngeal function during exercise in horses with grade-III left laryngeal hemiparesis at rest: 26 cases (1992-1995), *J Am Vet Med Assoc* 212:399-403, 1998.
4. Holcombe SJ, Derksen FJ, Stick JA et al: Effect of bilateral blockade of the pharyngeal branch of the vagus nerve on soft palate function in horses, *Am J Vet Res* 59:504-508, 1998.
5. King DS, Tulleners E, Martin BB Jr et al: Clinical experiences with axial deviation of the aryepiglottic folds in 52 racehorses, *Vet Surg* 30:151-160, 2001.
6. King DS: Axial deviation of the aryepiglottic folds. In Robinson NE, editor: *Current therapy in equine medicine,* pp 378-380, Philadelphia, 2003, WB Saunders.
7. Tulleners E: Transendoscopic laser surgery of the upper respiratory tract. In Traub-Dargatz J, Brown C, editors: *Equine endoscopy,* ed 2, pp 117-137, St Louis, 1997, Mosby, 1997.
8. Parente EJ, Martin BB, Tulleners EP: Epiglottic retroversion as a cause of upper airway obstruction in two horses, *Equine Vet J* 30:270-272, 1998.

CHAPTER 14

Miscellaneous Endoscopic Procedures

NATHAN M. SLOVIS

OTOSCOPY

The external ear consists of two parts: the auricle and the external acoustic meatus. The auricle, or pinna, is the "ear," as it is understood by the layman. The external acoustic meatus is the canal that leads from the base of the auricle to the eardrum (tympanic membrane) stretched across an opening in the temporal bone (Figure 14-1).

The external acoustic meatus begins where the rolled-up part of the auricular cartilage narrows and ends at the eardrum. The external meatus is lined with skin that contains sebaceous and tubular ceruminous glands. The latter secrete the earwax (cerumen), which is thought to prevent dust reaching the delicate tympanic membrane. The external meatus is curved, making the passage of a straight otoscope for the examination of the proximal part of the meatus and eardrum difficult (Figures 14-2 to 14-4).

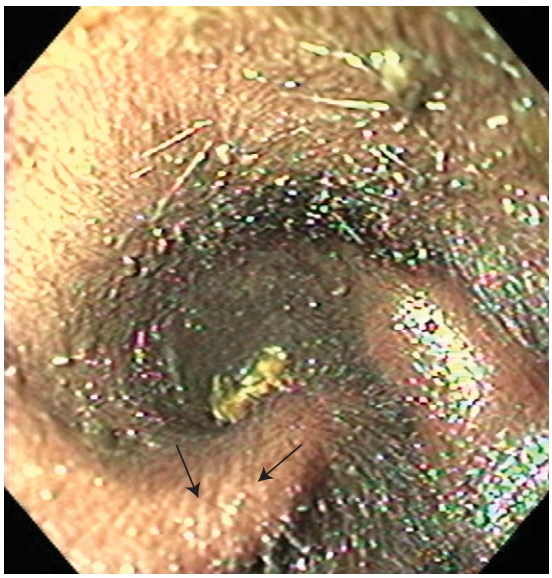

FIGURE 14-1. Vertical canal (proximal part of ear canal) of auricle. Anthelix *(arrows)* is present on medial wall of initial proximal part of ear canal.

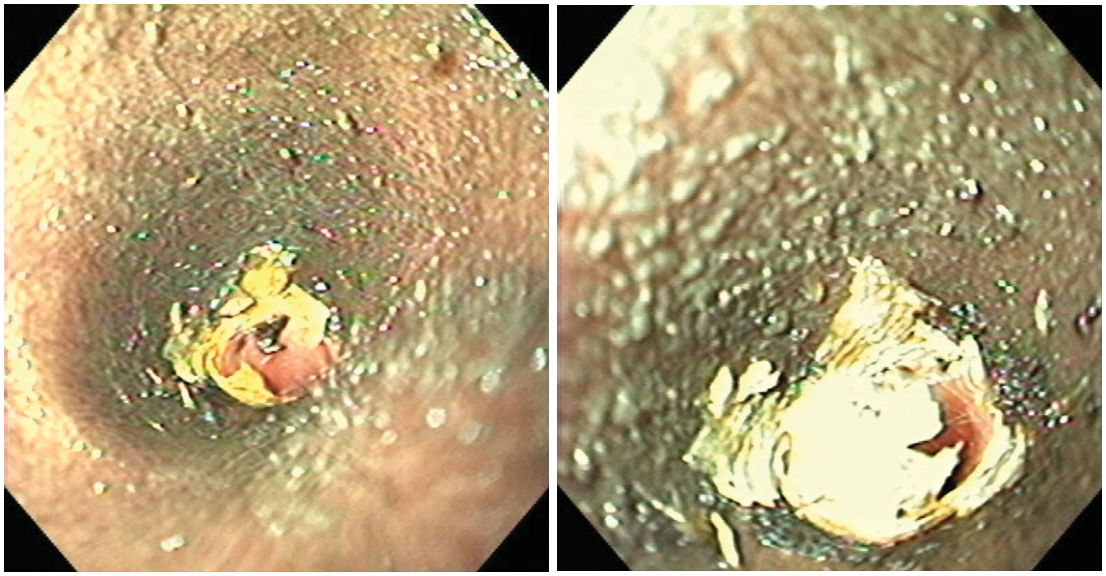

FIGURE 14-2. **A,** External acoustic meatus (horizontal canal) with cerumen. Note tympanic membrane (salmon color) in distance. **B,** Closer view of cerumen that has been pushed by otoscope to tympanic membrane. This is considered a normal otoscopic examination.

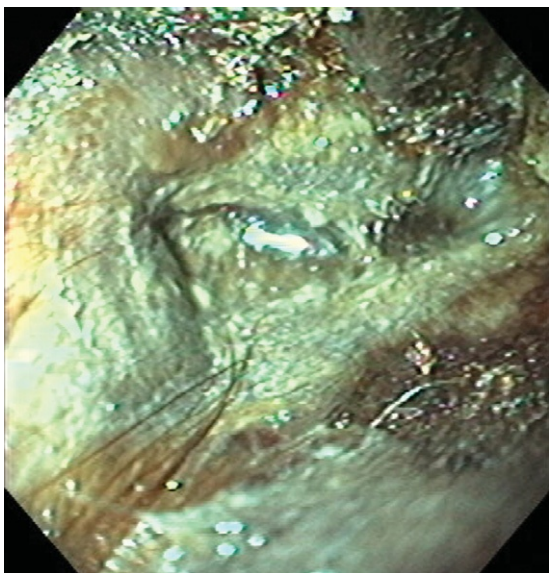

FIGURE 14-3. Vertical canal of a horse with severe otitis externa. This horse had unilateral cranial nerve VII and VIII deficits.

FIGURE 14-4. Five-year-old quarter horse with history of intermittent head tossing and scratching of the left ear. Otoscopy revealed a small mass in the vertical ear canal. A biopsy revealed that the mass was a sarcoid.

ORAL EXAMINATION (Figures 14-5 to 14-8)

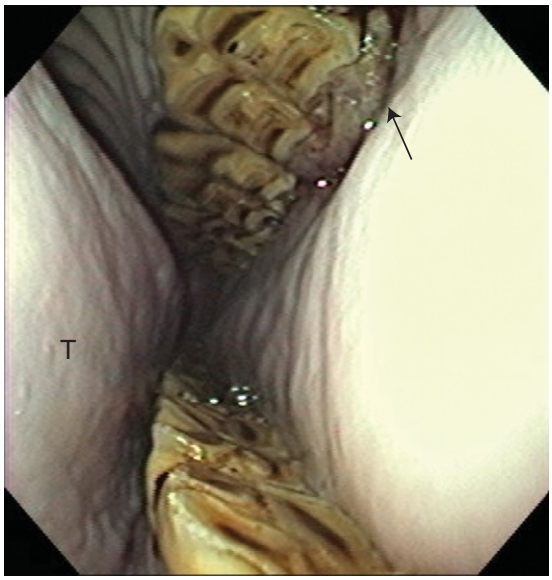

FIGURE 14-5. Oral examination via endoscope can be easily obtained with proper restraint. Horse is sedated and a full mouth speculum is in place. Endoscope is then placed in mouth and guided with a hand over tip of scope for protection. Dental caries, mucosal ulceration, oral tumors, and various other oral/dental diseases can be identified. Note mass on buccal aspect of 207 tooth *(arrow). T,* Tongue.

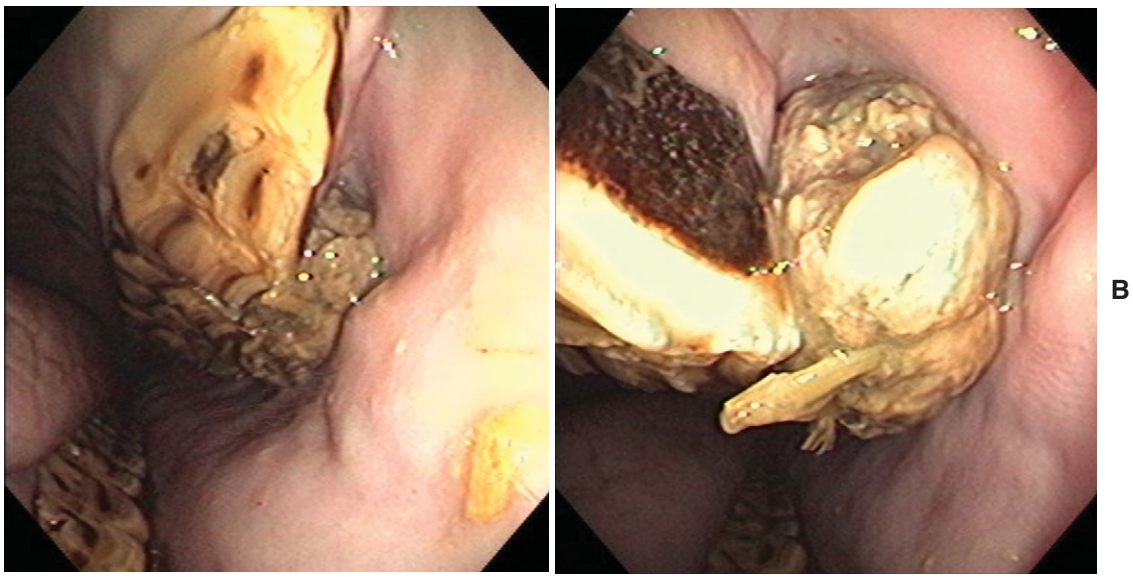

FIGURE 14-6. A and **B,** Two-year-old saddlebred stallion was seen with history of enlarging mass on left aspect of maxilla. Oral examination revealed a mass on buccal aspect of 207 tooth. A biopsy was performed and revealed ossifying fibroma. Surgical excision along with teletherapy was successful.

FIGURE 14-7. Four-year-old thoroughbred mare was seen with chronic history of weight loss and was dysphagic. Oral examination revealed ulcerative hard palate and buccal mucosal lesions. Biopsy specimens of lesions were characteristic histologically of lymphosarcoma. This mare also had severe ulcerative pharyngitis.

A

B

FIGURE 14-8. **A,** Five-year-old quarter horse gelding was seen with chronic draining tract on ventral aspect of mandible. Horse had 308 and 309 teeth extracted due to dental caries 2 years before presentation. Radiographs of head revealed osteomyelitis of mandible. **B,** Bone was débrided, and fistulous tract was packed with antibiotic-impregnated plaster of paris. Dental impression material was then used to cover oral aspect of tract. Horse's recovery was uneventful.

SHEATH (Figure 14-9)

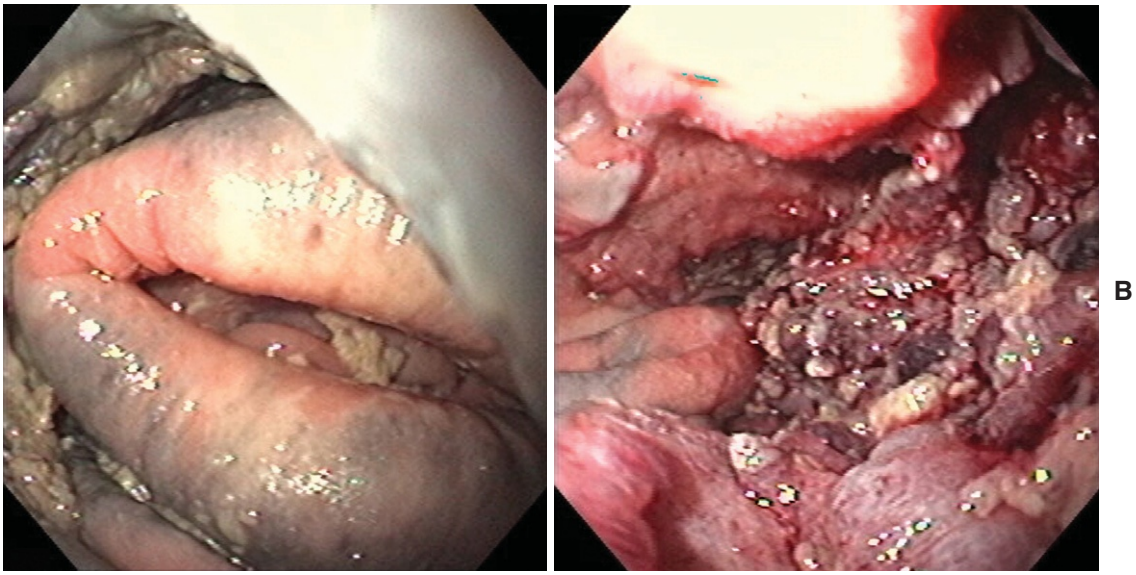

FIGURE 14-9. **A** and **B,** Twenty-five-year-old pony was seen with enlarged sheath. Animal had been noted not to be extending his penis during urination. Endoscope was placed in sheath and infiltrative mass was noted. Mass was biopsied and histologically resembled squamous cell carcinoma.

Index

Page numbers followed by "f" indicates figures, "t" indicates tables.